UNIVERSITY OF HULL

Investigating the Role of Arginine Methylation in Glioblastoma using Biomicrofluidics

A thesis submitted for the degree of Doctor of Philosophy to the University of Hull

By

Sabrina Francesca Samuel

BSc (Hons) University of Hull

MRes University of Birmingham

April 2021

Abstract

Despite intense research, the prognosis of patients with glioblastoma (GBM) remains extremely poor, with a median survival of 1.5 years after diagnosis. The need for new therapeutic options is therefore a vital step towards securing a better outlook for patients. Protein Arginine Methyltransferases (PRMTs) are novel targets in current oncology clinical trials due to their ability to augment a vast variety of cellular processes including growth factor signalling as well as Deoxyribonucleic acid (DNA) damage repair and proliferation. There are three known types of PRMT with varying target specificities and activities. All PRMT's are able to transfer a single methyl group onto the guanidino nitrogen on the target arginine, producing the monomethyl-arginine (MMA) mark. Type I PRMTs (PRMT1, PRMT2, PRMT3, PRMT4, PRMT6 and PRMT8) then transfer a second methyl group on the same nitrogen to produce the asymmetrical dimethyl-arginine (ADMA) mark. Type II PRMTs (PRMT5 & PRMT9) transfer a second methyl group to the opposite nitrogen on the arginine functional group, making symmetrical dimethyl-arginine (SDMA). The type III PRMT, PRMT7, is only able to carry out the first methylation step.

The generally accepted view is that PRMT expression is increased in tumour cells, including GBM. Therefore, the overarching hypothesis here is that GBM cells are dependent on PRMT expression, and the inhibition of these enzymes will result in cell death or reduced proliferation. This research aims to determine the efficacy of PRMT inhibitors as a therapeutic avenue in GBM treatment by measuring the anti-proliferative effects of PRMT inhibiting drugs on GBM cells. A further aim of this research is to characterise an *ex vivo* microfluidic model that would allow for patient specific testing of pharmacological drugs in a simulated tumour microenvironment.

Using the U-87MG glioma cell line as a model system, differing levels of efficacy of PRMT inhibitors were observed. PRMT1 inhibition by Furamidine resulted in a reduction in cellular viability, however, inhibition of PRMT1 and other type I PRMTs by MS023 had minimal effect, as measured by MTS assays in Two-dimensional (2D) and Three-dimensional (3D) culture U-87MG models. Western blotting revealed an increase in the symmetrical dimethylation of a ~70 kDa protein following inhibition of Type I PRMTs with MS023, suggesting cross-talk between Type I and Type II PRMTs.

To further investigate the use of PRMT inhibitors and possible cross-talk mechanisms, an *ex vivo* microfluidic model was utilised, where patient biopsies were perfused with growth medium with and without MS023. Patient samples could be maintained in a viable state on the microfluidic device for up to 192 hr (8 days), as determined by the minimal release of the membrane contained enzyme lactate dehydrogenase into the effluent (LDH assay). However, a reduction in proliferation was observed in samples incubated on chip compared with the matched fresh biopsies. Treatment of

patient samples with MS023 did not result in an increase in cell death as determined by LDH assay or a reduction in proliferation as determined by the quantification of ki-67 positivity by immunohistochemistry (IHC).

The cross-talk activity seen in the earlier cell line models was further demonstrated in the *ex vivo* microfluidic model. In patient biopsies six out of nine and four out of five patient samples showing increases in SDMA and MMA following MS023 treatment, respectively. To identify specific proteins that had undergone changes in methylation status, heavy methyl SILAC mass spectrometry was used. With this methodology, the RNA binding protein FUS was found to be methylated in the presence of MS023 only.

To further understand the effects of the *ex vivo* incubation of patient samples and explore the presence of intra-tumour heterogeneity, samples were treated with Temozolomide (TMZ), the current chemotherapy drug used is clinical practice, and cell death and proliferative activity determined by LDH assay and ki-67 positivity through IHC. Treatment with 10 µM TMZ did not result in an increase in cell death or a reduction in proliferation. However, a reduction in ki-67 was again seen in the samples incubated on chip compared with fresh biopsies. To explore intra-tumour heterogeneity, multiple slices from the same patient biopsy were ran in parallel. The slices appeared to have variation in ki-67 positivity, suggesting that the rate of proliferation is not uniform within the tumour mass and could perhaps mask any response to drug treatment during analysis.

In order to elicit a tumour response in GBM patient biopsies, MS023 was given in combination with TMZ, or GSK591, a PRMT5 inhibitor. Despite this aggressive approach, there were no significant changes in cell death or proliferative activity. It is hypothesised that the reduction in proliferative activity seen following incubation on the microfluidic device could reduce sensitivity to anti-tumour drugs and mute any changes that would otherwise be observed.

To conclude, this study has explored the feasibility of using a GBM-on-chip model to investigate emerging drugs, that is, PRMT inhibitors, towards the treatment of GBM. Further improvements to the microfluidic model, or broader analysis of the effect of TMZ and PRMT inhibitors on other cellular processes, such as apoptosis and senescence, are needed. This study has presented exciting cross-talk activity amongst PRMT enzymes not previously demonstrated in GBM tissue which warrants further investigation.

Acknowledgements

I would firstly like to thank my supervisor, Dr. Pedro Beltran-Alvarez, for guiding me through my project over the past three years. Thank you for pushing me to be my best, by encouraging me to step out of my comfort zone and to believe in my abilities. Your knowledge and support have been invaluable, and I have sincerely enjoyed every day of the lab. Thank you also to my secondary supervisor, Prof. John Greenman, for your knowledge and expertise. Your input is always appreciated! Thank you both of your unwavering faith and confidence in me.

Thank you to all of the other staff at the university including Kath Bulmer, Andrew Gordon, and Vicky Green, who have never hesitated in helping with my experiments and passing on their knowledge. Thank you to the other GBM researchers who have helped me over the years including Michael and Chris, and most importantly Srihari, who I had the pleasure of working beside throughout the majority of my studies. Thank you to my colleagues, Becca, Alistair, Quentin, and Antonia, who have made my PhD experience so much more memorable during the best of times, and bearable during the worst of times.

Thank you to my family for your patience and understanding, and apologies for my lack of communication during the intensive times.

Thank you to my partner, Lewis, for your continuous support, encouragement, and understanding. You have always celebrated my accomplishments and have been there to comfort me when my cells had perished.

I would also like to thank Dr Assam Allam for his generous contributions which have allowed my research to take place.

Publications to date

Related Peer Reviewed Publications:

Samuel, S. F., Barry, A., Greenman, J., & Beltran-Alvarez, P. (2021). Arginine methylation: the promise of a 'silver bullet' for brain tumours? Amino acids, 53(4), 489–506.

Samuel. S. F., Marsden, A. J., Deepak, S., Rivero, F., Greenman, J., & Beltran-Alvarez, P. (2018) Inhibiting Arginine Methylation as a Tool to Investigate Cross-Talk with Methylation and Acetylation Post-Translational Modifications in a Glioblastoma Cell Line. *Proteomes*, 6(4).

Conference Presentations:

November 2020 – Paper submission (First prize) – 17th International Medical Postgraduate Conference (Charles University, Prague)

July 2019 – Young Investigator Talk – British Society for Proteomic Research Annual Conference (University of Southampton)

March 2019 – Poster Presentation – Allam Lecture (University of Hull)

March 2019 – Poster Presentation – Life Sciences 2019: Post-Translational Modifications and Cell Signalling (University of Nottingham)

October 2018 – Poster Presentation – The East Midlands Proteomic Workshop (Lincoln University)

August 2018 – Poster Presentation & Chair – North of England Cell Biology Forum (University of Huddersfield)

Table of Contents

List of Figures

List of Tables

Abbreviations

2D	**Two-dimensional**
2-HG	**2-hydroxyglutarate**
3D	**Three -dimensional**
53BP1	**p53 binding protein 1**
ADMA	**Asymmetrical dimethylarginine**
APS	**Ammonium Persulfate**
ArgMe	**Arginine methylation**
ATP	**Adenosine triphosphate**
ATRX	**α thalassemia syndrome X-linked**
BBB	**Blood brain barrier**
BSA	**Bovine Serum Albumin**
CNS	**Central nervous system**
CO_2	**Carbon Dioxide**
CSF	**Cerebrospinal fluid**
DAB	**3,3′-Diaminobenzidine**
DMEM	**Dulbecco's Modified Eagle Medium**
DMSO	**Dimethyl sulfoxide**
DNA	**Deoxyribonucleic acid**
ECL	**Enhance Chemiluminescence**
EGFR	**Epidermal growth factor receptor**
EV	**Extracellular vesicle**
FBS	**Foetal bovine serum**
FGFR	**Fibroblast growth factor receptor**
GAR	**Arginine Glycine rich**
GBM	**Glioblastoma**
GO	**Gene Ontology**
HCl	**Hydrochloric acid**
HIF-1α	**Hypoxia-inducible factor 1-alpha**
hmSILAC	**Heavy methyl Stable Isotope Labelling of Amino Acids in Cell Culture**
HRI	**Hull Royal Infirmary**
IDH	**Isocitrate dehydrogenase**
KAT	**Acetyl-lysine transferase**
KEGG	**Kyoto Encyclopaedia of Genes and Genomes**
MEP50	**WD-repeat methylome protein 50**
MGMT	**O-6-Methylguanine-DNA Methyltransferase**
miRNA	**Micro RNA**
MMA	**Monomethyl arginine**
MMR	**Mismatch repair**
MRE11	**Meiotic recombination 11 homolog**
mRNA	**Micro RNA**
MTAP	**Methylthioadenosine phosphorylase**
NADP	**Nicotinamide adenine dinucleotide phosphate**
NF-κB	**Nuclear factor kappa B**
OCT	**Optimal cutting temperature**
P53	**Tumour Protein 53**
PARP	**Poly(ADP-ribose) polymerase**
PBS	**Phosphate buffered saline**
PDGFR α	**Platelet Derived Growth Factor Receptor α**
PI3K	**Phosphoinositide 3-kinase**
PI4K2A	**Phosphatidylinositol 4-Kinase Type 2 α**

PIP2	**Phosphorylate phosphatidylinositol-4, 5-bisphosphate**
PIP3	**Phosphatidylinositol-3, 4, 5-bisphosphate**
PRMT	**Protein arginine methyltransferase**
PTEN	**Phosphatase and tensin homolog**
PTM	**Post-translational modification**
qPCR	**Quantitative Polymerase Chain Reaction**
RB1	**Retinoblastoma 1**
RTK	**Receptor tyrosine kinase**
SAH	**S-adenosyl-L-homocysteine**
SAM	**S-adenosyl-L-methionine**
SDMA	**Symmetrical dimethylarginine**
SDS-PAGE	**Sodium dodecyl sulphate polyacrylamide gel electrophoresis**
SH3	**Src homology 3**
SMN	**Survival of motor neuron**
SNAIL	**Zinc finger protein SNAI1**
SPF30	**Splicing factor 30**
TCGA	**The Cancer Genome Atlas**
TDP1	**Tyrosyl-DNA phosphodiesterase**
TEMED	**Tetramethylethylenediamine**
TERT	**Telomerase reverse transcriptase**
TET	**Ten-eleven translocation**
TGFβ	**Transforming growth factor β**
TMZ	**Temozolomide**
TNF-α	**Tumour necrosis factor**
TTFIELDS	**Tumour Treating Fields**
VEGF	**Vascular endothelial growth factor**
α-KG	**α -ketoglutarate**

Chapter 1 - General Introduction

1.1) Glioblastoma

1.1.1) Introduction

Gliomas are the most common malignancy of the central nervous system (CNS), accounting for 26% of all primary CNS tumours as well as 81% of malignant CNS tumours. The most devastating form of glioma is grade IV astrocytoma, also known as Glioblastoma (GBM) (Ostrom et al, 2019). Despite intense research efforts, the prognosis of GBM patients remains poor, with a median survival of 1.5 years following initial diagnosis, with minimal progress being made in increasing this life expectancy over the past 20 years (Ostrom et al, 2015, Ostrom et al, 2018, Ostrom et al., 2019).

1.1.2) Cellular Origin

GBM is a cancer originating from astrocytic cells, which belong to the category of glial cells within the brain, alongside ependymal cells, oligodendrocytes, and microglia. These types of cells outnumber neurons by ten-fold, with astrocytes contributing 50% of total brain mass (Kimelberg, 1989). Astrocytes are responsible for the homeostasis of the CNS in a number of ways such as sustaining neurotransmission, synthesis of glycogen and energy substrates, the regulation of blood pH, and ion concentrations (Verkhratsky, 2018). Due to similarities in phenotypical characteristics, GBM cells may also arise from neuronal/glial stem cells at various stages of differentiation (Phillips et al., 2006).

1.1.3) Epidemiology

GBM is not only the most aggressive form of glioma but is also the most common, with an incidence of 3.21 per 100,000 people in the United States, accounting for 56.6% of all gliomas (Ostrom et al., 2018). The observed frequency of GBM can vary when considering different factors including age, sex and ethnicity. GBM is an age-related disease, with an increasing incidence of GBM in people of older ages, with a peak incidence being 15.13 per 100,000 in people aged 75 to 84 years (Ostrom et al, 2018). The increase in incidence is also accompanied by a decrease in survival rate. The median age of GBM diagnosed patients has increased over the years due to increased longevity of people in developed countries, meaning individuals who would have otherwise died of other causes, could now develop GBM.

There is a 1.6-fold higher incidence of not only GBM, but all malignant brain and CNS tumours, in men compared with women (Mehta et al., 2010, Tian et al., 2018, Ostrom et al., 2019). Differences in p53 (tumour protein P53) and RB1 (retinoblastoma 1) pathways are thought to play a part in this gender inequality, alongside other factors such as hormonal differences and differences in immunity (Sun et al., 2015). For instance, loss of p53 in neurofibromin (Nf1) negative astrocytes isolated from both male and female mice, resulted in the increased growth rate of male originating cells alone (Sun et al.,

2014). Conversely, when exposed to DNA damaging agents, female mice showed increased expression of cyclin dependant kinase (CDK) inhibitors, p16, p21, and p27 to induce cell cycle arrest, whereas male mice did not (Kfoury et al., 2018).

GBM also has a higher frequency in the Caucasian population compared with black or African American, whereas lower grade astrocytoma's are more prevalent in the black or African American population (Barnholtz-Sloan et al., 2003). Asian or Pacific Islander patients have an overall greater survival probability than other ethnicities, with a 3-year survival of 37% compared with 27.7%, 28.8% and 32.3% for Caucasian, black and Hispanic patients (Bohn, et al., 2018, Patel et al., 2019). It is unclear what the cause of these observed differences are, and further research is needed to identify possible molecular features that differ among these groups.

1.1.4) Aetiology

The only established known risk factor is exposure to ionising radiation such as from previous cancer treatments (Ellor et al., 2014). Little is known about other risk factors associated with GBM, with only a small percentage of patients (<5%) presenting with a germline predisposition, such as one associated with the Neurofibromatosis type 1 syndrome (D'Angelo et al 2019). Studies investigating the associated risk factors of GBMs have limited confirmed findings, due to small sample sizes and inconsistencies with tumour classification (Bondy et al., 2008). However, some studies have suggested that traumatic brain injury may predispose patients to glioma formation, including the development of GBM (Anselmi et al., 2006, Trapani et al., 1996, Zhou & Liu 2010). There are multiple hypotheses as to why this might occur: recruitment of inflammatory cells, migration of progenitor cells and the dedifferentiation of astrocytic cells (Al-Kharboosh et al., 2020).

1.1.5) Classification

Tumours of the CNS, including astrocytomas, are predominantly classified based on tissue histology and cellular origin and are graded on a scale of I-IV, with increasing malignancy (Figure 1.1) (Louis et al., 2007). Grade I astrocytomas are often benign and require only surgery, although gross total resection is not always possible, such as when the tumour has adhesions to surrounding brain tissue (Young et al., 2015). Grade II astrocytomas are more active in their progression and are more likely to recur. Grade III and IV astrocytomas, with grade IV being classed as a GBM, are considerably more aggressive and require a combination of surgery, radiation and chemotherapy. This aggressive nature is reflected in the poor patient prognosis and high rate of recurrence.

Patients within these different groups, as well as those diagnosed with non-astrocytic tumours, may present with differences in clinical characteristics. Following advances in genomics, molecular aberrations within these tumours have become accepted as an important factor in patient

stratification and now provide a more accurate and clinically relevant subtyping of brain tumours. The development of these narrow classification criteria, however, can leave large groups of tumours undesignated and so it is important to consider both the genotype and phenotype of tumours. Previously, gliomas originating from astrocytes or oligo dendrites were separated and further classified into their specific subtypes (Louis et al., 2007). With the observation of similarities in growth pattern and genetic features, all diffuse gliomas are grouped together and classified according to the presence of driver mutations: IDH (Isocitrate dehydrogenase) mutated, IDH wildtype, and NOS (not otherwise specified) (Figure 1.1) (Louis et al., 2016).

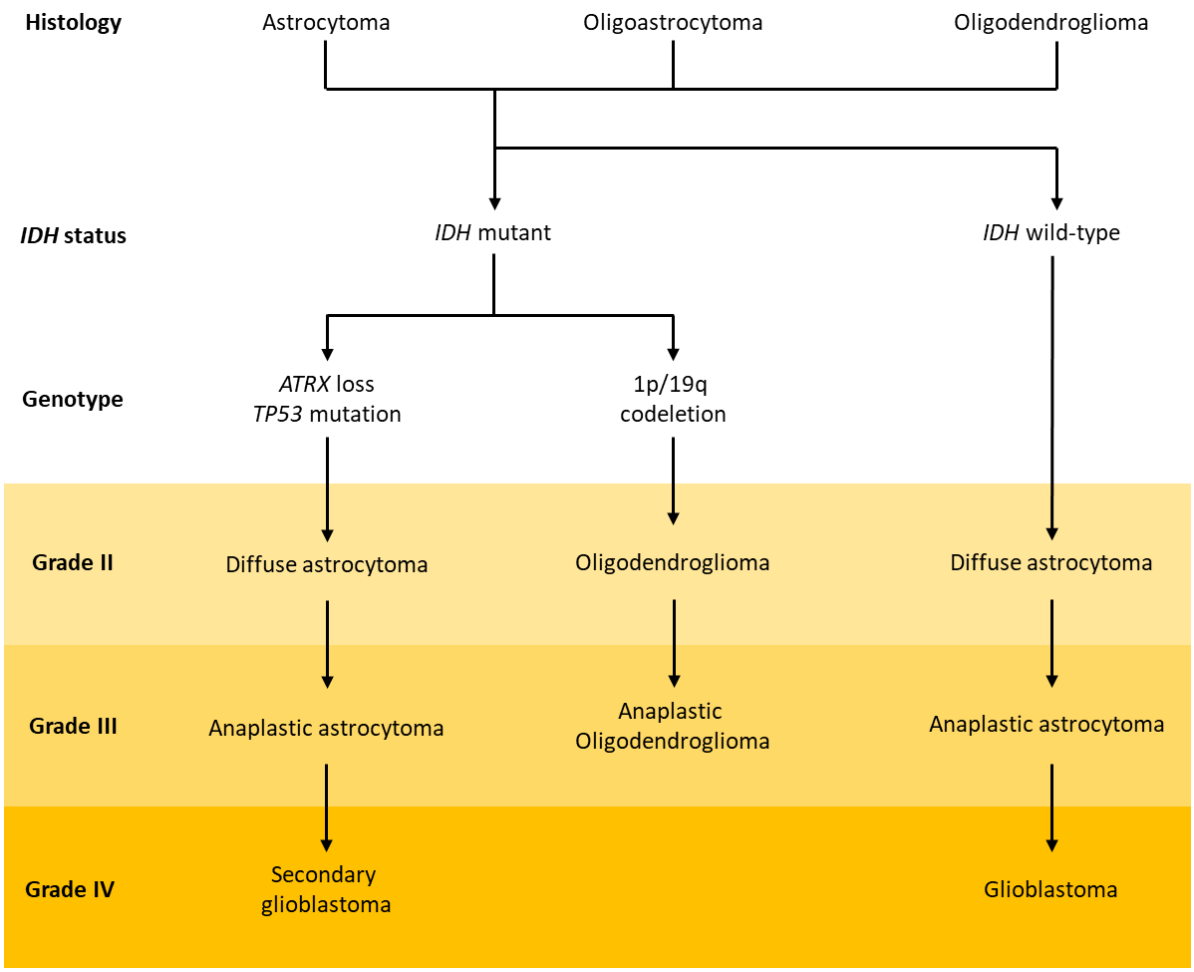

Figure 1.1: WHO classification of diffuse astrocytic and oligodendroglia tumours according to histopathological and genotypical characteristics. *Localised astrocytic tumours not included in the table are Pilocytic Astrocytoma (Grade I), Subependymal Giant Cell Astrocytoma (Grade I), Pleomorphic xanthoastrocytoma (Grade II) and Anaplastic pleomorphic xanthoastrocytoma (Grade III). (Adapted from Louis et al., 2016).*

Glioblastomas are considered either primary or secondary, with the latter referring to cases where the tumour has progressed from a lower grade glioma such as diffuse astrocytoma or anaplastic astrocytoma (Ohgaki & Kleihues, 2013). Primary tumours, also known as *de novo* GBMs, are more common and confer a poorer prognosis (90% of cases) than secondary tumours and are also more

frequent among older populations. Males are also more likely to develop a primary tumour, whilst females are more likely to develop a secondary GBM (Ohgaki et al., 2004). It is not possible to distinguish between primary and secondary tumours by histopathological means, although there are variations in molecular markers (Kleihues & Ohgaki, 2000, Kleihues & Ohgaki 2013).

1.1.6) Molecular Markers

1.1.6.1) IDH1 and IDH2

The presence of *IDH1* and *IDH2* heterozygous mutations are currently used to characterise patient tumours to allow for a more informed prognosis, with patients with mutations having a more favourable outcome (Louis et al., 2016). *IDH1* was the first to be identified and was found to be mutated in 12% of GBM patients (Parsons et al., 2008). It was then discovered that point mutations on residue R132 were present in a significantly greater proportion (80%) of lower grade gliomas as well as secondary GBMs (Yan et al., 2009, Cohen et al., 2013). *IDH1* mutations were found to occur early in glioma progression, taking place prior to mutations in other genes including *TP53* (Watanabe et al., 2009). Mutations in *IDH2* are less common in gliomas and are mutually exclusive with *IDH1* mutations and occur on the analogous residue R172 (Hartmann et al., 2009).

IDH1 and *IDH2* encode for enzymes involved in cytoplasmic and mitochondrial metabolism, and are often dysregulated in cancer (Parsons et al., 2008). IDH1/2 convert isocitrate into alpha-ketoglutarate (α-KG), generating reduced nicotinamide adenine dinucleotide phosphate (NADPH) from NADP+ (Figure 1.2). IDH1 carries out this reaction within the cytoplasm, whereas IDH2 can be found within mitochondria. Mutations in residues R132/R172 change the catalytic activity of the enzymes, resulting in a loss of function for the forward reaction due to a reduced binding affinity for isocitrate, and a gain in function of the reverse reaction involving the reduction of α-KG into 2-HG, due to an increased binding affinity for NAPDH (Dang et al., 2009, Turkalp et al., 2014). 2-HG differs from α-KG only by the presence of a hydroxyl group instead of a carbonyl group at the C2 position, and acts as a competitive inhibitor in α-KG dependant reactions (Xu et al., 2011). This inhibition results in dysregulation of multiple cellular processes including methylation of both histones and DNA as well as the response to hypoxia (Turcan et al., 2012). These changes can induce glioma development through inhibition of differentiation and upregulation of Hypoxia-inducible factor 1-alpha (HIF-1α) (Huang et al., 2019).

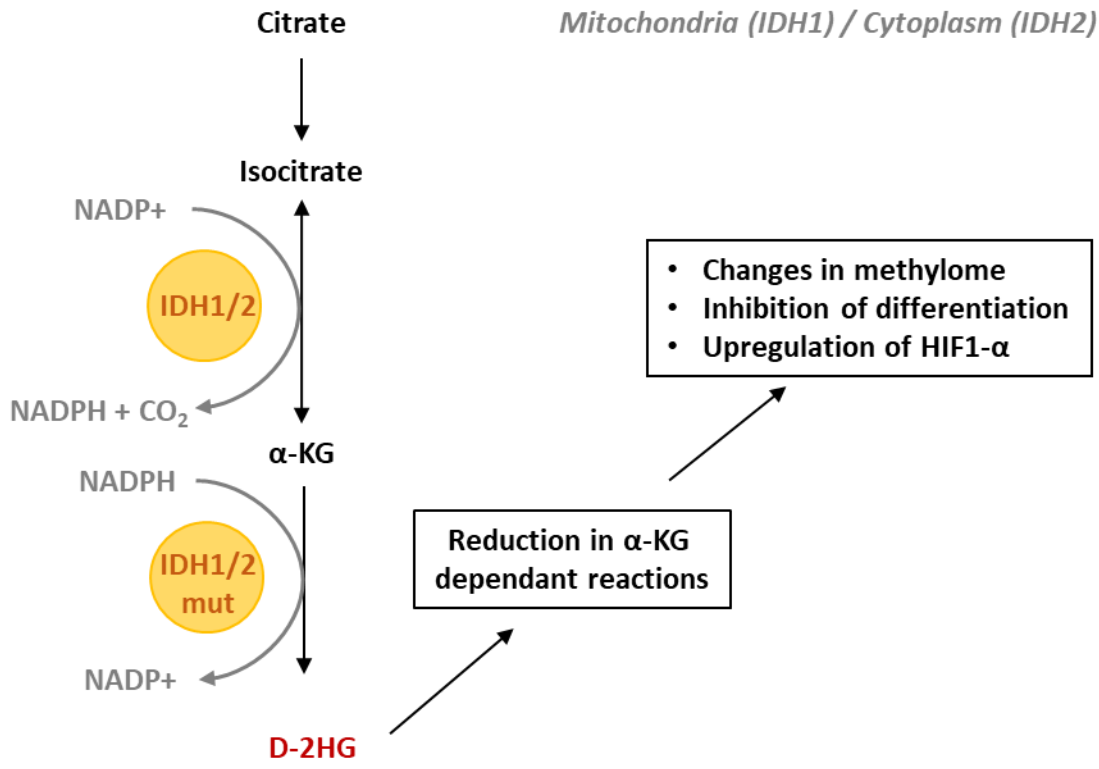

Figure 1.2: Activities of the IDH enzymes and the consequences of D-2HG production. *NADP+/NADPH(Nicotinamide adenine dinucleotide phosphate), IDH1/2 (Isocitrate dehydrogenase), α-KG(Alpha ketoglutarate), D-2HG(D-2-Hydroxyglutarate). (Adapted from Mondesir et al 2016).*

1.1.6.2) Chromosomal Gains and Losses

Common genomic amplifications include those on chromosomes 4, 7 and 12. These correspond to gene loci of platelet derived growth factor receptor alpha (*PDGFR*α), epidermal growth factor receptor (*EGFR*), mesenchymal epithelial transition (*MET*), cyclin dependent kinase 6 (*CDK6*), cyclin dependent kinase 4 (*CDK4*), mouse double minute 2 homolog (*MDM2*) (Brennan et al., 2013). Loss of heterozygosity of chromosome 10q is present in a high proportion of GBM samples ranging from 60-90% and has been shown to be a predictor of poor patient survival (Andreas et al., 1992, Ohgaki et al., 2004, Houillier et al., 2006, Kakkar et al., 2011). The loss of this region is thought to result in the loss of the key genes phosphatase and tensin homolog (*PTEN*) and phosphatidylinositol 4-kinase type 2 alpha (*PI4K2A*) (Fults et al., 1998, Waugh., 2016).

Chromosome 1p and 19q deletions have been shown to be useful prognostic tools in lower grade gliomas, however, they do not hold prognostic significance in GBM patients (Smith et al., 2000, Kaneshiro et al., 2009, Clark et al., 2013).

1.1.6.3) p53 and RB Pathway

Mutations in the *TP53* gene are implicated in almost all types of cancer, including GBM (Rivlin et al., 2011). Due to the role of p53 as a transcriptional regulator involved in cell cycle regulation and DNA

damage repair, mutations in this gene result in uncontrolled proliferation and an increase in genomic instability (Leroy et al., 2013). According to The Cancer Genome Atlas (TCGA) GBM report, the p53 pathway was dysregulated in 85.3% of GBM tumours (Cancer Genome Atlas Research Network, 2008). Dysregulations in this pathway include the mutation/deletion of *TP53* (27.9%), amplification of *MDM1/2/4* (15.1%) and/or deletion of *CDKN2A*, encoding for p16 and p14 (57.8%) (Brennan et al., 2013). *TP53* alterations were mutually exclusive with both the MDM family genes and *CDKN2A* and are more prominent in secondary GBM tumours (Figure 1.3) (Watanabe et al., 1996, Ohgaki et al., 2009).

A large percentage of GBM samples analysed (78.9%) have at least one alteration affecting the function of the retinoblastoma protein (RB) pathway (Brennan et al., 2013). This included mutations/deletion in *RB1*, amplification of *CDK4/6* and deletion of *CDKN2A*.

1.1.6.4) EGFR/ PI3K Pathway

EGFR is a type of receptor tyrosine kinase (RTK) and a well-known onco-protein that is dysregulated in GBM, particularly in primary tumours (Mischel et al., 2003, Cancer Genome Atlas Research Network, 2008). Alterations in *EGFR* itself occur in a large proportion of GBM patients (57.4%), with the most common alteration being an amplification of the *EGFR* gene (35-40%) (Halatsch et al., 2006, Rao et al., 2010, Brennan et al., 2013). These alterations result in constitutive activation, leading to constant proliferative signalling, and are correlated with increased cell proliferation, invasion and GBM recurrence (Kimmo et al., 2010). Despite its suggested role in glioma genesis, there are contradictory studies concerning the prognostic significance of *EGFR* alterations (Newcomb et al., 1998, Li et al., 2018). Many tumours possess a unique deleterious variant of *EGFR* known as EGFRvIII, which has a prevalence of approximately 40% (Humphrey et al., 1990, Huang et al., 2007). The presence of *TP53* mutations and *EGFR* alterations are mutually exclusive, with *TP53* mutations more frequent in younger patients with secondary tumours, and *EGFR* alterations occurring in older patients with primary tumours (Figure 1.3) (Ellor et al., 2014). Although to a lesser extent, other RTKs including *PDGFRα*, *MET,* and fibroblast growth factor receptor 2/3 (*FGFR2/3*) were also observed to be altered in GBM patients (Brennan et al., 2013).

One pathway triggered upon EGFR ligand binding is the PI3K/Akt/mTOR pathway. Activated EGFR binds the regulatory subunit of phosphoinositide 3-kinase (PI3K), releasing the PI3K catalytic subunit. PI3K is then able to phosphorylate phosphatidylinositol-4, 5-bisphosphate (PIP2) into phosphatidylinositol-3, 4, 5-bisphosphate (PIP3) (Riehle et al., 2013). PIP3 production can be altered by dephosphorylation by PTEN, and by the activation of PI3K by Ras GTPases (Smith et al., 2001, Suire

et al., 2002). PIP3 recruits and phosphorylates protein kinase B (Akt), allowing it to take part in mTOR-mediated signalling and other pathways associated with cell cycle progression (Sarbassov et al., 2005).

A proportion of 89.6% of GBM patients were found to have at least one genetic alteration in this pathway when including RTK alterations, and the PI3-Kinase family genes were found to be mutated in 25.1% (Brennan et al., 2013). Other components and associations of the PI3K pathway are altered in GBM patients including *PTEN* (41%), *NF1* (10%) and *RAS* (1%) (Figure 1.3). Activation of this pathway, determined by the expression of phosphorylated pathway components, was found to inversely correlate with patient outcome (Chakravarti et al., 2004).

1.1.6.5) PDGF Signalling

PDGF signalling begins with activation of the RTKs PDGFRα and PDGFRβ and has been shown to have a role in glial cell development. As previously stated, alterations of the gene encoding PDGFRα occurs in approximately 13% of GBM patients (Brennan et al., 2013). Half of these samples also showed concurrent alterations in other RTK genes including *EGFR* and *MET*. Higher expression of PDGF family subunits, particularly PDGFα was found to correlate with the loss of *PTEN* as well as the absence of an *IDH1* mutation (Cantanhede et al., 2017).

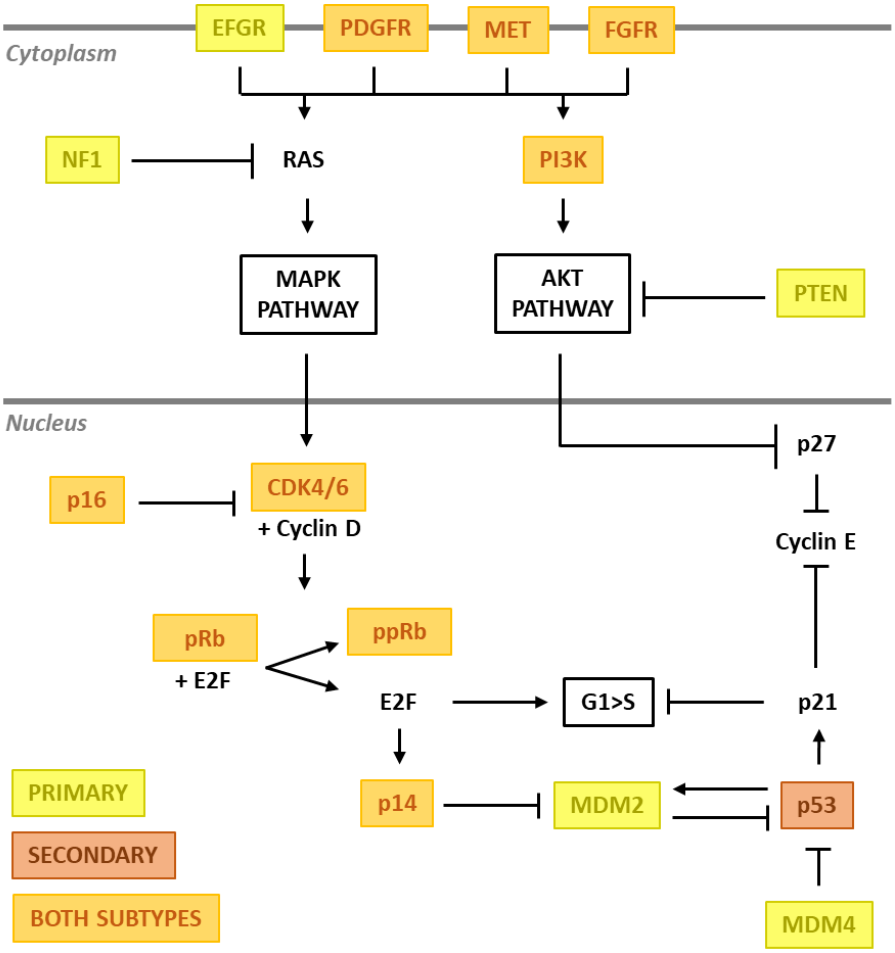

Figure 1.3: An overview of the most common signalling pathways frequently dysregulated in GBM patients. *Numerous interacting pathways are dysregulated in primary and/or secondary GBM tumours, including the p53, RB and EGFR pathways. Activation of growth factor receptors EGFR, PDGFR, MET or FGRE results in the activation of either the MAPK or AKT pathway via RAS and PI3K, respectively. Activation of the MAPK pathway results in the induction of the CDK4/6 and Cyclin D interaction, RB hyperphosphorylation and the progression of the cell cycle from G1 to S phase. Proteins involved in this signalling pathway are often upregulated in GBM and inhibitors of the pathway downregulated. Activation of the Akt pathway via PI3K results in the inhibition of p27 and therefore the upregulation of Cyclin E, resulting in progression of the cell cycle. Proteins involved in induction of this signalling pathway are often upregulated in GBM and inhibitors of the pathway downregulated. Further proteins involved in DNA repair and cell cycle regulation are also affected, including the down regulation of the tumour suppressors p53 and p14, and the upregulation of the oncogenes MDM2 and MDM4. Pointed arrows represent the activation of the following protein or pathway and flat headed arrows represent inhibition of the following protein or pathway. Definitions not previously stated: MET (Hepatocyte growth factor receptor) FGFR (Fibroblast Growth Factor Receptor) NF1 (Fibroblast Growth Factor Receptor) (Adapted from Ohgaki & Kleihues, 2007).*

1.1.6.6) TERT

Telomeres are protective structures made up of repeating lengths of DNA that cap the ends of chromosomes. With every round of mitosis, DNA is lost, and these telomeres act as buffers to ensure no loss of encoding DNA occurs. The telomerase reverse transcriptase (*TERT*) gene encodes for a protein involved in the reconstruction of these telomeres. Mutations in this gene are often acquired

by cancer cells and this is associated with an increased rate of proliferation. Mutations of the *TERT* promoter, in the form of a C228T and C250T substitution, occur in 55-83% of GBM cases, and is correlated with an increased *TERT* messenger RNA (mRNA) expression (Liu et al., 2013, Nonoguchi et al., 2013, Labussière et al., 2014). Loss of telomere length results in cell death or senescence. An increased expression and activity of the enzyme therefore allows cancer cells to escape this fate and removes this limitation on their proliferative capabilities. The presence of *TERT* promoter mutations is significantly more common in GBM patients without an *IDH1/2* mutation, and is associated with patient survival (Pekmezci et al., 2017, Labussière et al., 2014, Eckel-Passow et al., 2015).

1.1.6.7) ATRX

A telomerase-independent mechanism of elongating telomeres exists in the form alternative lengthening of telomeres (ALT), and is a common phenotype seen in GBM tumours (Bryan et al., 1997, Heaphy et al., 2011). The α thalassemia syndrome X-linked (*ATRX*) gene encodes for a SWItch chromatin remodelling protein that is involved in inhibiting this ALT pathway. The *ATRX* gene has been shown to be mutated in GBM, specifically in paediatric and secondary tumours, and is commonly mutated alongside *IDH1/2* and *P53* (Dyer et al., 2017). Loss of ATRX expression, either through mutation, deletion or gene fusion, is associated with WHO grade of glioma and so is therefore seen as a marker of glioma malignancy (Cai et al., 2015). However, in lower grade tumours, loss of ATRX is associated with a more favourable patient prognosis (Suzuki et al., 2015). Most likely due to the synonymous nature of *ATRX* and *TERT* mutations, they are found to be mutually exclusive (Hu et al., 2016).

1.1.7) Molecular Subtyping

Through further analysis of the TCGA data published in 2003, four subtypes of GBM were classified based upon clustering of gene expression (Verhaak et al., 2010). These subtypes were named as Proneural, Neural, Classical and Mesenchymal, and have distinct signatures (Table 1.1). Differences in treatment efficacy were evaluated and it was found that aggressive treatment reduced mortality in classical and mesenchymal with statistical significance, whereas efficacy was only suggested in the neural subtype. Aggressive treatment did not appear to reduce mortality in the proneural subtype.

Table 1.1: The genomic alteration signatures of the 4 main GBM subtypes *(Verhaak et al., 2010).*

Classical	Mesenchymal	Proneural	Neural
Increase in EGFR function by mutation/amplification	NF1 loss/mutation	PDGFRA alterations	Neuron markers (NEFL, GABRA1, SYT1 & SLC12A5)
PTEN loss/mutation	Mesenchymal markers CHI3L1 & MET highly expressed	IDH1 point mutations	
CDKN2A loci loss	Astrocytic markers CD44 & MERTK highly expressed	TP53 loss/mutations	
NES overexpression	Co-mutations of PTEN & NF1	Oligodentrocytic development genes highly expressed (PDGFRA, NKX2-2 & OLIG2)	
Notch/SHH pathways highly expressed	TNF superfamily & NF-kB pathway components highly expressed (TRADD, RELB & TNFRSFTA)	CDKN1A (p21) lowered expression	
Lack of TP53 alterations		High expression of proneural development genes (SOX, DCX, DII3, ASC1 & TCF4)	

1.1.8) Presentation

Diagnosis begins with symptomatic presentation and imaging. The initial clinical presentation of GBM is dependent upon tumour size and location, as well as the extent of surrounding inflammation. Symptoms occur as a result of intracranial pressure and can include headaches, nausea, seizures, memory issues and personality changes (Young et al., 2015). Seizures occur as an initial symptom in approximately 25% of patients, although this increases to 50% in later stages of the disease (Schiff et al., 2015).

Due to the non-specific nature of symptomatic presentation of GBMs, suggestive diagnosis is only possible following imaging. This is be done by CT and MRI, with MRI being the gold standard. Following presentation of the above symptoms, a CT scan may be used to identity intracranial masses such as GBM (Snyder et al., 1993), and should reveal a bright lesion when compared with surrounding grey matter (Johnson et al., 2015). Swelling in the surrounding brain tissue can also be seen, which is often diffuse due to the infiltrating nature of GBM. A CT scan may not identify smaller tumours and MRI will provide a more detailed and informative image (Figure 1.4). During an MRI, several measurements are taken, including T1 and T2: spin-lattice relaxation and spin-spin relaxation, respectively. These are then translated into T1 and T2 weighted images. T1 and T2 images highlight different tissue characteristics such as fat and water content, due to the differences in proton characteristics. A T1 weight image can also be produced following Gadolinium injection prior to the T1 weighted MRI scan, which is used to produce further contrast between the GBM tumour, surrounding tissue, and necrotic centre (Kalpathy-Cramer et al., 2014). Diagnosis can only be confirmed following surgical resection and histopathological staining using identifiers stated in Figure 1.1

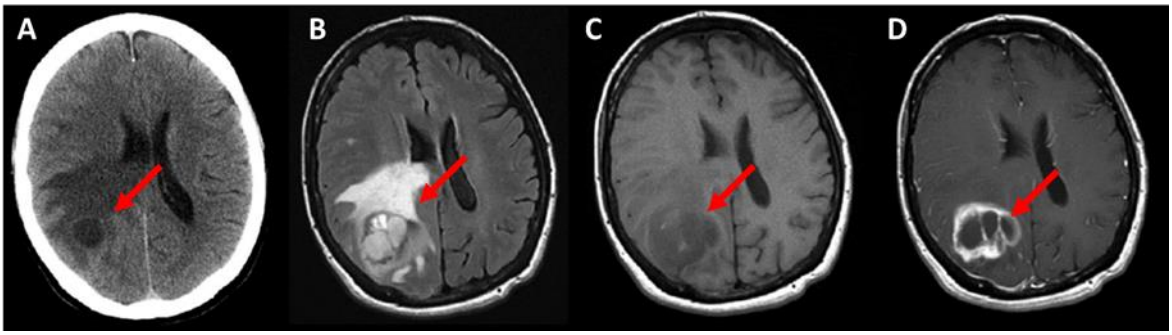

Figure 1.4: Imaging techniques used in GBM diagnosis. *Tumour location is indicated by a red arrow. (A) CT (B) T2 MRI (C) T1 MRI (D) T1 MRI following gadolinium injection. (Johnson et al., 2015).*

1.1.9) Current Treatment

1.1.9.1) Obstacles to GBM Treatment

Major obstacles in GBM treatment are faced during removal of the tumour. As GBM tumours are aggressive and diffuse in nature, they penetrate the surrounding normal tissue (Sahm et al., 2012), making it difficult to distinguish between what is tumour and what is not. To limit the risk of harming healthy brain tumour and normal neurological function, complete removal of the tumour is not always possible. (Simpson et al., 1993, Shanker et al., 2017).

Further limitations occur in the form of chemotherapy drug resistance. The cancer stem cell model describes small populations of undifferentiated self-renewing cells that give rise to the rest of the

tumour (Shackleton et al., 2009). The theory brings forward a mechanism for tumour initiation, progression and resistance to therapy. Following treatment with chemotherapy drugs, these resistant cells remain and can repopulate the tumour. For this reason, cancer stem cells have been the focus of many GBM investigations (Vieira de Castro et al., 2020).

Another obstacle faced during GBM treatment is physical and comes in the form of the blood brain barrier (BBB). The BBB was first demonstrated in 1885 by the use of Evan's blue dye intravenously injected into a rat, where it failed to penetrate the brain tissue (Ehrlich 1885). A further study published in 1913 showed that when injected into the CNS, only the brain tissue was stained (Goldmann, 1913). The BBB acts as a defence mechanism against pathogens and regulates the immune systems infiltration into the brain from the circulatory system. It is comprised predominantly of endothelial cells of the brains vasculature which have a high number of tight junctions to minimise the passage of ions, proteins and cells (Cipolla et al., 2009). The permeability of the BBB can be regulated by the release of signalling molecules by astrocytic cells (Deeken & Löscher, 2007). The BBB presents an issue for GBM treatment as it limits the diffusion of therapeutics to the sight of the tumour.

1.1.9.1) Resection and Radiotherapy

The first line of treatment for GBM is surgical removal, however as previously described, complete resection is often not possible due to both the likeness of tumour to normal tissue and the diffuse nature of the tumour (Simpson et al., 1993, Sahm et al., 2012, Shankar et al., 2017).

Following resection, approximately four weeks recovery time is given to allow for the craniotomy wound to heal (Davis 2016). Then, concurrent radiotherapy and chemotherapy are given, followed by adjuvant chemotherapy. Whole brain radiotherapy was originally used but caused serious long-term complications resulting from damage to the surrounding tissue. The use of involved field radiotherapy was then introduced that emitted radiation (a total of 60 Gy, fractionated) to the tumour with a 2-3 cm margin, providing similar or improved survival advantage over whole brain radiotherapy (Rusthoven et al., 2016).

1.1.9.2) Temozolomide

Following resection, the patient receives radiotherapy and the alkylating agent Temozolomide (TMZ) (Figure 1.5) (Stupp et al., 2009). This combination of treatment was demonstrated to provide a 2 month increase in life expectancy from 12.2 to 14.6 months, and a 16% increase in 2-year survival when compared with standard radiotherapy (Figure 1.6) (Stupp et al., 2009). In this study, TMZ was given concurrently at a low dose of 75 mg/m^2/day and an adjuvant dose alongside radiotherapy at 150-200 mg/m^2/day.

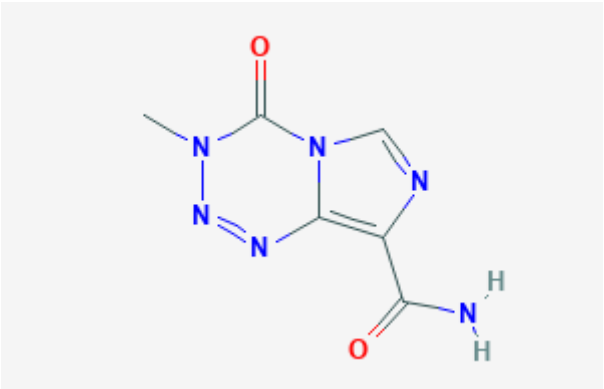

Figure 1.5: The skeletal formula for TMZ.

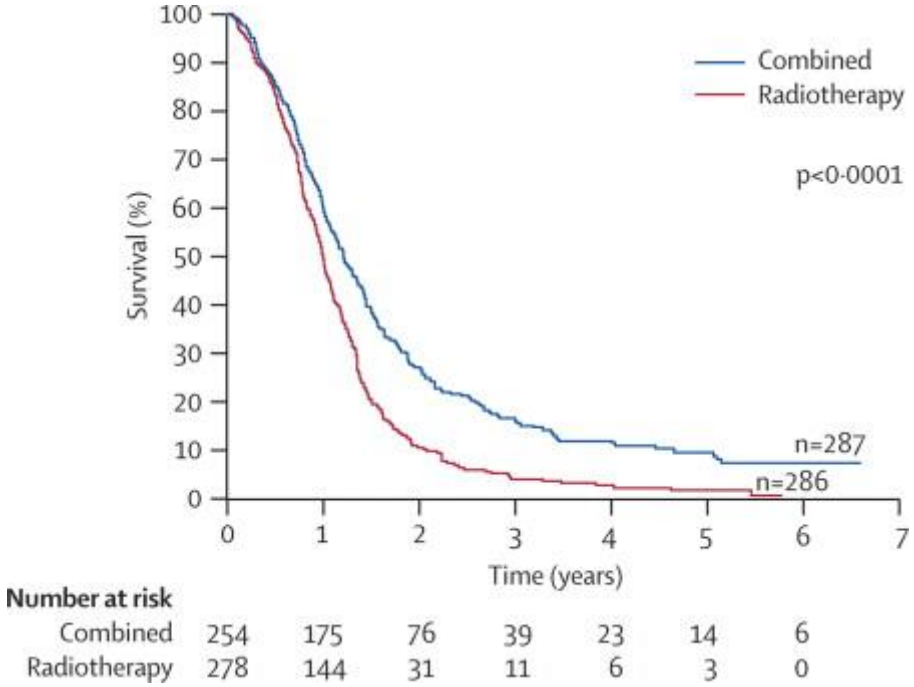

Figure 1.6: Kaplan-Meier demonstrating the increased survival of patients given TMZ. *The study was carried out over 7 years and patient were either given radiotherapy alone (red), or a combined treatment of radiotherapy with temozolomide (blue) (Stupp et al., 2009).*

TMZ works by alkylating DNA, creating adducts that induce DNA strand breaks (Thomas et al., 2017). It is administered orally in its pro-drug form and is spontaneously broken down to monomethyl triazene 5-(3-methyltriazen-1-yl)-imidazole-4-carboxamide (MTIC) once absorbed (Zhang et al., 2012). The pro-drug inactive form of TMZ has greater stability when in low pH conditions, becoming more prone to degradation with increasing pH. This increases its tumour specific action due to the relative alkaline conditions found in brain tumours (Rotternberg et al., 1984).

TMZ has near 100% bioavailability, meaning almost all of the drug is absorbed into circularity system following administration. Both TMZ and MTIC show similar pharmacokinetics in patient plasma with

an approximate half-life of 2 hr (Diez et al., 2010). Being a lipophilic compound, approximately 20% of TMZ is able to cross the blood brain barrier (Ostermann et al., 2004).

The metabolically active form of the drug alkylates DNA preferentially at N7 positions of guanine in guanine rich regions (N7-MeG; 70%), but also methylates N3 adenine (N3-MeA; 9%) and O6 guanine residues (O6-MeG; 6%). These lesions are repaired by specific mechanisms: base excision repair and suicide enzyme MGMT (O-6-Methylguanine-DNA Methyltransferase) repair. This repair response can lead to tumour resistance and treatment failure (Bobola et al., 2012).

During the study investigating TMZ adjuvant therapy, the methylation status of the *MGMT* gene promoter was found to be a statistically significant prognostic factor, with patients possessing a methylated promoter being more responsive to treatment (Stupp et al., 2009). This is due to the role of MGMT in the repair of the O6-MeG lesion and its restoration to guanine. MGMT repairs O6-MeG lesions by transferring the methyl group onto its own cysteine residue in its active site (Pegg et al., 1995). However, when the MGMT gene promoter is methylated, transcription of the gene is supressed, and fewer O6-MeG lesions can be repaired.

During replication, these unrepaired O6-MeG lesions are incorrectly paired with thymine rather than cytosine. The mismatched thymine is recognised by the mismatch repair (MMR) machinery and is removed from the daughter strand (Figure 1.7). However, the original O6-MeG lesion remains, and a cycle of thymine insertion and excision ensues, leading to replication fork collapse and DNA strand breakage, ATR dependant cell cycle arrest and apoptosis (Mojas et al., 2007). Functional MMR machinery alongside a low expression of *MGMT* is therefore required for an effective response to TMZ. The use of *MGMT* as a prognostic marker has been reinforced in more recent studies (Zhao et al., 2018, Alnahhas et al., 2020).

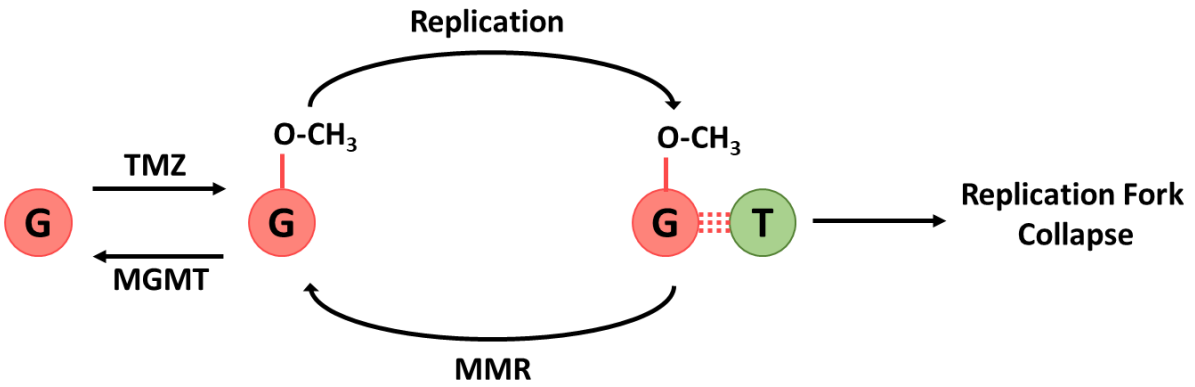

Figure 1.7: The mechanistic action of TMZ action in GBM*. Guanine (G) is alkylated by the active form of TMZ to produce the 6O-MeG lesion. During replication, if left unrepaired by MGMT, the alkylated Guanine is paired with Thymine (T) rather than Cytosine, prompting MMR mechanism. The MMR machinery removes the incompatible Thymine amongst other bases of the newly synthesised strand. The O6-MeG is not removed however, and these steps are repeated, leading to replication fork collapse, double strand breaks and apoptosis.*

1.1.9.3) Alternative Treatments

Vascular endothelial growth factor (VEGF) is a major player in blood vessel development (Carmeliet 2005) and has been shown to be approximately 200/300-fold more concentrated in the cyst fluid of GBM tumours when compared to serum (Takano et al., 1996). VEGF mRNA has been found localised to the areas surrounding hypoxic and necrotic foci in GBM tumours (Brat & Meir, 2001).

The anti-angiogenic drug, Bevacizumab, is an antibody that inhibits VEGF, and is also used for the treatment of recurrent GBM in the USA (Diaz et al., 2017). It binds to VEGF and inhibit its interactions with associated receptors, resulting in supressed signalling. Although Bevacizumab has no effect on overall survival, it was shown to give a significant improvement in progression free survival (Cohen et al., 2009). Due its role as an anti-angiogenic drug, it has been shown to reduce vascular permeability and oedema, improve oxygenation and reduce radiation associated necrosis (Niyazi et al., 2016). However, it can also result in life-threatening side effects including haemorrhage, blood clots and bowel perforation (Taal et al., 2014).

Carmustine (BCNU) is a nitrosourea drug that like TMZ, alkylates DNA in order to induce DNA damage and apoptosis. Nitrosourea drugs were investigated due to their lipid solubility and ability to cross the blood brain barrier (Fung et al., 1996). BCNU causes a high risk of severe pulmonary fibrosis and delayed hepatoxicity (Reithmeier et al., 2010). These risks are lowered by the use of wafer implantation during surgical resection for a localised delivery, which is most commonly used for the treatment of recurrent GBM (Chowdhary et al., 2015). This has been shown to increase patient survival, especially in combination with TMZ (Gutenberg et al., 2013, Chowdhary et al., 2015).

1.1.10) Recurrence

Following treatment, pseudo progression is observed in 10-30% of patients (Delgado-López et al., 2018). Pseudo progression is the indication of disease progression via appearance of contract-enhancing lesions seen in imaging techniques (Brandsma et al., 2008). This occurrence is followed by a spontaneous recovery or stabilisation, although it does complicate the management of treatment following radiation and chemotherapy.

Disease progression is, however, seen in 70% of GBM patients within one year of diagnosis (Stupp et al., 2005). Repeated resection is sometimes an option, and this can provide the opportunity to confirm the GBM recurrence and allows the possible screening of drug targets. Further surgery has been shown to provide an increase in patient survival if total gross resection is achieved (Bloch et al., 2012, Suchorska et al., 2016, Heiland et al., 2018). The genetic profile of the resulting recurring tumour is often very different from the original mass, making further treatment complicated due to lack of targets (Schäfer et al., 2019). Recurrence of GBM is most often treated in order to improve quality of life using chemotherapy and corticosteroids. The progression-free survival of recurrent GBM patients is 2-4 months (Gorlia et al., 2012).

1.1.11) Metastasis

As with other cancer cells, GBM cells can undergo Epithelial–mesenchymal transition (EMT) (Ortensi et al., 2013). This transformation is characterised by a change in protein expression towards a mesenchymal phenotype, involving the down-regulation of proteins such as E-cadherins and cytokeratins, and the upregulation of proteins such as matrix metalloproteinases (MMP) and those involved in the Akt-PI3K pathway (Lombard et al., 2015). This phenotypical change allows the cells to detach from the main tumour mass, enter the blood stream, evade the body's defence mechanisms, and establish themselves in distal locations. Evidence shows that GBM cells can spread via the cerebrospinal fluid (CSF), blood stream and lymphatic system (Lawton et al., 2012, Waite et al., 1999, Kalokhe et al., 2012). Metastasis of GBM tumours to areas outside of the CNS is uncommon, with only 0.4-0.5% of patients showing evidence of spread (Müller et al., 2014). This is a relatively low when compared to other cancers such as breast, lung and colorectal cancers, with some having up to 57% likelihood (Steeg et al., 2016, Howlader et al., 2013, Segelman et al., 2012). The low rate of metastasis in GBM patients is thought to be due to both the short survival of patients and the obstacle of the BBB (Lun et al., 2011).

1.1.12) Developing Treatments

1.1.12.1) The Landscape of GBM Developing Treatments

The ongoing development of GBM treatments spans a wide range of specialisations including cellular and molecular biology, immunology, and medical physics. Here, a summary of the significant advances in GBM treatment is provided. It should be noted that many of these clinical trials investigating such treatments encompass a range of high- and low-grade gliomas, including GBM.

1.1.12.2) Growth Factor Pathway Inhibition

Erlotinib is a small molecule inhibitor against EGFR that has had limited success in GBM patients when given alone (Raizer et al., 2010, Young et al., 2010). When combined with TMZ treatment however, an increase in overall survival has been observed (Prados et al., 2009). Studies investigating another EGFR inhibitor, gefitinib, have also failed to show a significant increase in patient survival, despite evidence of EGFR inactivation and detection of high drug concentrations within the tumour (Hegi et al., 2011).

Cetuximab is an anti-EGFR monoclonal antibody that demonstrated promising results in pre-clinical trials. However, the drug failed to cause an increase in patient survival when given following recurrence in high grade glioma (Neyns et al., 2009). Nimotuzumab is another anti-EGFR monoclonal antibody that has shown contradictory efficacy in GBM patients. One study showed an improved overall survival of high-grade glioma (both anaplastic astrocytoma and GBM) patients when Nimotuzumab was given in combination with radiotherapy (Solomón et al., 2013). Another study however did not show an improvement in either progression free survival or overall survival with Nimotuzumab combined with both radiotherapy and TMZ when compared with radiotherapy and TMZ alone (Westphal et al., 2015). However, an improved efficacy was seen in patients lacking methylation at the MGMT promoter. A further study showed a modest improvement in overall survival when patients were given Nimotuzumab alongside radiotherapy and TMZ (Wang et al., 2014). These studies suggest that Nimotuzumab may provide an improved patient survival compared with radiotherapy alone, but not as a replacement for TMZ. Other examples of EGFR targeted therapies currently under investigation in GBM include a variety of EGFR inhibitors, antibodies, immunotherapies and RNA based therapies (Oprita et al., 2021).

There has been an overall lack of efficacy in EGFR targeted therapy, most likely due to the abundance of other RTKs expressed in tumour cells such as PDGFR, MET and FRDR, as well as potential compensatory mechanisms in downstream signalling pathways (Stommel et al., 2007). For this reason, multi-RTK targeting inhibitors are being investigated. Despite this alternative strategy, the use of such inhibitors including Imatinib; an inhibitor of the RTKs PDGFRA, PDGFRB, c-Abl and c-Kit, and Sorafenib;

an inhibitor of PDGF and VEGF receptors, have failed to show a significant increase in patient survival in clinical trials (Raymond et al., 2008, Hainsworth et al., 2010).

Activation of RTKs results in the induction of downstream signalling pathways including PI3K/Akt/mTOR, p53, and Rb1. Similar to RTK inhibitors, inhibitors of these pathway components have shown limited clinical efficacy. For example, Buperlisib and Perifosine are PI3K and Akt inhibitors, respectively, that despite showing promising effects in preclinical model, failed to show a significant increase in patient survival (Kaley et al., 2019, Wen et al., 2019).

1.1.12.3) mutIDH inhibition

Ivosidenib is an optimised inhibitor specific against the mutated form of IDH1. It was the first to show a reduction in the oncogenic metabolite 2-HG in human trials (Popovici-Muller et al., 2018). There are a number of clinical trials including Ivosidenib and other mutIDH1 inhibitiors currently being carried out to characterise their effects in glioma, although not specifically GBM (Mellinghoff et al., 2019, Fan et al., 2020).

1.1.12.4) Calcium Channel Inhibition

The T-type and L-type calcium channels are involved in calcium influx in many types of cells, including GBM tumours, and play a role in cell cycle regulation. This calcium dependant signalling pathway is often dysregulated in tumours and result in resistance to chemotherapeutic treatments (Monteith et al., 2017). Such T-type calcium channels, Cav3.1, Cav3.2 and Cav3.3, can be inhibited alongside the use of TMZ to sensitise GBM cells by induction of cell cycle arrest, in a mechanism called “timed sequential therapy”. Here, the initial treatment induces the surviving population to enter S phase of the cell cycle, increasing their susceptibility to DNA damaging agents. This method has shown some promising results against recurrent GBM in clinical trials using the Cav3.3 channel specific inhibitor Mibefradil (Holdhoff et al., 2017, Lester-Coll et al., 2018), although there are currently no ongoing trials being conducted.

1.1.12.5) Laser Interstitial Thermal Therapy

Thermal therapy is the use of heat to destroy tumour tissue, most frequently by magnetic resonance guided laser therapy (Mahmoudi et al., 2018). Studies have shown Laser Interstitial Thermal Therapy (LITT) is safe and can provide a less invasive alternative to surgery for recurrent GBM tumours (Thomas et al., 2016). LITT also causes disruption of the blood brain barrier which provides an opportunity for improved transport of chemotherapeutic drugs (Leuthardt et al., 2016). Analysis has shown that use of LITT enhances progression free survival of GBM patients with difficult to reach tumours (Mohammadi et al., 2014, Kamath et al., 2019).

1.1.12.6) Tumour Treating Fields

Tumour Treating Fields (TTFIELDS) involve the application of low intensity, alternating electric fields to the tumour tissue to induce mitotic failure. Once the field is applied, dipole molecules involved in spindle alignment are disrupted and mitosis is prolonged resulting in cell death (Kirson et al., 2004). For this reason, TTFields are specific against highly proliferative cells, i.e., cancer cells.

Use of TTFields has shown to result in similar efficacy as chemotherapy, but with a more favourable safety profile and patient quality of life (Stupp et al., 2012). When used in combination with chemotherapy, TTFields have an increased efficacy, resulting in a statistically significant increase in overall survival in GBM patients (Stupp et al, 2017, Taphoorn et al., 2018). Clinical trials investigating the use of TTFields as a singular treatment are currently underway (Clinicaltrials.gov, 2020, NCT04492163). TTFields have currently been FDA approved under the branding of Optune (NovoTTF-100A). This technology has not yet been utilised in the UK due to low cost effectiveness (Brodbelt et al., 2018, National Institute for Health and Care Excellence, 2018).

1.1.12.7) Immunotherapies

1.1.12.7.1) Immune checkpoint inhibitors

T-cells are regulated by a number of inhibitory pathways, one of which is orchestrated by programmed cell death protein and its ligand (PD-1/PD-L1) (Topalian et al., 2015). Inhibitors of these pathways have provided an alternative mechanism for killing tumour cells, by reactivating the body's immune response. Antibodies against PD-1, such as nivolumab and pembrolizumab, have yet to show efficacy against GBM when given following surgery (Reiss et al., 2017, Kurz et al., 2018). However, an increase in patient survival has been seen when pembrolizumab was given both prior to and post-surgery (Cloughesy et al., 2019).

It has been suggested that failure of immune checkpoint therapies in GBM is due to a number of reasons, including a lack of PD-1 expression within the CNS, the presence of the blood brain barrier, and the differentiation of tumour infiltrating T-cells (Dutoit et al., 2016, Hodges et al., 2017, Park et al., 2019). GBM patients with a high level of mutational burden (over 100 exonic mutations), specifically patients with a germline biallelic MMR deficiency, were suspected to respond to immune checkpoint inhibition (Bouffet et al., 2016, Johanns et al., 2016). However, a more recent study showed there was no increased overall survival in patients with an in acquired MMR deficiency treated with PD-1 blockade (Touat et al., 2020).

1.1.12.7.2) Vaccines

Anti-tumour vaccines work by stimulating the body's immune response to induce recruitment of antigen specific effector T-cells to the tumour site (Weller et al., 2017b). These vaccines can be either cell based (e.g., T-cells or dendritic cells) or non-cell based (e.g. peptides).

Trials investigating the EGFRvIII specific peptide vaccine (Rindopepimut) showed initially promising results in phase I/II trials (Schuster et al., 2015). However, in a later trial, no increase in survival was seen with the drug (Weller et al., 2017a). In this study, ~60% of recurrent tumours lost expression of EGFRvIII when measured in recurrence samples, suggesting that these samples had experienced the clonal expansion of non EGFRvIII expressing tumour cells. To combat this potential for drug resistance, multi-target vaccines were also trialled. The IMA950 vaccine comprising of 11 peptides failed to show an increase in patient survival, despite an improved T-cell response in lower grade gliomas (Rampling et al., 2016, Dutoit et al., 2017).

An alternative to peptide vaccines is the use of the patients own dendritic cells (DCs). The cells are extracted and cultured to present tumour specific antigens, before being reintroduced (Weller et al., 2017). There have been a number of promising DC vaccines in newly diagnosed and recurrent GBM. The autologous tumour-lysate trained DC vaccine DCVax-L, for example, when combined with standard therapy, showed an increased overall survival (23.1 from 15-17 months) (Liau et al., 2018).

1.1.12.7.3) Chimeric antigen receptor T Cells

Chimeric antigen receptor (CAR) T cells recognise specific tumour cell antigens via receptors genetically engineered onto the cell surface. These patient cells are expanded *ex vivo* and reintroduced, where they further multiply. Limited success has been seen with CAR-T cells in GBM patients, due to the possible compensatory immunosuppressive mechanisms, tumour heterogeneity and loss of the target antigen (Brown et al., 2016, O'Rourke et al., 2017). Current studies focus on the identification of an antigen with a stable expression throughout tumour growth to prevent antigen loss, and additional binding proteins on the CAR-T cell surface to increase specific CAR-T cell-GBM binding and limit off target effects (Bielamowicz et al., 2018, Wang et al., 2020a).

1.1.12.7.4) Oncolytic Viruses

Viral therapy was initially developed as a method of delivering genetic material to provide tumour cells with chemotherapy susceptibility. They work by either hijacking the tumour cells replicative machinery or can be genetically altered to infect tumour cells specifically, inducing an innate immune system response. This innate immune response can trigger the development of anti-tumour immunity through the adaptive response (Peruzzi et al., 2018).

The oncolytic virus, DNX-2401, has shown promising results when tested in patients with recurrent high-grade gliomas (including GBM), with 20% of patients surviving >3 years following treatment (Lang et al., 2018). Another oncolytic virus, PVSRIPO, when given to recurrent GBM patients, resulted in 21% of patients surviving up to 36 months (Desjardins et al., 2018).

The delivery of oncolytic viruses can be used to pre-condition the tumour microenvironment for the administration of immune checkpoint inhibitors (Chen et al., 2018). The viruses induce an upregulation of PD-L1 protein expression and an increased infiltration of cytotoxic T cells, factors known to predict patient response to PD-1 inhibitors (Borghaei et la., 2015, Tumeh et al., 2014). The Reolysin virus was used to pre-condition tumours in this way in 6 recurrent GBM patients (Samson et al., 2018). The virus was able to cross the blood brain barrier when administered by infusion and this treatment resulted in the increased tumour leukocyte infiltration and a higher expression of the PD-L1 antigen. Phase 1 clinical trials have previously shown that the reovirus is well tolerated in human subjects (Auffinger et al., 2013).

1.1.12.8) Summary

Glioblastoma has been the focus of a plethora of clinical trials involving both conventional chemotherapy and targeted drugs thanks to advancements in preclinical research investigating the pathogenesis of the disease and its possible vulnerabilities. Numerous features of the tumour cell and its environment have been scrutinised with various success including growth factor signalling, metabolism and the immune system. Despite this intense effort, minimal changes in GBM patient life expectancy have been observed since the introduction of TMZ therapy over 10 years ago. For this reason, further aspects of GBM tumours should be investigated in order to identify new targets and develop life changing treatments.

1.1.13) Modelling Glioblastoma

In order to investigate the biology and pathogenesis of GBM, the disease is replicated in a number of different model systems. A widely used, ethical, and economical model of GBM is the use of cell lines. These are GBM cells originally taken from a patient, that have been immortalised and expanded to act as a biological standard. Use of these cell lines allows for greater reproducibility across institutions, although changes in culture conditions may result in an evolutionary shift in the cells genetic profile (Ben-David et al., 2019). There are a number of GBM cell lines available, each with varying culture requirements and genetic profiles. For example, the two common GBM cell lines U-87MG and T-98G, have a different mutation status of the tumour suppressor gene PTEN (Dong et al., 2018). The cells are easily grown in serum-supplemented medium, however, these conditions promote astrocytic differentiation of the tumour cells, shifting their profile away from the parental tumour (Lee et al.,

2006). This conserved biological model means that these cells lack patient specificity. However, it is possible to produce such cell lines for each individual patient (Kodack et al., 2017). This can be clinically relevant by their use to determine drug response ahead of treatment. Production of viable and culturable cell lines from solid tumours is not readily feasible, although progress is being made (Stringer et al., 2019). These patient derived cells also recapitulate the features of the primary tumour more accurately than classic cell lines, when grown in serum-free medium (Lee et al., 2006). This is because culture of cells in serum containing medium induces cellular differentiation and therefore loss of self-renewal properties.

Whole animal models provide the most accurate and disease-relevant models of GBM, as they incorporate the tumour-host interactions, including the immune system and endocrine signalling. Mice are often used due to their short breeding times and ease of genetic manipulation. Mouse models can be developed through a number of methodologies. One such method is through genetic engineering, to create *de novo* mutations. Here, genetic mutations that are common in human GBM tumours are introduced into the animal via numerous techniques such as the Cre system (Zhu et al., 2009). In this system, Cre recombinase can reverse, delete or transpose genes between specific sequences. An example of this method is the Ascl1-creER^{TM} model of GBM. Here, expression of Cre is driven by the Asl1 promoter, a CNS restricted gene, allowing for the tissue specific change in gene expression of GBM associated genes including *NP1*, *TP53* and *PTEN*. Changes in the expression of these genes results in a range of astrocytomas all high and low grades (Reilly et al., 2000), with a loss of all three genes resulting in GBM (Alcantara Llaguno et al., 2016). Another similar model uses RCAS/tv-a technology, which relies on the transfer of genes via viral vectors into mice expressing the RCAS receptor (Shih et al., 2004). Expression of this receptor is driven by the *nestin* promoter and following infection of the mice by a PDFG expressing virus, mice spontaneously develop tumours, with 30% developing GBM tumours (Shih et al., 2004). This model was shown to produce less proliferative tumours following treatment with TMZ (Momota et al., 2005).

Another method is through the transplantation of tumour-initiating cells directly into immunocompromised mice (allografts or xenograft), allowing for the representation of tumour heterogeneity (Patrizii et al., 2018). However, this model lacks the immune response aspect of the tumour microenvironment.

Patient samples can be taken and used as an *ex vivo* model of the human brain (Humpel, 2015), as well as to model GBM (Marques-Torrejon et al., 2018). This clinically relevant model is more representative of tumour biology compared with the culture of cells alone, as tumour infiltrating cells

will also be included within the tumour mass. Similar to patient derived cell lines, the use of patient samples allows for the testing of clinical drugs in a patient specific manor.

The way in which cells or patient samples are cultured will affect the closeness of the GBM model to the *in vivo* scenario. Cell lines can be cultured in agar, or an extracellular matrix-like material in order to induce the formation of spheroids. This allows for the modelling of tumour features such as necrotic and hypoxic gradients, that are excluded in monolayer culture (Hubert et al., 2016). Serum may also be excluded from the growing medium to induce the preferential proliferation of the cancer stem cell population (Lee et al., 2006).

A way in which researchers have increased the accuracy of GBM models is to introduce the flow of medium to represent the circularity systems role of removing waste and replenishing nutrients. These microfluidic models aim to recapitulate the tumour environment by incubating either cells or tissue in a specifically designed microfluidic device, to produce a "GBM on a chip". This method of culture has been widely used for the culture of GBM cell lines (Chanon et al., 2017, Jie et al., 2017, Logun et al., 2018). Although other studies have investigated the use of patient tumour slices in GBM research, the majority of these have used a static culture method utilising different ECM-like matrices (Ono et al., 2007, Merz et al., 2013, Bayin et al., 2016). A previous study was able to demonstrate the viability of the microfluidics methodology for the maintenance of GBM patient tissue (Olubajo et al., 2020). In this tumour tissue model, the patient tissue was enclosed inside of a screw on chamber, medium was perfused over the tissue, and effluent was collected (Figure 1.8).

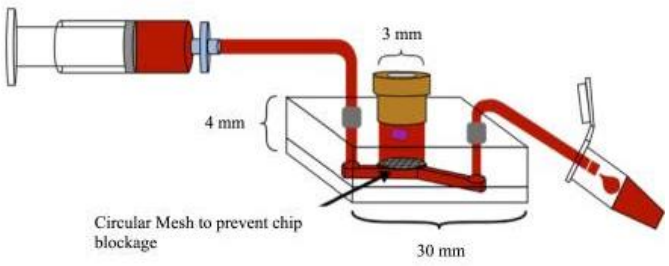

Figure 1.8 : Schematic of the microfluidic set up used by Olubajo et al. *Patient tumour tissue was enclosed within the tissue chamber and media perfused through the tubing, passing perpendicular to the tissue. A mesh layer was used to prevent possible tissue fragments blocking the microchannels. The bottom layers containing the microchannels is made from glass, whereas the tumour chamber is made from PDMS. (Taken from Olubajo et al., 2020).*

The microfluidic chip used in this previous study was made from glass and PDMA. Although PDMA is inexpensive and readily made, production of glass chips is costly. This coupled with the fact that glue was used to attach the tubing and chip components together, the chip quality varied between biological replicates and experiments. Although the mesh layer may limit the direct perfusion of media

over the tumour piece, this feature prevents blockage of these chip microchannels by the tumour tissue, a frequent issue in tissue microfluidic research. Another advantage of this chip design was the screw on adaptor for the tissue chamber. This design meant that the tumour tissue was readily accessible and could be inserted and removed without disruption to the tubing. The microfluidic chip used in this thesis is the fifth generation developed from the one used by Olubajo et al.

1.2) Arginine Methylation

1.2.1) Introduction

The structure and activity of proteins is determined by several factors, beginning with the sequence of oligonucleotides in DNA. The transcribed DNA can be altered through a number of mechanisms, including variations in splicing and by interactions with non-coding RNA. The translated protein is then open to a range of protein-protein interactions that can alter its characteristics, for instance, through blocking functional motifs or through addition of post-translational modifications (PTMs). PTMs are key aspects of both epigenetics and signal transduction due to their ability to change protein interactions and activity. Many types of modifications exist, including phosphorylation, SUMOylation, ubiquitination, acetylation, and methylation, and have varied specificities and effects. The most studied PTM for example, phosphorylation, often results in the activation of proteins involved in signalling cascades, causing signal amplification and transduction (Pawson, 2004). Ubiquitination, on the other hand, is predominantly known to target proteins for degradation through the proteasome (Komander & Rape, 2012). The addition of ubiquitin has also been found to play a role in non-degradative mechanisms including regulation of the NF-kB signalling pathway (Liu & Chen 2011). Protein methylation is a PTM involved in a vast number of processes, with a predicted 1% of the functional genome encoding for the enzymes catalysing protein methylation (Katz et al., 2003).

Methylation of proteins involves the transfer of a methyl group (CH_3) onto either an arginine or lysine residue. Recent studies have also demonstrated the methylation of histidine residues, including on the protein β-Actin (Zheng et al., 2020). Both types of post-translational methylation contribute to the balanced control of gene expression through modification of histone proteins. Lysine and arginine methylation also regulate a range of non-histone proteins including proteins involved in transcription and RNA binding, translation, chaperone, cytoskeletal and membrane proteins and adaptor/scaffold proteins (Guo et al. 2014; Lim et al. 2020). However, there are several and important differences between the methylation of lysine and arginine residues. Firstly, lysine methylation is highly dynamic and there are eight families of lysine demethyltransferases (Jones et al. 2019) whereas methylation of arginine is generally considered a stable mark (Bedford and Clarke, 2009). Secondly, lysine residues

can be mono-, di- and tri-methylated while arginine residues can only be mono- and di-methylated this is important because the different methyl lysine and methylarginine isomers can have very different impacts at the molecular level. Lastly, methylation of lysine is less common than methylation of arginine on the proteomic scale (Guo et al. 2014, Hornbeck et al. 2014).

Arginine methylation (ArgMe) was first identified in 1967 (Paik & Kim, 1967), but its significance has only been highlighted in recent years (Blanc et al., 2017). The availability of research tools including antibodies and specific inhibitors has allowed advances in knowledge of ArgMe and its role in health and disease. The side chain of arginine comprises of an aliphatic chain of 3 carbon atoms, ending with a guanidino group (Figure 1.9) (EMBL-EBI 2019). This structure allows arginine to form π-stacking interactions with aromatic amino acids/nucleic acids (Gallivan & Dougherty 1999). Arginine has the highest pKa value (13.8) of all amino acids and as such is positively charged at physiological pH (Fitch et al., 2015).

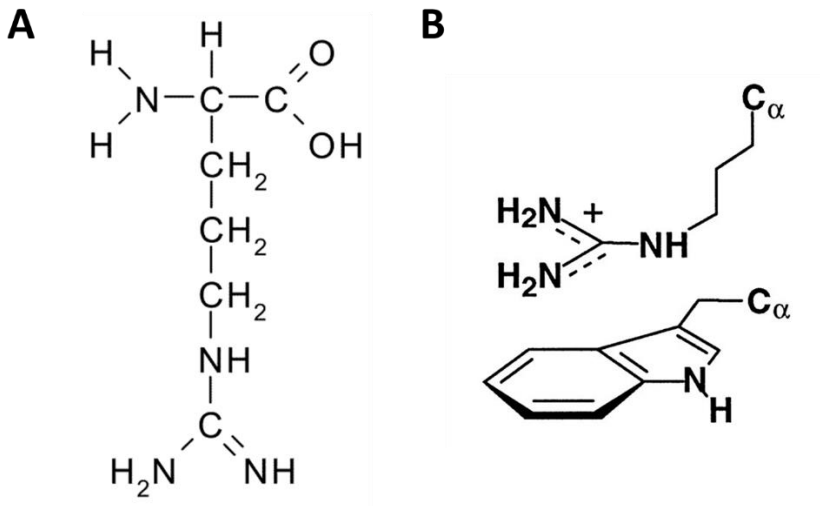

Figure 1.9: The structure of arginine and interactions of methylarginine. *(A) Chemical structure of Arginine (B) Parallel π-stacking interaction between arginine and tryptophan (an example of an aromatic amino acid) (Gallivan & Dougherty 1999).*

The addition of a methyl group removes a potential hydrogen bond donor from the recipient arginine, producing a bulkier and more hydrophobic residue than the unmethylated form (Bedford and Richard 2005). Although the overall cationic charge is maintained, it is dispersed towards the additional methyl groups, increasing the arginine's affinity for three-dimensional aromatic cages consisting of clusters aromatic amino acids (Figure 1.10) (Tripsianes et al., 2011, Beaver et al., 2016). This change in characteristics can either improve or hinder interactions with other proteins or nucleic acids.

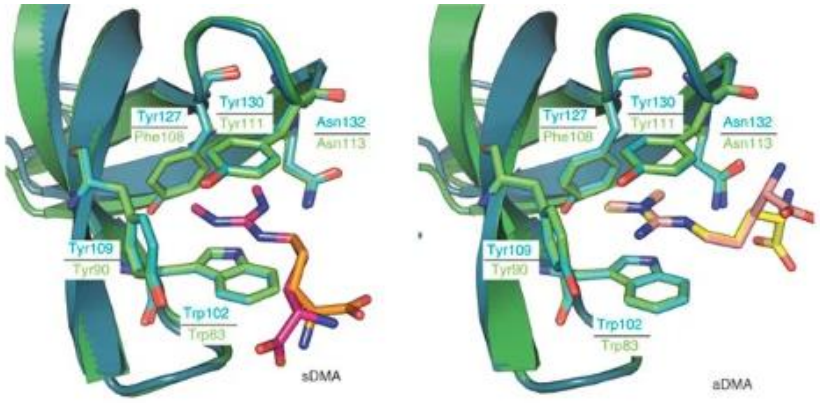

Figure 1.10: Examples of interactions between methylarginine and Tudor domain containing proteins. *An overlayed model of the interaction between survival motor neuron protein (SMN) (blue) and splicing factor 30 protein (SPF30) (green) and SDMA (left) and ADMA (right). SMN and SPF30 are both proteins that recognise methylated arginine and are both involved in mRNA processing. The guanidino group of the dimethylated arginine sits between a tryptophan (Trp102/Trp83) and a tyrosine residue (Tyr130/Tyr111) within the Tudor domain, and perpendicular to a further aromatic residue, Tyr127/Phe108 (Tripsianes et al., 2011).*

There are a number of proteins responsible for ArgMe recognition (Table 1.2) (Guccione and Richard, 2019) and the most studied contain Tudor domains, with approximately 30 known Tudor-domain containing proteins encoded in the human genome (Côté et al., 2005, Chen et al., 2011). Tudor domains contain numerous aromatic amino acids including tryptophan and phenylalanine, that form interactions, such as those illustrated in Figure 1.10, with the guanidino group of methylarginine, but not with the guanidino group of unmethylated arginine (Tripsianes et al., 2011). Proteins that contain such domains include Survival of motor neuron (SMN) and Splicing factor 30 (SPF30); which both recognise methylated SmB, and Tudor domain-containing proteins (TDRD1/2/3/6/9/11). The proteins responsible for ArgMe recognition act as the effectors, or readers of ArgMe, and translate specific methylation marks into defined molecular events such as gene transcription, mRNA splicing and a number of biochemical pathways (Yang and Bedford, 2013).

Table 1.2: Tudor domain containing proteins and recognised ArgMe containing protein.

Protein Name	Protein Recognised	Reference
SMN	SmD1, SmD3 and SmB/B'	Friesen et al., 2001 Côté & Richard, 2005
Splicing factor 30 (SMNDC1)	Sm B/B', D1, D2, and D3	Rappsilber et al., 2001 Côté & Richard, 2005
TDRD1	Mili, Miwi	Chen et al., 2009 Wang et al., 2009 Reuter et al., 2009 Vagin et al., 2009
TDRD2 (TDRKH)	Miwi	Zhang et al., 2017 Chen et al., 2009
TDRD3	H4R3me2a, H3R17me2a, RNAP II, TOP3B	Sims et al., 2011 Yang et al., 2010 Côté & Richard, 2005 Kim et al., 2006
TDRD6	Miwi	Chen et al., 2009 Kirino et al., 2010
TDRD7	Miwi	Chen et al., 2009
TDRD8 (STK31)	Miwi	Chen et al., 2009
TDRD9	Mili	Vagin et al., 2009
TDRD11 (SND1)	E2F-1 SmB and SmD1/D3 Miwi	Liu et al., 2010 Gao et al., 2012 Zheng et al., 2013

1.2.2) Protein Arginine Methyltransferases

Protein arginine methyltransferases (PRMTs) are the enzymes responsible for the methylation of arginine residues (Yang & Bedford, 2013). PRMTs catalyse the transfer of a methyl group from S-adenosyl-L-methionine (SAM/ AdoMet) onto the side chain nitrogen of arginine, producing the by-product S-adenosyl-L-homocysteine (SAH/ AdoHcy). There are three known types of PRMT with varying target specificities and activities. All PRMT's are able to transfer a single methyl group onto the guanidino nitrogen on the target arginine, producing the monomethyl-arginine (MMA) mark. Type I PRMTs (PRMT1, PRMT2, PRMT3, PRMT4, PRMT6 and PRMT8) then transfer a second methyl group on the same nitrogen to produce the asymmetrical dimethyl-arginine (ADMA) mark. Type II PRMTs (PRMT5 & PRMT9) transfer a second methyl group to the opposite nitrogen on the arginine functional group, making symmetrical dimethyl-arginine (SDMA). The type III PRMT, PRMT7, is only able to carry out the first methylation step. (Figure 1.11). As such, all three types of PRMTs are able to transfer a

single methyl group, although only types I and II are able to transfer a second one. Other PRMTs may exist however, and there are numerous putative PRMTs being investigated including NDUFAF7, which was found to play a role in embryonic development (Zurita Rendón et al., 2014). Type I PRMTs include PRMT1, -2, -3, -4, -6 and -8. PRMT5 and -9 are type II PRMTs. PRMT7 was initially described as a Type II PRMT and subsequently characterised as type III (Zurita-Lopez et al., 2012).

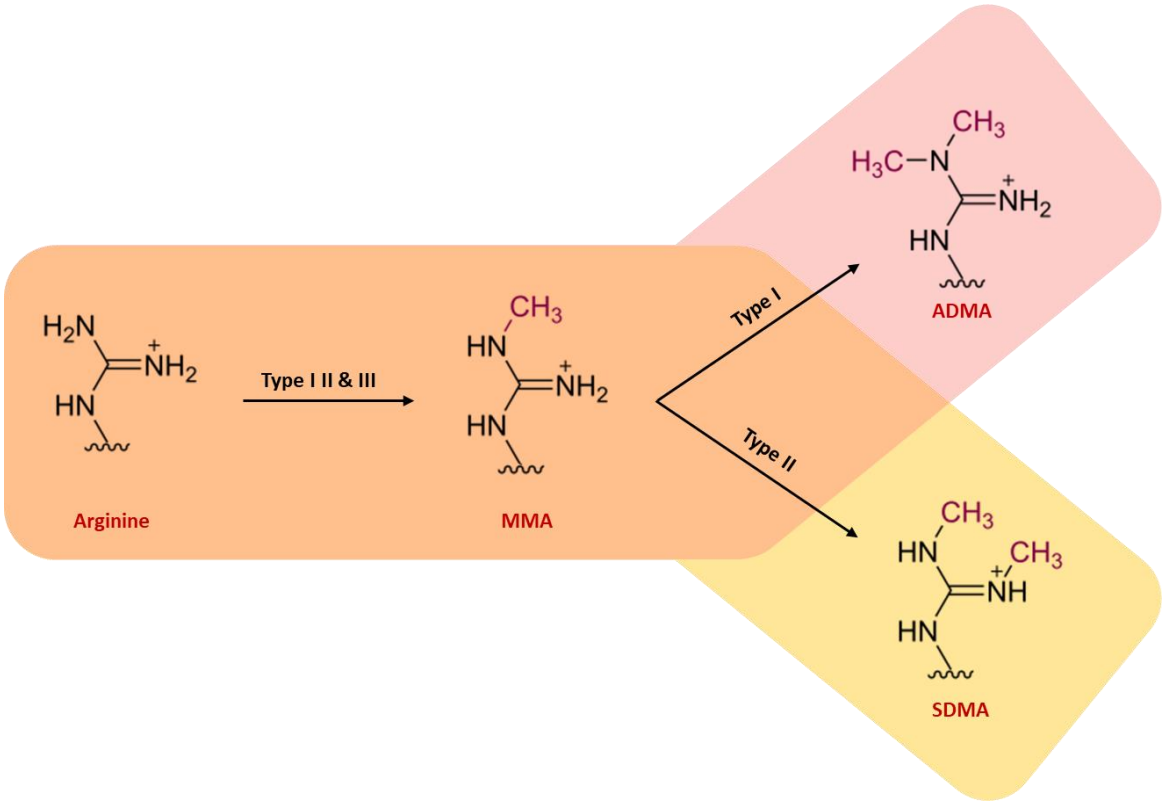

Figure 1.11: Schematic to show the different enzymatic activities of type I, II and II PRMTs. *Type I, II and III PRMT enzymes catalyse the transfer of a methyl group from SAM to the side chain nitrogen on arginine residues on the target protein to produce MMA. Type I enzymes are then able to catalyse the transfer of a further methyl group, asymmetrically onto the same nitrogen atom. Type II enzymes are able to catalyse the transfer of a second methyl group symmetrically, onto the opposite nitrogen on the side chain of arginine.*

1.2.3) PRMT Structure and Function

1.2.3.1) Overall Structure

PRMTs are highly conserved and can be found in a wide range of eukaryotes. All mammalian PRMTs contain a conserved catalytic domain within the core of the protein. The main structures within this region are a Rossman fold and a β-barrel, responsible for cofactor and substrate binding, respectively (Figure 1.11) (Schapira and Ferreira, 2014). Within the β-barrel structure is a dimerization arm, which interacts with the Rossman fold of another subunit to produce the catalytically active dimer. Additional sequences that are specific to PRMTs include a double E-loop and threonine-histidine-tryptophan (THW) loops (Cheng et al., 2005).

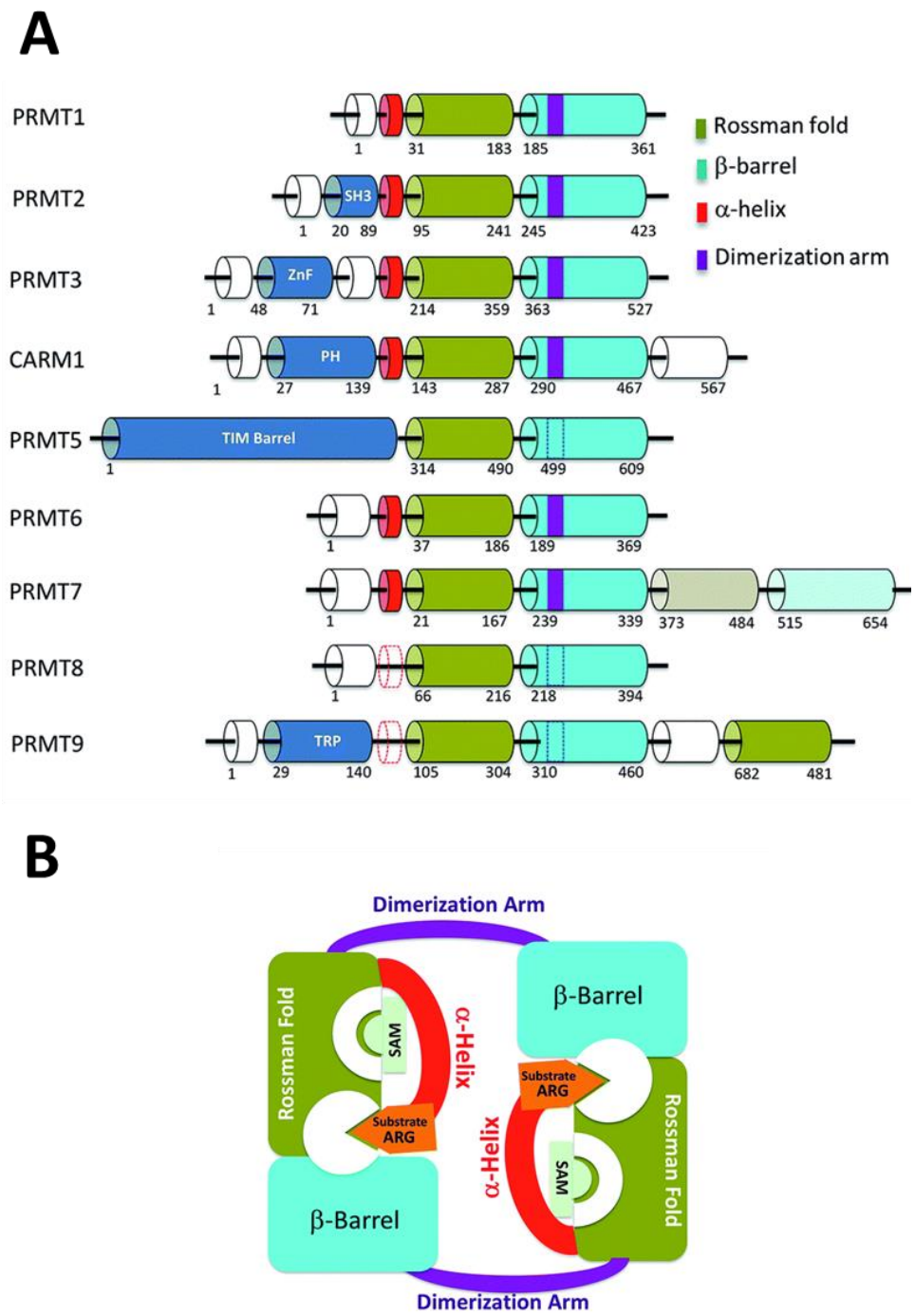

Figure 1.12: Schematic to show domain organisation on the various PRMT genes and the tertiary structure of a type I PRMT enzyme. *(A) Domain organisation of PRMTs1-9. PRMT7 contains two core domains, with the second Rossmann fold (grey) and ß-barrel (light blue) being unconserved and inactive. White areas represent unconserved non-functional domains. Dashed lined domains indicate unknown structures yet to be characterised. (B) The dimer structure of PRMTs represented by CARM1 (PRMT4) (Shapira & Ferreira de Freitas 2014).*

The most significant level of variability amongst PRMTs can be found in the N-terminal domain (Morales et al., 2016). Here, differences in sequence, length, and the presence of particular domains contribute to the substrate specificity of the enzymes, cellular localisation and regulation. Such

domains include the SH3 domain (PRMT2), TIM barrel (PRMT5), zinc finger (PRMT3), and pleckstrin homology domain (CARM1) (Antonysamy et al., 2012, Troffer-Charlier et al, 2007).

The combination of neighbouring residues on the target protein influences the specificity of PRMTs. For example, the presence of glycine immediately downstream or upstream of the target arginine is thought to enhance accessibility of the enzyme to target arginine residues (Miranda et al., 2004). Most PRMTs target Arginine Glycine rich (GAR) or RG motifs, however, CARM1 mainly acts upon Proline-Glycine-Methionine (PGR). PRMT6 will also methylate arginine residues surrounded by charged residues such as in the HIV associated Tat protein (Boulanger et al., 2005). PRMT7 favours multiple arginine residues surrounded by lysine rich areas (Feng et al., 2013). Although each PRMT type has varying target sequence preferences and specificities, it has been shown that they are able to methylate the same residue, such as on splicing factor SmB.

1.2.3.2) Type I Structure and Function

1.2.3.2.1) PRMT1

PRMT1 is the predominant PRMT responsible for asymmetric methylation and was first discovered as a binding partner to TIS21 and BTG1 (Lin et al., 1996, Tang et al., 2000). Partial loss of the protein in mice embryonic fibroblasts results in a loss of proliferation and a drastic increase in genomic instability and complete loss of PRMT1 is embryonically lethal, suggesting a multifunctional capacity within the cell (Pawlak et al., 2000). Seven isoforms of PRMT1 are produced as a result of alternate splicing, each with differing N-terminal sequences and substrate specificity (Goulet et al., 2007). Its catalytic activity has been shown to be dependent upon two residues (M48 and M115), as mutations in these residues result in imbalances in MMA and ADMA production, and also allows the production of SDMA (Gui et al., 2014). PRMT1 is predominantly localised to the nucleus but has substrates found in the cytoplasm and other cellular compartments (Herrmann et al., 2005; Onwuli et al., 2019), and has in fact been shown to play a role in protein shuttling between these areas (Herrmann et al., 2004).

PRMT1 functions as a transcriptional co-activator through the deposition of an ADMA mark onto histone H4R3, resulting in the recruitment of histone acetyltransferases (Huang et al., 2005). The TDRD3-TOP3B protein complex is also recruited to sites of H4R3 methylation and act to dampen R-loop formation (Yang et al., 2014). PRMT1 is also able to alter transcription by modification of non-histone proteins, including through the methylation of the H3K4 methyltransferase complex subunit Ash2L, although the consequences of this are unclear (Butler et al., 2011), and by the methylation of the transcription factor RelA, resulting in a lowered DNA binding ability (Reintjes et al., 2016).

PRMT1 takes part in a range of cellular processes including DNA damage repair, cell signalling, and ion flux. PRMT1 methylates the repair protein meiotic recombination 11 homolog (MRE11), enabling its

exonuclease activity on double stranded DNA which is required during the S-phase DNA damage response (Boisvert et al., 2005b). Another DNA repair protein, p53 binding protein 1 (53BP1) is also methylated by PRMT1, enabling its recruitment to DNA (Boisvert et al., 2005a). PRMT1 also alters the cofactor activity of a further DNA damage repair associated protein, breast cancer gene 1 (BRCA1) (Guendel et al., 2010), a modification recently found to contribute towards the defence of breast cancer cells against ionizing radiation (Montenegro et al., 2020).

PRMT1 has been shown to take part in cell signalling though the Akt pathway. The growth factor signalling receptor EGFR, as previously discussed, is a receptor responsible for activation of the Akt pathway and has been found to be methylated by PRMT1 (Wang et al., 2019). This methylation at R198 and R200 augments ligand binding and enhances receptor activation. PRMT1 also methylates Estrogen receptor (ERα) at R260, enabling the formation of the ERα/Scr/PI3K complex (Le Romancer et al., 2008). Transforming growth factor beta (TGFβ) signalling is also influenced by PRMT1 activity. PRMT1 methylates the inhibitory protein SMAD6 at R74, allowing the recruitment of the Bone Morphogenetic Protein (BMP) effectors SMAD1 and SMAD5 (Xu et al., 2013) and also methylates both the inhibitory proteins SMAD6 and SMAD7 (at R57 and R67), leading to the activation of the SMAD3 effector (Katsuno et al., 2018). These activities have a crucial role in epithelial-mesenchymal transition and epithelial stem-cell generation.

1.2.3.2.2) PRMT2

PRMT2 was first discovered in 1997 as the human homolog of the rat protein (Katsanis et al., 1997). Complete loss of the enzyme produces viable mice with minimal difference in tissue structures (Yoshimoto et al., 2006). In addition to the original PRMT2 protein, 4 alternatively spliced isoforms have been identified in breast cancer cells (Zhong et al., 2012). It is mainly localised to the nucleus but is also found at lowered levels in the cytoplasm (Kzhyshkowska et al., 2001). PRMT2 contains a unique Src homology 3 (SH3) domain that enables binding to proline rich motifs on other proteins (Pawson & Gish 1992, Cura et al., 2017). Despite having high sequence homology with the other enzymes, PRMT2 was initially not thought to process methyltransferase activity (Scott et al., 1998). Later studies revealed a weak methyltransferase activity of PRMT2 on the Histone 4 tail (Lakowski & Frankel, 2009).

Similar to PRMT1, PRMT2 methylates histone proteins in order to influence transcription. Following its recruitment by β-catenin, PRMT2 methylates H3R8 and activates the transcription of β-catenin target genes (Blythe et al., 2010, Su et al., 2014). Also, similarly to PRMT1, PRMT2 alters transcription by interactions with non-histone proteins. PRMT2 was shown to interact with RB1 and repress the activity of the transcription factor E2F. Although this repression was not found to be dependent on

PRMT2 methyltransferase activity, it was suggested that PRMT2 may recruit further co-activators (Yoshimoto et al., 2006).

PRMT2 is thought to play a role in mRNA processing by interactions with splicing related proteins including SRC associated in mitosis of 68 kDa (SAM68), to induce the pro-apoptotic protein BCL-X in response to inflammatory stressed triggered by tumour necrosis factor alpha (TNF-α) (Vhuiyan et al., 2017). This inflammatory response activates the NF-κB Nuclear factor kappa B (NF-κB) pathway, which has also been shown to be regulated by PRMT2 through an interaction with IκB-α (Ganesh et al., 2006). PRMT2 also interacts with nuclear hormone receptors including oestrogen receptor alpha and androgen receptors to increase their transcriptional activity (Qi et al., 2002, Meyer et al., 2007).

1.2.3.2.3) PRMT3

PRMT3 was discovered due to its association with PRMT1 (Tang et al., 1998). Full knockout of the gene in mice results in smaller, but viable embryos that achieve full size at adulthood (Swiercz et al., 2007). It contains a unique zinc finger structure within the N-terminal domain, as well as the Rossmann fold, β-barrel and dimerization arm (Zhang et al., 2000). Zinc fingers are common protein motifs responsible for protein-protein and protein-nucleic acid interactions (Laity et al., 2001). PRMT3 is exclusively expressed in the cytoplasm, although the enzyme has been shown to migrate to the nucleus upon treatment with palmitic acid or the liver X receptor α (LXRα) agonist T0901317 (Kim et al., 2015a).

PRMT3 methylates the ribosomal protein S2, a process required for the formation of the 40S ribosomal subunit; in cells depleted of PRMT3, an imbalance between the 40S and 60S ribosomal subunits is produced (Swiercz et al., 2007). PRMT3 has been shown to methylate nuclear poly(A)-binding protein (PABPN1); a protein implicated in oculopharyngeal muscular dystrophy, and the voltage-gated sodium channel isoform $Na_V1.5$ (Beltran-Alvarez et al., 2013); which is often dysregulated in cancer (Djamgoz et al., 2019, Luo et al., 2020). The tumour suppressor proteins VHL30 and ARF, recruit PRMT3 to p53, resulting in its methylation (Lai et al., 2011). The functional consequences of this methylation are not yet clear.

1.2.3.2.4) PRMT4

PRMT4, also known as CARM1, was discovered as an enhancer of transcriptional activation by nuclear hormone receptors (Chen et al., 1999). The absence of PRMT4 in mice results in a block to thymocyte differentiation at embryonic day 18.5 due to a defect in the foetal hematopoietic compartment, and mice do not survive past birth (Yadav et al., 2003, Li et al., 2013). PRMT4 consists of a total of 608 amino acids and in addition to the catalytic core domain, it harbours a PH domain, a conserved structure that enables the formation of large multi-protein complexes and protein-protein interactions (Troffer-Charlier et al., 2007).

PRMT4 is able to regulate transcription through methylation of histone tails, predominantly histone H3 at R17, R26 and R42, contributing to transcriptional activation (Schurter et al., 2001). PRMT4 also methylates non-histone proteins in a both activating and repressive manor. For example, methylation of CREB-binding protein (CBP) at R742 by PRMT4 increases its histone acetyltransferase activity (Ceschin et al., 2011), whereas methylation at R580 hinders CREB recruitment (Xu et al., 2001).

PRMT4 has been shown to play a role in the formation and regulation of paraspeckles (Hupalowska et al., 2018), membraneless organelles within the nucleus made up of specific proteins and long non-coding RNA (lncRNA) (Fox et al., 2018). PRMT4 acts by repressing NEAT1 expression, an important component in paraspeckle function paraspeckles (Hupalowska et al., 2018). PRMT4 is also able to methylate another paraspeckle component, p54nrb, resulting in its redistribution. PRMT4 is able to regulate splicing mechanisms by direct methylation of RNA binding proteins (Larsen et al., 2016), for example, CA150, which is involved in repressing transcription-elongation (Cheng et al., 2007).

1.2.3.2.5) PRMT6

PRMT6 was first identified following the sequencing of the human genome (Lander et al., 2001). It was found to be a nuclear enzyme with differing substrate specificity to PRMT4, and with limited substrate overlap with PRMT1 (Frankel et al., 2002). Although knockout mouse embryo fibroblasts are viable, they show hallmarks of cellular senescence and have growth defects (Neault et al., 2012).

The enzymes nuclear localisation corresponds with its role in DNA repair and gene expression. PRMT6's predominant role is as a transcriptional co-repressor by methylating H3R2 and H2AR29 (Iberg et al., 2008, Waldmann et al., 2011). Asymmetrical methylation of the H3R2 residue blocks interactions between the neighbouring H3K4me3 activation mark and Mixed Lineage Leukaemia (MLL), halting transcriptional activation. PRMT6 is also able to activate transcription through the methylation of H3R42 (Casadio et al., 2013).

PRMT6 can function as an oncogene through the inhibition of important regulatory cell cycle proteins including p53, p21 and p16 (Neault et al., 2012, Nakakido et al., 2015, Wang et al., 2012d). It has also been found to act in a tumour suppressive manor, through the methylation of PTEN at R159, allowing for PTEN activation and therefore down regulation of the PI3K/Akt signalling pathway (Feng et al., 2019). PRMT6 also harbours antiretroviral activity through the methylation of HIV proteins Tat, Rev and Nucleocapsid, restricting HIV-1 replication (Boulanger et al., 2005). Recently, a level of redundancy between PRMT6 and PRMT4 has been described as they were both shown to deposit the H3R17me2a mark and when inhibited together, cause a synergistic effect (Cheng et al., 2020).

1.2.3.2.6) PRMT8

The PRMT8 gene was first identified in a screen of neural precursor cells from Sox1-gfp knock-in mice, and its structure later described (Aubert et al., 2003, Lee et al., 2005a). Although PRMT8 knock out embryos are viable, the mice present with motor behaviour defects including hindlimb clasping and hyperactivity (Kim et al., 2015b). PRMT8 is a type I enzyme with a similar structure to PRMT1, sharing greater than 80% sequence homology and differing only by its N-terminal domain. Unlike PRMT1 however, PRMT8 is exclusively expressed in CNS tissue (Lee et al., 2005a). PRMT8 also differs in the fact that it is membrane bound due to its myristoylation motif found on its N-terminal domain.

PRMT8 is able to interact with multiples members of the Ten-eleven translocation (TET) family including FUS, EWS and TAFII68, which are all transcriptional cofactors involved in splicing (Pahlich et al., 2008). Due to its exclusive expression within the CNS, PRMT8 plays a more focused role within neural biology. For example, loss of PRMT8 results in a change in gene expression of certain glial differentiation related genes including *CXCR4*, *DHFR* and *EFEMP1* (Simandi et a., 2015), and also causes the aberrant formation of perineuronal nets (Lee et al., 2017), extracellular matrix structures surrounding neurons that provide stabilisation and protection (Fawcett et al., 2019). PRMT8 was found to localise to presynaptic and postsynaptic sites, where it methylates voltage-gated sodium channels (Baek et al., 2014) and its deletion causes a change in synaptic proteins and alters context-dependant fear learning (Penney et al., 2017). In addition to its methyltransferase activity, PRMT8 has been found to harbour phospholipase activity that may play a role in in the maintenance of dendritic arborisation in Purkinje cells (Kim et al., 2015b).

1.2.3.3) Type II Structure and Function

1.2.3.3.1) PRMT5

PRMT5 is the major methyltransferase responsible for SDMA within the cell. It can be found expressed in both the nucleus (Lacroix et al., 2008) and cytoplasm, including within the Golgi apparatus (Zhou et al., 2010), and has a role in a number of processes. Unique from other PRMTs, PRMT5 relies on its interaction with WD-repeat methylome protein 50 (MEP50) within a hetero-octameric structure for substrate binding to the catalytic domain. The combination of PRMT5, MEP50, also known as WD Repeat Domain 77, and a further protein known as plCln is termed the methylome (Friesen et al., 2002). Although dimerised PRMT5 alone is able to perform the transfer of methyl groups, the enzyme activity is much greater in the MEP50:PRMT5 hetero-octamer structure (Antonysamy et al., 2012). This increase in activity is attributed to a greater affinity for the target protein and methyl donating SAM domain. Other proteins have also been identified that have a role in this complex, including RIOK1 and COPR5, which have been suggested as possible targets to disrupt PRMT5 activity (Krzyzanowski et al., 2021). Studies have determined that the activity of PRMT5, both alone and in complex with

MEP50 act in a non-processive manner, meaning formation of SDMA only occurs once the concentration of MMA is higher than that of non-methylated arginine (Antonysamy et al., 2012).

PRMT5 is perhaps the most studied of the PRMTs, with roles found in a great range of cellular functions including transcription, translation, splicing, DNA damage repair, and growth factor signalling. PRMT5 methylation of histones H2AR3, H4R3 (Pollack et al., 1999), H3R8 (Pal et al., 2004), and H3R2me2a (Migliori et al., 2012) is repressive for transcription. The symmetrical dimethylation of H2AR3 and H4R3 was later associated with reduced histone tail acetylation and therefore DNA unravelling (Scaglione et al., 2018).

PRMT5 plays a key role in splicing regulation as it methylates multiple RNA binding proteins, including three Sm proteins, which then go on to bind small nuclear RNAs (Meister et al., 2001). The methylated Sm proteins are also recognised by the SMN protein, promoting the maturation of small nuclear ribonucleoproteins (Meister et al., 2001). Depletion of PRMT5 activity is related to a reduction in spliceosome assembly, causing exon skipping and retention of introns (Bezzi et al., 2013). An example of mis-splicing following PRMT depletion is the production of the short human ortholog of mouse double minute 4 (MDM4) isoform, leading to a reduction in p53 pathway repression (Bezzi et al., 2013).

PRMT5 has been shown to play a role in translation through a number of mechanisms. One of which is the methylation of the heterogeneous nuclear ribonucleoprotein hnRNPA1 (Gao et al., 2017). Methylation of hnRNPA1 facilitates its interactions with internal ribosome entry sites (IRES) on RNA, promoting translation of mRNAs such as MEP50, CCND1, MYC, HIF1α, MTIF and CDKN1B (Gao et al., 2017). hnRNPA1 is also known to be methylated by PRMT1 (Rajpurohit et al., 1994). Although some methylation sites of hnRNPA1 are exclusively methylated by type I PRMTs, site R206 is both symmetrically and asymmetrically methylated (Noto et al., 2020).

Depletion of PRMT5 results in aberrant p53 expression and leads to cell cycle arrest and defects in homologous recombination. These consequences are a result of PRMT5 activity in several pathways. For example, PRMT5 methylates the TIP60 complex subunit, RUVBL1 at R205, a modification required for the acetylation of H4K16 by TIP60, blocking the binding of 53BP1 to neighbouring H4k20me2 (Clarke et al., 2017). This then causes a switch from non-homologous end joining, to homologous recombination. PRMT5 also methylates other substrates involved in DNA damage repair including flap endonuclease 1 (FEN1) (Guo et al., 2010), RAD9 (He et al., 2011) and tyrosyl-DNA phosphodiesterase (TDP1) (Rehman et al., 2018).

Two of the most important growth factor signalling receptors, EGFR and PDGFRα, both contain residues methylated by PRMT5. Methylation of EGFR at R1175 allows the autophosphorylation of surrounding tyrosine residues and the binding of the protein-tyrosine phosphatase SHP1 (Hsu et al., 2011). The bound pair are then able to remove phosphor groups from various members of the RAS pathway, inhibiting the pathway. PRMT5 is required to block the degradation of PDGFRα by the Cbl E3 ligase, through methylation of its cytoplasmic tail (Calabretta et al., 2018). This blocks binding of the ligase to phosphorylated residues on PDGFRα.

1.2.3.3.2) PRMT9

PRMT9 was first described as a candidate PRMT alongside PRMT8 (Lee et al., 2005a). As seen in Figure 1.12, PRMT9 contains a repeated Rossman fold and β-barrel, although the functional consequence of this is not yet clear (Hadjikyriacou et al., 2015).

The two type II PRMTs, PRMT5 and PRMT9, have distinct substrate specificities and their functions are non-redundant, most likely due to the fact that PRMT9, unlike PRMT5, does not recognise GAR motifs (Hadjikyriacou et al., 2015). PRMT9 plays a role in the regulation of splicing through methylation of the U2 snRNP component, spliceosome-associated protein 145, promoting the affinity of U2 snRNP for SMN (Yang et al., 2015).

Loss of PRMT9 has been found to promote HIF-1α expression by increasing its mRNA stability, suggesting that PRMT9 acts a repressor of HIF-1α, a crucial protein involved in the hypoxia response (Ju et al., 2015, Zhang et al., 2017). PRMT9 has also been shown to inhibit the stability of BCL6 (B-cell Lymphoma 6) (Duan et al., 2012) and Zinc finger protein SNAI1 (SNAIL) (Shao et al., 2020).

1.2.3.4) Type III Structure and Function

1.2.3.4.1) PRMT7

Currently, the only known PRMT with type III activity is PRMT7 (Zurita-Lopez et al., 2012). PRMT7 was first discovered by a genetic screen to reveal sensitivities to chemotherapeutic drugs (Gros et al., 2003). Unlike type I PRMTs, PRMT7 contains two core domains in tandem which allows a single protein to mimic the dimer confirmation established by other members of the PRMT family (Cura et al., 2014, Hasegawaa et al., 2014).

Site directed mutagenesis studies have identified specific residues in PRMTs that are crucial for enzyme activity. By switching a glutamate residue (Glu181) within the double E-loop, a conserved region of the catalytic domain of the Rossman fold of PRMT7, with an aspartate residue, the enzymatic activity of PRMT7 to is widened to the production of ADMA (Debler et al., 2016). It was hypothesised

that this extra enzymatic activity was made possible due to an increase in available space within the active site due to the shorter side chain of aspartate.

Being a type III enzyme, it is only able to catalyse the production of MMA, although other research has suggested it could also produce the SDMA mark (Lee et al., 2005b; Jeong et al., 2020; Vuong et al., 2020; Liu et al., 2020). However, these studies relied on the use of SDMA antibodies or mass spectrometry in cells under or over expressing PRMT7. This methylation may have in fact been a result of dimethylation by PRMT5, as evidence has shown cross-talk between the two PRMT enzymes (Tarighat et al., 2016). The Liu et al. paper has since been retracted due to the possible role of PRMT5 in the methylation of the protein studied. This evidence, alongside the biochemical studies showing the altered activity of PRMT7 following widening of its active site, has meant it is generally accepted that PRMT7 is an exclusively type III enzyme (Halabelian & Barsyte-Lovejoy, 2021).

Although there has been no evidence to show PRMT7 is able to methylate histone proteins *in vivo*, *in vitro* experiments have indicated histone H2B and histone H4 to PRMT substrates at multiple residues (Feng et al., 2013, Feng et al., 2014). Difficulty in identifying PRMT7 substrates has largely been due to the enzyme's low activity (Feng et al., 2014). Experiments have also suggested that PRMT7 acts by methylating non-histone proteins. Changes in PRMT7 expression for example, affect the methylation state of Sm proteins and elongation factors (Gonsalvez et al., 2007, Jung et al., 2011).

More recently, PRMT7 activity has been linked with the stress response, through the methylation of the heat shock protein HSP70 (Szewczyk et al., 2020). Methylation of HSP70 at R249 was found to be important for the stress granule response following proteasome inhibition.

1.2.4) Regulation of Arginine Methylation

1.2.4.1) Micro RNAS

Micro RNAS (miRNA) are short non-coding lengths of RNA that function by regulating gene expression via base-pairing with complementary mRNA sequences (Jin et al., 2019). As with other DNA that can be transcribed, miRNAs may be regulated by ArgMe of their associated histone tails prior to transcription (Tao et al., 2017). PRMTs themselves, however, can be regulated by miRNAs by their binding to PRMTs 3' untranscribed regions (3'-UTRs). For example, miR-4518, miR-92, miR-96, miR-32 and miR-19, all target PRMT5 mRNA and prevent its translation, ultimately leading to reduce cell proliferation (Pal et al., 2007, Wang et al., 2008a, Fu et al., 2018). miR-543 was shown to bind the 3'-UTR of PRMT9, inhibiting its expression and leading to reduced PRMT9-enhanced cell oxidative phosphorylation and increased HIF-1α stability in osteosarcoma cells (Zhang et al., 2017). PRMT1 translation is inhibited by binding of miR-503 and was linked to a reduced epithelial-mesenchymal transition in hepatocellular carcinoma cells (Li et al., 2015). miR-195 was found to reduce PRMT4

expression and reduce proliferation in colorectal cancer cells (Zheng et al., 2017). Of note, PRMT1 has recently been shown to play an important role in the regulation of miRNA synthesis (Spadotto et al., 2020), which could open a new avenue for self-regulation of PRMT expression.

1.2.4.2) Alternate Splicing

Many of the PRMTs undergo alternate splicing during mRNA maturation, resulting in differences in amino acid sequence. This can have consequences in terms of enzyme activity, as is seen in an isoform of PRMT1, named PRMT1v2. This isoform is uniquely localised to the cytoplasm and has a functional nuclear export sequence (Goulet et al., 2007). PRMT2 also forms multiple isoforms following alternate splicing, producing PRMT2α, PRMT2β, PRMT2γ, PRMT2L2, as well as the original PRMT2 protein. These alternative isoforms have reduced methyltransferase activity and varied localisation due to losses to domain III and the THW loop (Zhong et al., 2012). Two isoforms of PRMT4 have been identified in human tissue: full length PRMT4 and a shorter PRMT4Δ15 isoform. Exon 15 of PRMT4 is excluded in this shorter isoform, resulting in a loss of auto methylation capacity, but no change in methyltransferase activity (Wang et al., 2013).

1.2.4.3) Protein Interactions

As PRMT5 is a member of a multimeric complex, it interacts with many cofactors which regulate its activity. As previously described, its most important cofactor is MEP50, with which it creates a hetero-octameric structure. The PRMT5:MEP50 complex is able to bind further cofactors including pICln and RioK1, allowing for the recruitment of distinct methylation substrates (Guderian et al., 2011). More recently, a further PRMT5 interacting partner has been identified (Chakrapani et al., 2020). FAM47E was shown to enhance PRMT5 association with chromatin and histone methylation through inhibition of PRMT5 proteasomal degradation (Chakrapani et al., 2020).

Other PRMT-protein interactions contribute to the regulation and substrate specificity of PRMTs. These include human CCR4-associated factor 1 (hCAF1), which inhibits PRMT1 methylation of Sam68 (Robin-Lespinasse et al., 2007), and actin filament-associated protein (AFAP1), which is known to inhibit PRMT3 (Singh et al., 2004). Other PRMT:protein interactions can facilitate PRMT recognition of substrates, for instance nucleosomal methylation activator complex (NUMAC), which targets PRMT4 to H3 in vivo (Xu et al., 2004). Other examples of PRMT protein partners are high mobility group AT-Hook 1 (HMGA1) and CCCTC-binding factor (CTCFL), which increase the methylation activities of PRMT6 (Sardo et al., 2013) and PRMT7 (Jelinic et al., 2006), respectively. PRMTs have also been found forming homomers and heteromers with other PRMT isoforms, generally to enhance PRMT activity (Pak et al., 2011).

1.2.4.4) Posttranslational Modification

Phosphorylation of PRMTs can allow, inhibit or switch their methyltransferase activity, depending on the site of modification. For example, phosphorylation of PRMT5 at T132, T139 and T144 is required for its activity, whereas phosphorylation of Y304 and Y307 downregulates methyltransferase activity by disrupting the PRMT5-MEP50 interaction (Liu et al., 2011). Phosphorylation of PRMT5 at residue S15 by protein kinase C is induced by interleukin-1β and is required for the PRMT5 mediated activation of NF-κB (Hartley et al., 2020), a major transcription factor involved in the innate and adaptive immune response (Lawrence 2009).

PRMT1 and PRMT4 are also known to be phosphorylated. Casein kinase 1 isoform alpha 1 phosphorylates PRMT1 between the regions 55-57, 102-105 and 284-289 to control PRMT1 targeting to chromatin and therefore regulate self-renewal pathways by changing gene expression (Bao et al., 2017). PRMT1 is also phosphorylated at Y291, altering substrate specificity (Rust et al., 2014). PRMT4 is phosphorylated at residues S217 and S229, inhibiting methyltransferase activity through promoting cytoplasmic localisation (Feng et al., 2009) and preventing dimerization (Higashimoto et al., 2007), respectively. PRMT4 is also phosphorylated at S572 by p38γ MAPK, inhibiting its translocation to the nucleus, where it would methylate PAX7 and activate myogenic factor 5 to induce myogenesis (Chang et al., 2018).

Like all other proteins, PRMTs may be subject to degradation by the proteasome. PRMT1, PRMT4 and PRMT5 for example, are substrates of ubiquitin E3 ligases. PRMT1 is ubiquitinated by E4B (Bhuripanyo et al., 2018), PRMT4 by SKP1-cullin-F-box protein (SCF) (Shin et al., 2016), and PRMT5 by heat shock cognate 70-interacting protein (CHIP) (Zhang et al., 2016). Recently, an orphan F-box protein, FBXO24, has been shown to modify PRMT6 by ubiquitination at K369 (Chen et al., 2020). Due to the minimal number of studies investigating the effect of ubiquitination of PRMTs, the physiological relevance of this modification is still unclear. Questions still remain about the specific ubiquitination sites on other PRMTs, and whether ubiquitination leads solely to proteasomal degradation, or carries out other functions independent of this process (Hartley and Lu, 2020).

Glutathionylation is a PTM that can target proteins exposed to oxidative stress and can also modulate protein structure and function. Cys sulfhydryl groups are particularly responsive to the redox state of cells and can be post-translationally modified by glutathionylation. Recently, glutathionylation at C42 has been reported to decrease methyltransferase activity of PRMT5 by affecting PRMT5-MEP50 interactions (Yi et al., 2020). PRMT5 C42 glutathionylation was increased in aged mice and in cell lines treated with H_2O_2, and the modification was reversed by Glutaredoxin-1. This finding contributes to growing evidence that PRMT activity can be affected by oxidative stress (Morales et al., 2015).

As methylation of target substrates can alter their interactions and activity, methylation of the PRMTs themselves can also have a regulatory affect. Some PRMTs are able to methylate themselves in order to control their function. These PRMTs include PRMT4, PRMT6 and PRMT8. PRMT4 is automethylated at R551 within its C-terminal domain. This modification does not directly alter catalytic activity, but instead facilitates protein-protein interactions required for transcriptional regulation of other proteins (Kuhn et al., 2011). PRMT6 is also able to undergo auto methylation, specifically at the residue R35. This modification was found to be required for PRMT6 stability and for the inhibition of HIV-1 replication (Singhroy et al., 2013). PRMT8 was also found to be auto methylated within its N-terminal domain (Sayegh et al., 2007), resulting in blockage of the catalytic site and inhibition of further methylation (Dillon et al., 2013). Asymmetrical methylation of PRMT5 by PRMT4 at R505 increases PRMT5 oligomerisation and was found to be critical for PRMT5 methyltransferase activity (Nie et al., 2018).

1.2.4.7) Arginine Demethylases

Lysine demethylation is now a well-established activity and numerous responsible enzymes have been identified, of which there are two families: flavin-dependant methyl lysine demethylases and Fe(II) and 2-oxoglutarate dependant JmjC-domain-containing enzymes (Böttger et al., 2015). As yet however, no arginine demethylation enzymes have been confirmed.

JMJD6, a Jumonji C domain containing protein, was thought to be an arginine demethylase, acting on the histone positions H3R2 and H4R3 (Chang et al., 2007). Further studies showed that JMJD6 was in fact a hydroxylase that acts predominantly on nucleic acids (Hong et al., 2010). The exact activity and role of JMJD6 is controversial and remains unclear (Böttger et al., 2015), although it has been shown to demethylate the stress granule nucleating protein G2BP1 *in vivo* (Tsai et al., 2017). Particular lysine demethylases (KDM4E, KDM4A, KDM5C, KDM3B, and KDM3A) have recently been shown to also have arginine demethylase activity in vitro (Walport et al., 2016, Li et al., 2018). The arginine demethylase activity been shown to differ amongst these enzymes and was also found to be lower than their lysine demethylase activity (Walport et al., 2016). Inhibitors of KDM4E were also found to reduce both the lysine demethylase and arginine demethylase activity of the enzyme (Bonnici et al., 2018). Although it has been shown that the levels of arginine methylation can be dynamic and alter depending on cellular environment (Katsuno et al., 2018), suggesting the existence of arginine demethylases, there is a lack of arginine demethylase activity demonstrated in cells, and the existence of such enzymes remains in dispute. If the existence of arginine demethylases was confirmed, this could potentially present novel therapeutic avenues for cancer treatments.

The degradation of proteins bearing methylated arginine residues leads to the proteolytic products NG-monomethyl-L-arginine (monomethyl arginine, mMA), NG,NG-dimethyl-L-arginine (asymmetric dimethylarginine, aDMA) and NG,N′G-dimethyl-L-arginine (symmetric dimethylarginine, sDMA) (Tsikas et al., 2018). These metabolites exercise a range of functions when released into circulation, notably related to nitric oxide synthase inhibition. sDMA is primarily eliminated through renal excretion while mMA and aDMA are mainly excreted as mono- and di-methylamine, respectively (Said et al., 2019). The enzyme responsible for the hydrolysis of mMA and aDMA into mono- and di-methylamine, and citrulline, is dimethylarginine dimethylaminohydrolase (DDAH) (Jarzebska et al., 2019). The metabolism of aDMA and sDMA can also include transamination into asymmetric or symmetrical α-keto-dimethylguanidinovaleric acid, catalysed by alanine:glyoxylate aminotransferase 2 (AGXT2), (Jarzebska et al., 2019). However, DDAH and AGXT2 activities have only been observed towards methylarginine metabolites, and not towards proteins modified ArgMe and, therefore, cannot be considered true protein arginine demethylases. Similarly, peptidyl-arginine deaminases (PADs) are enzymes that convert methylarginine into citrulline through hydrolysis (Wang et al., 2004) but citrulline has different chemical properties to unmethylated arginine and PADs cannot therefore be considered authentic demethylases either. PADI enzymes also have a preference for unmodified arginine, suggesting their primary function is not to remove methyl groups, but prevent the addition of alkyl groups instead (Cuthbert et al., 2004).

1.2.5) PRMT Inhibition

1.2.5.1) Early PRMT Inhibitors

The first small molecule inhibitors of PRMTs were discovered by Bedford and others in 2004, with the development of the AMI compounds (Arginine Methyltransferase Inhibitors) (Cheng et al., 2004). These compounds were identified through the detection of decreased methylation of the RNA-binding protein, Npl3p, by Hmt1p (yeast homolog of PRMT1). Some of the molecules found to cause a significant decrease in PRMT activity were analogues of SAM, the methyl donor used by PRMTs. They were, however, found to be unspecific and inhibited the activity of all PRMTs tested excluding PRMT5. All compounds excluding AMI-1 and AMI-6 also inhibited the activity of lysine methyl transferases. AMI-1 was shown to inhibit methylation of PNp13 and Sam68 in HeLa cells and also reduce the effect of PRMT1 on nuclear receptor dependant transcription in MDF7 cells. The molecules identified in this study have since been used as a basis for discovery of other similar structures.

1.2.5.2) Type I Inhibitors

Allantodapsone and Stilbamidine are further PRMT1 inhibitors found through the virtual screening of 1990 compounds using a homology model of human PRMT1 and *Aspergillus nidulans* RmtA (fungal

PRMT homolog) created using rat PRMT3 X-ray structure (Spannhoff et al., 2007a). Compounds with suitable docking into the binding pocket of the structure were then tested in an *in vitro* assay to evaluate their ability to inhibit RmtA. Allantodapsone was found to inhibit PRMT1 with an IC50 of 1.7 µM. Compounds discovered in this study share a basic motif that mimics the guanidine nitrogen of the substrate protein. Further discoveries have been made based on the structure of these compounds, all with varying activities (Bissingera et al, 2011). Other PRMT1 inhibitors have also been identified by similar methods using different datasets of compounds such as RM65 (Spannhoff et al., 2007b) and A9 (Wang et al., 2012a).

Due to the similarities between the guanidine structure in substrate arginines and the amidine group of diamidine-based compounds, as well as the existence of the diamidine PRMT inhibitor Stilbamidine, Yan et al explored the use of such compounds as PRMT inhibiting drugs (Yan et al., 2014b). Two compounds, including Furamidine (also known as DB75), were identified to selectively inhibit PRMT1, with an IC50 of less than 10 µM for PRMT1 and greater than 160 µM for PRMT5, and even greater for PRMT4 and PRMT6. Furamidine is thought to act as a competitive substrate inhibitor.

Both the inhibitors EPZ020411 and CMPD-1 (inhibitors of PRMT6 and PRMT4 respectively) contain an ethylenediamine which is thought to mimic the structure of arginine. Following experiments with negative control compounds lacking this ethylenediamine group confirmed its importance by a lack of inhibition by these compounds. This was then used to rationally design a broader PRMT type I inhibitor, MS023. The cyclobutoxy group found in EPZ020411 was thought to provide the specificity against PRMT6. Therefore, its replacement with a smaller functional group (i.e., isopropoxy) allowed the inhibitory actions against other type I PRMTs. MS023 was found to have a strong inhibitory action against a range of type I PRMTs exclusively with IC50 in the nano molar range when tested *in vitro*; PRMT1 (30 nM), PRMT3 (119 nM), PRMT4 (83 nM), PRMT6 (4 nM) and PRMT 8 (5 nM). Cell based assays were used to confirm the activity of MS023, utilising the fact that PRMT1 is the main enzyme responsible for the deposition of the H4R3me2A methylation mark. In MCF7 cells, it was found that MS023 was able to cause a 50% decrease in the H4R3me2a mark at 9 nM.

1.2.5.3) Type II Inhibitors

Type II PRMT inhibitors have also been developed and extensively investigated. In a landmark paper by a multi-pharmaceutical collaboration, a fluorescence assay was used to monitor the monomethylation of the PRMT5 target H4R3 and to screen a library of small molecules. Following re-testing and counter screens, a subset of 17 compounds were identified with IC_{50} ranging from 0.4-7 µM (Chan-Penebre et al, 2015). The most successful compound was EPZ007345, which was then structurally developed to increase potency and other pharmacokinetically favourable characteristics

including absorption, distribution, metabolism and excretion. The end product, EPZ015666, acts as a competitive substrate inhibitor and has an IC_{50} of 22 nM *in vitro* and 64-902 nM in cell assays. A second study optimised the structure for use as an *in vitro* tool known as EPZ015866, also known as GSK591, that has an IC_{50} of 4 nM (Duncan, et al., 2015).

In contrast to these substrate binding inhibitors, LLY-283 is a SAM pocket competitive inhibitor of PRMT5 which was found to have an IC50 of 22 nM in terms of inhibiting the PRMT5:MEP50 complex (Bonday et al., 2018). When tested *in vivo*, the drug had an IC_{50} of 25 nM, measured by the levels of methylated SmBB.

Recently, a novel allosteric inhibitor of PRMT5 has been reported, which leads to occlusion of both the SAM and substrate binding sites through displacement of the loop ELLGSFADNEL spanning PRMT5 residues 435-445 (Palte et al., 2020). The question of whether the combination of Type I and Type II inhibitors would synergise against tumour cells is a logical step and has recently been addressed by several research groups (Fedoriw et al., 2019; Fong et al., 2019; Gao et al., 2019). Both groups have independently reported that the combination of PRMT1 and PRMT5 inhibition has synergistic effects on tumour cell growth, most likely through the attenuation of splicing mechanisms.

1.2.5.4) Type III Inhibitors

PRMT7, the only recognised Type III PRMT, has also been targeted for development of specific inhibitors. DS-437 is a SAM analogue inhibitor of PRMT5 that also shows activity against PRMT7 (Smil et al., 2015). More recently, specific PRMT7 inhibition by SGC8158, a SAM-competitive inhibitor, has been described (Szewczyk et al., 2020). A list of inhibitors sorted by their PRMT targets is shown in Table 1.3.

Table 1.3: Summary of preclinical PRMT inhibitors.

PRMT	Inhibitors	Target Site
PRMT1	Furamidine	Competitive substrate inhibitor
	MS023	Type I Competitive substrate inhibitor
	Allantodapsone	Competitive substrate inhibitor
	Stilbamidine	Competitive substrate inhibitor
	RM65	Competitive substrate inhibitor
	A9	Competitive substrate inhibitor
PRMT2	MS023	Type I Competitive substrate inhibitor
PRMT3	MS023	Type I Competitive substrate inhibitor
PRMT4	MS023	Type I Competitive substrate inhibitor
	CMPD-1	Competitive substrate inhibitor
PRMT5	JNJ-64619178	Small molecule inhibitor of SAM and substrate binding pockets
	LLY-283	SAM competitive inhibitor
	EPZ015866/GSK-591	Competitive substrate inhibitor
	DS-437	SAM analogue inhibitor
PRMT6	MS023	Type I Competitive substrate inhibitor
	EPZ020411	Competitive substrate inhibitor
PRMT7	SGC8158	SAM competitive inhibitor
	DS-437	SAM analogue inhibitor
PRMT8	MS023	Type I Competitive substrate inhibitor

1.2.5.5) Clinical Trials Involving PRMT Inhibitors

PRMTs play key roles in many cellular processes and PRMT dysregulation has been associated with cancer, which has prompted the development of PRMT inhibitors into Phase I clinical trials. These clinical trials involve several tumour types, including a range of blood and solid cancers, and are summarised in Table 1.3. Over the past few years, there has been great interest in understanding the mechanistic basis that supports the use of PRMT inhibitors in cancer. As described above, a prominent role of PRMTs is in RNA splicing. In cancer, RNA splicing is often dysregulated including by mutations in RNA splicing factors (RNA-SF), and inhibition of Type I PRMT and PRMT5 by MS023 and GSK591, respectively, has been shown to effectively target cells bearing RNA-SF mutations, both in vitro and in vivo (Fong et al., 2019). GSK3368715, an inhibitor of Type I PRMTs, alters exon utilisation and RNA splicing most likely by inhibiting ArgMe of heterogeneous nuclear ribonuclear (hnRNP) proteins

(Fedoriw et al., 2019). The PRMT5 inhibitor GSK3326595 has been shown to promote the alternative splicing of MDM4, which leads to the activation of the tumour suppressor p53 protein and reduced tumour cell viability (Gerhart et al., 2018). GSK3326595 was developed from GSK3235025 (Chan-Penebre et al., 2015) with both compounds having potent antiproliferative effects both in vitro and in vivo (Chiang et al., 2017; Gerhart et al., 2018). These basic and translational science efforts have been paralleled by much interest from large pharmaceutical companies in developing and trialling PRMT inhibitors, including in gliomas and GBM populations as expansion cohorts (Table 1.4).

Table 1.4: Current clinical trials taking place involving PRMT inhibitors.

Compound Name	Target	Dose Escalation Cohort	Expansion Cohort	Trial Identifier
GSK3368715	Type I PRMTs except PRMT3	Relapsed/refractory diffuse large B-cell lymphoma and selected solid tumours with frequent MTAP deficiency	Diffuse large B-cell lymphoma and relapsed/refractory solid tumours including pancreatic, bladder, and non-small cell lung cancer	NCT03666988
EPZ015938 (GSK3326595)	PRMT5 PRMT9	Myelodysplastic Syndrome and Acute Myeloid Leukaemia	Newly diagnosed myelodysplastic syndrome	NCT03614728
EPZ015938 (GSK3326595)	PRMT5 PRMT9	Non-Hodgkin's lymphoma and solid tumours (inc. recurrent GBM)	Triple-negative breast cancer, metastatic transitional cell carcinoma, recurrent GBM, non-Hodgkin's lymphoma p53 mutant gene, adenoid cystic carcinoma, hormone receptor-positive adenocarcinoma of the breast, human papillomavirus positive solid tumours of any histology (including cervical cancer and squamous cell carcinoma of the head and neck) and P53 wild-type non small-cell lung cancer	NCT02783300
EPZ015938 (GSK3326595)	PRMT5 PRMT9	Early stage Hormone Receptor (HR) positive breast cancer	NA	NCT04676516
JNJ-64619178	PRMT5	Non-Hodgkin's lymphoma and solid tumours	Myelodysplastic syndromes	NCT03573310
PF-06939999	PRMT5	Advanced solid tumours (non-small cell lung cancer, head and neck squamous cell carcinoma, oesophageal cancer, endometrial cancer, cervical cancer, and bladder cancer)	Advanced solid tumours	NCT03854227
PRT811	PRMT5	Advanced solid tumours	GBM	NCT04089449

1.3) PRMTs in Glioblastoma

1.3.1) PRMT1 in Glioblastoma

PRMT1 expression is considerably high in the foetal brain when compared with adult tissue, suggesting a role in development (Huang et al., 2011, Pawlack et al., 2000, Ikenaka et al., 2006). Further research has suggested a role for PRMT1 in astrocytic differentiation through the methylation of STAT3 (Honda et al., 2017). STAT3 is part of the JAK/STAT signalling cascade and works to activate the expression of astrocytic genes in order to promote tumorigenesis (Levy & Darnell. 2002).

PRMT1 is upregulated in both GBM tissue and cell lines, including U-87MG, U-251 and A-172, at both the RNA and protein level (Wang et al., 2012c). Its knock down through siRNA causes a loss of cell proliferation as seen through a reduction of S-phase cells by flow cytometry and also by MTT assay. An induction of apoptosis was also seen by TUNEL assay (Wang et al., 2012c).

PRMT1 is recruited by chromatin associated proteins in GBM cells to induce the expression of proliferative genes (Takai et al., 2014). Chromatin target of PRMT1 (CHTOP), when associated with 5hmC, recruits PRMT1 as part of the methylosome complex which then causes the expression of cancer related genes *EGFR*, *AKT3*, *CDK6*, *CCND2*, and *BRAF*, through the methylation of H4R3. Knock down of CHTOP as found to decrease sphere formation of GBM cells.

The production of 5hmC from 5mC is dependent upon the TET family of enzymes. The activity of the TET enzymes is inhibited by 2-HG, a product of the mutated version of the IDH1 enzyme, a major prognosis marker of GBMs (Figure 1.2). This activity involving PRMT1 could therefore provide an additional mechanism for the positive prognosis seen in IDH mutated GBM patients. This study is supported by previous findings of interactions between PRMT1 and CHTOP at chromatin, also named as “friend of PRMT1” (Van Dijk et al., 2010, Izumikawa et al., 2014).

Co-Immunoprecipitation, western blot, sliver staining and mass spectrometry were used to identify possible binding partners of PRMT1 in glioma cells (Wang et al., 2012b). In this study, SEC23-IP, ANKHD1-EIF4EBP3 protein, and 1-phosphatidylinositol-3-phosphate 5-kinase were found to have at least two methylated arginine sites in U-87MG cells.

Altogether, the current literature suggests that PRMT1 plays a role in GBM pathogenesis. This is based on the observations of increased PRMT1 expression in GBM cells and tissue, GBM cells dependency on PRMT1 activity for proliferation, and the correlation of PRMT1 expression with disease stage and poor patient survival. A number of interacting partners and targets that contribute to its activity in GBM have also been identified, perhaps the most interesting being CHTOP and 5hmC, the activity of which may be altered in mutant IDH1 GBM.

1.3.2) PRMT2 in Glioblastoma

In a study carried out by Dong et al, PRMT 1, 2, 4 and 6 mRNA expression were found to be correlated with tumour grade and high expression to be predictive of patient prognosis (Dong et al., 2018). On the other hand, expression of PRMT5, 7, 8 and 9 correlates with a more favourable prognosis. The group found that knocking down PRMT2 by shRNA resulted in loss of proliferation in both T98G and U-87MG cells, each having different PTEN status (wild type and deleted, respectively). Because of this, focus was taken on PRMT2, excluding other PRMTs in protein expression analysis. IHC was carried out on 21 cases of gliomas of different grades and quantification of PRMT2 showed an increased expression in higher grade samples. Knockdown of PRMT2 by shRNA in T98G and U-87MG cells resulted in a decrease in cell number and a decrease in spheroid formation, suggesting a role in self-renewal. To further investigate this, limiting dilution assays were carried out and it was shown that cells depleted of PRMT2 were less able to produce spheroids and also showed a decreased expression of stem cell-associated genes by quantitative reverse transcription PCR. Oncogenic transcriptional programmes were also reduced including PI3K-AKT, MAPK, JAK-STAT and Wnt signalling pathways. T98G and U-87MG cells were then transduced with a luciferase expressing virus with either an unspecific control shRNA (shScrambled), or shPRMT and injected into mice. Cells depleted of PRMT2 were less able to form tumours and the mice showed significantly prolonged survival. These changes were linked with the methylation mark on H3R8me2a. Although there are limited studies investigating PRMT2 in GBM, it is clear that PRMT2 contributes to the pathogenesis of GBM, most likely through promoting cell stemness.

1.3.3) PRMT5 in Glioblastoma

PRMT5 has been shown to be expressed and active in normal neuronal cells and has a role in neuronal stem cell proliferation (Han et al., 2014, Chittka et al., 2010, Chittka et al., 2012). When dysregulated, it thus has the potential to cause uncontrolled cell growth in such cell types.

PRMT5 has been shown to be overexpressed in numerous GBM cell lines when compared to those originating from normal brain tissue (Yan et al., 2014a). More importantly, a significant increase in expression of PRMT5 was observed in grade III and IV astrocytoma patients when compared with normal or grade I and II brain tissue by IHC. This expression was localised to the nucleus. PRMT5 mRNA was not found to be differentially expressed however, meaning dysregulation of the proteins expressions occurs at the level of translation, most likely by micro-RNAs. This observation has also been made by other groups through the immunofluorescence and IHC (Han et al., 2014).

Braun et al. observed a loss of proliferation in U-87MG cells following treatment with the PRMT5 specific inhibitor EPZ015666, indicating a dependency on PRMT5 activity (Braun et al., 2017). Cell cycle

profiling suggested this reduction in growth was due to activation of senescence as an upregulation of senescence associated markers and beta-galactosidase positive cells were seen accompanied by no increase in G2/M cells which would otherwise indicate activated p53 and apoptosis.

Due to its role in neuronal stem cell proliferation, and the increasing significance of cancer stem cells, Banasavadi-Siddegowda et al. investigated the differential effects of PRMT5 silencing through pooled siRNA in stem-like and differentiated glioblastoma cells (Banasavadi-Siddegowda et al., 2017). Loss of PRMT5 caused a decrease in cell proliferation in only stem-like cells but did not cause in an increase in apoptosis. Following differentiation of the cells by prolonged incubation with serum-containing media, sensitivity to PRMT5 knock down was achieved. Cell cycle analysis by propidium iodide staining revealed a G1/S cell cycle arrest in only stem-like cells suggesting the apoptosis in differentiated GBM cells was cell cycle independent. An increase in senescence using the beta-gal assay was seen in stem-like GBM cells which was supported by cell cycle arrest, decreased proliferation and increased cell size. Further investigation showed an increase in the activation of Akt and its upstream target PTEN following knock down of PRMT5 in stem-like GBM cells, contrasting with results from Han et al, where no increase in Akt activation following PRMT knock down by shRNA in U373MG cells. Proliferation of these cells was rescued following a combinational knock down of both PRMT5 and PTEN, indicating a role for PTEN in the induction of senescence in the absence of inhibition by PRMT5.

Han et al. showed an increase in ERK1/2 signalling following knock down of PRMT5 through shRNA (Han et al., 2014). As over-activation of this pathway has previously been shown to cause cell death in GBM cells, Han et al. stipulated this mechanism may be regulated by PRMT5 in order to allow for tumour growth. More indirect evidence of the relevance of PRMT5 in GBM includes the report that the long non-coding RNA, small nucleolar RNA host gene (SNHG16), has been found to be upregulated in glioma tissues, such as GBM. SNHG16 was shown to have oncogenic properties by “sponging” cellular miR-4518, a known regulator of PRMT5 expression (Lu et al., 2018).

Work by Mongiardi et al. has suggested a role for N-Myc in the tumorigenic nature of PRMT5 in GBM (Mongiardi et al., 2015). Expression of the Omomyc protein, an effective inhibitor of specific N-Myc interactions, correlated with a decreased prevalence of the H4R3me2 histone mark, a post translational modification dependent upon PRMT5, in both U-87MG and patient derived cells. Inhibition of N-Myc, as expected, resulted in a loss of expression of its target proteins, cad and cyclin D1. Their expression returned, however, through the knock down of the PRMT5 associated protein CORP50. These findings are supported by the known stabilising interactions between N-Myc and PRMT5 (Park et al., 2015). Further investigations suggested a role for PRMT1 in these interactions, and it was found that N-Myc was both symmetrically and asymmetrically demethylated and that these

modifications were required for its activity and turnover, respectively (Favia et al., 2019). PRMT5 has also been associated with Myc-driven primary medulloblastoma tumours (Chaturvedi et al., 2019). This group has shown that PRMT5 is overexpressed in these tumours, compared to normal tissue, and that PRMT5 expression inversely correlated with survival. Knocking down PRMT5 in Myc-driven medulloblastoma cells led to a significant inhibition of cell growth (Chaturvedi et al., 2019).

Finally, a paper by Holmes and colleagues explored possible synergies between PRMT5 inhibition and other treatments in glioblastoma (Holmes et al. 2019). This is an important issue, because it is unlikely that any novel treatment will be introduced to neuro-oncology clinics unless it has been investigated in combination with the standard of care. Although combinations of PRMT inhibitors and TMZ have not yet been fully investigated, the paper by Holmes et al. sheds light on a different class of inhibitors that has also been explored for GBM treatment through clinical trials, that is, mammalian target of rapamycin (mTOR) inhibitors. They found that PRMT5 activity was stimulated by mTOR inhibitors, which could explain resistance to mTOR inhibition, and that the concurrent inhibition of PRMT5 and mTOR pathways led to synergistic anti-proliferative effects both in GBM cell lines and in a xenograft model (Holmes et al. 2019).

To summarise, PRMT5 is expressed at greater levels in both GBM cell lines and patient tissue and PRMT5 expression correlates with disease stage. Similar to PRMT2, PRMT5 activity in GBM cells has been linked to cell stemness and tumour cell ability to self-renew. A number of mechanisms have been suggested for this activity including through the regulation of PTEN and Akt signalling as well as Myc and ERK1/2 signalling.

1.3.4) PRMT8 in Glioblastoma

In contrast to other PRMTs, PRMT8 was found to have a reduced transcript expression in GBM patient tissue when compared with normal, suggesting it may be down regulated during tumour development (Simandi et al., 2015). This decrease in expression was accompanied by a significant increase in the expression of genes *CXCR4* and *EFEMP1*. Silencing of PRMT8 in embryonic stem cell derived neurons, through the use of shRNA, causes a differential expression pattern in genes including *CXCR4* and *EFEMP1*. These genes are also known to be implicated in Glioma (Idbaih et al., 2008). *CXCR4* has been shown to have a role in GBM proliferation and invasiveness, most likely through activation of the MAPK or PI3K/Akt pathways (Barbero et al., 2003, Ehtesham et al., 2006)). *CXCR4* has also been implicated in the resistance to TMZ treatment (Wang et al., 2020b) and glioma stemness (Calinescu et al., 2017). *EFEMP1* on the other hand has been shown to a tumour suppressor gene with roles in EGFR/AKT-mediated growth signalling the reduction of MMP activity (Hu et al., 2014).

Knock down of a previously unknown PRMT8 transcript variant, names PRMT8 variant 2, was shown to reduce proliferation of the GBM cell line U-87MG (Hernandez & Dominko 2016). This variant of PRMT8 shows nuclear localisation, due to the loss of the myristoylation motif in the N-terminal domain, so most likely acts through epigenetic regulation of gene expression (Hernandez, et al., 2017). However, a similar loss in proliferation was also observed in nontumorigenic cells.

In conclusion, PRMT8 does not seem to play a role in the pathogenesis of GBM and is, in fact, associated with a better patient prognosis, although the significance of this is still unclear. However, upon nuclear localisation through the loss of its myristoylation motif, PRMT8 appears to have a switch in molecular targets, which confers a tumorigenic phenotype, most likely similar to PRMT1.

1.4) Hypothesis and Aims

PRMTs present a novel target for GBM treatment due to their ability to augment a vast variety of cellular processes including growth factor signalling, DNA damage repair and proliferation, that has resulted in their increased expression in GBM tumour cells. Here, the overarching hypothesis is therefore that GBM cells are dependent on PRMT expression, and their inhibition, as demonstrated by other groups (Wang et al., 2012c, Dong et al., 2018, Braun et al., 2017), will result in cell death or reduced proliferation.

Investigation of such novel treatments in classic cell culture models is limited by the lack of representation of interactive systems and the tumour microenvironment. For this reason, the central aims of this thesis are 1) to investigate a novel GBM-on-chip model for maintenance of GBM patient samples in microfluidic devices and 2) to determine the efficacy of PRMT inhibitors as for GBM treatment on-chip.

Chapter 2 – General Materials and Methods

2.1) Cell Culture

2.1.1) Cell Line Model

U-87MG cells were acquired from colleagues at the University of Hull. Cells were incubated with DMEM (Dulbecco's Modified Eagle Medium) supplemented with 10% (v/v) Foetal bovine serum (FBS) (Sigma) and 1X antibiotic/antimycotic solution (100 units/mL penicillin 0.1 mg/mL streptomycin, 0.25 µg/mL amphotericin B (Sigma) at 37˚C at 5% Carbon Dioxide (CO_2) and passaged every 3-4 days once they had reached roughly 75% confluency. To passage, cells were washed with warm 10/20 mL Phosphate buffered saline (PBS) (1.34 M NaCl, 26.8 mM KCl, 101.4 mM Na_2HPO_4, 13.7 mM K_2PO_4) and detached by incubation with 2 mL of warm Trypsin-EDTA solution (Sigma) at 37˚C for 5 mins. DMEM growth medium was then added to make 10 mL and 1/5 of the volume transferred to a 15 mL centrifuge tube and centrifuged at 250 g for 5 min. The supernatant was then discarded, and cell pellet resuspended in appropriate volume of DMEM medium and transferred to a new T25/75/175 flask.

2.1.2) Microfluidic Model

2.1.2.1) Patient Samples

Patients at the Hull Royal Infirmary suspected to have a high-grade astrocytoma were given an information sheet and the project explained to them by Mr Srihari Deepak, a registrar at the Neuro-oncology Department of the Hull Royal Infirmary and collaborator of this project. They were then asked to sign the consent form. Ethics approval was provided by the Integrated Research Application System (IRAS) with the chief investigator being Prof John Greenman and NHS contact being Shailendra Achawal (Project ID: 131630, LREC ethics code: 13/YH/0238).

During surgical resection, tissue that was not needed for pathology and further diagnosis, was placed in a 15 mL centrifuge tube containing DMEM medium at room temperature and given to either myself or Srihari Deepak. This sample varied greatly in size which ranged from 0.25 g to 2.5 g. The tube was then stored in a tissue transportation box and transported via a taxi to the university. This journey took between 20 and 45 minutes.

2.1.2.2) Microfluidic Device

The microfluidic devices (Figure 2.1), made of polymethyl methacrylate (PMMA), were laser cut in house, as 3 individual pieces which were then bonded together using chloroform (Akhil et al., 2016). During this process, small amounts of chloroform are pipetted onto each section of the unassembled chip, dissolving the exposed areas of PMMA. These sections are then held together and the dissolved PMMA hardens as one following evaporation of the chloroform liquid. The tubing used is 1/32” Tygon

Silicon material (Coleparmer) which are connected to the device via female/male elbow luer connects (Ibidi).

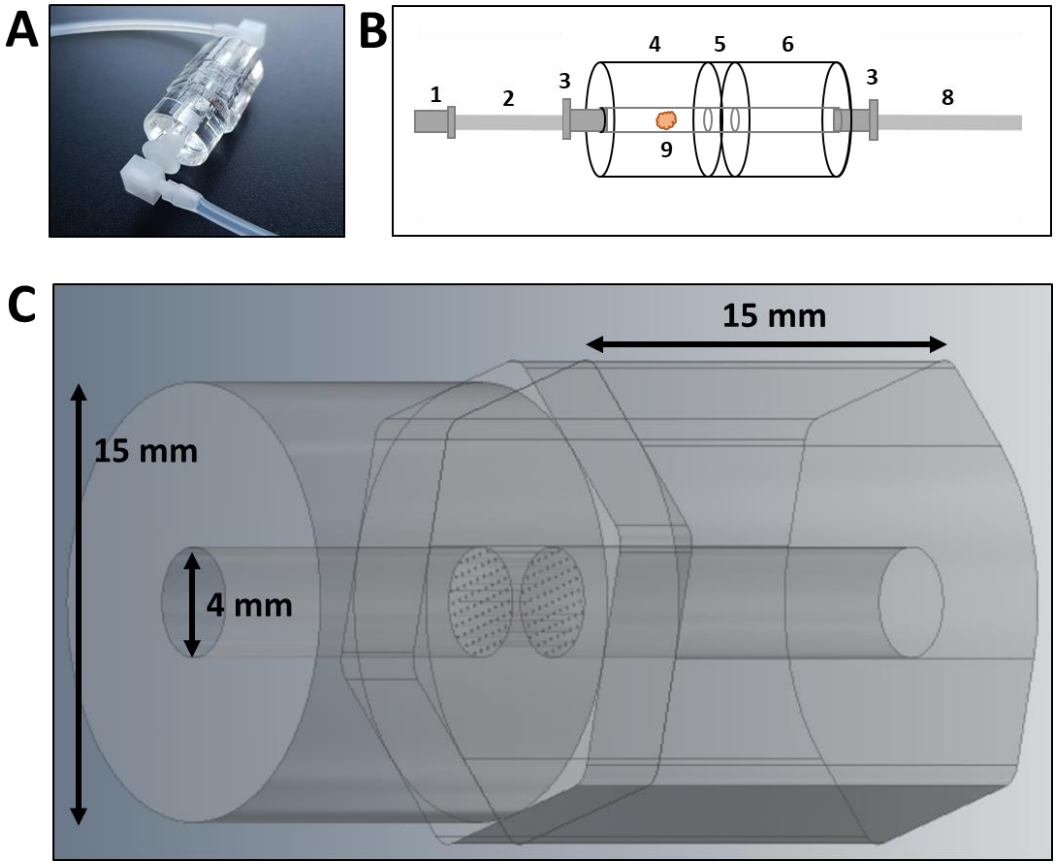

Figure 2.1: The miniature chip used in microfluidic experiments. (A)*Photograph of the microfluidic device used in patient sample incubations* ***(B)*** *schematic of the microfluidic device: 1- female connector 2- inlet tubing 3- male connector 4- inlet chamber 5- perforated chamber 6- outlet chamber 8- outlet tubing 9- tissue sample* ***(C)*** *3D rendering of the microfluidic device including measurements.*

2.1.2.3) Workflow

During surgery, some of the resected tumour is transported to laboratory and cut into multiple slices. Most of these slices are incubated on chip and then processed for various different techniques in order to quantify differences in cell proliferation, cell death, metabolic capacity, gene expression and protein expression (Figure 2.2). A slice was also reserved for baseline comparisons.

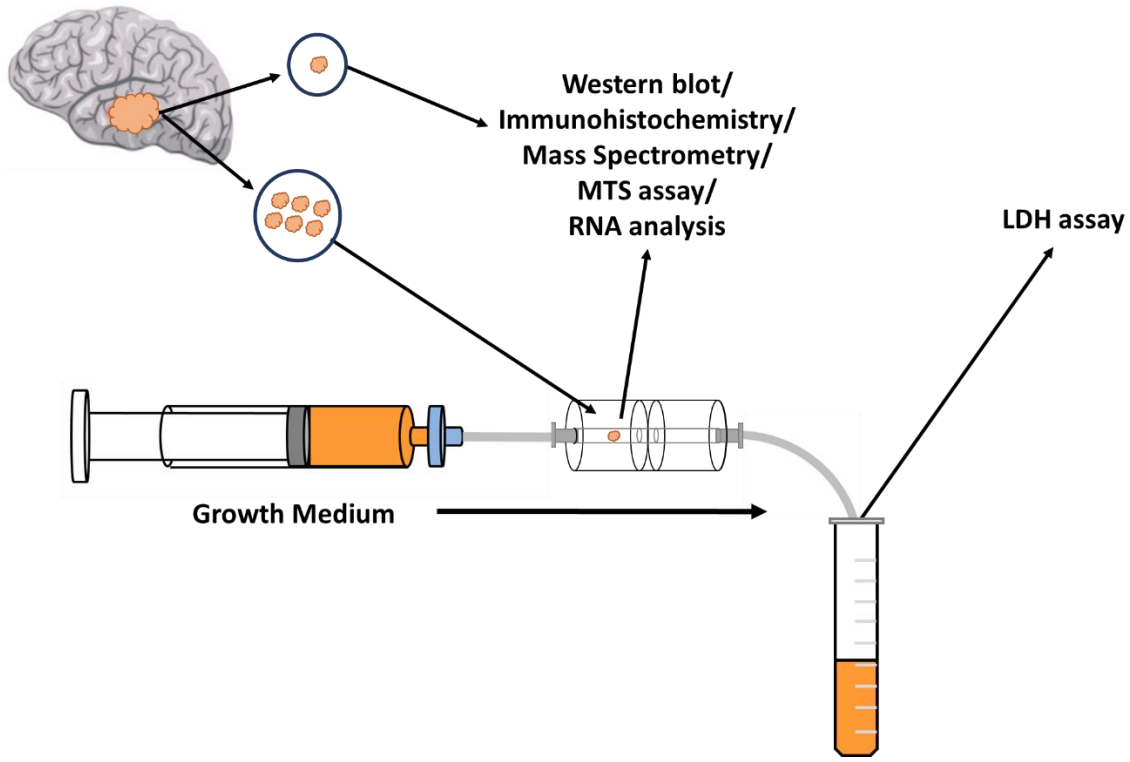

Figure 2.2: Schematic to demonstrate the workflow involved in the microfluidic experiments. *The patient samples are sectioned and transferred to the microfluidic devices and connected to the syringes holding growing medium. For every patient sample, pre-chip sections are set aside and processed for either western blot, IHC, mass spectrometry, and/or RNA analysis, depending on the requirements of the experiment. The on-chip sections are perfused with growth medium containing different treatments and are also then processed for either western blot, IHC mass spectrometry, RNA analysis, and/or MTS assay. The effluent that flows over the incubated samples is also collected at intervals and processed for LDH assay.*

2.1.2.4) Pre-Sample Preparation

All handling and preparation of tissue and equipment was carried out under sterile conditions in an Air Stream Esco class II hood. Prior to sample collection, the required number of syringes were filled with DMEM medium with the appropriate dilution of drug. The syringes were then connected to a filter and via the tubing, to the microfluidic device. Media was then pumped manually through the device until the tubing was filled and no bubbles were present.

2.1.2.5) Sample Preparation

Patient samples were sliced with two surgical blades on a 10 cm petri dish into multiple sections of equal size and their weight measured and recorded (average of 20 mg depending on mass of sample collected). The inlet tubing was removed, and sections were transferred to the inlet chamber of the microfluidic device with forceps. Any air space remaining in the inlet chamber was replaced with media, and the inlet tubing reconnected.

During this process, it was important to minimise the existence of gaseous bubbles within the syringes, tubing and device. To ensure this, all materials were maintained at 37˚C prior to sample collection and a filter was attached to the syringes (Figure 2.3).

2.1.2.6) Sample Incubation

The syringe, tubing, and device containing the patient sample was fitted into the Harvard pump (Figure 2.3). The media was then perfused through the tissue at a rate of 3 µL per minute. The effluent initially collected after 3 hr and then at 24 hr intervals up to 168-244 hr. The effluent was stored at 4 °C until analysed. At the end of the incubation period, the samples are either processed for western blot, MTS assay, LDH assay, IHC and/or mass spectrometry.

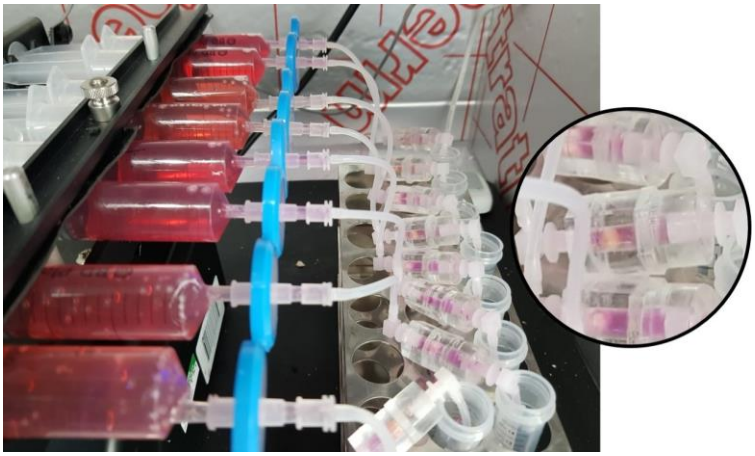

Figure 2.3: ***Photograph encompassing the main materials involved in the patient sample incubations.*** *Includes syringes, filters, tubing, microfluidic devices and collection tubes. This set up is placed in a temperature-controlled incubator set to 37 °C using a heat mat.*

2.2) Western Blot

2.2.1) Cell Lysis

U-87MG cells were dislodged from either a T25/75/175 flask or 6-well plate using a cell scraper and collected into a 15 mL centrifuge tube alongside the media. The cells were centrifuged in a 15 mL tube for 5 min at 4˚C at 400 g and supernatant discarded. The cell pellet was resuspended in cold PBS and centrifuged for 5 min at 4˚C at 400 g and supernatant discarded. This washing step was then repeated.

2.2.1.1) Cell lysis for analysis of 2D cell line model

The cell pellet was resuspended in 1% NP40 + 1% Triton X-100 in PBS plus protease inhibitor cocktail (Pierce Protease Inhibitor Tablets (Thermo Fisher)) and incubated at 4˚C whilst rotated for 1 hour and centrifuged for 20 min at 4˚C at 16200 g and the supernatant transferred to a cold 1.5ml microcentrifuge tube, stored at -20˚C and pellet discarded.

2.2.1.2) Cell lysis for analysis of spheroid cell line model

The cells were resuspended in 5% (w/v) sodium dodecyl sulphate (SDS), sonicated for 10 min on the Bioruptor (Diagenode) on the high setting with 30 second intervals and incubated at 4˚C for 15 minutes, and allowed to reach room temperature to solubilise the SDS. Cells were then centrifuged for 20 min at 4˚C at 16200 g and supernatant transferred to a 1.5ml microcentrifuge tube and pellet discarded.

2.2.1.3) Cell Lysis of Patient samples

The samples were removed from the inlet chamber using forceps and transferred to a microcentrifuge tube and grinded with a plastic douncer in 300 µL 1 % (v/v) Triton X-100 in PBS for approximately 30 strokes. Once homogenous, 100 µL was stored at 4°C for use in the LDH assay (section 2.5) and 200 µL was processed for western blotting as follows.

2.2.2) Protein Determination and Protein Reduction

To allow for even loading of protein lysates, the concentration of protein in each sample was determined using the Pierce BCA Protein Assay kit (Thermo Fisher) according to manufacturer's instructions. The absorbance of the samples was measured at 595 nm using the BioTek™ ELx800™ absorbance microplate reader. The absorbance of Bovine Serum Albumin (BSA) standards were plotted against protein concentration to produce a standard curve from which an equation was used to calculate the protein concentrations of samples. Volumes equivalent to 10-40 µg of protein for each lysate were then aliquoted into new tubes and more lysis buffer added to make a total volume the same for each sample. The lysates were then incubated with appropriate volume of x4 SDS buffer (40% (v/v) Glycerol, 8% (v/v) SDS, 10% (v/v) Beta-Mercaptoethanol, TBS (20 mM Tris-base, 1.5 M NaCl, pH 7.6)) at 100 ˚C for 5 min.

2.2.3) SDS-PAGE and Western Transfer

Acrylamide gels were prepared at 12% (Tris, 0.1% (v/v) SDS/ 12% (v/v) acrylamide/ tetramethylethylenediamine (TEMED)/ammonium persulfate (APS)) and placed in a running buffer (0.1% (v/v) SDS, 50 mM Tris-base, 0.4 M Glycine).

10-40 µg of lysates were loaded into wells and resolved through the gel at 80 V for 2 hr at room temperature using the Mini-PROTEAN Tetra Cell (Bio-Rad). Proteins were then transferred to a nitrocellulose membrane (GE Healthcare) through a transfer buffer (20 mM Tris-base, 0.15 M Glycine, 0.1 % (v/v) SDS (in 20% methanol in distilled water) for 2 hr at 100 V on ice using the Mini Trans-Blot® Cell (Bio-Rad). Membranes were retrieved and proteins revealed by incubation with Ponceau S for 5 min. Ponceau S was removed by washing with TBST (1x TBS + 0.1% (v/v) Tween). Membranes were blocked in 5% (w/v) milk in TBST for 1 hr at room temperature and incubated in primary antibody overnight at 4 ˚C according to the dilutions in Table 2.1.

Table 2.1: Primary and secondary antibodies used in this study with species, dilution, company purchased from and catalogue numbers.

Target	Host species	Dilution	Source	Catalogue Number
Primary				
GAPDH	Mouse	1/5000	Cell Signalling Technologies	97166
Actin- HRP conjugated	Rabbit	1/1000	Cell Signalling Technologies	12620S
PRMT1	Rabbit	1/1000	Abcam	Ab73246
PRMT2	Rabbit	1/1000	Abcam	Ab66763
PRMT3	Rabbit	1/1000	Abcam	Ab191562
PRMT4	Rabbit	1/1000	Abcam	Ab50214
PRMT5	Rabbit	1/1000	Abcam	Ab109451
PRMT6	Rabbit	1/1000	Abcam	Ab190902
PRMT7	Rabbit	1/1000	Abcam	Ab22110
PRMT8	Mouse	1/1000	Abcam	Ab168134
PRMT9	Rabbit	1/1000	Abcam	Ab122374
ADMA	Rabbit	1/1000	Cell Signalling Technologies	13522S
SDMA	Rabbit	1/1000	Cell Signalling Technologies	13222S
MMA	Rabbit	1/1000	Cell Signalling Technologies	8015S
Acetyl-Lysine	Rabbit	1/1000	Cell Signalling Technologies	9441S
Secondary				
Mouse	Goat	1/3000	Dako	P0161
Rabbit	Goat	1/5000	Dako	P0448

Membranes were then washed twice in TBST for 10 min and TBS once for 10 min and incubated with the corresponding HRP conjugated-secondary antibody for 1 hr at room temperature according to the dilutions in Table 2.1. Membranes were washed as above. 1 mL of Enhance Chemiluminescence (ECL) was added to each membrane and proteins were visualised using the ChemiDoc machine (Bio-Rad).

2.3) MTS Assay

2.3.1) MTS Assay Concept

The MTS assay is a substitute for a cell proliferation assay and is often used to investigate the action of anti-tumour drugs in cancer cell lines (Primon et al., 2013). The assay utilises the cell's metabolic ability to convert a tetrazolium salt into a formazan salt using nicotinamide adenine dinucleotide + hydrogen (NADH), a reaction which is detectable by a change of colour from yellow to red.

2.3.2) Monolayer cell Line model

The MTS reagent (Abcam) was added to the cells at 10% (v/v) concentration and incubated for 3 hr. Three wells containing only media and the MTS reagent were used as blanks. Absorbance was read at 490 nm using the BioTek™ ELx800™ absorbance microplate reader, with correction reading at 680 nm. This correction removes any alterations to absorbance values caused by plate variation and surface marks. The average blank absorbance value was subtracted from each sample absorbance value, the average absorbance calculated amongst biological replicates, and the resulting values normalised against a non-treated control when applicable. This normalisation was done by dividing each average by the control, including itself.

2.3.3) Spheroid cell Line model

The MTS reagent was added to the cells at 10% (v/v) concentration and incubated for 3 hr. Following incubation, the plates were shaken to evenly distribute the MTS product in the wells. Then, 80 µL was transferred to a clean flat bottomed 96-well plate, as to not have interference from the agarose or well curvature. The procedure was then carried out as in section 2.3.2.

2.3.4) Microfluidic model

Following incubation, samples were transferred with forceps into a well of a 96 well plate containing 100 µL of media. The media used was taken from the remainders in the syringes. 10 µL of MTS reagent was added to each well and incubated for 6 hr at 37 °C. Like the spheroid model, following incubation, the plates were shaken to evenly distribute the MTS product in the wells. Then, 80 µL was transferred to a clean flat bottomed 96-well plate. The procedure was then carried out as in section 2.3.2.

2.4) LDH Assay of Patient Samples

The Lactate Dehydrogenase (LDH) assay works by a similar mechanism to the MTS assay previously explained, however, it does not depend on the ongoing metabolic activity of the cells. Included in the reagents used, are all the components required for the reaction (Figure 2.4) to take place, excluding LDH. This means LDH is the limiting factor of this process, and therefore the production of the coloured formazan salt is dependent upon the LDH present in the effluent.

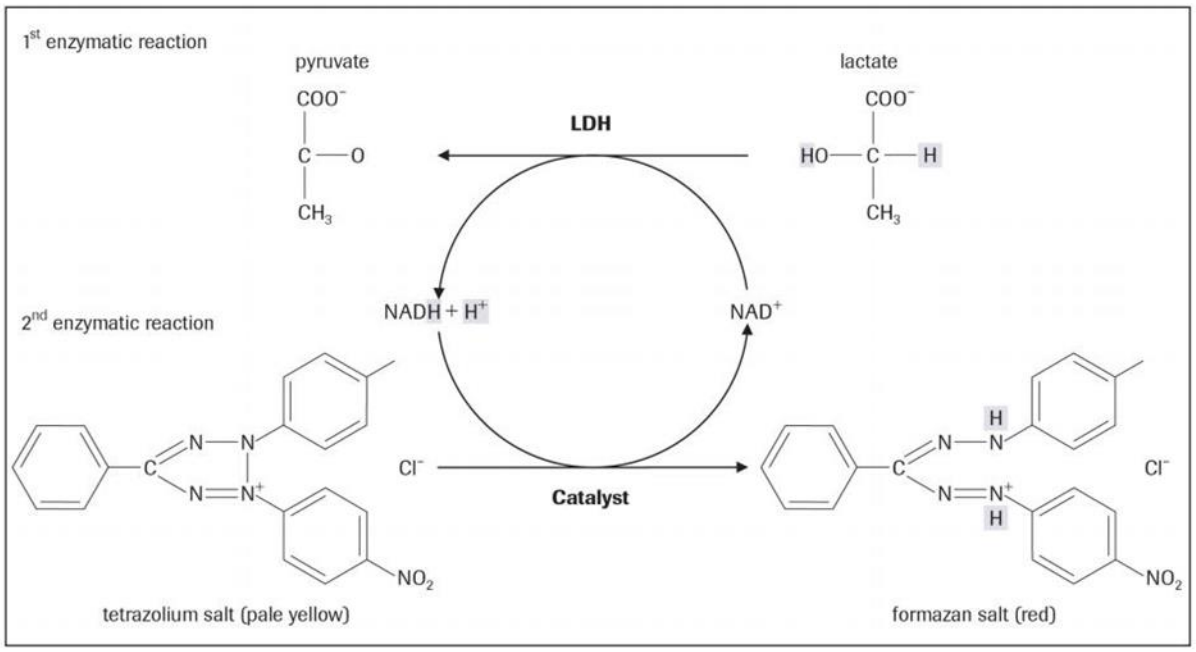

Figure 2.4: The mechanistic action of the LDH assay. *LDH that is released into the effluent converts lactate into pyruvate, producing NADH + H+ as an additional product. This is then used by the catalyst to convert a tetrazolium salt into a formazan salt.*

LDH assays were carried out using the Cytotoxicity Detection KitPLUS (Roche). The patient samples were removed from the inlet chamber using forceps and transferred to a microcentrifuge tube and grinded with a plastic douncer in 300 µL 1 % (v/v) Triton X-100 until homogenous. 100 µL was stored at 4°C for use in the LDH assay and 200 µL was processed for western blotting.

A serial dilution of LDH was first prepared and plated onto a 96 well plate in triplicate, starting from 1 Unit of LDH to 0.002 Units. The lysed samples and effluent samples were transferred onto the plate by adding 50 µL of each sample in triplicate. 50 µL of DMEM media was also added to the plate to act as a background control. 50 µL of the reaction mixture (Diaphorase/NAD+ mixture/Iodonitrotetrazolium and sodium lactate) was added to each well and the plate was incubated at 37°C for 30 minutes in the dark. 25 µL of stop solution (1M Hydrochloric acid (HCl)) was added and then plate was read at 490 nm with a correction of 680 nm using a spectrophotometer. Actual LDH concentration would then have been calculated in the samples by using the equation of the line of an LDH standard curve produced by a dilution series of known LDH concentrations. However, neither a linear or logarithmic relationship was produced, and so calculations made from a line of best fit would not have been accurate (Figure 2.5). Therefore, absorbance at 490 nm has been substituted for a marker of cell death, rather than an actual LDH concentration.

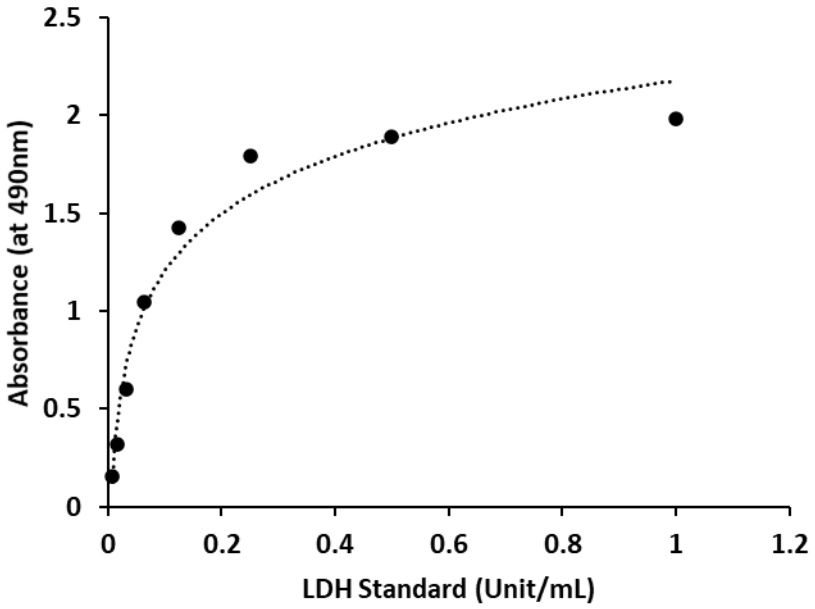

Figure 2.5: A standard curve of LDH standard vs absorbance used to quantify the LDH concentration in the effluent and lysed samples. *Here, a logarithmic model is used to fit the data (y = 0.4224ln(x) + 2.1782). However, multiple points do not fit this model. N=15.*

2.5) Immunohistochemistry of patient samples

2.5.1) Immunohistochemistry Staining Introduction

IHC can be utilised to quantify various cellular processes within tissue samples such as proliferation, apoptosis and senescence. The tissue is incubated with antibody specific against markers of these particular pathways.

Ki-67 is a marker of proliferation widely used in IHC and is especially useful in cancer cell activity. It is expressed at the protein level in all stages of the cells cycle, apart from G0, when the cells are in a quiescent state (Gerdes et al., 1984). Because of this, it is possible to quantify and compare the rate of proliferation of tissue by calculating the proportion of positively stained nuclei (Ki-67 index) (Zeng et al., 2015).

2.5.2) Sample Preparation

2.5.2.1) Samples prior to SD0033

Samples were removed from the inlet chamber with forceps and transferred to a microcentrifuge tube and fixed in 4% (v/v) paraformaldehyde for 2 hr at 4 °C. The sample was then incubated in 30% (w/v) sucrose for 24 hr at 4 °C and then placed on a piece of cork and frozen in optimal cutting temperature (OCT) (Agar Scientific) medium at -80 °C until ready for cryosectioning. Sucrose acts as cryo-protection by dehydrating the sample and reducing freezing damage caused by ice crystal formation, a

methodology currently utilised in GBM IHC (Dodd et al., 1986, Gao et al., 2019a). During cryosectioning, samples were cut into 10 µM thick slices and placed onto poly-L-lysine (Sigma) treated microscope slides and stored at -20 °C.

2.5.2.1) Samples from SD0033

For later samples (SD0033, SD0034, & SD0035) an alternative protocol was utilised to prepare the tissue for IHC. This minimised freezing artefacts by speeding up the freezing process. For these samples, an aluminium beaker was filled three quarters with 2-Methylbutane (Sigma) and placed into a dewar containing liquid nitrogen. The tissue was acclimatised in OCT for 10 minutes and placed into a cryomold (Agar Scientific) containing fresh OCT. The mould was then lowered into the cold methyl-butane until a small area of OCT (around 1 mm) remained unfrozen, to prevent cracking of the sample. The samples were then immediately transferred to a -80 °C freezer.

2.5.3) Slide Processing

2.5.3.1) Initial Steps for Samples prior to SD0033

Slides were rehydrated in increasing grades of alcohol and boiled in antigen retrieval buffer (10 mM Citric acid pH 6) for 20 minutes in a 700 W domestic microwave.

2.5.3.2) Initial Steps for Samples from SD0033

As samples SD0033-36 were not fixed prior to freezing, they required fixing before staining and this was done by incubating in cold 100% methanol for 15 minutes. However, these samples did not require rehydration or antigen retrieval.

2.5.3.4) Following Steps for all Samples

The Vector stain Elite Kit (Sigma) and the Vector block kit (Sigma) were used to prepare and probe the slides (Carr et al., 2014). The slides were rinsed in running water before endogenous peroxidase activity was blocked with 3% (v/v) H_2O_2 in methanol for 15 minutes. Following another rinse with water, slides were assembled into sequenza racks and washed 3 times with TBS. The slides were blocked for non-specific binding by incubating with normal horse serum provided with the Vector stain Elite kit for 15 minutes. Non-specific binding was further blocked by incubation with Avidin and Biotin solutions, with three TBS washes in between. Slides were incubated with primary antibody (Table 2.2) overnight at 4 °C or for 1 hr at room temperature and washed three times in TBS.

Table 2.2: The primary antibodies utilised in immunohistochemical staining of GBM samples.

Target	Host Species	Dilution	Source	Catalogue number
Ki-67	Mouse	1/200	Dako	M7240

Slides were then incubated with secondary antibody for 30 minutes (included the Vector stain Elite Kit - biotinylated horse anti-mouse/rabbit IgG). A mixture of Avidin and Biotinylated HRP was added for 30 minutes, and slides washed three times in TBS. Slides were incubated with 3,3′-Diaminobenzidine (DAB) and H_2O_2 for 5 minutes and rinsed with water. Slides were counterstained with Harris haematoxylin for 20 seconds and rinsed with water. The samples were dehydrated in increasing grades of ethanol and mounted onto coverslips using histomount (Scientific Laboratory Supplies).

2.5.4) Immunohistochemistry Quantification

Brightfield photos of the slides were taken on an Olympus microscope at x40 magnification. Photos were then processed in Cell Profiler 4.0.6. and the number of DAB stained cells (Ki-67 positive) and total cells (haematoxylin-stained) were automatically counted. Approximately 24 images were taken per microscope slide, with 3 microscope slides per biopsy slice. Images were taken across the entire section, moving the microscope platform horizontally in alternating fashion and fields chosen at random. All images for one tissue treatment were inputted into Cell Profiler and the pipeline run, with data exported to a spreadsheet. The number of positive cells was divided by the total number of cells to give the Ki-67 index (Figure 2.6).

$$\frac{\text{Total positive cell counts per sample}}{\text{Total cell counts per sample}} = \text{Ki-67 Index}$$

Figure 2.6: The calculation of Ki-67 index.

The Cell Profiler pipeline, developed by my colleague Antionia Barry, is depicted in Figure 2.7. The Cell Profiler pipeline was validated using images from sample SD0032, which had been DAB stained for Ki-67 protein positivity. The 'Unmix Colours' module transforms the coloured images into greyscale, allowing the 'IdentifyPrimaryObjects' modules to distinguish cell borders. Diameter range of the cells was determined using the scale bar included in the Olympus microscope images. The 'threshold strategy' was set to global, which calculates a single threshold value based on the unmasked pixels of the input image and 'threshold method' was set to Otsu, with three class thresholding. This separates the cell gradient into three-pixel intensities, of which the middle intensity is set to background. In this way, the 'Identify ObjectIntensity' module will only count the brightest intensity as a cell and will eliminate any background noise. Cell objects were distinguished by shape, as intensity tended to differ due to the quality of tissue staining and the changes to the threshold correction factor were able to overcome some object distinctions. For positive cells, the smoothing filter was set manually to 15, to aid in the distinction of positive cells between clumped objects. Suppression of local maxima at a pixel distance of 30 was found to most effectively separate clumped objects, by disregarding any high intensity pixels within a 30-pixel distance between two individual objects. For total cells, the pipeline

to was set to automatically calculate the ideal smoothing filter and distance between local maxima, based upon the typical object diameter. This is because there is more variation between object diameter for total cells.

Parameters to identify the cells were refined in 'Test Mode', modifying the threshold correction factor and the lower and upper bounds on the threshold of the module 'IdentifyPrimaryImages', to account for differences in staining and tissue characteristics. All other parameters were kept the same, with the exception of the option to fill in the holes within identified objects, which was done after both thresholding and declumping for total cell count (module indicated by red arrow, Figure 2.7) and after declumping only for positive cell counts (module indicated by green arrow). This is because the pipeline tended to disregard lower intensity, positive cells when the threshold correction factor was increased, which was necessary to eliminate some high intensity negative cells from being included in the positive cell count. The 'OverlayImages' module (indicated by purple arrow) produced alternately coloured outlines around each object it had identified as a cell and saved this image. These images were then reviewed manually, and any incorrect object designations reassigned before calculating positive protein index.

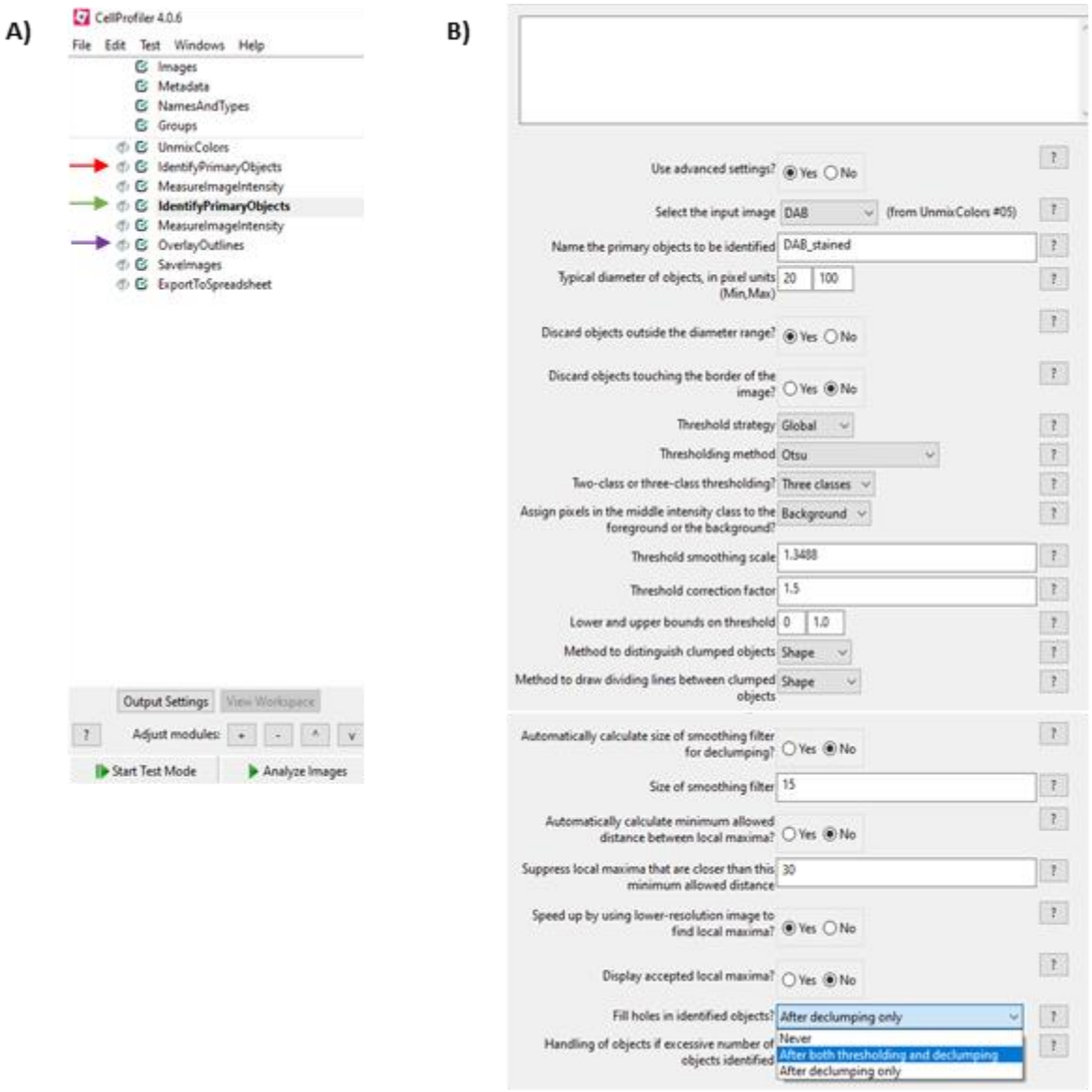

Figure 2.7: The cell profiler pipeline *(A) Cell Profiler 4.6.0 pipeline for automated IHC-image cell counting and (B) IdentifyPrimaryObjects module for positive cell counting. Red arrow indicates the module in which parameters were changed to determine total cell counts. Green arrow indicates the module in which parameters were changed to determine positive cell counts. Purple arrow indicates the module which set outlines over the processed images.*

For the SD0032 validation image sets, these counts were compared with manual cell counts and percentage error and standard deviation calculated for Ki-67 index, per sample. For all samples, percentage error for total sample Ki-67 index was calculated to be under 5% for both positive and total cell counts, and standard deviation was <0.01. Manual object reassignment was still performed for each slide, due to some of the validation images having a higher percentage error than the average – however, this is to be expected in many cases due to the lower numbers of positive cells.

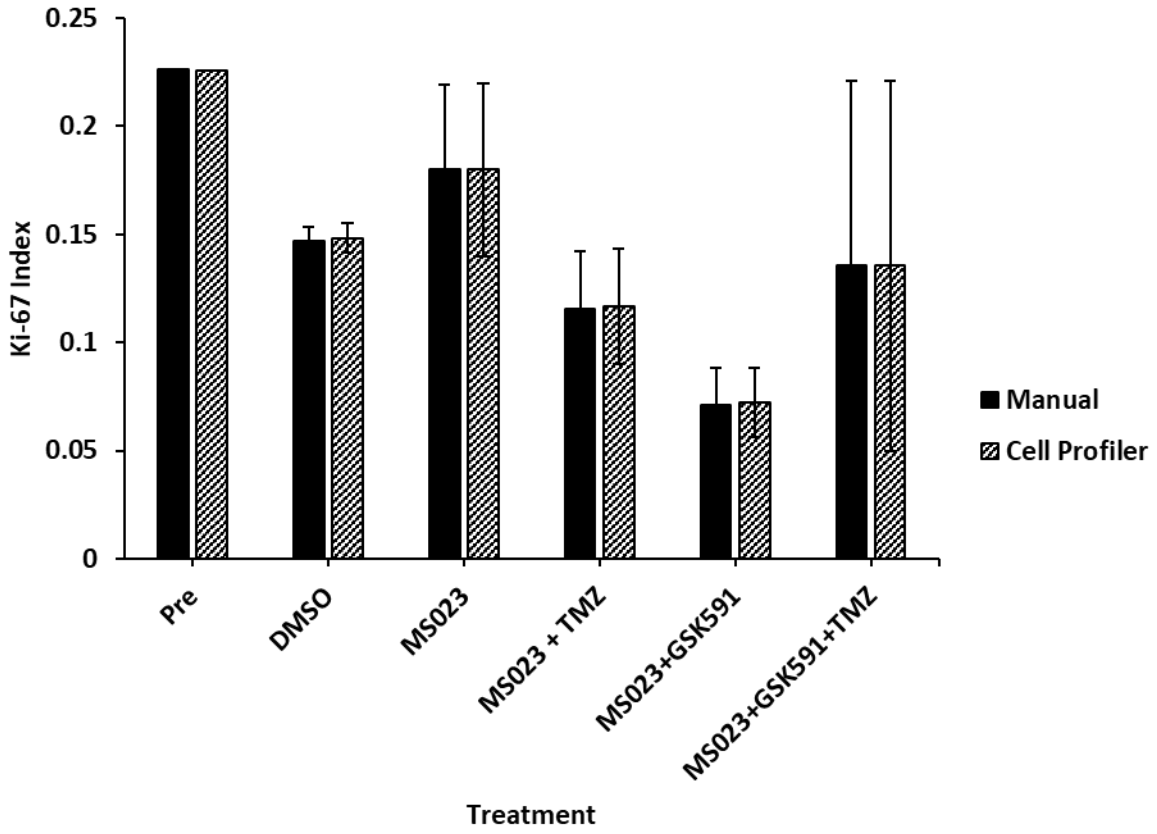

Figure 2.8: Ki-67 of control and treat patient biopsies measured both manually and through the Cell Profiler pipeline. *Error bars represent standard deviation between two biopsy slices ran in parallel.*

Chapter 3 – Investigating Arginine Methylation in GBM Using 2D and 3D Cell Models

Results in this chapter have been published in *Proteomes*

Samuel, S. F., Marsden, A. J., Deepak, S., Rivero, F., Greenman, J., & Beltran-Alvarez, P. (2018). Inhibiting Arginine Methylation as a Tool to Investigate Cross-Talk with Methylation and Acetylation Post-Translational Modifications in a Glioblastoma Cell Line. Proteomes, 6(4), 44.

3.1) Introduction

3.1.1) PRMT Inhibition as a GBM Treatment

PRMTs are involved in numerous cellular processes, such as those linked to tumorigenesis, including proliferation and DNA repair. Certain PRMTs, including PRMT1, PRMT2 and PRMT5 have been found to be upregulated in GBM. This increase in expression of PRMTs results in a dependency upon the enzymes which can possibly be exploited as a new therapeutic option.

A number of PRMT inhibiting drugs are commercially available with varying specificities. These include the broad acting inhibitor AMI-1, that inhibits all PRMTs excluding PRMT5; GSK591, a PRMT5 specific inhibitor; MS023, a type I PRMT inhibitor; and Furamidine, a PRMT1 inhibitor. The bioavailability of some PRMT inhibitors has been investigated, with GSK591 and LLY-283 being able to cross the BBB, as demonstrated by either an anti-tumour effects in xenograft models (Chan-Penebre et al., 2015), or direct measurement of the drug in brain samples (Sachamitr et al., 2021).

Interactions between ArgMe and other PTMs are becoming more apparent and have been demonstrated predominantly in the form of genetic regulation through histone modifications (Guccione and Richard 2019). Similar forms of interactions exist which involve non-histone proteins, including the methylation of apoptosis signal-regulating kinase 1 (AKS1) at R89, that interacts with S83 phosphorylation by Akt (Chen et al. 2016). The relevance of this interplay in the development of cancer is becoming more and more apparent and has been shown to play a role in breast and lung cancer (Hsu et al., 2011, Liu et al., 2020). Certain PTMs have been implicated in GBM progression, including PRMTs, as previously stated, and lysine acetylation (Panicker et al., 2010). Possible interplay amongst these enzymes were therefore investigated through the inhibition of PRMTs.

3.1.2) Aims and Objectives

The objectives of the experiments in this chapter are:

- To determine whether PRMT -1 to -9 are expressed in the GBM cell line U-87MG using western blotting.

- To evaluate efficacy of PRMT inhibiting drugs on the GBM cell line U-87MG in a 2D monolayer model and in a 3D spheroid model using an MTS assay.
- To confirm drug specificity and explore cross-talk between inhibition of ArgMe and other PTMs using western blotting of treated U-87MG samples.

3.2) Materials and Methods

3.2.1) Cell Plating

For MTS assay experiments, U-87MG cells were plated in triplicate in a flat bottomed 96 well plate at 2000 cells/well in 100 µL growing medium and allowed to settle for 24 hr. For spheroids, U-87MG cells were plated at 20,000 cells/well in 100 µL in a round bottomed 96 well plate onto 100 µL of 1.5% (w/v) agarose in PBS and incubated for 72 hr prior to treatment. During this time, the cells came together to form a spheroid shape, approximately 500 µM in diameter. The high cell number allowed for an earlier formation of larger spheroids.

For western blotting experiments, U-87MG cells were plated in duplicate on a six well plate at 250,000 cells/well in 1 mL and allowed to settle for 24 hr. For spheroids, U-87MG cells were prepared as above.

3.2.2) Drug Treatment

For serial dilution treatments (3.3.2), a serial dilution of GSK591 (Sigma) and Furamidine (Tocris Bioscience) was prepared at double concentration (12.5-200 µM) in a 6-well plate. For each concentration, 100 µL was then added to the cells (already containing 100 µL medium) to make final concentrations of 6.25-100 µM; cells were then incubated for 48 hr.

For time course treatments (3.3.3-6) drug dilutions of GSK591 (Tocris Bioscience), AMI-1 (Sigma), MS023 (Tocris Bioscience) and Furamidine (Tocris Bioscience) were prepared at double the desired concentrations and 100 µL added to the cells to give a final concentration of 100 µM in 200 µL. Cells were incubated for 72, 96 and 144 hr.

3.3) Results

3.3.1) Expression of PRMT1, 2, 3, 4, 5, 6, 7, 8, and 9 found in U-87MG cell line

The first aim of this project was to determine the expression of the currently known PRMTs (PRMT1-9) in the GBM cell line U-87MG. PRMT1, PRMT2, PRMT3, PRMT5, PRMT6, PRMT7, PRMT8 and PRMT9 were found to be expressed by U-87MG cells as determined by western blotting (Figure 3.1) with the majority of bands appearing at the correct molecular weight. PRMT4 could not be detected but this was not confirmed with further antibodies. PRMT8 and PRMT9 antibodies detected bands 10 kDa

higher and 15 kDa lower, respectively. There are two PRMT9 isoforms produced by alternate splicing, this second isoform is 82 kDa (Q6P2P2-2) and so is likely to be responsible for the band recognised here. PRMT8 on the other hand does not have any currently known isoforms approximately 60 kDa in weight. The observed weight of PRMT8 could be due to modifications such as methylation (Dillon et al., 2016) and myristoylation (Sayegh et al., 2007). Other bands can also be seen for other PRMTs, including PRMT1. These are either isoforms of different molecular weights or non-specific binding.

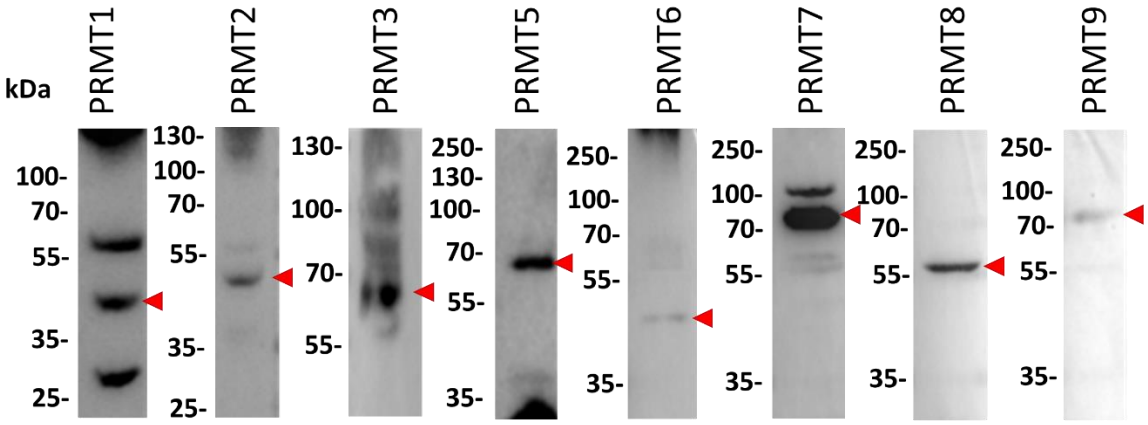

Figure 3.1: Expression of PRMT1-9, excluding PRMT4 in U-87MG cell line. *U-87MG cells were harvested from 75 cm² culture flasks and processed for western blotting according to section 2.2. Expected molecular weight: PRMT1- 42 kDa, PRMT2- 46 kDa, PRMT3- 60 kDa, PRMT5- 73 kDa, PRMT6- 42 kDa, PRMT7- 78 kDa, PRMT8- 45 kDa, PRMT9- 94 kDa. Multiple bands can be seen in all samples which are most likely due to the various isoforms of each PRMT and unspecific binding. The blots shown are representative of 2 independent experiments (N=2).*

3.3.2) Determining sensitivity of U-87MG cells to type I and type II PRMT inhibitors

As the majority of PRMTs were found to be expressed in U-87MG cells, these cells could be used to investigate treatment with PRMT inhibiting drugs. The next aim of this project was to determine the efficacy of such PRMT inhibiting drugs by assessing cell viability following treatment, via an MTS assay.

U-87MG cells, grown as a monolayer, were treated for 48 hr with a dilution set of Furamidine and GSK591, to establish concentrations that would be used for further treatments. Little to no effects were observed at lower concentrations (<50 µM). Although cell viability was not reduced to 50%, the most effective concentration, out of those tested, for Furamidine was 100 µM. GSK591 treatment did not cause any loss in cell viability, regardless of drug concentration (Figure 3.2). Previous studies using a similar analogue of GSK591, GSK3235025 or EPZ015666, had shown mild inhibition of cell proliferation in GBM cell lines at 10 µM, and so higher concentrations of drug were not tested here (Braun et al., 2017).

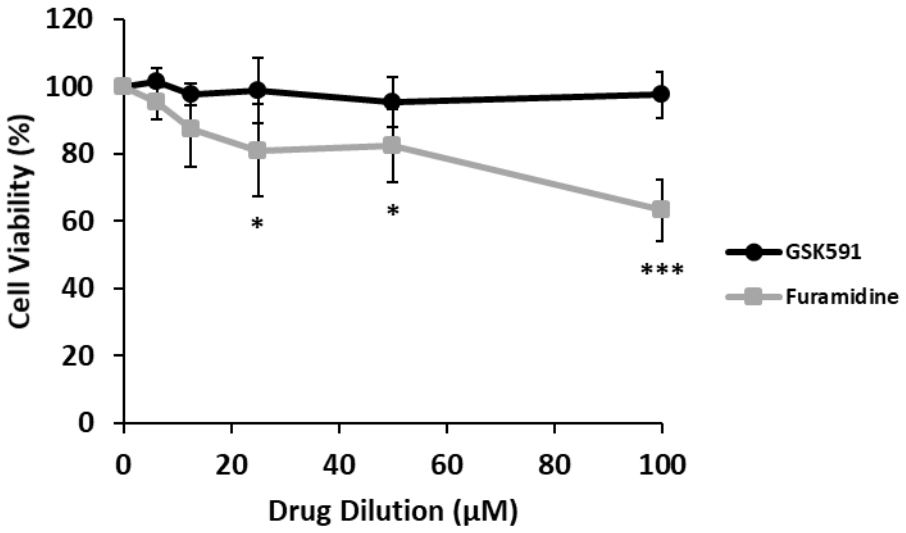

Figure 3.2: The effect of increasing concentrations of Furamidine and GSK591 on cell viability of U-87MG cells. *U-87MG cells were plated in triplicate at optimal density and treated with either GSK591 or Furamidine for 48 hr at concentrations 6.25, 12.5, 25, 50 & 100 µM. Cell viability was determined by MTS assay. Error bars represent standard deviation. Statistical analysis by two-way ANOVA showed no significant decrease in cell viability for any dilution of GSK591 but significant decreases for 25, 50 and 100 µM of Furamidine were observed compared with no drug. * p<0.05 *** p<0.005. N=4.*

3.3.3) The effect of PRMT inhibitors on U-87MG cell growth in both 2D and 3D spheroids

Treatment of U-87MG cells with PRMT inhibitors resulted in a range of responses. In the 2D model (Figure 3.3), GSK591, AMI-1, and MS023 did not result in a significant loss in cell viability according to the MTS assay, despite a high concentration (100 µM) of drug being used. Furamidine treatment caused the greatest loss of cell viability, with a reduction of 80% at 96 hr.

In order to improve the likeness of this model to the true tumour environment, the U-87MG cells were also grown on agarose gel to induce the formation of spheroids. These spheroids were then treated with PRMT inhibitors for 96, 120, and 144 hr. An increased incubation time was used to allow for penetration of the drug into the spheroid structures (Wang et al., 2013). A similar trend was observed, with little to no effect observed following treatment for all drugs, apart from Furamidine. Furamidine treatment (100 µM) caused a 30% reduction in cell viability; a less severe effect than that observed in the 2D model.

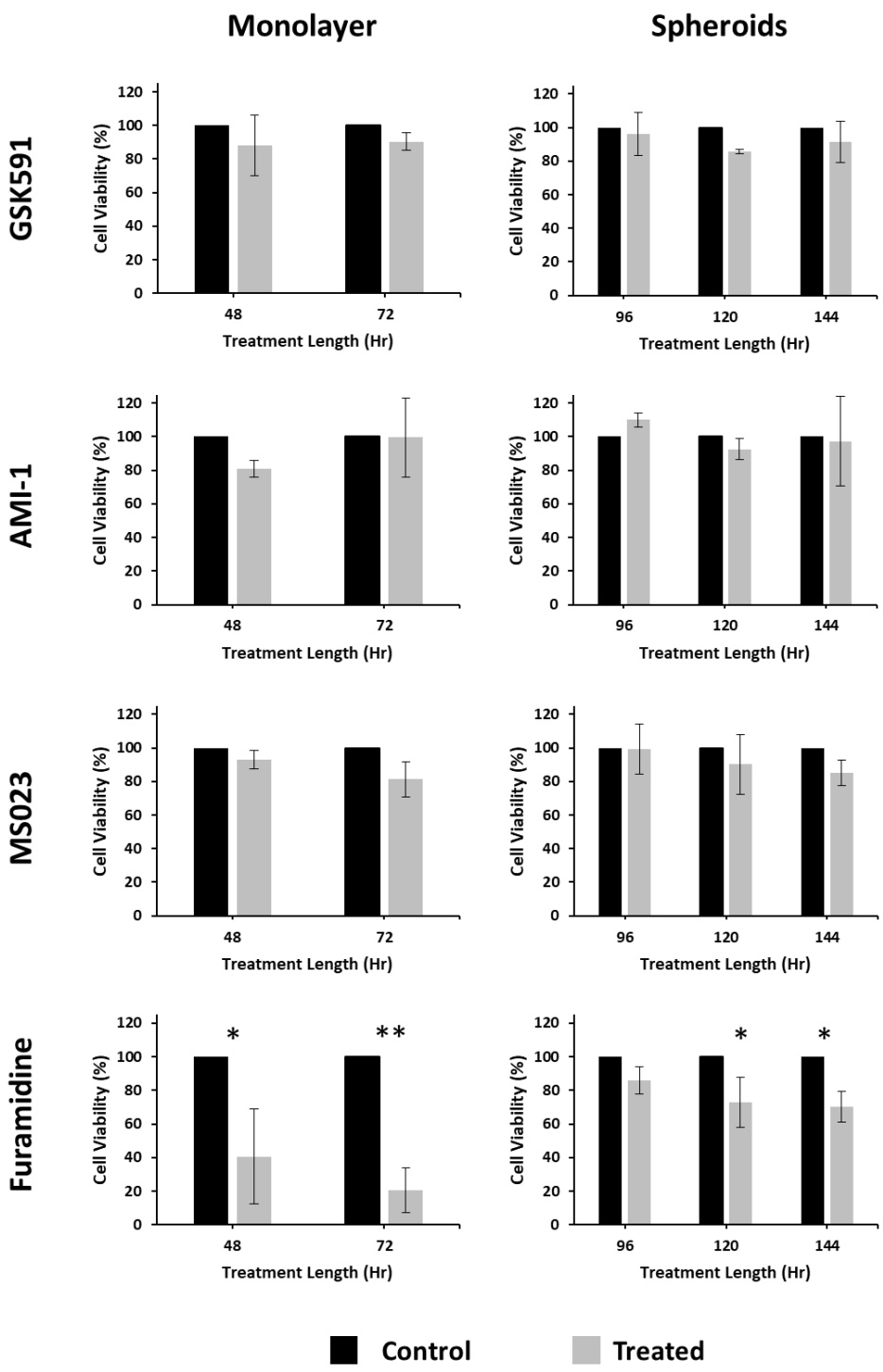

Figure 3.3: MTS assay on U-87MG cells shows a sensitivity to PRMT inhibition by treatment with Furamidine. *U-87MG cells grown in either a monolayer or as spheroids treated with 100 µM of GSK591, AMI-1, MS023 and Furamidine for 48 and 72 hr or 96, 120 and 144 hr, respectively. A one sample students t-test was then carried out using percentage values to determine if changes in cell viability at different time points were statistically significant when compared to the expected value of 100. * p<0.05 ** p<0.01. Error bars show standard deviation. N=3.*

3.3.4) Treatment with PRMT inhibiting drugs resulted in decreased Arginine Methylation in a 2D Model

In order to confirm the efficiency of the PRMT inhibiting drugs in leading to decreased ArgMe activity, treated cells were lysed, processed for western blotting, and probed with antibodies specific for either symmetric or asymmetric dimethylation. As expected, treatment with GSK591, a PRMT5 inhibitor, caused a decrease in the symmetric dimethylation of arginine residues (Figure 3.4A, red box). Likewise, treatment with MS023, a type I PRMT inhibitor, resulted in a decrease in asymmetric dimethylation of arginine residues (Figure 3.4B, yellow box). Unexpectedly, MS023 caused a decrease in certain SDMA marks (Figure 3.4A, yellow box). This may be due to unspecific activity due to the high concentration of drug used. A new band at approximately 75 kDa was produced following MS023 treatment (Figure 3.4A, yellow arrow), which will be discussed further.

Treatment with Furamidine, a PRMT1 inhibitor, resulted in the loss of ADMA of a protein with the weight of 100 kDa (Figure 3.4B, blue box), but the increased ADMA of protein at the 55 kDa marker (Figure 3.4B, green box). Given that Furamidine inhibits only PRMT1, and that MS023 is a broader acting PRMT type I inhibitor, it can be argued that this increase in ADMA at the lower band protein following Furamidine treatment is due to compensatory mechanisms by other type I PRMTs. Furamidine is a diamidine compound and has an unusual crescent shape that is able to inhibit both the active site, and substrate binding site of PRMT1 simultaneously, a characteristic thought to provide its PRMT1 specificity (Yan et al., 2014).

A broad acting PRMT inhibitor, AMI-1, was also used, and as expected, caused a decrease in both SDMA and ADMA marks (Figure 3.4A/B, orange box).

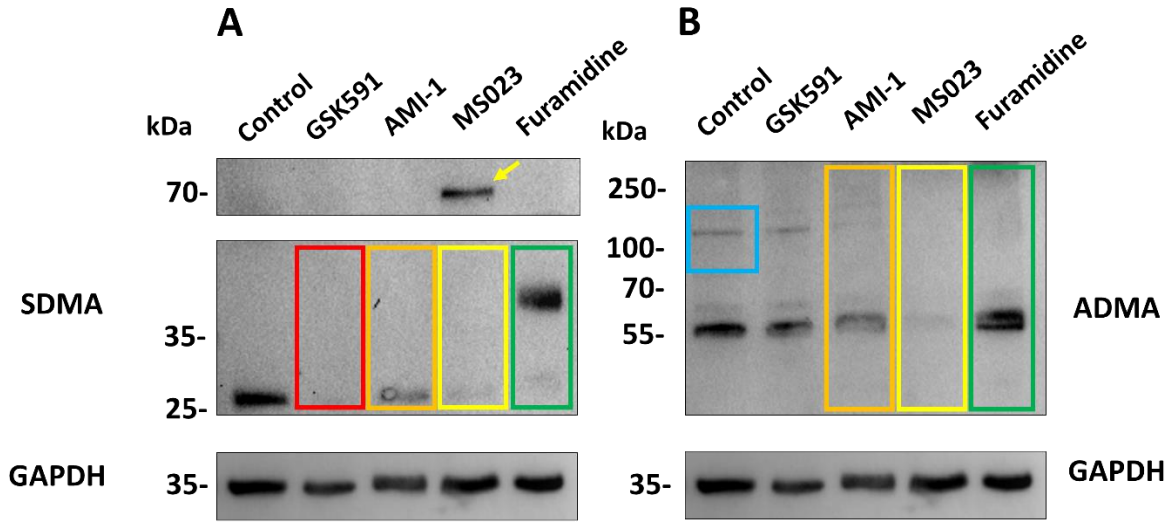

Figure 3.4: Inhibition of PRMTs in U-87MG cells results in the decrease in corresponding methylation marks. *Cells were treated with no drug (control), GSK591, AMI-1, MS023 and Furamidine at 100 µM for 48 hr and processed for western blotting. 20 µg of protein was loaded into each well. GAPDH acts as loading control. N=2. Band densitometry carried out on Image J software (Appendix 1).*

3.3.5) Treatment with PRMT inhibiting drugs resulted in decreased Arginine Methylation in a Spheroid Model

To study the effect of ArgMe in a 3D model, U-87MG cells were grown as spheroids before being treated with PRMT inhibitors. Like the monolayer model of U-87MG cells, inhibition of PRMT5 by GSK591 treatment caused a decrease in SDMA as shown through western blotting (Figure 3.5A, red box). GSK591 did however cause a reduction in ADMA marks (Figure 3.5B, red box). Inhibition of type I PRMTs by MS023 caused a decrease in ADMA (Figure 3.5B, yellow box), as expected, but also caused a decrease in SDMA marks (Figure 3.5A, yellow box). Similar to the 2D model, this may be due to the high concentration of drug used and resulting non-specific activity. AMI-1 was less effective in the spheroid model, with a minimal reduction in ADMA and SDMA marks (Figure 3.5A/B orange boxes).

The effects of Furamidine treatment on the methylation of arginine residues was not conclusive, as the loading control, GADPH, was significantly decreased, suggesting denaturation of the sample.

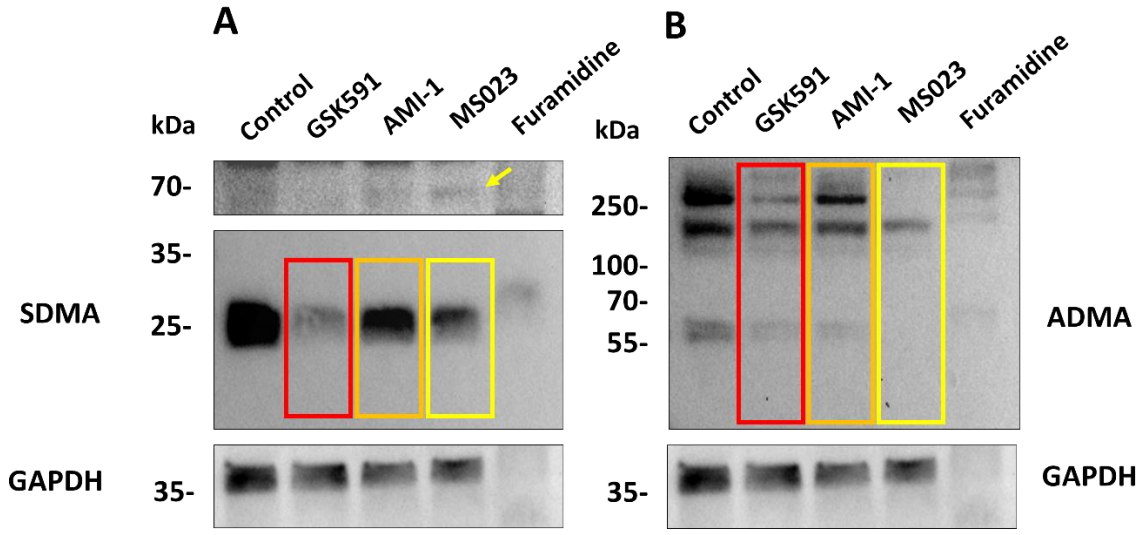

Figure 3.5: Inhibition of PRMTs in U-87MG spheroids results in the decrease in corresponding methylation marks*. Cells were grown as spheroids and treated with no drug, GSK591, AMI-1, MS023 and Furamidine at 100 µM for 96 hr and processed for western blotting. 40 µg of protein was loaded into the wells. GAPDH acts as loading control. The blots shown are representative of 2 independent experiments (N=1). Band densitometry carried out on Image J software (Appendix 2).*

3.3.6) Treatment with Furamidine Results in Cross-talk with Acetyl Lysine Modifiers in U87-MG cells and Human Platelets

The modification of proteins is a dynamic process that can involve multiple interacting mechanisms. For example, the expression of a gene is determined by the combination of PTMs on histone tails surrounding the promoter region, making up a "histone code". ArgMe has been found to co-localise on cardiac associated proteins with other PTMs, including lysine acetylation (Onwuli et al., 2017). Methylation of Arginine residues has also been suggested to interfere with the acetylation of such surrounding lysine residues (Chen et al., 2014).

The possible interactions between ArgMe and Lysine acetylation were therefore also investigated. Incubation with Furamidine resulted in loss of lysine acetylation of proteins of molecular weights of roughly 75 kDa and 10 kDa when investigated in U87-MG cells (Figure 3.6 A, red arrows). Furamidine was then used in human platelets as a further independent model, with consistent results (Figure 3.6 B, red arrow). Platelets provide a unique model to investigate post translational modifications as they have limited protein turnover due to being anucleated cells (Malchow et al., 2017). Due to their short life-span, a much shorter 4 hr incubation had to be used.

This loss of acetyl-lysine marks could have occurred due to a number of explanations. Firstly, Furamidine could act as a direct inhibitor of acetyl-lysine transferase (KAT), which has not been described, or there may be cross-talk activity present between PRMTs and KATs. Furamidine could

also induce changes in gene expression, protein stability or localisation of KATs or deacetylases, all of which may result in the observed loss in acetyl-lysine marks.

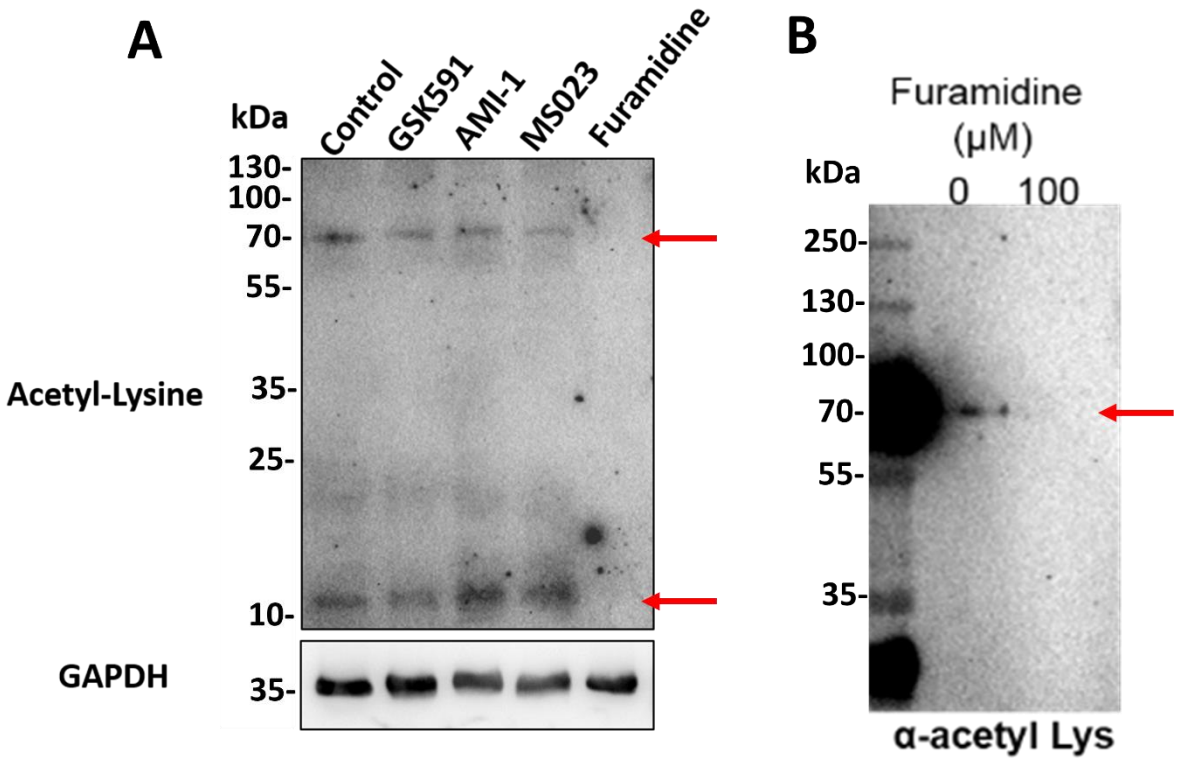

Figure 3.6: Inhibition of PRMTs in U87-MG cells and human platelets and the resulting changes in the acetyl-lysine modification. *(A) U87-MG cells grown as a monolayer were treated with treated with no drug, GSK591, AMI-1, MS023 and Furamidine at 100 μM for 48 hr (B) Human platelets were incubated with and without Furamidine for 4 hr (N=4). Platelet experiments were carried out by Alistair Marsden.*

3.4) Discussion

3.4.1) Expression of PRMT1-9 in U-87MG cell line

PRMT1, PRMT2 and PRMT5 have been shown to be expressed at relatively high levels in GBM cells compared with cell lines representing healthy astrocytes (Mongiardi et al., 2015 Braun et al., 2017, Wang et al., 2012c, Yan et al., 2014). The protein expression of other PRMTs have previously not been described in GBM cell lines, and so western blotting was used to demonstrate the expression of all PRMTs, excluding PRMT4, in U-87MG cells.

The Human Protein Atlas is a publicly available online database of protein and transcript expression data across numerous cell lines and patient samples. Data was available for the transcript expression of PRMTs1-9 (excluding PRMT8) in U-87MG cells (The Human Protein Atlas). This data was used to verify the detection of PRMT4 in U-87MG cells in previous studies as no band was identified in this current experiment. PRMT4 was found to be expressed at 49.2 transcripts per kilobase million (TPM)

with 1 TPM being a threshold of protein expression. PRMT4, however, could not be detected in this study using western blotting in U-87MG cells. PRMT4 has repeatedly been shown to be expressed in GBM patient samples and to correlate with patient survival, when analysed by microarray (Kappadakunnel et al., 2010, Dong et al., 2018). These previous studies refer to PRMT4 expression at the RNA level, suggesting there may be regulation of the transcript or protein that results in loss of PRMT4 protein expression, or that the antibody used here failed to detect the appropriate band. The latter may be the case as further antibodies were not tested and a positive control was not used.

3.4.2) U-87MG cells sensitive to PRMT1 inhibition by Furamidine and not MS023

To determine whether U-87MG cells were sensitive to PRMT inhibition, and therefore perhaps be dependent on its activity for proliferation, the cells were treated with a number of PRMT inhibiting drugs, and cell viability determined by MTS assay. Despite Furamidine and MS023 both being inhibitors of PRMT1, MTS assay revealed that the cells were sensitive only to Furamidine treatment. Western blotting also showed a mixed biological response in terms of SDMA, ADMA and acetyl lysine marks.

A possibility as to why no effect was seen with MS023 treatment was that the incubation time was not sufficient. A study investigating PRMT inhibition and proliferation treated the GBM cell line, A-172, with MS023 and then the rate of proliferation was determined by cell counting. Although they demonstrated a reduced cell count in treated samples, a significant difference in proliferation was only seen after 6 days of incubation in this monolayer culture model, with the greatest effect seen at 8 days (Gao et al., 2019b). The treatments in the monolayer culture model carried out in this chapter were only up to 72 hr. It should be noted that although cell proliferation and cell viability are both indicators of drug efficacy, they are not interchangeable, and this may also be an explanation for these contradicting results. Cell proliferation describes the rate of division in a population of cells whereas cell viability refers to the ratio of living *vs* dead cells. The treatment of GBM spheroids may require further incubation time to allow for drug penetration.

Differing cellular responses to these drugs may be due to their different specificities. Furamidine was found previously to have PRMT1 inhibiting effects with an IC_{50} of 9.4 µM (Yan et al., 2014), whereas MS023 has been shown to inhibit multiple PRMTs including PRMT1 (IC_{50} 30 nM) (Eram et al., 2018, Yan et al., 2014). Its other activity includes against PRMT3 (IC_{50} 119 nM), PRMT4 (IC_{50} 83 nM), PRMT6 (IC_{50} 4 nM) and PRMT8 (IC_{50} 5 nM). Although the original publication describing the activity of MS023 could not identify any activity against PRMT2, a study has since demonstrated this by a decrease in the PRMT2 specific histone mark, H3R8me2a, following treatment with MS023 in hepatocellular

carcinoma cells (Hu et al., 2020). This difference in specificities would have influenced which PRMTs were responsible for the changes in cell proliferation.

Furamidine has also previously been found to have an inhibitory effect on TDP1 (IC_{50} of approximately 30 µM), an enzyme involved in the repair of both nuclear and mitochondrial DNA (Antony et al., 2007). This additional activity may have contributed to the different response seen in U-87MG cells, although studies have yet to find whether inhibition of TDP1 alone results in a lower rate of proliferation. However, TDP-1 has been found to act synergistically with topoisomerase inhibitors by preventing the repair of DNA damage (Zakharenko et al., 2019). An alternative explanation to the reduction in cell viability following Furamidine treatment may be the subsequent changes in SDMA and acetyl-lysine deposition, which are specific to Furamidine. Due to the lack of response in GSK591 treated cells, it may be more likely that changes in acetyl-lysine induce the changes in cell proliferation. This is also suggested by the fact that Furamidine has a higher IC50 for PRMT enzymes and should therefore require a longer incubation time to see effects, indicating the changes in proliferation seen here are due to the off-target effects of Furamidine. To eliminate the potential interference from TDP1 inhibition, a lower dilution of Furamidine may be used, as the inhibitor has greater activity against PRMT1 (IC50 of 9.4 µM vs 30 µM). To further investigate the cause of proliferative changes, knock-down experiments could also be conducted using siRNA's against both PRMT1 and TDP1 to identify which protein is required for U-87MG cell growth, or if the mutual loss of both proteins is needed to reduce cellular proliferation.

As well as changes in proliferation, it is important to consider other changes that may be taking place upon PRMT inhibition. The findings in this chapter show that inhibition of type I PRMTs with MS023 did not result in a reduced proliferation of U-87MG cells when incubated for 48-72 hr in monolayer culture and 72-144 hr in a spheroid model. However, PRMT1 has been shown to play a role in the promotion of astrocyte differentiation (Honda et al., 2017) and is required for the activation of astrocytes in response to injury (Hashimoto et al., 2020). These effects will not be detectable with the MTS assay and thus, additional methods of determining cellular response to PRMT inhibition should be used, perhaps quantitative Polymerase Chain Reaction (qPCR) to detect changes in the expression of differentiation associated transcripts.

Treatment with GSK591 failed to induce a reduction in proliferation according to the MTS assay. As mentioned earlier, a previous study demonstrated a reduction in proliferation with 10 µM of GSK3235025, an optimised compound produced from GSK591 (Duncan et al., 2016), in U-87MG when treated for 96 hr (Braun et al., 2016). In this study, cell proliferation was measured by the reduction in strength of a fluorescent dye in proliferating cells. Since this study, another group inhibited PRMT5

through GSK3235025 treatment for 48 hr in 3 GBM cell lines (LN229, LN18 and GBM39) but failed to show a reduction in cell viability when using the Cell Titer-Glo® luminescent cell assay (Holmes et al., 2019). Similar to the MTS assay used in this chapter, the Cell Titer Glo assay determines the relative number of metabolically active cells. However, they were able to induce an effect when in combination with the mTOR inhibitor, PP242. Taken together, these studies suggest that to see an effect in GBM cells, a longer incubation time will be needed, or the drug should be used in combination with another inhibitor.

Inhibition of PRMT5 through GSK591 has also been shown to reduce the formation of spheroid structures when incubated for 5 days in breast cancer cells (Chiang et al., 2017). In the experiments in this chapter, GBM spheroids were allowed to form for 3 days prior to drug treatment. However, inhibition of PRMT5 may have a greater effect on the early formation of these spheroid structures immediately following plating. In future experiments, GSK591 could be added during initial cell plating to determine if the spheroid formation is affected through measuring spheroid size and MTS assay.

3.4.3) Inhibition of type I PRMTs by treatment with MS023 caused novel cross-talk events in both 2D and Spheroid Models

When confirming drug activity by western blotting, it was revealed that inhibition of type I PRMTs by MS023 caused the increased symmetrical dimethylation of a protein at approximately 70 kDa. Due to the non-specific nature of MS023, it is unclear whether this cross-talk is between PRMT1, PRMT4, PRMT6, or PRMT8 and type II PRMTs. To investigate the possible identity of this methylated protein, or other proteins symmetrically demethylated as a result of MS023 treatment, mass spectrometry will be utilised in chapter 6.

Since completing these studies, similar cross-talk events have been demonstrated by other groups in GBM cell lines but not yet in patient tissue (Gao et al., 2019b, Musiani et al., 2019, Fedoriw et al., 2019). Fedoriw et al. found increases in MMA and SDMA marks, as seen by western blotting, following inhibition of PRMT1 by a small molecule inhibitor (GSK3368715). They were then able to reverse this increase in SDMA marks by the use of a PRMT5 inhibitor (GSK3203591, the inhibitor used in this chapter), but were not able to reverse the increase in MMA. This indicates that the increase in SDMA marks were a result of an increase PRMT5 activity, whereas the increase in MMA deposition was independent of PRMT5 activity. The increase in MMA marks may therefore be due to an increase in the activity of other type I and type II PRMTs. When used in isolation, the PRMT5 inhibitor did not cause any changes in ADMA, meaning the cross-talk events seen here are specific to type I PRMT loss. Gao et al. knocked down PRMT1 expression in mouse embryonic fibroblasts (MEF) cells by a Tamoxifen inducible system and detected increases in global MMA marks and increases in certain SDMA marks,

as seen by western blotting, including a band at roughly 70 kDa. They also used a PRMT5 specific inhibitor (EPZ015666) and like Fedoriw et al. (2019), did not see a change in ADMA marks. However, they demonstrated a reduction in MMA marks, contradicting the increase seen by Fedoriw and colleagues. Musiani et al. did not investigate the loss of PRMT1, however, they were able to demonstrate that loss of PRMT5 activity, by using GSK3203591, results in an increase in MMA marks as seen by mass spectrometry. These marks were at the same residues as the SDMA marks detected in control samples, suggesting that substrate scavenging was taking place.

These studies have all shown that although loss of PRMT5 activity results in increases in ADMA, loss in PRMT1 does not cause an increase in SDMA marks. This may be due to the greater abundance of PRMT1 in cells compared with PRMT5. PRMT1 and PRMT5 share many target proteins and compete for such substrates, so it is logical to assume that loss in activity of either enzyme, will result in the increased deposition of marks associated with the other. However, the abundance of both enzymes should also be considered; PRMT1 is the most abundant PRMT in mammalian cells, whereas PRMT5 has a much lower abundance (Tang et al., 2000). Loss of PRMT5 can therefore we compensated by the activity of PRMT1, whereas PRMT5 activity may not be sufficient to carry out the methylation events of PRMT1 upon its inhibition.

In this chapter, treatment with MS023 also caused a reduction in certain SDMA marks, alongside the increase in SDMA of the 70 kDa protein. I hypothesise that due to the high concentration of drug used, this may be due to inhibition of some type II PRMTs. This may have significance in understanding these cross-talk events. The presence of both an increase and decrease in different SDMA marks suggests a protein specific cross-talk activity amongst PRMT enzymes.

Cross-talk events have previously been identified between PRMTs and KATs /histone acetyltransferases (HATs). PRMT1 for example, has been shown to stimulate the acetylation of lysine residues in histone tails by p300 (Wang et al., 2001, Geoghegan et al., 2015). Loss of PRMT1 activity would therefore result in the reduction in such acetyl lysine marks, as seen in these experiments in this chapter (Figure 3.6). The lysine marks identified to be lost in this chapter are of molecular weights 10 and 70 kDa, with only the 10 kDa protein being of a histone weight. There is minimal literature relating to possible cross-talk mechanisms involving higher molecular weight proteins, as most investigations concern the histone code. Although p300 predominantly acts has a HAT, it is also able to acetylate non-histone proteins such as transcription factors. These include HBP1 (HMG box-containing protein 1) (Wang et al., 2012), AFF1(AF4/FMR2 family member 1) (Kumari et al., 2019), and the ~70 kDa protein Foxo1 (Forkhead box class O) (Perrot & Rechler 2005).

3.4.4) Conclusions

The expression of all PRMTs were identified in U-87MG cells, excluding PRMT4. This is thought to be an issue with the antibodies as PRMT4 should be expressed within glial cells, as demonstrated by studies in human GBM tissue (Kappadakunnel et al., 2010, Dong et al., 2018), and in U-87MG cells at the RNA level (The Human Protein Atlas). Following confirmation of PRMT expression within U-87MG cells, PRMT inhibitors were utilised to investigate the tumour response to the loss of PRMT activity. Treatment with 100 μM Furamidine for 48-72 hr in the 2D cell culture model and 96-144 hr in the 3D cell culture model resulted in a statistically significant loss in metabolic capacity (used as a substitute for cell proliferation), when measured by MTS assay. Treatment with other PRMT inhibitors drugs, MS023, AMI-1 and GSK591 did not result in a decrease in metabolic capacity. As MS023 is a type II inhibitor with a much lower IC50 against PRMT enzymes, it was surprising that a similar effect was not observed, despite a reduction in ADMA marks. Taken with the fact that inhibition with Furamidine did not cause a global decrease in ADMA marks, it is tempting to speculate that the observed cell response may be due to specific changes in type II PRMT (Figure 3.4A) and KAT activity (Figure 3.6) upon Furamidine treatment. Due to the uncertainty surrounding Furamidine activity and the cellular response, MS023 were used in further experiments.

In conclusion, the GBM cell lines, U-87MG, responds to treatment with some PRMT inhibitors both at the molecular level through changes in ArgMe and Lysine acetylation, and through change in cell viability. The following chapters will optimise and investigate the response of GBM tissue to PRMT inhibitors alone, and in combination with the chemotherapy agent TMZ. Due to a lack of investigations into response to MS023 in tissue, the following experiments focus on the use of this inhibitor using patient biopsies in a microfluidic device. The levels of ADMA, SDMA and MMA will also be investigated.

Chapter 4 – Treatment of Patient Samples with TMZ on-chip

4.1) Introduction

4.1.1) Microfluidic Culture of GBM Cells

Monolayer and spheroid culture of cell lines are simple and reproducible models for the study of disease; however, they do not produce a completely accurate representation of the tumour in terms the tumour micro-environment. During their incubation, cells take in nutrients from growing medium, meaning the concentration of the glucose and essential amino acids is constantly decreasing. The cells also produce waste which accumulates in the surrounding area. In the *in vivo* environment, there is a dynamic diffusion of molecules as the various circulatory systems remove waste and replenish oxygen and nutrients in the tissues. A microfluidic model aims to reincorporate this aspect of the tumour environment by the perfusion of fresh medium over cells and has been used for the investigation into possible GBM treatments with varying levels of complexity (Logun et al., 2018, Cai et al., 2020).

The use of extracellular matrix-like gels in microfluidics can incorporate a further aspect of the *in vivo* environment that may alter cell behaviour. Such gels include various components of the extra-cellular matrix including laminin , collagen, and elastin, each providing different mechanical and signalling effects on cultured cells and tissues. Collagens provide strength and support for cells both in vivo and in vitro and can be used to study cell growth, migration and differentiation (Kleinman et al., 1981). Laminin on the other hand binds cells together and holds cells within the ECM. When sued in cell culture, laminin therefore aids in cell adherence and can be used to study growth, signalling pathways and cell motility (Gamm et al., 2008). Chanon et al. developed a two micro-channel device containing human umbilical vein endothelial cells (HUVECs) either side of a channel holding glioma initiating cells seeded onto Polydimethylsiloxane (PDMS) with a collagen 1 scaffold in order to recapitulate the interactions between tumour and blood vessel within the brain and the extracellular matrix (Chanon et al., 2017). This method produced a more accurate representation of some of the cellular interactions that occur in the tumour environment and, using this model, the group were able to demonstrate that HUVECs promote the invasion of GBM stem cells.

Orally administered drugs are initially processed by the intestine and liver prior to arrival at the tumour site, often altering treatment efficacy. Traditional 2D and 3D cell culture methods are unable to account for this metabolism pathway. Jie et al created a model where colon cells were incubated in a hollow fibre structure to represent the intestinal tissue, and liver cells were incubated alongside the GBM tumour cell line U-251 cells in chambers to mimic the liver and hepatocellular metabolism (Jie et al., 2017). This enabled for the pre-clinical testing of potential anti-tumour treatments whilst considering pharmacokinetic activity of the drug. In this study, the combinational treatment of

Camptothecin (CPT-11), a topoisomerase inhibitor, and TMZ, showed a synergistic effect when compared to single treatments.

The use of microfluidics in GBM research allows for the better representation of the tumour microenvironment, however, a current major drawback is expense in terms of both time and cost. Accessibility of materials and infrastructure is more limited when compared to the ease of static culture and can especially become difficult when attempting high-through studies. Another limitation is the variability and inconsistency during chip manufacture, that can influence the reproducibility in tumour-on-chip investigations. However, with the increasing commercialisation of microfluidic devices, this aspect should become more consistent and robust.

Although these studies described here have overcome some of the limitations of static cell cultures, they predominantly utilise only cancer cell lines, not considering the heterogeneity seen amongst patient tumours. Patient tumours even of the same cell type are rarely the same genetically and phenotypically, and so the use of cell lines disregards a significant proportion of the patient population, jeopardising clinical relevance. The use of patient samples provides are greater resemblance to the tumour-host environment, as the tissue will contain multiple cell types, allowing for more complex and biologically relevant interactions to take place. It also allows for a personalised medicine approach, as the tumour tissue used is directly related to the patient and can therefore be used to influence clinical decision making. There are limited studies involving the use of microfluidics on GBM patient samples (Logun et al., 2018). One such recent study performed by the group of Prof Greenman in Hull has described the development of a microfluidic model where GBM patient samples were maintained “on-chip” for up to 72 hr (Olubajo et al., 2020). LDH assay, Ki-67 quantification, and cleaved caspase quantification were used to demonstrate the viability of tissue following incubation on the device. The experiments in this chapter aim to describe a next generation “on-chip” maintenance of GBM patient tissue on an alternative device and for longer periods of incubation.

4.1.2) Aims and Objectives

Investigation of novel treatments in classic cell culture models is limited by the lack of representation of interactive systems and the tumour microenvironment. Therefore, an *ex vivo* microfluidic model that recapitulates the tumour environment by the maintenance of patient tissue on a chip under the perfusion of medium is characterised in this chapter. Changes in cellular processes including cell death and proliferation were measured. It was also examined whether there were any differences in proliferative activity amongst these slices when incubated with and without treatment with TMZ.

The aim of this chapter is to characterise a microfluidic model that supports GBM patient samples. I will assess tumour viability and characterise cellular processes and molecular signatures of GBM biopsies using LDH and MTS assays, and western blotting and IHC through the following objectives:

- To identify an appropriate incubation period for patient samples on the microfluidic device, which ensures sample viability, by measuring the release of LDH at regular intervals into the effluent and upon lysis of the sample.
- To assess intra-tumour heterogeneity by measuring the release of LDH into the effluent from multiple sample sections from the same patient tumour piece and proliferative markers by immunohistochemical staining.
- To determine the response of the GBM biopsies maintained in the microfluidic model to TMZ, by measuring the release of LDH into the effluent medium and by MTS assay.

4.2) Materials and Methods

4.2.1) Patient Samples

Ten samples were used in the following experiments to evaluate the microfluidic model. These samples were collected from the hospital as previously described in chapter two. Patient information available including sex, age, GBM type and molecular markers are included in the table 4.1 below.

Table 4.1: Patient information supplied by the clinical team at HRI. *MGMT Status: MGMT gene promoter methylation status, with positive being methylated and negative being non-methylated. NA: not available.*

Sample Name	Sex	Age	Primary vs Recurrent	MGMT Status	IDH Mutation	EGFR Amplification	TERT Mutation	ATRX Mutation
SD0003	F	29	Recurrent	NA	Mutant	NA	Positive	Negative
SD0002	F	76	Primary	Negative	Wild Type	NA	NA	NA
SD0022	M	48	Primary	Negative	Wild Type	NA	Positive	Negative
SD0023	M	66	Primary	Negative	Wild Type	NA	NA	Negative
SD0024	M	48	Primary	Negative	Wild Type	NA	Positive	Negative
SD0025	M	68	Primary	Negative	Wild Type	NA	NA	Negative
SD0027	F	83	Primary	Negative	Wild Type	NA	NA	Negative
SD0029	M	55	Primary	Negative	Wild Type	NA	Positive	Negative
SD0004	M	75	Recurrent	Positive	Wild Type	NA	NA	NA
SD0026	F	73	Primary	Positive	Wild Type	NA	NA	Negative

4.2.2) Incubation of Non-treated Patient Samples

Patient samples SD0002, SD0003 and SD0004 were collected from Hull Royal Infirmary (HRI) and prepared as in section 2.1.2. Each sample was cut into 4 equally weighted sections and incubated for increasing lengths of time (48-192 hr), with some samples being lysed at the end of their incubation. LDH release was then measured using the LDH assay as in section 2.5.

4.2.3) TMZ Treatment in GBM Patient Samples

Patient samples SD0022, SD0023, SD0024, SD0025, SD0026, SD0027 and SD0029 were collected from HRI and prepared as in section 2.1.2. Each sample was cut into 8-10 equally weighted sections and treated with either 10 µM TMZ or equivalent volume of dimethyl sulphoxide (DMSO) for 192 hr, excluding SD0026, which was ran for 240 hr. Following incubation, samples SD0022, SD0023 and SD0024 were processed for IHC as in section 2.4. Samples SD0025, SD0026, SD0027 and SD0029 were processed for MTS and LDH assay (5 slices), and IHC (3-5 slices).

4.3) Results

4.3.1) GBM Patient Samples Remain Viable on Chip for up to 8 days

The first aim of these microfluidic experiments was to show that GBM patient tissue can be maintained in a viable state during incubation on the microfluidic device. To do this, an LDH assay was used that measured the concentration of LDH in both the effluent samples and lysed tissue. LDH is an enzyme released by damaged and dying cells through perforations in the membrane. In a viable sample, it is therefore expected that there would be minimal release of LDH in the effluent samples but a large release of LDH following lysis of the sample.

A relatively high release of LDH into the effluent, comparable with the release during cell lysis, was observed at between 2 and 48 hr (Figure 4.1). This can be explained by the expected damage caused to the tissue during removal and handling. Minimal LDH release was then seen during the incubation time, rising slightly at 120 hr, most likely due to the changing of syringes when the 20 mL of growing medium was replaced. When the tissue was removed from the microfluidic chip and it was lysed, a greater concentration of LDH was detected in the lysate (Figure 4.1, red circles). These results indicate that although damage occurs to the tissue during initial handling and during syringe changing, the tissue remains viable as suggested by maintained membrane integrity. This is demonstrated by the minimal LDH release throughout the incubation, and by the release of LDH from cells at the end of incubation following lysis.

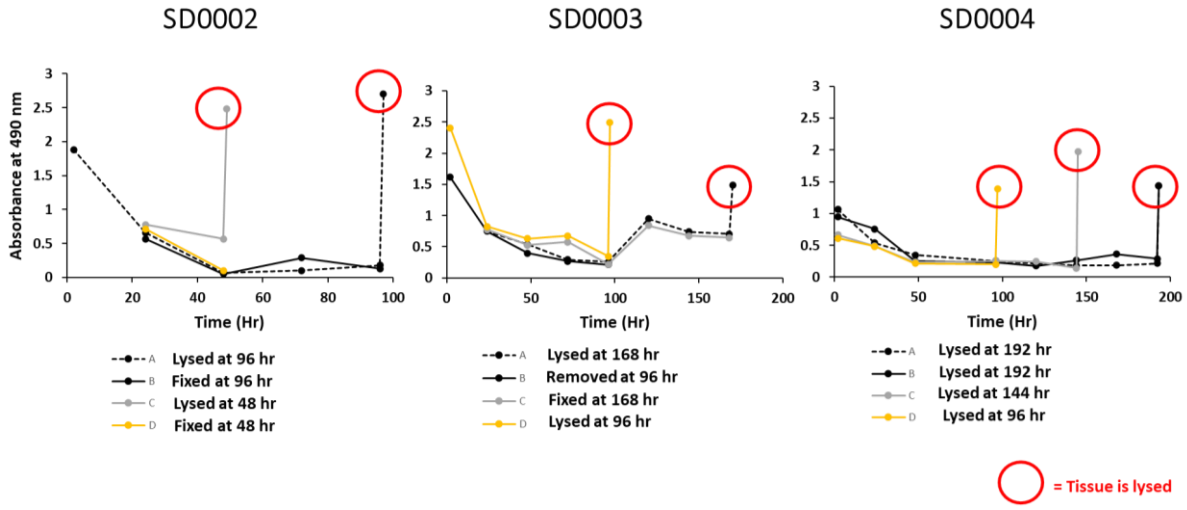

Figure 4.1: LDH assay demonstrates maintenance of GBM patient tissue on chip for up to 192 hr. *GBM Patient samples were sectioned into various sections and incubated on the microfluidic set up for increasing amounts of time and lysed. LDH release represented by absorbance per mg of tissue. LDH assays were carried out on the effluent and lysed samples.*

4.3.2) Incubation of GBM Patient Samples with TMZ Did Not Result in Cell Death Using LDH Assay

GBM is a very heterogenic disease with differences in the molecular phenotype and other characteristics from patient to patients. This heterogeneity can also be seen in the tumour itself, with clusters of varying clonal populations each competing for space and nutrients (Barthel et al., 2019). For this reason, it was speculated that during processing of the GBM samples, sections may be taken from different clonal populations and would therefore perhaps respond differently to treatment during incubation on the device. To investigate intra-tumour heterogeneity, samples were treated with the alkylating agent TMZ, the chemotherapeutic option for GBM patients. In the clinic, GBM patients receive between 75-200 mg/m^2/day, depending on whether this is the initial low or following adjuvant dose (Stupp et al., 2009). When tested in non-human primates, a dose of 150-200 mg/m^2 was shown to result in a peak blood plasma concentration of 3–15 µg/mL, corresponding to 15–77 µM (Patel et al 2003). Lower daily doses of 75 mg/m^2 were found to produce similar concentrations (10–25 µM) in the CSF (Ostermann et al., 2004, Diez et al., 2010). In these experiments, samples were treated with 10 µM of drug to replicate the clinical use of TMZ.

Incubation with TMZ is expected to result in an elevated LDH release into the effluent of treated samples, compared with control. It must be noted however that the methylation status of *MGMT* gene promoter is a major prognostic marker, with patients with a methylated promoter having a higher likelihood of response. The mechanism behind this change in sensitivity was visualised in Figure 1.4. However, it should be noted that the MGMT methylation status of the patients was not known until weeks following sample collection.

For each biopsy, 6 sections were treated with the same concentration of TMZ, in order to observe if there were any differences in the response. Two sections were treated with DMSO alone to act as a control. It was found that treatment of patient GBM samples with 10 µM TMZ did not result in an increased release of LDH when compared with control (Figure 4.2, A, C, E). There were slight differences in the release of LDH between TMZ treated samples, with the disparity differing amongst patients. Patient SD0023, for example, showed consistent release of LDH across all tissue slices. On the other hand, the release of LDH from patient SD0024 tissue slices varied more greatly, particularly at 168 hrs (following disruption due to syringe changes). To further investigate the differences in tumour response to TMZ in heterogenic tissue, the levels of proliferation were measured through the quantification of Ki-67 positive cells as a proportion of total cells (Ki-67 index). This was done by immunohistochemical staining of the proliferative marker. The Ki-67 index appeared to differ between sections sliced from the same biopsy, with standards deviations from 25% to 50% of the average index. A peak in ki-67 expression can be seen in patient SD0024 in the “TMZ 4” tissue slice in

Figure 4.2 F. This slice corresponds to the one that produce the peak in LDH release seen in Figure 4.2 E, suggesting a greater release of LDH could be a result of great proliferative and so metabolic activity within the cells.

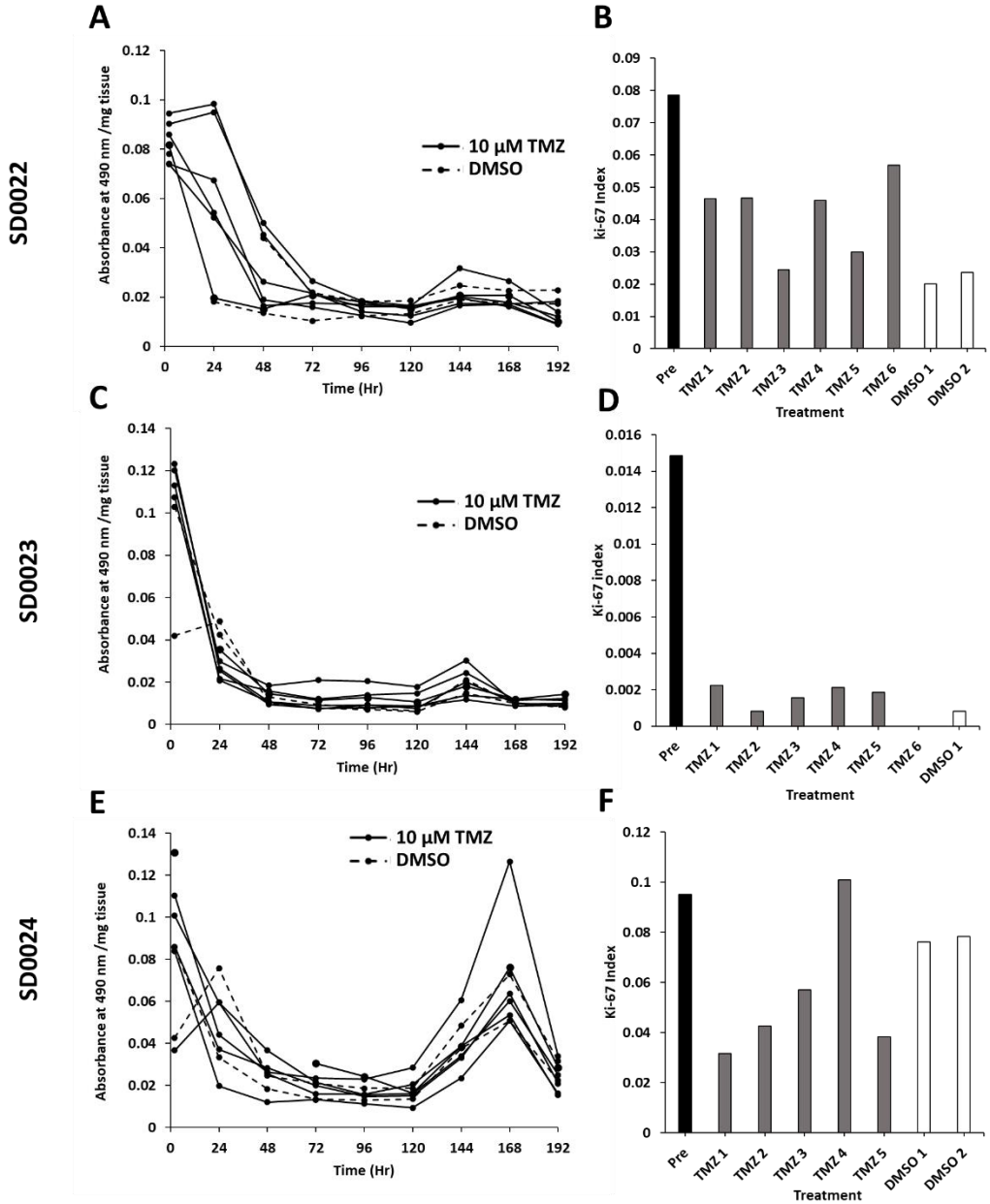

Figure 4.2: LDH assay and Ki-67 staining of GBM patient samples to demonstrate intratumour heterogeneity. *Three GBM patient biopsies were sectioned into 8 samples and incubated on the microfluidic device for 192 hr. For each patient sample, 6 tumour slices were treated with 10 µM TMZ and 2 were treated with an equal volume of DMSO. Following incubation, effluent samples were processed for LDH assay (A, C, E) and biopsies samples processed for IHC (B, D, F).* ***(A, C, E)*** *Points represent absorbance values per milligram of tissue. Elevated LDH levels can be seen at the early time points due to tissue handling, as well as at time points 144 and 168 hr due to the disruption caused by changing syringes.* ***(B, D, F)*** *Bars represent the Ki-67 index (number of ki-67 positive cells/total number of cells). Standard deviation amongst TMZ treated samples: SD0022- 0.011, SD0023- 0.00079, SD0024- 0.025. Representative images can be found in Appendix 3.*

4.3.3) LDH, Ki-67 and MTS assays Produce Similar Results of GBM Sample Response to TMZ

The LDH assay allows for the quantification of cell death by the measurement of LDH enzyme release from damaged cells. In order to consolidate the findings of GBM tissue response to TMZ, a further assay was used: the MTS assay. This assay differs by being a measure of cell viability, through the availability of NADH in cells. In the four patient samples tested, both LDH and MTS assays showed no response of the patient tissue to treatment with 10 µM TMZ (Figure 4.3 and 4.4). The LDH assay showed greater reproducibility as shown by the smaller size of the error bars representing standard deviation.

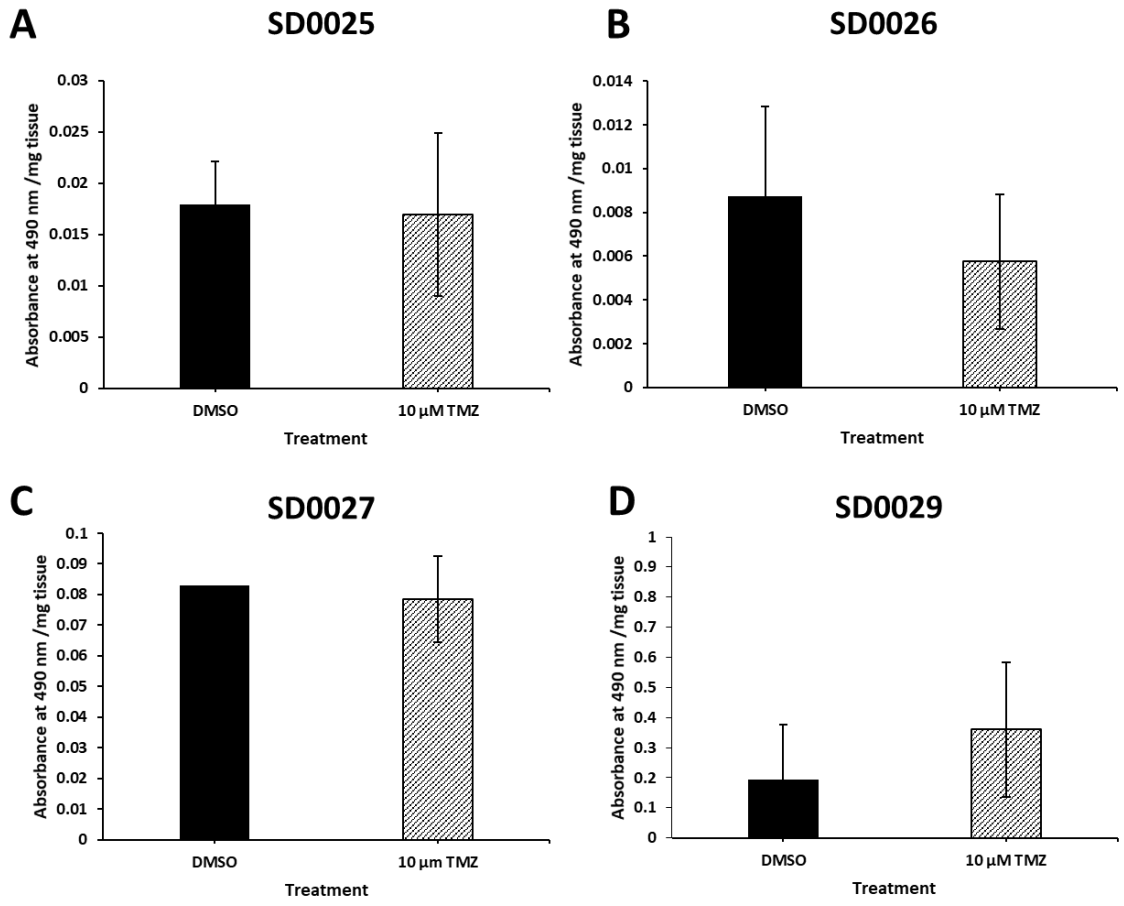

Figure 4.3: MTS assay to show changes in cell viability of GBM patient samples following treatment with TMZ. *Absorbance values measured using MTS assay on four patient samples treated with 10 µM TMZ or DMSO for 192 (SD0025, SD0027 & SD0029) or 240 hr (SD0026). Error bars represent standard deviation of duplicate/triplicate sample slices. It should be noted that the y-axis does not have the same scale for each sample above. Due to the size of tissue collected following surgery, only one replicate was used for the DMSO control for SD0027 for MTS experiments.*

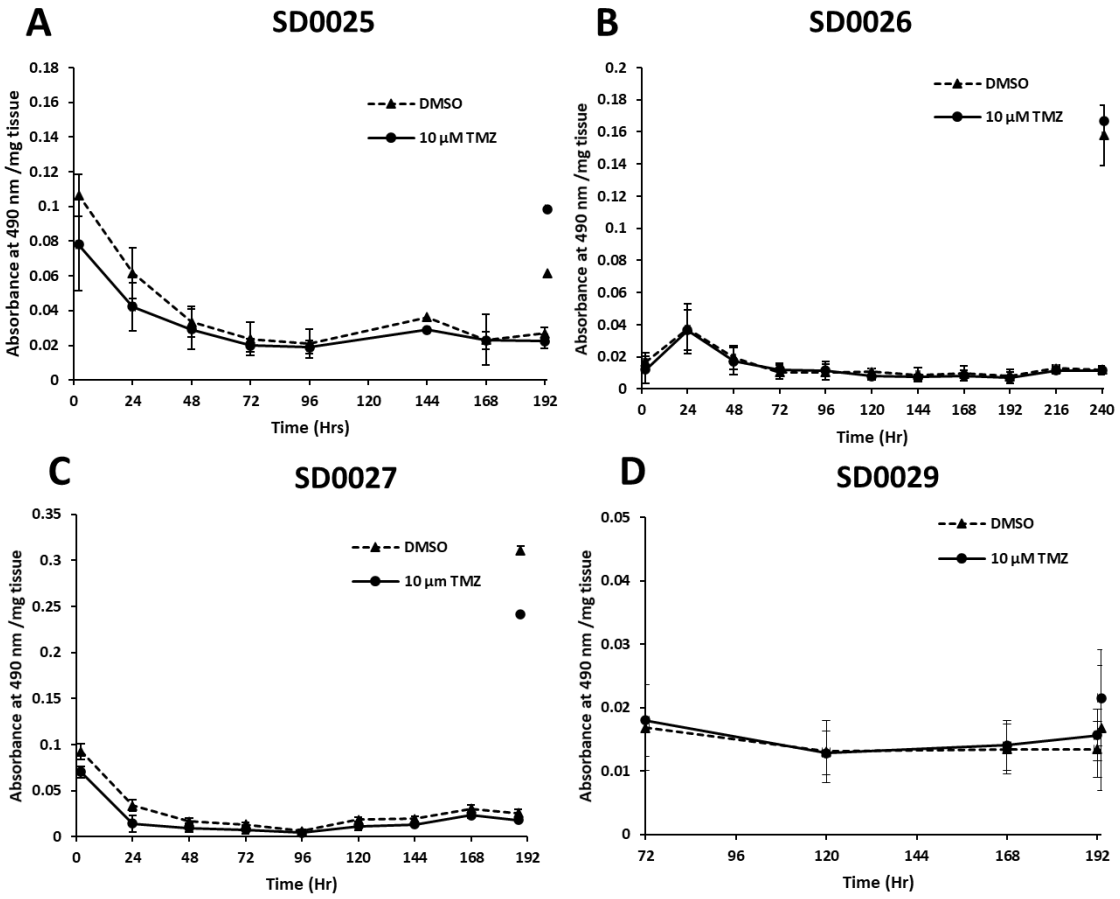

Figure 4.4: LDH assay to demonstrate changes in cell death following treatment with TMZ. *Absorbance values measured using LDH assay on four patient samples treated with 10 µM TMZ or DMSO for 192-240 hr. Following incubation with MTS reagent (non-toxic), samples were lysed, and LDH measured to demonstrate viability (excluding SD0029). Data not available for all time points for SD0025 and SD0029. Error bars represent standard deviation of duplicate/triplicate sample slices.*

The relative proportion of proliferating cells was also used to determine any response to TMZ treatment. Treatment with TMZ did not result in a reduction in Ki-67 index, however, similar to Figure 4.2, Ki-67 was reduced following incubation on-chip. The pre-chip sample for SD0027 shows a significantly low Ki-67 index but this is most likely a staining error as there appeared to be no background staining on any of the pre-chip tissue slices (Appendix 4). It is also very unlikely that incubation on chip would induce an increase in proliferation.

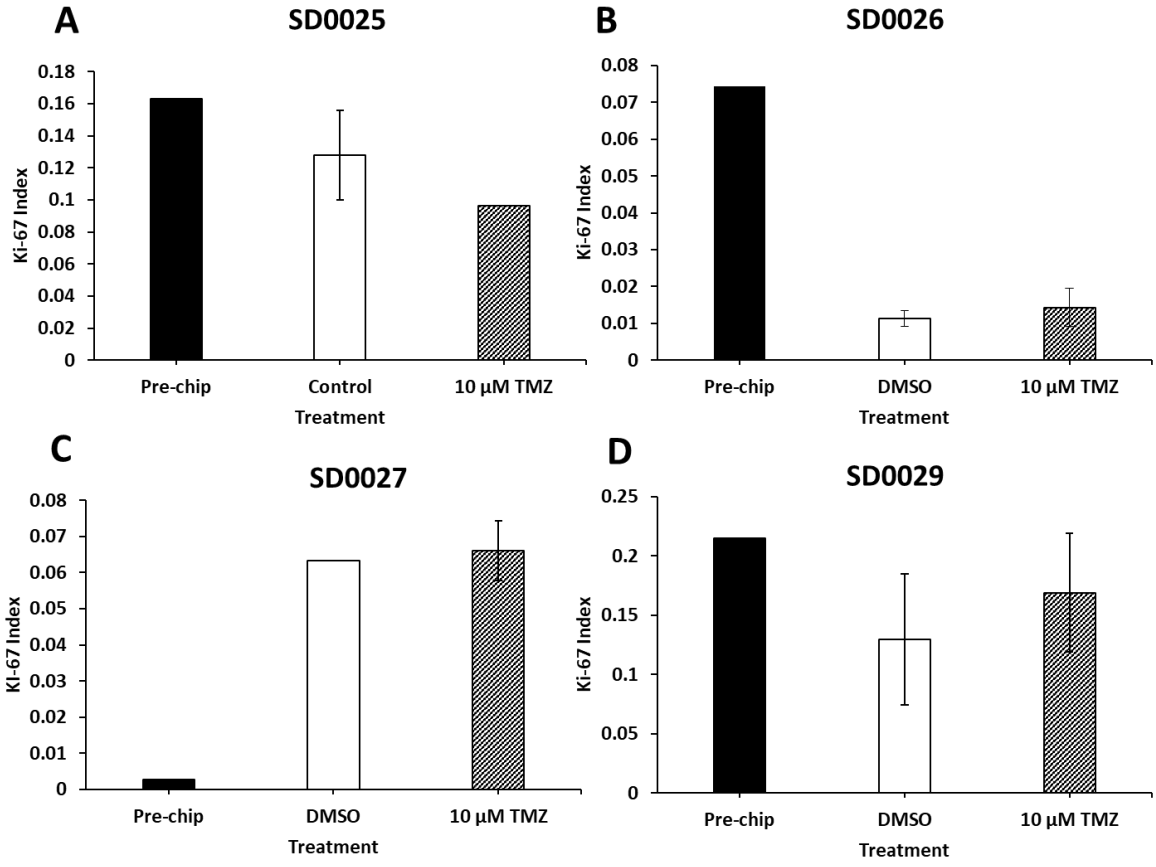

Figure 4.5: Quantification of Ki-67 to demonstrate changes in proliferation following treatment with TMZ. *Ki-67 index values measured following IHC of four patient samples treated with 10 µM TMZ or DMSO for 192-240 hr. Error bars represent standard deviation of duplicate/triplicate sample slices. Due to the size of tissue collected following surgery, only one replicate was used for the DMSO control for SD0027 for IHC experiments. Representative images can be found in Appendix 4.*

4.4) Discussion

4.4.1) On-chip Incubation Maintained at 192 hr

GBM patient samples were maintained on-chip with incubation times of between 48 and 192 hr. The concept that GBM tumour samples remained viable was supported by the minimal release of LDH into the effluent samples, and a large increase in LDH release upon lysis of the samples. These extended incubation times compared to the original work of Olubajo et al. would be beneficial in future experiments as it would allow more time for drug penetrance and activity (Olubajo et al. 2020). A compromise was made between longer incubation times and time restraints, and so 192 hr incubation time was carried forward. This incubation time allowed for the extended treatment with both TMZ and PRMT inhibiting drugs (see chapter 5). For some patient biopsy incubation, circumstances required a longer on-chip incubation of up to 240 hr (SD0026). Similar to other samples, there was no increase in LDH release past 192 hr.

4.4.2) Presence and Consequences of Intra-tumour heterogeneity

Intra-tumour heterogeneity is a possible source of variation amongst the sectioned slices from each patient biopsy. This is particularly important when studying GBM response, as it is highly evident in GBM tumours (Sottoriva et al., 2013, Patel et al., 2014, Barthel et al., 2019). Intra-tumour heterogeneity is often incorporated into model design, such as through the production of patient-derived cell lines (Jacob et al., 2020). In these models, it enables the investigation of clonal evolution and drug resistance (Golebiewska et al., 2020). However, in the circumstances of this microfluidic model, variances in the characteristics of biopsy slices could influence the observed response to different treatments when used as biological replicates.

To evaluate this aspect of GBM tumours in this microfluidic setup, patient biopsies were sliced into 8 samples, 6 of which were treated with TMZ and two of which were treated with a DMSO control. The LDH assay carried out the effluent samples from these biopsies did show small differences amongst treated samples, but no trends separating treated and control samples. Expression of the proliferative marker, Ki-67, was found to vary amongst sections slices from the same biopsy, also indicating the presence of intra-tumour heterogeneity. This variance in endogenous levels of Ki-67 expression could cause either the under estimation or over estimation of Ki-67 changes following treatment. To over-come this model characteristic, an increase in the number of biopsy slices per treatment should be used, to encapsulate a more representative response of the patient's tumour.

During collection of the tissue slices, it was only possible to access the heterogeneity of tissue sections given by the surgical team at HRI. In future experiments, arrangements could be made to receive sections from different areas of the tumour, increasing the likelihood of identifying areas of heterogeneity if present. This may be limited by the fact that the priority for tissue distribution should be with histopathology, as the biopsy taken during surgery is used to confirm the diagnosis of GBM and advise treatment options.

4.4.3) Influence of MGMT Promoter Methylation

Methylation of the MGMT promoter results in silencing of the gene, and therefore a reduced expression of the suicide protein MGMT. As MGMT is required for the repair of TMZ induced legions, loss of the protein results in sensitisation to the drug. Methylation of the MGMT promoter is therefore used as a predictive marker in TMZ response and is used in the clinic to guide treatment options.

Methylation of the MGMT promoter is seen in approximately 50% of GBM patients (Hega, 2005, Wick, 2015). Despite this, only 37% of patient samples (10 out of 27) were reported to have an MGMT methylation status of positive amongst the samples collected. The methylation status of these samples was known retrospectively, and very few MGMT promoter methylated samples were actually

treated in these experiments. The lack of response seen in TMZ treated samples may therefore be a result of a functional MGMT protein. It could also not be determined if heterogeneity amongst tissue slices from the same patient resulted in a differential response to drugs in the microfluidic set up. This is because the patient samples used (SD0022, SD0023 and SD0024) were non *MGMT* promoter methylated and are more likely to show resistance to TMZ treatment (Bobola et al., 2012, Alnahhas et al., 2020). This is a limitation of this study, as the *MGMT* promoter methylation status of the patient is only known following incubation. A larger patient cohort will be needed in future, to investigate a greater proportion of *MGMT* promoter methylated samples. Methylation of the MGMT promoter is known to be homogenous within GBM tumours (Grasbon-Frodl et al., 2007), and so there should be limited variation amongst slices taken from the same biopsy.

Both the MTS and LDH assays showed no changes in cell viability or cell death in GBM patients in response to TMZ treatment. There was greater accuracy in the LDH result however, as seen by the minimal size of the error bars compared with the MTS assay. LDH and MTS assays did not show an increase in cell death or a decrease in cell viability in the patient samples tested following treatment with TMZ.

However, it was found that sample SD0026 was in fact MGMT methylated, meaning that the sample was theoretically sensitive to TMZ treatment (Bobola et al., 2012, Alnahhas et al., 2020). It should be noted that although methylation status of the MGMT promoter is provided as a positive or negative result, there are intermediate levels of DNA methylation (Bady et al., 2016). The definition of what is methylated or not depends on techniques used to quantify the methylation and there is a lack of standardisation in this biomarker (Wick et al., 2014). Therefore, the methylation levels of the SD0026 biopsy may be relatively low, and perhaps not enough to result in a sensitivity to TMZ treatment.

4.4.4) Limitations of the Microfluidic Set-up

The LDH assay is widely used in GBM cancer research to quantify changes in cell death and proliferation, depending on the protocol utilised (Turkez et al., 2019, Ni et al., 2020), and has also been previously used in similar microfluidic experiments (Riley et al., 2019, Khot et al., 2020, Olubajo et al., 2020). However, results indicating a lack of sensitivity to TMZ treatment on-chip may also be due to a lack in sensitivity of these assays to minor changes in cell viability and cell death. A proof of concept experiment was also carried out where two biopsy slices were incubated with lysis buffer on chip for 3 hr to demonstrate an increase in LDH detection in the effluent (Appendix 12). This treatment was successfully able to induce a measurable increase in LDH release.

Although there were observed variation amongst all samples in Figure 4.2, there were no trends in Ki-67 expression amongst treated and control samples, suggesting treatment with TMZ did not result in

the reduction of proliferation. This was also the case in the treated vs control samples in Figure 4.3. In samples sensitive to TMZ treatment, this was unexpected as other studies have shown a reduction in Ki-67 expression following TMZ treatment in both GBM cell lines and patient tissue (Prabhu et al., 2017, Liu et al., 2019). It should be noted that there was a significant decrease in Ki-67 expression in the "on-chip" samples compared with the "pre-chip" samples. This suggests that although incubation on-chip does not cause cell death, the proliferative capacity of these patient samples is reduced. This may mute any response of the tissue to pharmacological treatment as drug activity may be dependent upon cells undergoing multiple rounds of replication, such as with TMZ. As TMZ works by introducing DNA damage during replication, this decrease in proliferation may mask any changes caused by drug treatment, as fewer DNA adducts will accumulate.

4.4.5) Conclusion

It is unclear whether the lack of response to TMZ was due to the lack of MGMT promoter methylation, lack of proliferative activity, or the presence of tumour heterogeneity. In the next chapter a new type of drug that has recently entered clinical trials in the oncology setting was used that is independent of DNA methylation, that is, PRMT inhibitors.

Chapter 5 – Investigating the Effects of PRMT inhibitors in GBM Patient Samples in a Microfluidic Device

5.1) Introduction

5.1.1) Use of Arginine Methylation Inhibitors in Clinical Trials

Due to promising results of preclinical studies involving PRMT inhibition of PRMT1 and PRMT5 in cancer cells, the use of type I and type II PRMT inhibitors is currently under investigation in patient clinical trials. Some of these trials, including those involving the drugs GSK3326595 and PRT811, involve a recurrent GBM cohort (see sections 1.2.5 and 1.2.6). There is therefore a need to understand the molecular and cellular effects of PRMT inhibitors in GBM tissue.

5.1.2) Aims and Objectives

Results in the previous chapter indicate that GBM patient tissues can be maintained in a viable state when incubated in the microfluidic chips through the minimal release of LDH. This model was then used to investigate PRMT inhibition in patient tissue.

- To evaluate the effect of PRMT inhibiting drugs (MS023, GSK591 and Furamidine) on tumour cell integrity by measuring the release of LDH from GBM samples maintained on-chip.
- To determine the response of patient samples on-chip to PRMT inhibition by MS023 through the quantification of the proliferative markers by immunohistochemical staining in treated *vs* nontreated samples.
- To preliminarily determine the response of patient samples on-chip to PRMT inhibition by MS023 through the sequencing of RNA and gene enrichment analysis.
- To determine the response of patient samples on-chip to a combinational treatment incorporating type I PRMT and type II PRMT inhibitors and induction of DNA damage through TMZ.

5.2) Materials and Methods

5.2.1) Patient Samples

Fifteen patient samples, collected from HRI, were used in the investigations in this chapter.

Table 5.1: Patient information supplied by the clinical team at HRI. *MGMT Status: MGMT gene promoter methylation status, with positive being methylated and negative being non-methylated. NA: not available.*

Sample Name	Sex	Age	MGMT Status	IDH Mut	EGFR Amp	TERT Mut	ATRX Mut	Histology
SD0020	M	68	NA	Wildtype	NA	NA	Negative	GBM
SD0034	NA	NA	NA	NA	NA	NA	NA	GBM
SD0035	F	51	NA	Wildtype	NA	NA	NA	GBM
SD0008	M	66	Negative	Wildtype	NA	NA	Negative	GBM
SD0012	F	31	Negative	Mutated	Negative	NA	Negative	Secondary
SD0014	M	51	Negative	Wildtype	Negative	Positive	NA	GBM
SD0016	F	69	Negative	Wildtype	Positive	Positive	Negative	GBM
SD0017	F	38	Negative	Wildtype	Positive	Positive	Negative	GBM
SD0018	F	71	Negative	Wildtype	NA	NA	Negative	GBM
SD0030	M	79	Negative	Wildtype	NA	NA	Negative	GBM
SD0031	F	45	Negative	Mutated	NA	Positive	Positive	Recurrent
SD0015	F	55	Positive	Wildtype	Negative	Negative	Negative	Secondary
SD0019	M	72	Positive	Wildtype	NA	NA	Negative	GBM
SD0021	F	42	Positive	Wildtype	NA	Positive	Negative	GBM
SD0033	M	34	Positive	NA	NA	NA	Negative	GBM

5.2.2) MS023 Treatment in GBM Patient Samples

Patient samples (SD0008, SD0012, SD0014, SD0015, SD0018, SD0019, SD0020 and SD0021) were collected from HRI and prepared as in section 2.1.2. Eight or ten equally weighted slices were separated, two of which were set aside. The remaining samples were incubated on chip for 192 hr. For SD0008, SD0011, and SD0012, three slices were incubated with only growing medium and three slices incubated with growing medium containing 100 nM MS023 (from a 50 mM MS023 stock in water). For SD0014, SD0015, SD0018, SD0019, SD0020 and SD0021, four slices were incubated with only growing medium and four slices incubated with growing medium containing 100 nM MS023. MS023 has an IC50 of between 4 nM to 119 nM, with a specific IC50 of 30 nM against PRMT1 (Eram et al., 2016), and so a concentration of 100 nM was used. Although published studies have used a higher molarity of drug (1 μM) such as one conducted by Gao et al., this was a shorter 6-day incubation (Gao et al., 2019b).

Following incubation, slices and effluent samples were processed for either LDH assay, IHC, RNA sequencing, western blotting (see chapter 6), or mass spectrometry (see chapter 6).

5.2.3) RNA Sequencing

5.2.3.1) RNA Isolation

Following incubation on the microfluidic device, the tissue samples were harvested in one of two ways: placed into a microcentrifuge tube, submerged in liquid Nitrogen and stored at -80 °C (pre-chip sample) or fixed in 4% (v/v) formaldehyde for 2 hr, incubated in 30% (w/v) sucrose overnight and stored in -80 °C in OCT compound (control and MS023 treated samples).

RNA isolation was carried out using the RNeasy mini kit (Qiagen) or the RNeasy FFPE mini kit (Qiagen), for liquid Nitrogen frozen samples and fixed samples, respectively, according to the manufacturer's instructions. Tissue samples were grinded with a glass douncer in 350 µL of RLT buffer (from kit) and homogenised using a 20-gauge needle. Once the lysate was cleared and nucleic acids precipitated and collected on the column and solution washed, the RNA was eluted in 30 µL of RNAse-free water and stored at -20 °C for two weeks before being posted to Novogene facilities in Cambridge in dry ice.

5.2.3.2) Initial RNA Quality Control

Prior to transport of the RNA samples to Novogene, the concentration and 260/280 ratio of the RNA was tested using a Nanodrop Spectrophotometer to ensure a sufficient concentration of RNA and a lack of DNA contaminants. Once these parameters were identified, the samples were shipped in dry ice by express delivery to Novogene's labs in Cambridge.

5.2.3.3) Novogene RNA Sequencing Workflow

The remaining RNA processing, sequencing and expression analysis were carried out by Novogene

5.2.3.3.1) Further Total RNA Quality Control

Once delivered to Novogene, similar quality control procedures were carried out, with the addition of an agarose gel electrophoresis to test for RNA degradation and potential contaminations and Agilent 2100 automated electrophoresis to determine RNA integrity.

5.2.3.3.2) Library Preparation

Samples sent to Novogene contained total RNA, therefore, mRNA was enriched using oligo(dT) beads. This protocol utilises the fact that eukaryotic mRNA possesses a polyadenylic acid tail that forms stable bonds with oligo(dT) under high salt conditions. The isolated mRNA will contain strands of varying length, and some strands may be more readily sequenced in later steps. To combat this, the mRNA was fragmented into uniform length strands. These mRNA strands were then converted into cDNA using reverse transcriptase. After the first strand is synthesised, a "second strand synthesis buffer" was added, containing dNTPs, RNase H and polymerase I to generate the second strand by nick-translation. The cDNA library was then purified, a non-templated nucleotide to the 3' end, a

sequencing adapter ligated and finally enriched by PCR. The library concentration was quantified using a Qubit 2.0 fluorometer. Sequencing was then carried out using Illumina and all data processing carried out by Novogene (read depth: 20 million, read length: Illumina PE150, unique machine identifier: HWI-ST1276).

5.2.3.3.3) Gene expression analysis

Kyoto Encyclopedia of Genes and Genomes (KEGG) pathway analysis was carried out to identify any biological processes or pathways were enrichment in certain samples and Gene Ontology (GO) was carried out to identify biological functions that were enriched in different samples. Each condition has one biological replicate.

Prior to differential gene expression analysis, for each sequenced library, the read counts were adjusted by edgeR program through one scaling normalized factor. Differential expression analysis of two conditions was performed using the DEGseq R package. The P values were adjusted using the Benjamini and Hochberg methods. Corrected p value of 0.005 and log2 (Fold Change) of 1 were set as the threshold for significantly differential expression.

KEGG analysis was carried out using KOBAS software. KEGG terms with an adjusted P value less than 0.05 were considered significant.

GO enrichment analysis of differentially expressed genes was implemented by the GOseq R package, in which gene length bias was corrected. GO terms with corrected P value less than 0.05 were considered significantly enriched by differential expressed genes

5.3) Results

5.3.1) Treatment of Patient Samples with MS023 Resulted in ADMA Loss in 4 out of 9 Samples Tested

In order to confirm the activity of MS023 as a type I PRMT inhibitor, western blot analysis was carried out on patient samples to observe changes in ADMA after incubation of biopsies on-chip with MS023 for 8 days. Similar to previous treatments in U87MG cells, treatment with the type I PRMT inhibitor, MS023, should result in a decrease in ADMA marks. A clear reduction of ADMA signals in treated samples compared to control was seen in 4 out of 9 samples analysed by western blot (green arrows in Figure 5.1). Two treated samples were analysed for western blot for sample SD0012 and appeared to have differing levels of ADMA compared with control, with some higher molecular weight proteins having greater levels of ADMA and lower molecular weight proteins having lower levels of ADMA. The loading control also made it difficult to interpret the changes in ADMA for SD0020, however band densitometry revealed that there was in fact a decrease in ADMA. Due to a low concentration of

protein and/or issues with the antibody, a loading control could not be provided for samples SD0018 and SD0019, as reprobing did not result in any visible banding.

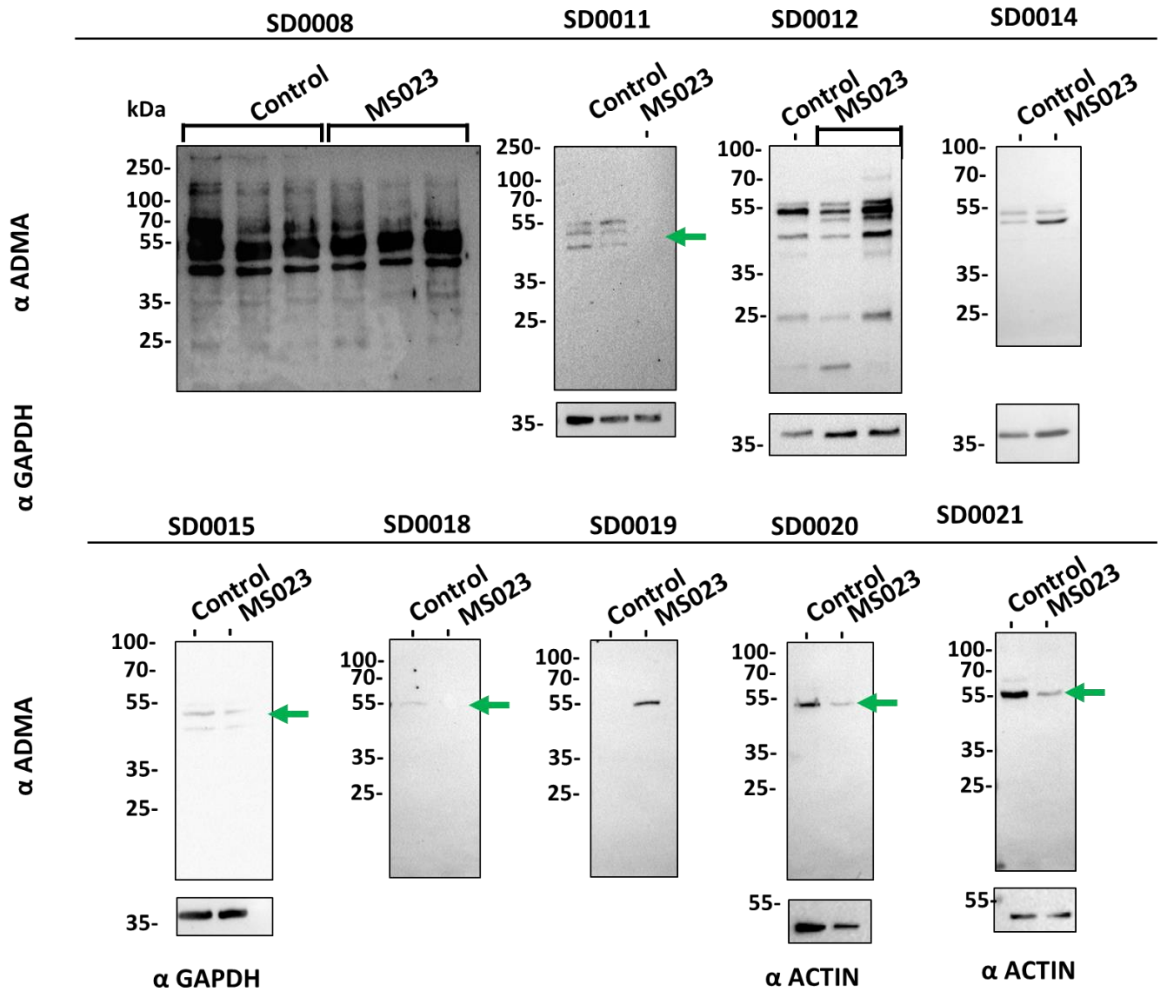

Figure 5.1: Western blot of GBM patient samples treated with and without MS023 showing changes in ADMA *(green arrows). Nine patient samples are shown each treated with and without 100 nM MS023 for 192 hr. ADMA is decreased following treatment in 4 out of 9 samples, increased in 2 and remains unchanged in 1. Loading controls could not be successfully probed for patients SD0008, SD0018 and SD0019.*

5.3.2) RNA Analysis of Patient Samples

5.3.2.1) Coverage of the RNA Seq

Patient sample SD0021 was treated with 100 nM MS023 as described in 5.2.2, with four slices being treated with drug, and four slices acting as a no treatment control. A single treated and a single non-treated control slice was processed for RNA seq following incubation on-chip. A pre-chip sample was also processed. Although RNA from pre-chip, control and treatment samples were sent from 3 different patients, not all passed quality control, and so it was not possible to compare RNA expression amongst different non treated samples from different patients. The only comparison possible was between differently treated replicates of the same patient.

Following RNA sequencing, a number of transcripts were identified in the three samples. A slightly higher percentage of the transcripts identified in the pre-chip samples were intronic when compared with the control and MS023 treated samples (Figure 5.2A). A total of 20,405 transcripts were identified in the pre-chip sample, 18,019 in the control sample, and 17,751 in the MS023 treated sample (Figure 5.2B). Out of these transcripts, 16445 were shared amongst all samples, 725 transcripts were shared between the pre-chip and control sample, 489 between the control and treated samples, and 463 between the pre-chip and treated samples (Figure 5.2B).

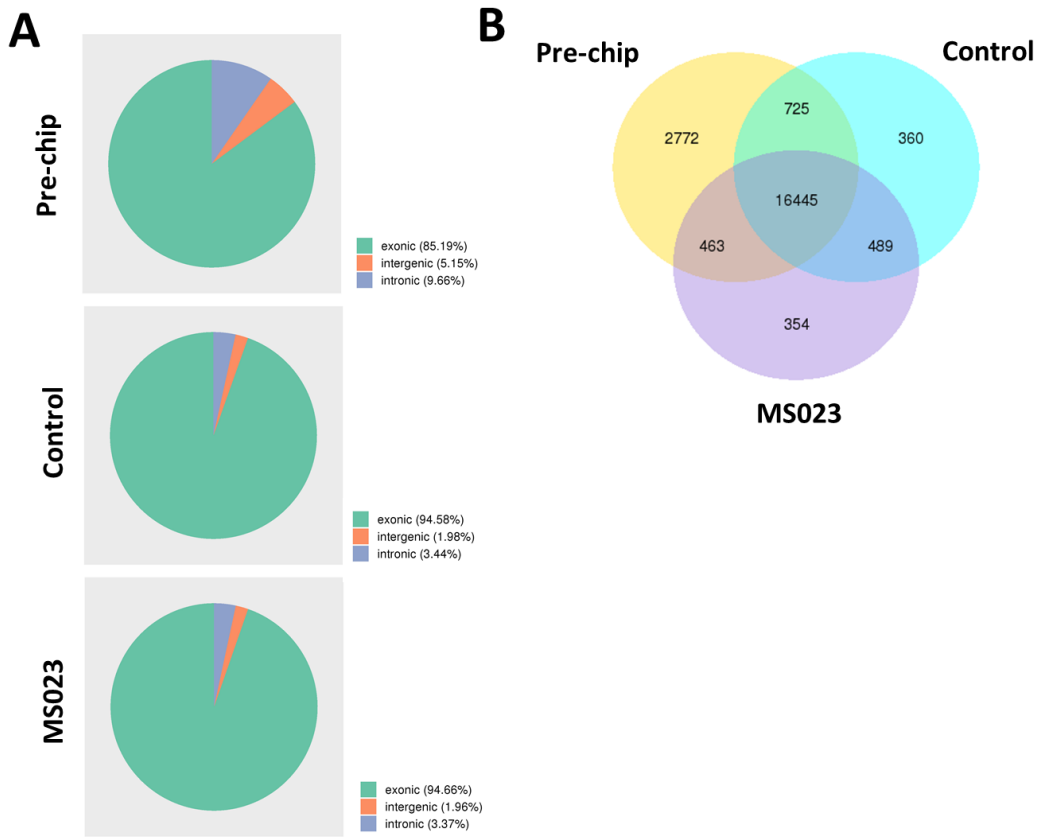

Figure 5.2: Initial summery of the RNA data. *(A) Mapping of samples to regions in a reference genome. At least 85% of reads were exonic. (B) A venn diagram to visualise the number of transcripts detected in each biopsy from 1 patient sample.*

5.3.2.2) RNA Analysis

Both incubation of biopsy slices on-chip without any treatment, and treatment of biopsy slices with 100 nM MS023 resulted in changes in gene expression. From the heatmap in Figure 5.3A, it is evident that there are clusters of genes differently expressed across all samples.

The greatest difference observed was between pre-chip and control samples, with 2562 transcripts being upregulated, and 4151 being downregulated, in the incubated control sample ("Control") compared with the fresh tissue (Pre-chip) (Figure 5.3B). Fewer genes appeared to have an altered

expression between the incubated control and treated samples, with 248 being downregulate, and 132 being upregulated in the treated sample compared with control (Figure 5.3C).

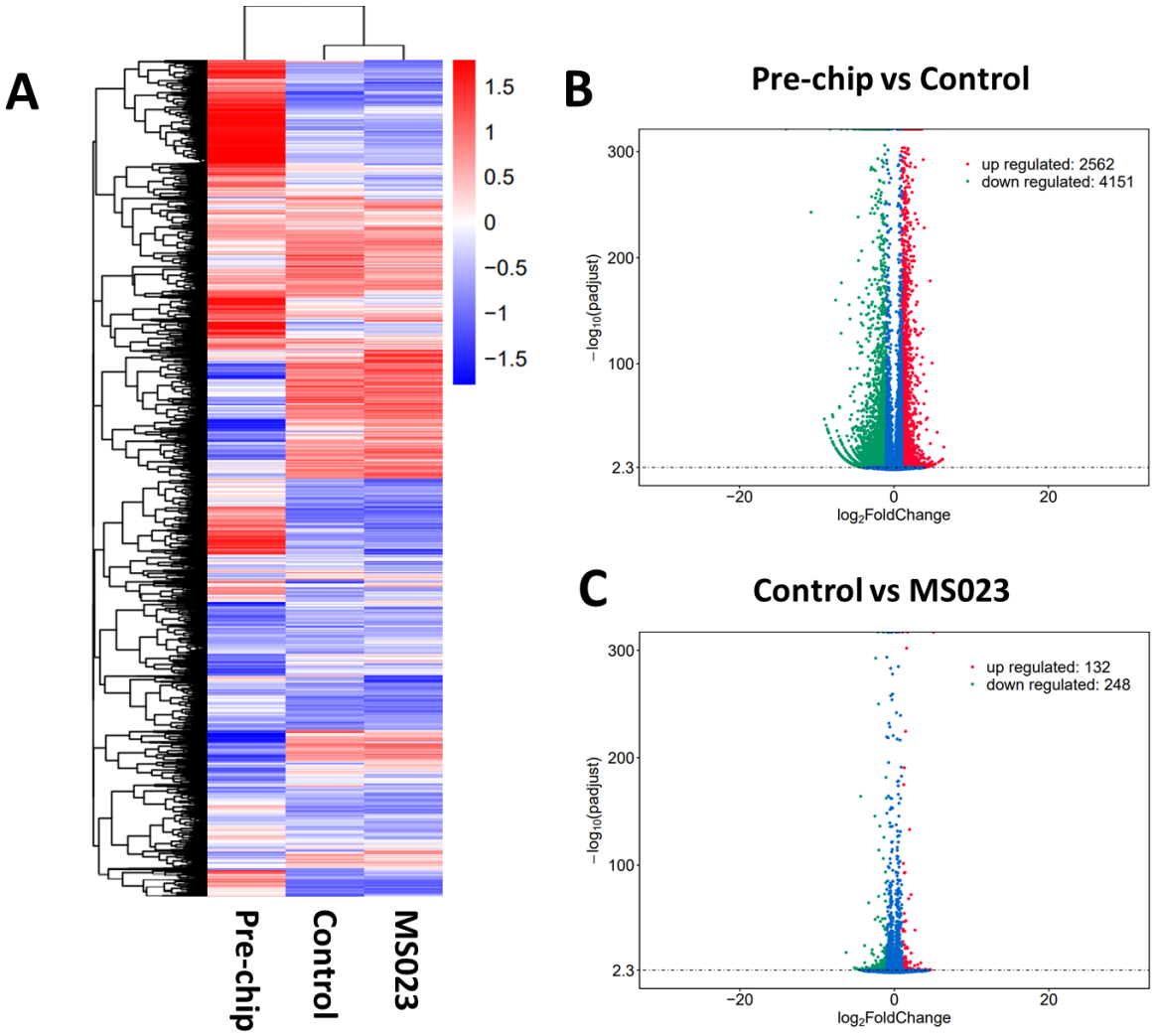

Figure 5.3: Different expression analysis of the GBM patient sample treated with MS023 on-chip*. (A) Heatmap depicting the differential expression of gene sets in pre-chip, control and treated GBM biopsy sections (B) Volcano plot depicting the differential expression of genes in pre-chip and control samples (C) Volcano plot depicting the differential expression of genes in control and treated biopsies from a single patient.*

Gene enrichment analysis allowed for the identification of pathways and biological functions that were associated with these upregulated and downregulated transcripts. Transcripts with a $\log_2$(fold change) ($\log_2$(FC)) of greater than 1 and an adjusted p-value of less than 0.05 were assigned as differentially expressed. Gene ontology revealed that the genes differentially expressed between pre-chip and control samples were related to cell adhesion, immune system process, transmembrane transport activity, the extracellular region, peptidase activity and transport (Figure 5.4A). KEGG analysis revealed that these genes differentially expressed between pre-chip and control samples were associated with metabolic pathways, ribosomes, cell adhesion molecules, phagosomes, the PI3K-

Akt signalling pathway, lysosomes, pathways related to cancer, cytokine-cytokine receptor interaction, focal adhesion and hematopoietic cell lineage, among others (Figure 5.4B). Gene ontology also revealed that the genes differentially expressed between control and treated on chip samples were associated with immune processes and the extracellular region (Figure 5.4c). KEGG analysis revealed that these genes differentially expressed between control and treated on-chip samples were associated with TNF signalling, complement and coagulation processes, AGE/RAGE signalling, and other processes related infection and disease. A list of the GO terms and gene names identified during these comparisons can be found in Appendix 13.

The transcript with the greatest increase in the MS023 treated sample compared with the control sample was ribosomal protein S17 (RPS17), with a $\log_2$(FC) of 5.05. RPS17 is a ribosomal protein found within the 40S subunit of the ribosome and known to be modified by arginine methylation (Larsen et al., 2016). The transcript with the greatest loss in MS023 treated samples was chemokine (C-C motif) ligand 20 (CCL20) ($\log_2$ FC: -6.23), a proinflammatory chemokine.

Other significantly differentially expressed genes include some GBM molecular markers which are often mutated or amplified in the disease and have been summarised in Table 5.2.

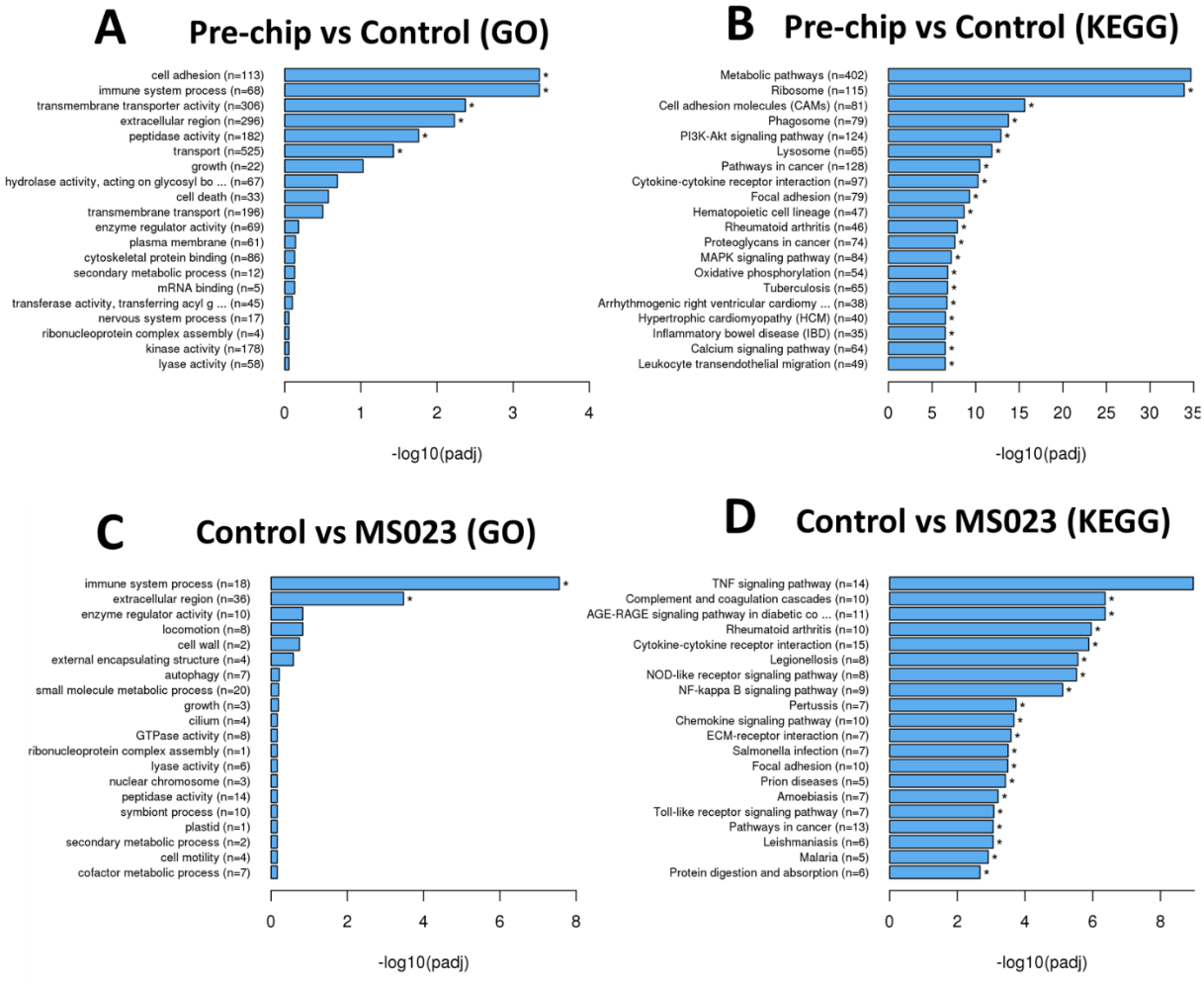

Figure 5.4: Functional grouping analysis of differentially expressed genes. *(A) GO analysis of Pre-chip and Control samples. (B) KEGG analysis of Pre-chip and Control samples. (C) GO analysis pf Control vs MS023 treated samples. (D) KEGG analysis of Control vs MS023 treated samples.*

Table 5.2: Significantly differentially expressed genes associated with GBM in the on-chip vs pre-chip sample. Negative values indicate a reduction in expression on chip.

Gene	Log_2 (Fold Change)
TERT	-2.11
MDM4	-1.64
CDK1	-1.41
PTEN	-1.03
EGFR	1.08
ATRX	1.29
IDH1	1.34
CDK6	1.49
PDGFRA	1.51
RB1	1.56

5.3.3) Treatment of Patient Samples with MS023 Did Not Result in An Increase in Cell Death or a Reduction in Proliferation

Following the demonstration of maintained cell viability “on-chip”, the microfluidic model was used to explore the potential of PRMT inhibiting drugs as a treatment for GBM using patient samples on-chip. Although previous experiments using the GBM cell line U87-MG did not show a reduction in cell viability by MTS assay, it was speculated that the 96-hour incubation time may not have been sufficient, as other studies have demonstrated changes in cell number in response to MS023 only after 6 days (Gao et al., 2019b). For this reason, patient GBM samples were treated with 100 nM of MS023 for a total of 192 hr (8 days). MS023 is a PRMT type I specific inhibitor that has recently become a gold standard for cancer biology preclinical research and demonstrates a consistent decrease in ADMA in other studies (Eram et al., 2016, Choucair et al, 2019, Gao et al., 2019b, Plotnikov et al., 2020).

Effluent samples were collected every 24 hr and at the end of the incubation period, the tissues were lysed. An LDH assay was carried out in order to confirm sample viability on chip and determine any changes in cell death with treatment. Similar to previous experiments, a relatively high absorbance was seen within the first 48 hr, followed a period of minimal LDH release. A peak in absorbance was then seen in the lysed samples, confirming that the GBM tissue could be maintained on the device for 192 hr. There was no difference, however, in the absorbance between control and treated samples. This was confirmed by a “repeated measures ANOVA”, giving a p-value of 0.375.

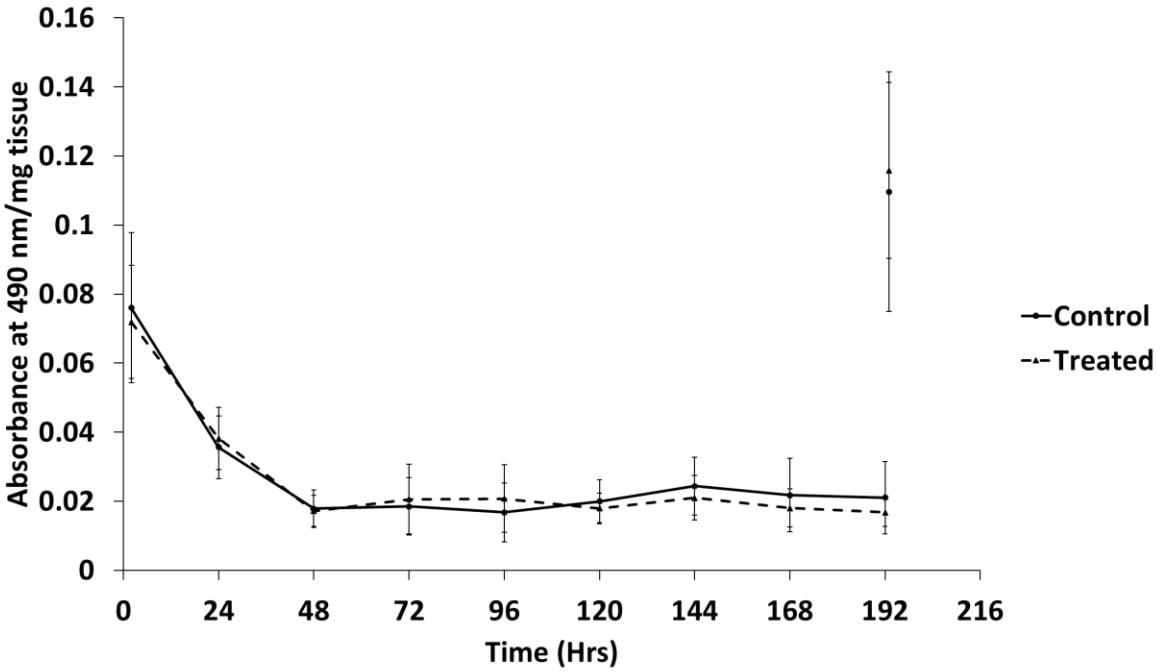

Figure 5.5: Treatment with MS023 did not result in an increase in cell death judged by LDH assay. *Treated with 100 nM MS023 and control samples incubated with growing medium alone for 192 hr. Effluent samples were taken at regular intervals and samples were lysed at the end of the incubation. Here, absorbance represents the concentration of LDH, and therefore indicates cell death. Error bars represent standard deviation. 2-192 hr, N=7. Lysed, N=4. P-value=0.375. LDH release of individual patient samples can be found in Appendix 5.*

The LDH assay qualitatively assesses the levels of cell death through the release of an otherwise membrane enclosed protein. These results demonstrate that patient samples do not release greater detectable levels of LDH when treated with 100 nM of MS023 on-chip when compared with untreated samples (Figure 5.5). However, LDH measurements do not uncover any changes in other cellular processes such as cell proliferation. In order to determine whether any changes in proliferative capacity of the patient samples occur upon PRMT inhibition, pre-chip, control and treated samples were prepared for IHC and probed for Ki-67, a protein only expressed during the active stages of the cell cycle. Of the three samples tested in this manner, no significant decrease in Ki-67 expression was observed in the MS023 treated samples compared with the controls (Figure 5.6). It was observed that incubation of the patient samples on the microfluidic device resulted in a decrease in Ki-67, indicating that although the samples remain viable, as seen by the lack of LDH release, the patient samples lose a level of proliferative capacity when compared with samples prepared for IHC upon removal from the patient. Similar to treatment with TMZ, the cells are required to activity proliferative and carry out cycles of protein synthesis in order to be sensitive to PRMT inhibition. Although there are studies to argue that ArgMe is a dynamic process, the marks are relatively stable, and so in order for the

inhibition of a PRMT enzyme to induce a reduction in its associated methylation mark, there should be a level of protein turnover within the cells.

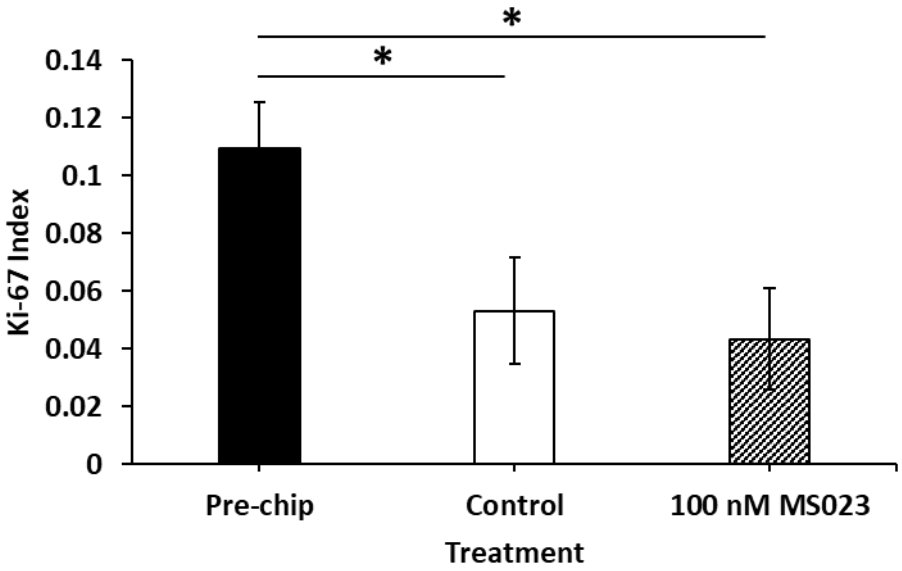

Figure 5.6: Immunohistochemical staining of Ki-67 in three patient samples treated with MS023. *Prior to chip incubation ("pre-chip"), incubation on the chip for 192 hr with no treatment ("control"), and incubation on the chip for 192 hr with 100 nM of MS023. Error bars represent standard deviation among 3 patient samples. An ANOVA was carried out with Tukey Post hoc tests. Pre-chip vs Control: P=0.039, Pre-chip vs 100 nM MS023: P= 0.02, Control vs 100 nM MS023: P=0.84. Ki-67 index for individual patient samples and representative images can be found in Appendix 6.*

5.3.4) Treatment of Patient Samples with MS023 in Combination with TMZ Did Not Result in Reduction in Proliferation or an Increase in Cell Death

TMZ's mode of action involves the induction of DNA breaks through alkylation of DNA. Numerous DNA repair mechanisms are involved in this process including the MMR machinery and nonhomologous ending joining or homologous recombination, during removal of the alkyl group and repairing of the DNA break, respectively. Due to the role of PRMTs and ArgMe in DNA repair (Boisvert et al., 2005b, Clarke et al., 2017), it was hypothesised that treatment with TMZ and PRMT inhibitors may have a synergistic effect. Other groups have demonstrated that two GBM cell lines, U-251 and A-172, when pre-treated with 100 µM of TMZ, showed a greater than additive increase in cell death following PRMT5 knock-down (Yan et al., 2014a). As this has yet to be shown with PRMT1 inhibition, GBM patient samples were incubated with both 10 µM TMZ and 100 nM MS023 and compared with singular treatment to determine if a combinational treatment was more effective at inducing cell death or led to a reduction in cell proliferation.

No increase in LDH release was seen in any treated samples compared with the DMSO control throughout the 192 hr incubation (Figure 5.7), suggesting that neither the singular nor combinational treatments resulted in an increase in cell death as measured by LDH release. There was also no reduction in Ki-67 index in treated samples compared with the DMSO control in the patient biopsies at the end of the incubation.

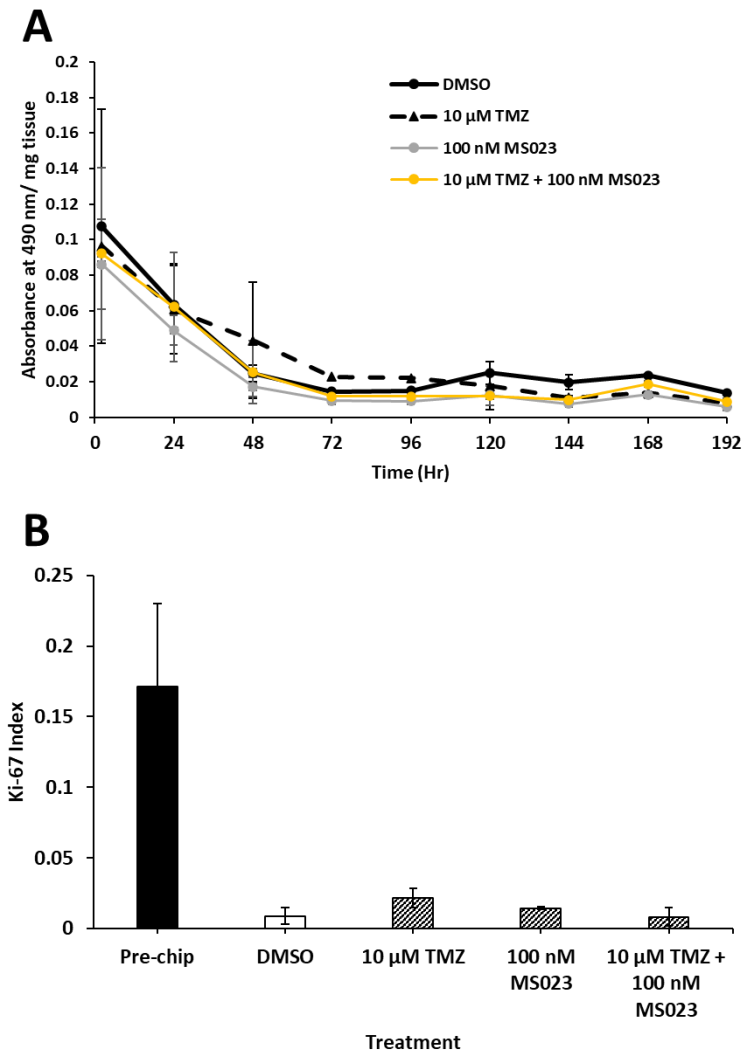

Figure 5.7: LDH assay and Ki-67 quantification to show changes in cell death and proliferation following treatment with combinations of MS023 and TMZ. *GBM Patient samples (SD0030 & SD0031) were treated with DMSO, TMZ, MS023 or a combination of TMZ and MS023 for 192 hr using the microfluidic set up. The two GBM patient biopsies were sectioned into 8 samples and incubated on the microfluidic device for 192 hr. For each patient sample, 6 tumour slices were treated with a combination of MS023 and TMZ and 2 slices with an equal volume of DMSO. Following incubation, effluent samples were processed for LDH assay and biopsies samples processed for IHC. Points represent absorbance values per milligram of tissue. Elevated LDH levels can be seen at the early time points due to tissue handling. (A) LDH assay to show the release of LDH, measured by absorbance at 490 nm, into the effluent. (N=2) LDH release of each patient samples can be found in Appendix 7. (B) Ki-67 index measured by IHC. Error bars represent the standard deviation of two patient samples. (N=2) Ki-67 index for individual patients and representative images can be found in Appendix 8.*

5.3.5) Treatment of Patient Samples with MS023 in Combination with GSK591 and TMZ Did Not Result in Reduction in Proliferation or an Increase in Cell Death

As well as possible synergistic activity of PRMT inhibition and TMZ treatment, dual inhibition of PRMT1 and PRMT5 was considered. Loss of PRMT1 expression alongside PRMT5 inhibition has been seen to produce a synergistic effect in MEF cells, with an increased loss of proliferation when compared to the predicted reduction of the separate treatments (Gao et al., 2019b). Together with the findings that inhibition of type I PRMTs results in the increased activity of type II PRMTs (sections 3.3.3 and 3.3.4), this suggests that there are redundancies between the two sets of enzymes, and that inhibition of both would result in a synergistic effect. To investigate this, patient biopsies were treated with different combinations of TMZ, MS023 and GSK591. As no change in LDH release of Ki-67 expression was seen in previous experiments, drug concentration was increased from 10 µM TMZ and 100 nM MS023, to 100 µM TMZ and 1 µM MS023, with GSK591 being given at 1 µM.

Due to the extended storage of the drugs between these experiments as a result of the COVID19 March 2020 lockdown, drug treatments were initially carried out on U-87MG cells to demonstrate inhibitor activity. Cells were treated with 1 µM and 100 µM of MS023 and GSK591 for 96 hr and harvested for western blot (Figure 5.8). Like experiments in chapter three, the levels of both ADMA and SDMA were determined by probing with specific antibodies. Treatment with MS023 resulted in the decrease in ADMA marks (green arrow), and the induction of some SDMA marks (red arrow). Treatment with GSK591 resulted in the loss of SDMA marks (orange arrow) and no change in ADMA marks (yellow arrow).

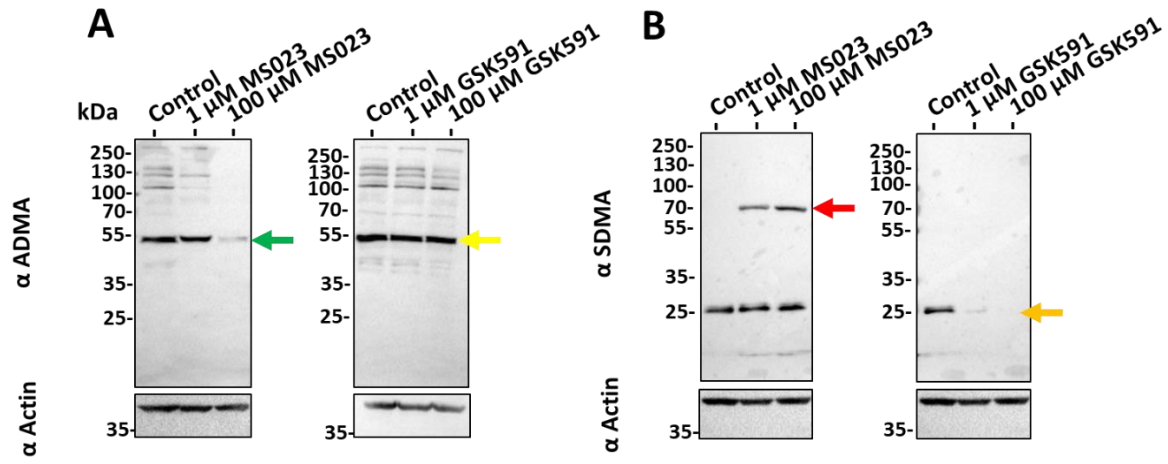

Figure 5.8: Western blot to demonstrate drug activity of PRMT inhibitors. *(N=1). Note the reduction in ADMA and SDMA upon treatment with MS023 and GSK591, respectively. Actin was used as a loading control.*

First, the LDH release from GBM patients (SD0033, SD0034 & SD0035) maintained on-chip and treated with MS023 alone, MS023 together with TMZ, a cocktail of MS023 and GSK591, and PRMT inhibitors plus TMZ, were evaluated. (Figure 5.9). A higher concentration of MS023, GSK591 and TMZ were used compared with previous experiments, as a lack in response was seen when judged by LDH, MTS, and IHC. Although the biopsies remained viable, as seen by the minimal release of LDH during the incubation, no combination of drugs resulted in an increase in LDH release.

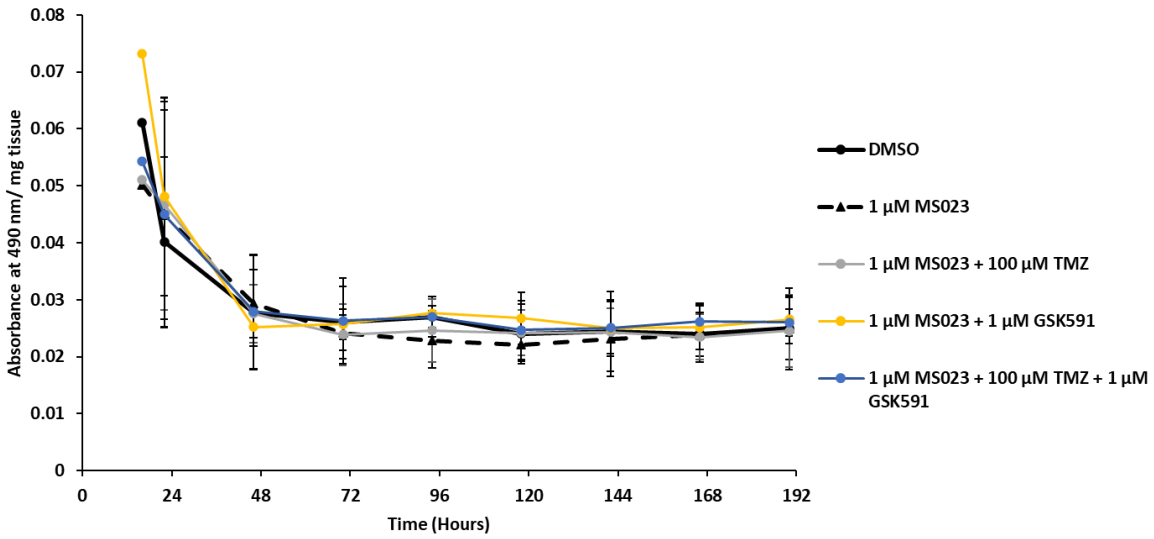

Figure 5.9: LDH assay of GBM patient biopsies treated with different combinations of PRMT inhibitors and chemotherapeutic drugs (TMZ). *Three GBM patient biopsies were sectioned into 10 samples and incubated on the microfluidic device for 192 hr. For each patient sample, 2 tumour slices were treated with a different combination of drug and 2 were treated with an equal volume of DMSO. Following incubation, effluent samples were processed for LDH assay and biopsies samples processed for IHC (Figure 5.12)**.** Points represent absorbance values per milligram of tissue. Elevated LDH levels can be seen at the early time points due to tissue handling. N=3 (SD0033, SD0034 & SD0035). Error bars represent standard deviation amongst different patient samples. LDH release for individual patients can be found in Appendix 9.*

Following incubation on the device, the patient biopsies were prepared, according to section 2.5, for immunohistochemical staining. In order to quantify any changes in the proliferative activity of the biopsies, Ki-67 was probed for, using specific antibodies, and the Ki-67 index calculated from the proportion of positive nuclei *vs* total nuclei. A large decrease was observed on biopsies incubated on the microfluidics devices when compared to the fresh sample. This was also observed in earlier experiments e.g., in Figure 5.8. No treatment combinations resulted in a decrease in Ki-67 positive nuclei (Figure 5.10). Due to the decrease in Ki-67 staining in the on-chip samples, it may be the case the cells do not have enough proliferative activity for the changes hypothesised to occur.

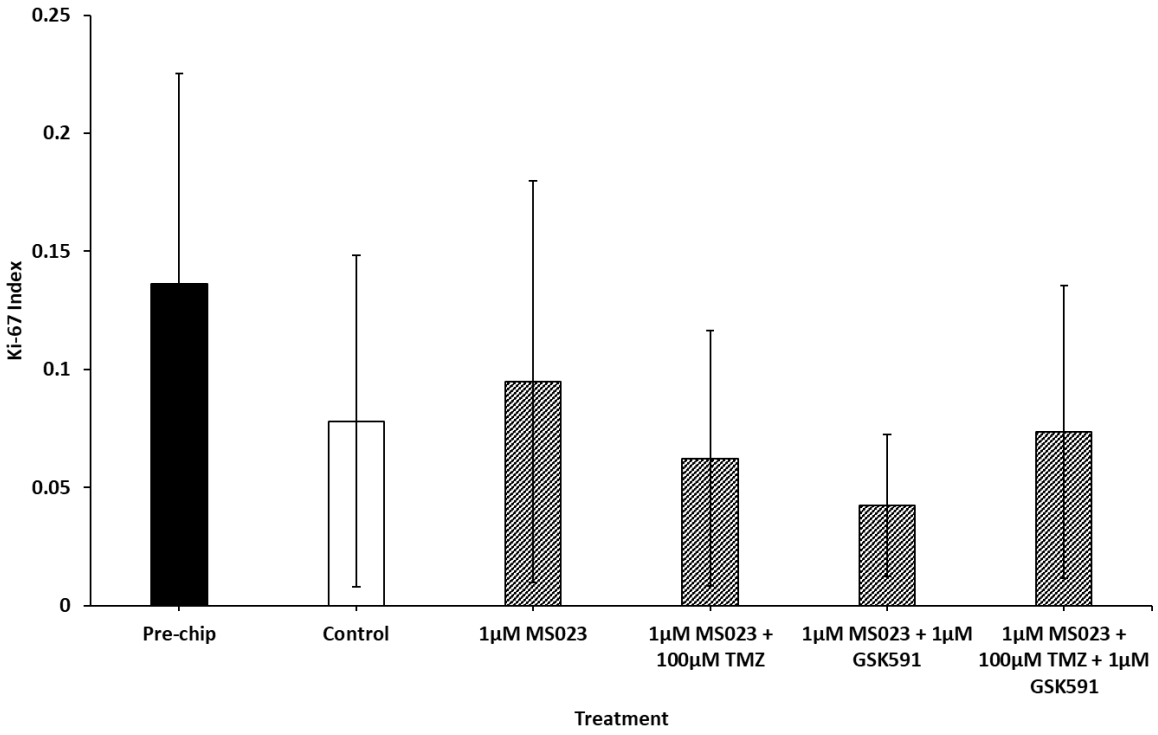

Figure 5.10: The Ki-67 index of GBM patient biopsies treated with different combinations of PRMT inhibiting drugs and the alkylating agent TMZ. *Sample SD0033 and SD0034 biopsies were treated in duplicate with either growing media alone or with 1 µM MS023, 1 µM MS023 and 100 µM TMZ, 1 µM MS023 and 1 µM GSK591 or 1 µM MS023 with 100 µM TMZ and 1 µM GSK591. (N=2) Error bars represent standard deviation between biological replicates. Ki-67 index for individual patients and representative images can be found in Appendix 10.*

5.3.6) Patient Tissue Treated with Furamidine

Incubation of U-87MG cells with the PRMT1 inhibiting drug Furamidine (Chapter 3) resulted in a decrease in cell viability as measured by MTS assay, although the mechanism behind this was unclear, due to the lack of response following MS023 treatment, another type I PRMT inhibitor. The next aim of this chapter was to determine if this response was also seen in patient tissue using the microfluidic model. Although no significant difference was observed overall (Figure 5.11), out of the two patient biopsies tested, one biopsy showed a minor increase in LDH release following Furamidine treatment when compared to the DMSO control (Appendix 11). It is unclear why these two patients showed a different response to Furamidine treatment, as they share similar characteristics and molecular markers (Table 5.1). Unfortunately, there was no tissue availability after these experiments for other cell viability and proliferation assays such as MTS and Ki-67 assays, to further interrogate these samples.

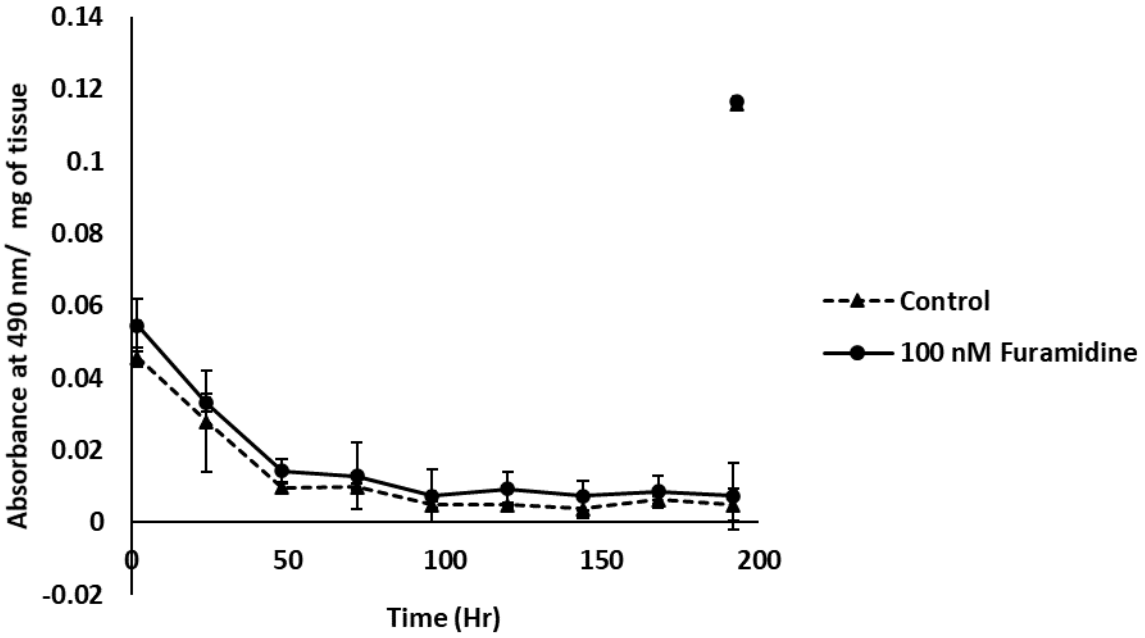

***Figure 5.11: LDH assay of GBM patient biopsies treated with* Furamidine.** *GBM Patient samples (SD0016 & SD0017) treated with and without Furamidine for a total of 192/288 hr. For each patient sample, 3 tumour slices were treated with 100 µM Furamidine and 2 slices with growing media only. Following incubation, both effluent samples and biopsy slices were processed for LDH assay. Points represent the average absorbance values per milligram of tissue. Elevated LDH levels can be seen at the early time points due to tissue handling and a peak of LDH release seen upon tissue lysis. (N=2) Error bars represent standard deviation between two patient samples. LDH release for individual patient samples can be found in Appendix 11.*

5.4) Discussion

5.4.1) Differential Expression of Genes on Chip

Differential expression analysis carried out on pre-chip and control samples showed a much greater alteration of gene expression when compared with the control vs MS023 treated analysis. Although preliminary, these data suggest that the samples undergo a phenotypical change during incubation using this microfluidic model. The genes with the most significantly altered expression were those related to cell adhesion, perhaps due to removal of the tissue from the tumour environment, and the immune response (Figure 5.6A).

The three most differentially expressed genes between the off-chip and on-chip samples were β-haemoglobin, α-haemoglobin 1 and α-haemoglobin 2 (Log_2FC: -9 to -13.9). Together these subunits form the Haemoglobin structure of red blood cells used for the transport of oxygen in the circulatory system. It is likely that these transcripts were expressed in red blood cells within the tumour and

although red blood cells have a lifespan of approximately 120 days (Franco, 2012), they were most likely shed into the effluent during incubation.

Out of all the PRMTs, only PRMT5 was found have a differential expression following sample incubation on-chip, showing an upregulation in expression, perhaps due to a stress response mechanism (Gao et al., 2017). It was also found that certain genes associated with GBM were also differentially expressed on-chip (Table 5.2). It is unknown whether these changes in transcript expression are translated into changes in protein expression, although this could be elucidated by the using of western blotting with specific antibodies. It is unclear to what extent these gene expression changes may alter the characteristics of the tumour, as the expression patterns of these genes are used to designate GBM tissues into classical, mesenchymal, neural and proneural subtypes. This could have consequences in terms using this microfluidic model to replicate the patient response seen in the clinic. For instance, a reduction in the gene expression of the tumour suppressor gene, *PTEN,* in samples incubated on chip, could induce a resistance to PRMT inhibition. This is because one of the ways PRMT5 is thought to induce gliomagenesis is through the inhibition of PTEN to induce proliferation in GBM cells (Banasavadi-Siddegowda et al., 2018).

Quantification of gene expression could be used in the future to valid this or a similar microfluidic model. As a model should replicate the in vivo scenario as accurately as possible, there should be minimal changes in gene expression when comparing samples from the same patient that have been incubated on chip, compared with fresh tissue. The gene expression of samples incubated on-chip could also be compared with samples incubated for the same length of time in a static culture method to demonstrate any improvements in the retention of the original patient gene expression profile.

It should be noted that the pre-chip and on-chip control samples were prepared using different methodologies prior to RNA isolation as described in 2.6.1.1. This also meant that two different RNA isolation methodologies needed to be utilised for these samples. For samples fixed in paraformaldehyde, the cross-links formed during fixation were first broken down prior to RNA isolation. These different techniques could have introduced differences in mRNA integrity of certain transcripts and therefore the resulting gene expression analysis.

5.4.2) Differential Expression of Genes Following Type I PRMT Inhibition

RNA analysis of MS023 treated samples demonstrated that inhibition of type I PRMTs alters a large number of mechanisms and pathways. Included in these pathways are some involved in tumorigenesis and/or immune cell signalling, including TNF signalling, cytokine-cytokine receptor interaction, NOD-like receptor signalling and NF-kappa B signalling. This is not surprising given the role of PRMTs in cancer (Bryant et al., 2021) and immunosurveillance (Nagai et al., 2019).

CCL20, a chemokine that has been shown to be a poor prognostic marker in GBM tissue (Wang et al., 2012), was found to have the greatest loss in expression upon treatment with MS023. A possible explanation for this is the increased activity of PRMT5 as seen by the upregulation of SDMA marks seen by western blotting (Figure 4.6). This is because PRMT5 has been shown to inhibit Targeting TNF-related apoptosis-inducing ligand (TRAIL) to bind the Death receptor, DR4, and reduces NF-κB activation and CCL20 expression (Kim et al., 2016).

5.4.3) Involvement of Immune Cells

As whole tumour biopsies were lysed prior to RNA isolation, it is important to consider what other cells of the tumour micro-environment may have contributed to the changes in gene expression seen. Studies have demonstrated that despite the brains isolation from the immune system, immune cells can still be found within GBM tumours. Tumour infiltrating lymphocytes (TILs) can be found in up to 38.5% of GBM samples, with varying levels of infiltration (Orrego et al., 2018). Some patients with a low number of TILs were found to have a sequestration of T-cells within the bone marrow, an adaptive response of the tumour to evade the body's immune system (Chongsathidkiet et al., 2018). Other immune cells including macrophages and microglial have also been found within GBM tumours with different infiltration patterns (Bowman et al., 2016, Frohne et al., 2019).

Due to identification of immune response pathways during the enrichment analysis of both pre-chip vs control and control vs MS023 treated samples, it is likely that these non-tumour cells are taking an active part in the drug response. For instance, IL-1β, a chemokine that showed a reduced expression in treated samples, has been shown to promote tumorigenesis is gliomas when released by tumour associated macrophages (Lu et al., 2020).

It is also possible that these cells also contribute to the effects seen in the immunohistochemical staining of Ki-67. This is a more representative model of the tumour environment, as these cells would also be present during clinical treatment of GBM patients.

5.4.4) Limitations of RNA Expression Analysis

As previously explored in chapter four, intra-tumour heterogeneity is likely to result in variance in the population of cells found in the different samples sectioned from a patient biopsy. Unfortunately, only one slice for control and one slice for treated were available to carry out the RNA analysis, and so these results should be treated as preliminary. In future experiments, a greater number of biological replicates should be used for each condition to accommodate for this.

Although preliminary, these experiments have identified a set of candidate genes that could be important in the response to PRMT inhibition. To further investigate this, qPCR experiments could be conducted to validate their expression following treatment with MS023.

5.4.5) Cellular Response Seen in U-87MG cells Replicated in Patient Samples

In chapter 3, the potential use of PRMT inhibiting drugs as a therapeutic option was evaluated using the GBM cell line U-87MG. In these experiments, only Furamidine was able to elicit a measurable response, observed by the decrease in absorption of the MTS product in treated samples. There was uncertainty concerning Furamidine activity, i.e., the irregular loss of ADMA marks, as well as the loss of acetyl lysine. Other PRMT inhibitors, including MS023, did not show a response U-87MG cells, however, MS023 did show a reliable inhibition of type I PRMT activity. This lack of response, despite the evident decrease in ADMA deposition in 4 out of 9 samples, was also seen in the *ex vivo* microfluidic model used in this chapter. Like immunohistochemical experiments conducted in chapter 4, the on-chip samples had a lower Ki-67 index compared with the pre-chip sample. This may have muted any effects MS023 had on the proliferative activity of the biopsies. Although MS023 was the focus of this chapter, Furamidine was also investigated, and a small response was observed in one out of two of the Furamidine treated samples. This supports the previous findings in U-87MG cells, where Furamidine treatment resulted in a decrease in cell viability. It also reiterates the presence of intertumoral heterogeneity seen amongst GBM patients, and the need to identify predictive markers for treatment.

5.4.6) Combinational Therapy of PRMT Inhibitors and TMZ did Not Result in Synergistic Effects

No synergistic effect was observed in the experiments in this chapter, however, no decrease in Ki-67 was observed with any treatment in the microfluidic model. This may be the case due to the reduction in Ki-67 staining in the on-chip slices when compared to the fresh biopsy as previously explored in 4.4.4.

The loss of PRMT1 and PRMT5 has previously been investigated, with cells with altered splicing found to be crucial in the combinational effects (Fong et al 2019). Through inhibition of PRMTs by GSK591 and MS023, Fong et al. were able to demonstrate an increased sensitivity in cells with splicing factor mutations. They hypothesised that methylation of these RNA associated proteins weakened cation π interactions of their RGG/RG-rich motifs and effect the assembly of regulatory RNA processing organelles. This previous study suggests that the cells used here most likely have functional splicing factors.

5.4.7) Conclusion

RNA analysis of patient samples incubated on the microfluidic device compared with fresh tissue suggested changes in expression of a wide range of genes, including those associated with cell adhesion, the immune system, and genes associated with different GBM phenotypes. Further analysis using biological replicates in multiple patient samples will need to be carried out in order to identify significant changes in the genes explored here. Similar to previous cell model work, treatment with MS023 did not result in a reduction in cell viability, judged by the minimal release of LDH and no reduction in Ki-67 index, although the incubation period was extended to 192 hr. This lack of response was also seen when a combination of PRMT inhibitors and TMZ was evaluated. As previously stated in chapter 4, incubation of samples on-chip results in a reduced proliferative activity. This was also found in the samples tested in this chapter, and so responses to MS023 treatment may not be apparent by measuring the Ki-67 index. MS023 has been used in these experiments to specifically inhibit type I PRMTs in both cell lines and patient biopsies. Although it is repeatedly used in pre-clinical studies in many cancers including GBM, other inhibitors are now available that are also used in clinical studies, including GSK3368715. This would bring further clinical relevance to these experiments.

There are a number of ways to determine tumour response to either the classic chemotherapeutic drugs, i.e., TMZ, or novel therapies, i.e. PRMT inhibitors. Here, an LDH assay was used to determine cell death, MTS to determine cell viability, and ki-67 staining to measure proliferative activity. These methods may not have been sensitive enough to detect other changes in cell biology following treatment of the GBM cells. Other approaches that could be carried out in the future include flow cytometry to identify proportions of proliferating and apoptotic cells to a much greater level of accuracy and precision. An alternative methodology to inhibit PRMT activity to understand the enzymes' role in GBM tumour biology would be the use of siRNA to silence genes rather than inhibiting the enzymes activity. This will allow for a more specific loss of PRMT activity compared with MS023, which inhibits the majority of type I PRMTs.

The intriguing results seen in earlier chapters involving the visualisation of PTM cross-talk between the inhibition of asymmetric arginine dimethylation and the appearance of new protein bands recognised by symmetric arginine dimethylation antibodies will form the basis of the following chapters.

Chapter 6 – Identification of Cross-Talk Amongst PRMT Enzymes in GBM Cells and Patient Samples

6.1) Introduction

Interplay amongst PRMTs was identified in U-87MG cells in chapter 3 due to the increase in SDMA marks when assessed by western blotting. This has also since been demonstrated by other research groups tissue (Gao et al., 2019b, Musiani et al., 2019, Fedoriw et al., 2019), who have investigated the interactions specifically between PRMT1 and PRMT5, suggesting that these are the enzymes responsible for the cross-talk activity seen here. To date, all studies involving interactions between ArgMe have utilised cell-line models and cross-talk events have yet to be investigated in tissue.

6.2) Aims and Objectives

The presence of cross-talk between PRMT enzymes was identified in chapter 3 due to induction of SDMA marks following type I PRMT inhibition. As treatment with MS023 successfully reduced the levels of ADMA marks in these patient samples, the following chapter will investigate the presence of any cross-talk events and what proteins may be responsible.

- Demonstrate any changes in SDMA and MMA marks in patient biopsies through western blotting in order to identity cross-talk activity amongst PRMT enzymes.
- Further investigate cross-talk activity by SILAC mass spectrometry to identify specific proteins methylated as a result of type I PRMT inhibition by MS023.

6.3) Materials and Methods

6.3.1) Heavy Methyl SILAC

6.3.1.1) The Heavy Methyl SILAC Method

Heavy Methyl Stable Isotope Labelling of Amino Acids in Cell Culture (hmSILAC) is a technique where cells are incubated with a heavy form of methionine (Figure 6.1). This is then converted into a heavy form of SAM, the methyl donor required for methylation by PRMTs (Ong and Mann 2006, Musiani et al., 2019). PRMTs within the cell transfer the heavy methyl group of SAM onto target proteins, labelling them for identification by mass spectrometry. Sensitivity can be increased by prior enrichment of the PTM of interest using anti-methylarginine antibodies by immunoprecipitation (Onwuli et al., 2019).

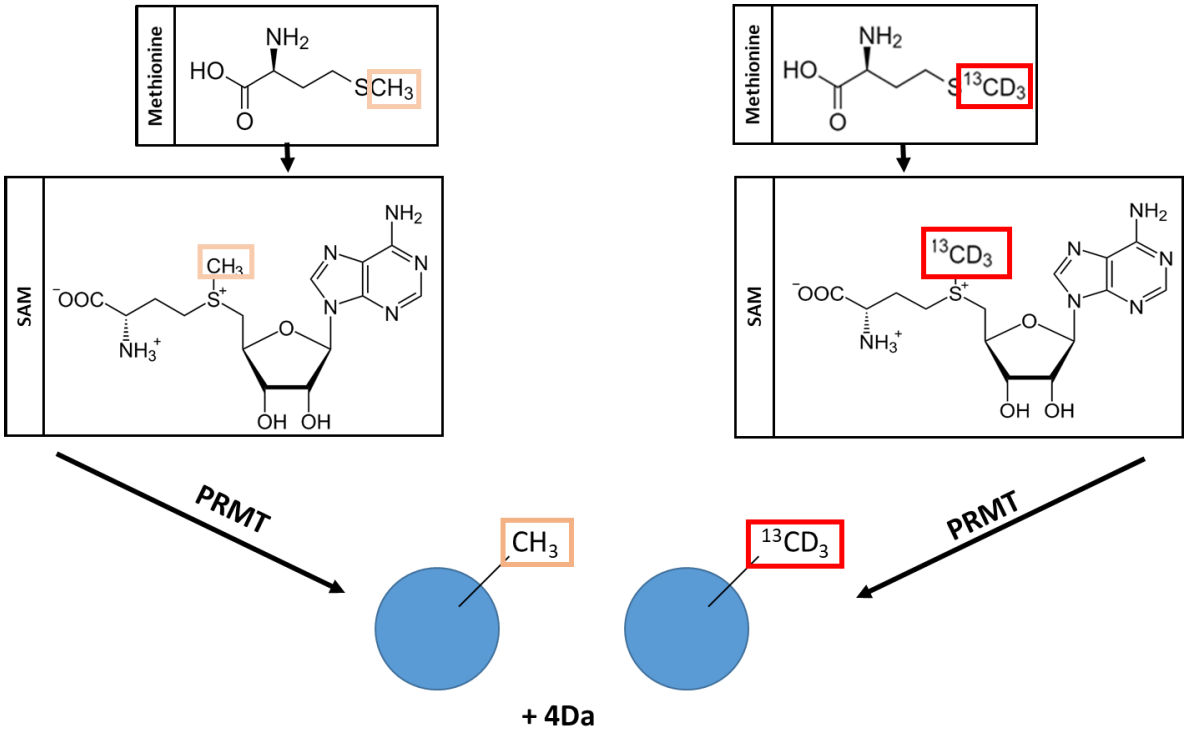

Figure 6.1: Scheme of the hmSILAC method*. Methionine, containing either a light ($^{12}CH_3$) or heavy ($^{13}CD_3$) methyl group, is converted into SAM by methionine adenosyl transferase (MAT), in an Adenosine triphosphate (ATP)-dependant reaction. The light/heavy methyl group is maintained and is transferred from SAM onto the target arginine by a PRMT enzyme. There is a +4 Da mass shift difference between the light (+14 Da or +28 Da for mono- and di-methylation, respectively) and heavy (+18 Da or +36 Da for mono- and di-methylation, respectively) methylarginine residues. This mass change is detectable by mass spectrometry.*

6.3.1.2) hmSILAC in Patient Samples

6.3.1.2.1) hmSILAC Media Preparation

DMEM containing no glutamine, no methionine and no cysteine (Fisher) was used to prepare the heavy and light methionine media. Glutamine (Sigma), methionine (light or heavy) (Sigma) and cystine (Sigma) were added at the following concentrations: Glutamine: 584 mg/L, Methionine (light/heavy): 30 mg/L, Cystine: 62.6 mg/L.

6.3.1.2.2 Sample Preparation

Patient sample SD0014 (patient information in section 5.2.1) was incubated on the microfluidic device as in section 5.2.2 for 192 hr. Four out of the eight slices were set up according to Figure 6.2. LDH release was comparable with previous samples using regular DMEM medium.

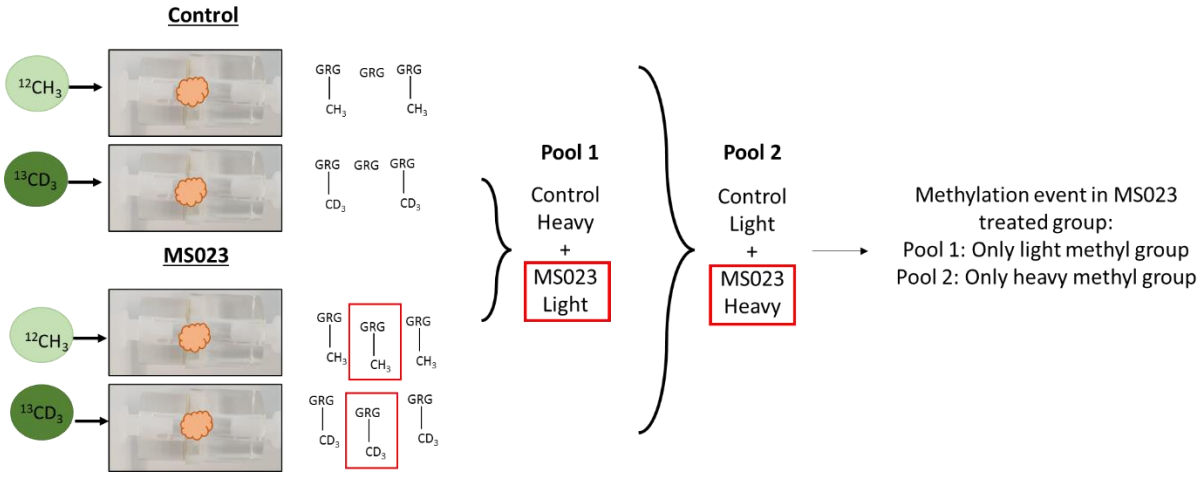

Figure 6.2: GBM patient samples were incubated with and without 100 nM of MS023*. One control sample contained light methionine and the other contained heavy methionine in the growing medium. One treated sample contained light methionine and the other contained heavy methionine in the growing medium. The tissue was then lysed, and control with heavy Met and MS023 samples treated with light Met were pooled (Pool 1). Similarly, control with light Met and MS023 samples treated with heavy Met were separately pooled (Pool 2). Certain methylation events would produce an identifiable heavy/light pair signature. If a methylation event was present in only the treated samples, a light methyl group (but no heavy methyl group) would be observed in Pool 1 and a heavy methyl group (but no light methyl group) would be observed in Pool 2.*

Following incubation, samples were snap frozen in liquid nitrogen for storage. When thawed, all samples were placed into a douncer individually, containing 500 µL of urea lysis buffer (20 mM HEPES, 9 M Urea and protease inhibitor cocktail (Pierce Protease Inhibitor Tablets (Thermo Fisher)). The lysates were then sonicated on a high setting for 5 minutes with 30 second intervals. The lysates were then cleared by centrifugation at 20,000 *g* for 15 minutes and the supernatant transferred to a new tube.

6.3.1.2.3) Protein Determination by Bradford Assay

Protein concentration was determined by Bradford assay according to manufacturer's instructions.

Control with heavy Met and MS023 samples treated with light Met were pooled (Pool 1). Similarly, control with light Met and MS023 samples treated with heavy Met were separately pooled (Pool 2). Samples were pooled in a 1:1 ratio and made up to a volume of 1 mL with lysis buffer.

6.3.1.2.4) Sample Preparation

Proteins were reduced by incubation with 3.6 µL of 1.25 M DTT (4.5 mM total) for 30 minutes at 55 °C with frequent shaking. When the solution had cooled to room temperature, the proteins were alkylated by incubation with 100 µL of 102 µM iodoacetamide (in water).

The lysate was diluted to 8 mL with 20 mM HEPES, to dilute the urea to 1 M. TPCK-treated Trypsin (in 1 mM HCl) was added to a final concentration of 10 µg/mL and incubated over night at room

temperature. 400 µL of 20% (w/v) trifluoroacetic acid (TFA) was added and a precipitate formed following a 15 minute incubation on ice. The precipitate was removed by centrifugation at 1780 *g* for 15 minutes.

Peptides were purified by elution through a HyperSep C18 column (Thermo Fisher). The column was pre-wet with 100% acetonitrile and washed with 3 washes of 0.1% (w/v) TFA. The lysate was loaded and cleaned with 3 washes of 0.1% (w/v) TFA and two washes with 0.1% (w/v) TFA, 5% (w/v) acetonitrile. The lysate was then eluted with 0.1% (w/v) TFA, 40% (w/v) acetonitrile, snap frozen in liquid Nitrogen and lyophilised for 2 days.

6.3.1.2.5) Immunoaffinity Purification

The lyophilised peptides were collected by centrifuging at 5000 *g* for 5 minutes. The pellet was resuspended in 1.4 of immunoaffinity purification buffer (50 mM MOPS/NaOH pH 7.2, 10 mM Na_2HPO_4, 50 mM NaCl) and transferred to a 1.5 microcentrifuge tube. The solution was cleared by centrifuging at 10,000 *g* at 4 °C for 5 minutes and cooled on ice.

The antibody-bead slurry contained MMA-specific antibodies conjugated to protein A agarose beads (Cell Signal #12235). This slurry was washed 5 times in 1 mL PBS and centrifuged at 2,000 *g* for 30 seconds. The antibody-beads were then resuspended in 40 µL PBS. The peptide solution was added to the antibody-beads and incubated for 2 hr at 4 °C with rotation. The mixture was centrifuged at 2,000 *g* for 30 seconds and the supernatant transferred to a new microcentrifuge tube. The beads were washed in 1 mL of immunoaffinity purification buffer twice and in water 3 times. The peptides were eluted by adding 55 µL of 0.15% (w/v) TFA allowing to stand at room temperature for 10 minutes. The eluate was centrifuged at 2000 *g* for 30 seconds and transferred to a new microcentrifuge tube. The elution step was repeated with 50 µL of TFA and both eluates were pooled.

6.3.1.2.6) Concentration and Purification of Peptides

Peptides were concentrated by Hypersep SpinTip C18 tips (Thermo Fisher). The tips were wet with 50 µL of 0.05% (w/v) TFA plus 60% (w/v) acetonitrile and washed 3 times with 0.05% (w/v) TFA. The sample was loaded and washed with 0.05% (w/v) TFA two times. The peptides were eluted with 0.05% (w/v) TFA plus 60% (w/v) acetonitrile and concentrated in a Speed-Vac.

6.3.1.2.7) Liquid Chromatography and Mass Spectrometry Analysis

The eluted peptides were transported to the mass spectrometry facilities at the University of York where the analysis took place. Here, samples were acquired over 1 hr acquisitions with elution from a 50 cm C18 EN PepMap column onto an Orbitrap Fusion Tribrid mass spectrometer using a Waters mClass UPLC. Resulting LC-MS chromatograms were peak picked and searched against the human

subset of the SwissProt database using PEAKS Studio X. To identify "light" methylated peptides, a mass shift of +14 Da was searched for, and to identify "heavy" methylated peptides, a mass shift of +18 Da was searched for.

6.3.1.3) hmSILAC of U-87MG Cells

6.3.1.3.1) Cell Plating

Cells were passaged when at 80% confluency into 4x T75s. One control and one treated sample contained light methionine and the other control and treated samples contained heavy methionine in the medium (Figure 6.3). When at 80% confluency, the cells were passaged into 8x 150 mm plates, with 2 plates for each above condition. Again, once at 80% confluency, the cells were passaged into 32x150 mm plates, with 8 plates per condition. Once these cells reached 80% confluency, the flasks were harvested as described in the following steps.

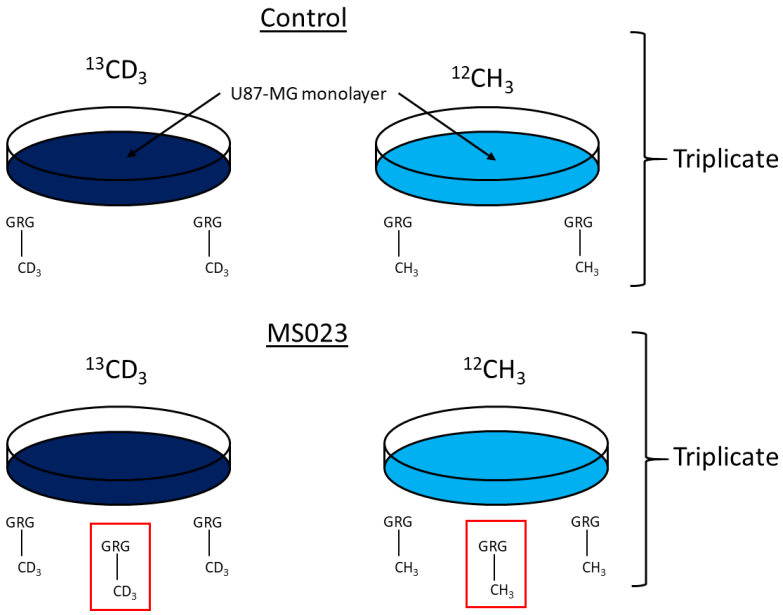

***Figure 6.3: U-87MG cell were treated with and without 100 nM of MS023**. One control sample contained light methionine and the other contained heavy methionine. One treated sample contained light methionine and the other contained heavy methionine in the medium. Control with heavy Met and MS023 samples treated with light Met were pooled (Pool 1). Similarly, control with light Met and MS023 samples treated with heavy Met were separately pooled (Pool 2).*

6.3.1.3.2) Cell Lysis

Cells were scraped and washed in PBS and transferred to a 1.5 microcentrifuge tube and lysed in 500 µL of urea lysis buffer (20 mM HEPES, 9 M Urea and protease inhibitor cocktail (Pierce Protease Inhibitor Tablets (Thermo Fisher)). The lysate was sonicated on a high setting for 5 minutes with 30 second intervals. The lysate was then cleared by centrifugation at 20000 g for 15 minutes and the supernatant transferred to a new tube. The samples were processed for mass spectrometry according

to steps 6.2.1.2 – 6.2.1.10, with some slight differences. These differences are that the antibody-bead slurry contained antibodies specific against SDMA marks, therefore changing the mass shift used to identify methylated peptides. As SDMA marks contain two methyl groups, a mass shift of 28/34 Da m/z was used to identify methylated proteins rather than 14/18 Da in the patient samples. The 28 Da mass shift would identify two light methyl groups on the guanidino Nitrogen. Although two heavy methyl groups on the guanidino Nitrogen would produce a mass shift of 36 Da, the efficiency of the uptake and conversion of heavy isotopes was not clear, and it would be possible for such Nitrogen's to have both a light and a heavy methyl group associated, producing a mass shift of 32 Da. Therefore, a compromised mass shift of 34 Da was chosen to maximise identification of "heavy" methylated peptides as this would be more representative of the average mass shift amongst a peptide population/peak.

6.4 Results

6.4.1) Treatment of Patient Samples with MS023 Induced Cross-Talk Between Type I and Type II PRMTs

Inhibition of type I PRMTs in U-87MG cells resulted in cross-talk events as observed by the induction of symmetrical dimethylation. In this chapter, these cross-talk events are further elucidated through the use of PRMT inhibitors in patient tissue, western blotting and mass spectrometry. Patient samples were treated with MS023, and western blotting was used to demonstrate any changes in symmetrical arginine dimethylation. Six of the samples appeared to present cross-talk between type I and type II PRMTs, suggested by the increase in SDMA marks in MS023 treated samples (SD0008, SD0012, SD0014, SD0015, SD0020 & SD0021) (Figure 6.4A). Conversely, sample SD0011 did not show a change in SDMA following treatment with MS023. It was not possible to determine whether there was an increase in SDMA marks due to the lack of a successful loading control for SD0019.

Type I and type II PRMTs catalyse the transfer of a single methyl group before then catalysing the transfer of a second. Considering this, western blot analysis was used to determine if there were any changes in MMA following inhibition of type I PRMTs. Out of the 5 patient samples analysed, 4 showed an increase in MMA with MS023 treatment (SD0012, SD0015, SD0020 & SD0021), with the other two samples showing minimal change (SD0014) (Figure 6.4B). This shows that upon inhibition of the type I enzymes, type II and type III PRMTs were still able to transfer single methyl groups onto proteins, producing the MMA mark. These marks would then be converted into SDMA by type II PRMTs, resulting in an increase in both MMA and SDMA marks. Surprisingly, these increases in MMA and SDMA were not completely global, as some marks were simultaneously lost (Figure 6.4, green arrows).

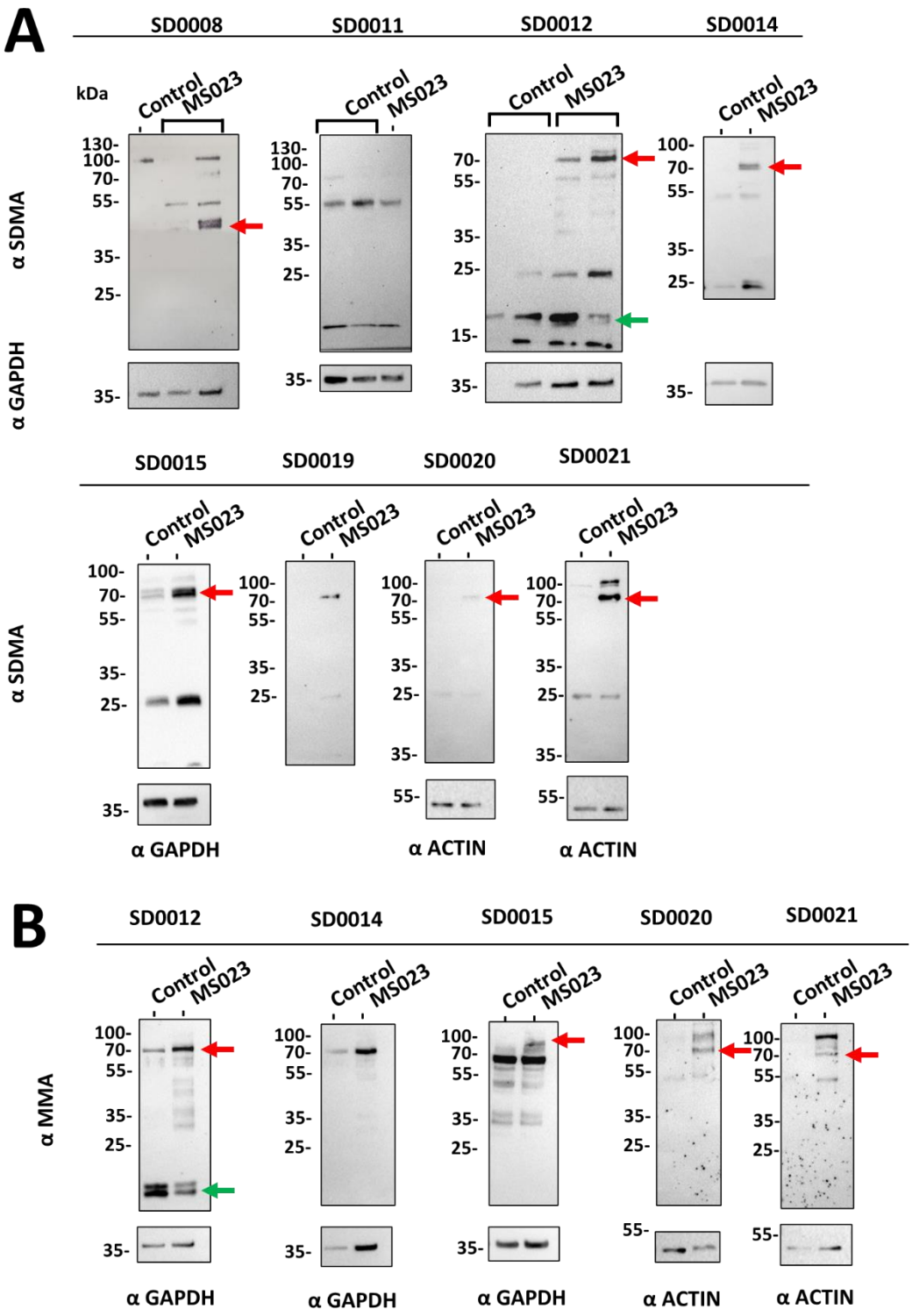

Figure 6.4: Western blot analysis of GBM patient samples treated with MS023 showing presence of cross-talk activity amongst PRMT enzymes. *(A) Western blot of GBM patient samples treated with and without MS023 showing changes in SDMA. Nine patient samples are shown each treated with and without 100 nM MS023 for 192 hr. SDMA is increased in 6 out of 9 samples (for examples see red arrows). Certain SDMA marks were decreased in some samples (green arrow). Loading controls could not be successfully probed for SD0019. (B) Western blot of GBM patient samples treated with and without MS023 showing changes in MMA. Five patient samples are shown each treated with and without 100 nM MS023 for 192 hr. MMA is increase in 4 out of 5 samples (Red arrows). Certain MMA marks were decreased in some samples (green arrow). GAPDH and ACTIN used as loading controls.*

6.4.2) FUS is Methylated in the Presence of MS023

Treatment of both a GBM cell line (chapter 3) and GBM patient cell lines (Figure 6.4) with the type I PRMT inhibitor MS023 resulted in an increase in SDMA marks, suggesting cross-talk activity between PRMT types. Changes from ADMA to SDMA marks may have significant consequences for protein-protein interactions and tumour biology, for this reason, it is crucial to determine the identity of these modified proteins. HmSILAC is a mass spectrometry technique involving the detection of mass differences between methyl groups containing heavy and light Carbon and Hydrogen/Deuterium isotopes. This technique was utilised in order to identify proteins that are monomethylated and symmetrically dimethylated only as a result of MS023 treatment in both U-87MG cells and GBM patient samples, respectively. In addition to treatment with and without MS023, both tissue samples and U-87MG cells were incubated with either a light or heavy version of methionine (containing either a $^{12}CH_3$ or $^{13}CD_3$ methyl group, respectively), which was then converted into SAM within the cells. As PRMTs can transfer the light or heavy methyl group from SAM onto their target proteins, the methylation of proteins can be identified through mass spectrometry by the existence of light and heavy methyl combinations as explained in Figure 6.2.

For the patient biopsy samples, mass spectrometry experiments identified a total of 133 peptides with light methyl modifications and 10 peptides with heavy methyl modifications in Pool 1. These shorter peptides are a result of protein digestion during tissue processing and may or may not originate from the same number proteins. In Pool 2, there were 183 peptides with light methyl modifications and 9 peptides with heavy methyl modifications identified. Only one peptide presented with a light/heavy signature that indicated being methylated in the samples treated with MS023 only, and not in the untreated sample. This peptide had a light methyl modification in Pool 1 with the absence of a heavy modification, and a heavy methyl modification at the same residue in Pool 2 with the absence of a light modification. This peptide belongs to the RNA binding protein known as Fused in Sarcoma (FUS).

The peptides associated with the FUS protein that were found to be methylated following both the patient tissue and U-87MG cell line mass spectrometry experiments can be found in Table 6.1. Analysis showed that FUS was methylated at arginine 394 in the MS023 treated samples alone (Table 6.1). This is because a light methyl group was identified at R394 in Pool 1, with an absence of a heavy methyl group; and a heavy methyl group was identified at R394 in Pool 2, with the absence of a light methyl group. Although methylation events were identified in other residues, these did not show the pattern representing methylation in the MS023 treated samples alone.

In U-87MG cell experiment, in Pool 1, 77 peptides were identified with light methyl modifications and 25 peptides were identified with heavy methyl modifications. In Pool 2, 59 peptides were identified

with light methyl modifications and 35 peptides were identified with heavy methyl modifications. No peptides were identified as fully fitting the criteria previously described, although a methylation event was identified on R394 (Table 6.1).

Table 6.1: Identification of FUS peptides in U-87MG cells and GBM patient sample. *A total of 6 FUS peptides were identified as methylated in patient samples and U-87MG cell lines, each containing either one or two methylation marks. In the patient sample (top), two FUS peptides were identified as being methylated in Pool 1, with light MMA modifications at R407, R394 and R407. One peptide was identified as being methylated in Pool 2 for the patient sample, with two heavy MMA modifications at R388 and R394. In the U-87MG cell line sample, two FUS peptides were also identified as being methylated in Pool 1, with each containing two light SDMA modifications, the first at R394 and R407, and the second at R216 and R218. One peptide was identified as being methylated in Pool 2 in the U-87MG cell line sample, with two heavy SDMA modifications at R248 and R259. Patient sample pool were immunoprecipitated with antibodies specific for MMA epitopes. U-87MG cell line pools were immunoprecipitated with antibodies specific SDMA epitopes. Pool 1: Light treated and heavy control (LTHC), Pool 2: Light control and heavy treated (LCHT).*

Pool	FUS Peptide (P35637)	FUS Position	Expected MW	Observed MW	Mass Error	Retention time	m/z
Patient Sample (IP: MMA)							
1 (LTHC)	GGYGGGGSGGGGR(+14.02)GGFPSGGGGGGGQQR	407	2250.9862	2265.002	-0.5	25.19	756.0076
1 (LTHC)	GGPMGR**(+14.02)**GGYGGGGSGGGGR(+14.02)	394 & 407	1549.6803	1577.7117	1.1	25.51	789.864
2 (LCHT)	GGRGR(+18.04)GGPMGR**(+18.04)**GGYGGGGSGGGGR	388 & 394	2032.9469	2069.0227	-0.4	41.85	690.6812
U-87MG (IP: SDMA)							
1 (LTHC)	GGPMGR**(+28.03)**GGYGGGGSGGGGR(+28.03)GGFPSGGGGGGGQQR	394 & 407	2806.2449	2862.3076	-0.6	29.49	716.5837
1 (LTHC)	GGR(+28.03)GR(+28.03)GGSGGGGGGGGGGYNR	216 & 218	1705.7740	1761.8367	1.1	28.02	441.4669
2 (LCHT)	GR(+34.07)GGGRGGRGGMGGSDR(+34.07)GGFNK	248 & 259	2048.9782	2117.1162	-1.8	46.54	1059.5635

To further investigate the methylation of FUS following MS023 treatment, western blot membranes previously used to confirm drug activity following COVID-19 lockdown (Section 5.3.4), were stripped, and reblotted using a FUS antibody. When overlapping the original membrane image (Figure 5.7 B, left) with the FUS reblot (Figure 6.5), the upregulated SDMA mark (red arrow of Figure 5.10) overlapped approximately with the new FUS band, suggesting the proteins are of a similar molecular weight (Figure 6.5, green arrow). Further investigation will need to take place to confirm the identity of the ~70 kDa band observed in these western blot experiments and these possibilities will be discussed further.

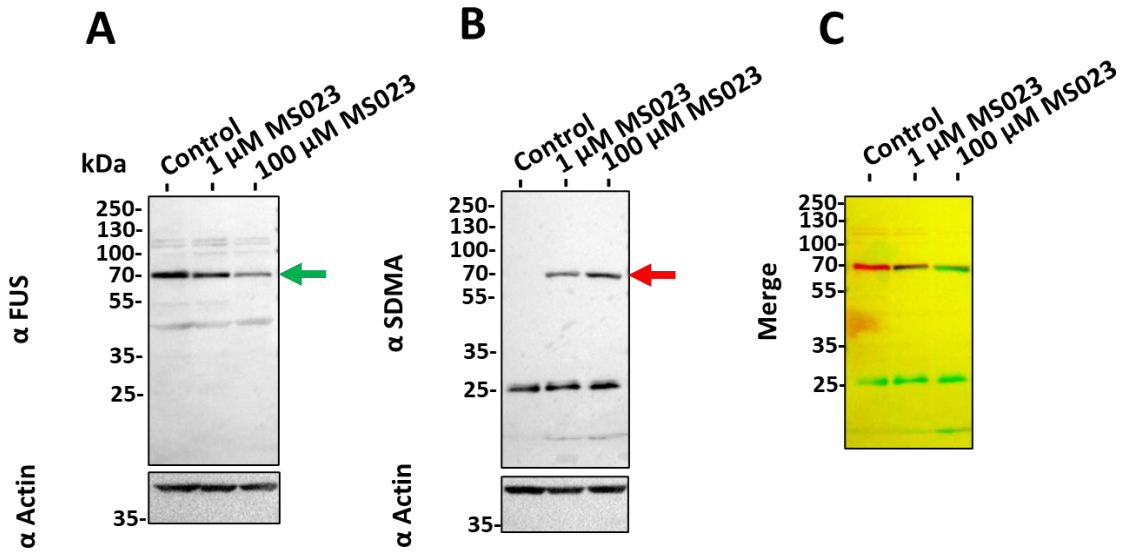

Figure 6.5: Western blot analysis of U-87MG cells treated with MS023 suggesting the SDMA of FUS. *(A) FUS antibody (B) SDMA antibody (blot taken from Figure 5.10) (C) A & B blots merged with A coloured green and B coloured red. Actin was used as a loading control.*

6.5) Discussion

6.5.1) Presence of Cross-talk in Samples with no Decrease in ADMA

Some patient samples did not show a reduction in ADMA following incubation with MS023 but did in fact show cross-talk activity between type I and type II PRMTs by an increase in SDMA. The antibodies used recognise the epitope of asymmetrically or symmetrically methylated arginine residues but may have slightly different specificities and biases toward different residues. This means that a symmetrically methylated epitope may be recognised by the anti SDMA antibody, but the asymmetrically methylated version of the same epitope may not be recognised by the corresponding anti ADMA antibody used. Western blotting may also not be sensitive enough to detect more subtle changes in the quantity of ADMA marks, as detection of post translational modifications requires a relatively large concentration of sample (Mishra et al., 2017).

6.5.2) PRMT1 is Most Likely Responsible for Type I Cross-Talk

When patient GBM samples were treated with the type I PRMT inhibitor, MS023, 6 out of 9 showed an increase in SDMA marks and 3 out of 5 samples showed an increase in MMA marks. From these results, it is not certain whether this cross-talk is a result of inhibiting a single type I PRMT, or whether inhibition of multiple enzymes is needed. Studies carried out by others, however, have shown similar increases in SDMA and MMA as a result of down regulating PRMT1 specifically by shRNA or inhibiting its activity with small molecule inhibitors (Dhar et al., 2013, Fedoriw et al., 2019, Hartel et al., 2019, Gao et al., 2019b). A similar study has also been carried out to investigate the loss of PRMT2 in GBM cells (Dong et al., 2018). Although there was not a focus on cross-talk activity amongst PRMT enzymes, no change was seen in the type II PRMT specific histone mark H4R3me2s, indicating that there was no induction in type II PRMT activity following PRMT2 inhibition.

Although it is possible that the inhibition of PRMT2, PRMT3, PRMT4, PRMT6 and PRMT8, contributed to the induction of type II PRMT activity, through the availability of substrates, the specific loss of PRMT1, which is responsible for approximately 80% of type I PRMT activity, is sufficient for the induction of type II PRMT activity.

6.5.3) Possible Cross-Talk Mechanisms

Previous studies using cell lines suggest that loss of type I PRMTs, specifically PRMT1, may result in substrate scavenging by the remaining active PRMTs, causing a global increase in type II PRMT specific ArgMe (Gao et al., 2019b, Musiani et al., 2019, Fedoriw et al., 2019). Upon inhibition of type I PRMTs, sites that would otherwise be asymmetrically methylated, would be now available for symmetrical dimethylation by the type II PRMTs. This would explain the increases in SDMA marks, and perhaps the increase in MMA marks. PRMT1 is a partially processive enzyme (Obianyo et al., 2008), meaning it can catalyse both methylation reactions during a single binding step whilst bound to its substrate. Because of this, the increase in MMA is most likely due to other PRMT enzymes, such as PRMT5, which is unprocessive (Antonysamy et al., 2012), and is therefore more likely to add a single methylation mark.

The reductions in SDMA marks seen following MS023 treatment could be a result of more specific cross-talk activity, rather than substrate scavenging. Although increases in the symmetrical dimethylation of some proteins was observed in this chapter, this change was not consistent amongst all proteins and all patient samples. For example, some proteins showed either no change in methylation status, or an increase in symmetrical dimethylation with MS023 treatment (Figure 4.6 & 4.7 green arrows). This suggests either a patient-specific mechanism, perhaps as a result of variance in PRMT expression, or a protein specific mechanism. Inhibition of a type I PRMT could prevent the addition of an ADMA mark onto an uknown protein which could then result in a change of protein-

protein interactions with a possible binding partner which then prevents the symmetrical dimethylation of a further protein. The fact that proteins that were symmetrically methylated in response to MS023 treatment had different molecular weights to asymmetrically methylated proteins in the control samples opens the possibility that this cross-talk may not always occur on the same residue or even protein.

6.5.4) Consequence of PRMT Cross-talk

Due to the immunoprecipitation steps of the mass spectrometry experiments, it is not clear whether FUS was unmethylated in the control samples, or simply methylated in a different manner (asymmetrically). Therefore, both the consequences of a shift of methylation status from unmethylated to symmetrically and monomethylated, and from asymmetrically to symmetrically methylated should be considered.

A switch from asymmetrical dimethylation to symmetrical dimethylation is known to have effects on gene expression when involving histone proteins. For example, the histone modification H4R3me2a is an activating histone mark whereas H4R3me2s is a repressive histone mark (Blanc & Richard 2016). Although histone proteins may be affected by MS023 treatment, the proteins with increased SDMA marks have molecular weights of between 25 and 75 kDa whereas histone proteins are much lighter (Mongiardi et al., 2015).

Any changes to protein interactions that occur when a protein is asymmetrically methylated rather than symmetrically methylated could cause unwanted effects such as a reduced activity of a tumour suppressor protein or signal other cellular mechanisms that could produce adverse effects during cancer treatment. Any changes to protein-protein interactions as a result of an ADMA to SDMA switch may in fact be the mechanism behind type I PRMT inhibiting drugs. For example, Myc is known to be methylated by both PRMT1 and PRMT5, where PRMT5 is required for Myc/PRMT1 binding (Favia et al., 2019). Inhibition of PRMT1 resulted in the increased SDMA of Myc and it was suggested that they both compete for Myc as a substrate. The neuronal specific Myc family member, NMyc, is also methylated by both PRMT1 (Eberhardt et al., 2016) and PRMT5 (Park et al., 2015). Inhibition of PRMT1 was shown to reduce Myc recruitment to the SOX2 promoter in stem cell conditions, and CCND1 and EGFRvIII promoters in differentiated conditions (Favia et al., 2019). PRMT1 and PRMT5 have also been found in complex with MEP50, and enhancer of rudimentary homolog (ERH) and CHTOP, in GBM (Takai et al., 2014). The study found that this complex was associated with genes including *EGFR, AKT3, CDK6, CCND2*, and *BRAF*. These studies demonstrate that inhibition of PRMT1 could disrupt a number of mechanisms leading to changes in protein interactions and gene expression, that could have significant consequences in GBM.

6.5.5) FUS Protein Function and Methylation

Substrates of PRMT1 and PRMT5, including CHTOP and Myc, have been found to play a role in GBM. To evaluate whether proteins such as these could be undergoing changes in their arginine methylation status following PRMT inhibition, the presence of relevant heavy/light methyl pairs was determined. CHTOP was found to be monomethylated in one of the pools of patient samples but did not appear to be methylated at all in the accompanying pool, and therefore these results are inconclusive. If uptake of exogenous methionine was improved, the desired methylation signature may have been produced. Myc was not found to be methylated in any of the samples tested. One other protein, however, demonstrated the heavy and light pairing associated with being methylated only in treated samples: FUS, an RNA binding protein, also known as Translocated in Liposarcoma Protein (TLS). Following hmSILAC experiments, it was found to be dimethylated only in the presence of MS023 in U-87MG cells and was also found to be monomethylated only in the presence of MS023 in a GBM patient sample.

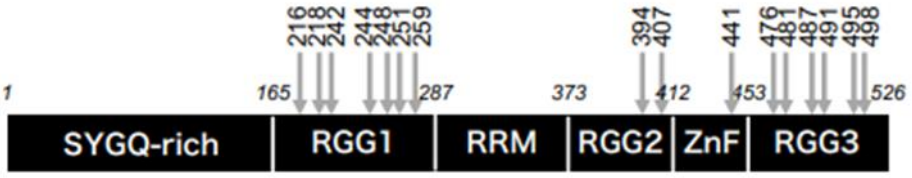

Figure 6.6: A summary of the known methylation sites on FUS *(Cui et al., 2018).*

FUS is known to take part in a number of cellular mechanisms, mainly those associated with RNA processing, and has been found to play in role in tumorigenesis (Ghanbarpanah et al., 2018). FUS is phosphorylated by ataxia-telangiectasia mutated (ATM) and DNA-dependent protein kinase (DNA-PK), two factors required for DNA double strand break repair. Loss of FUS is associated with both reduced non-homologous end joining and homologous recombination, as well as an induction of DNA damage (Deng et al., 2014, Wang et al., 2018).

FUS has been shown to play a role in a number of human cancers including lung, cervical cancer, and GBM, with its expression being associated with poor differentiation, poor prognosis and greater extend of metastasis (Xiong et al., 2018, Zhu et al., 2018). Due to FUS's role in RNA processing, it is not surprising that it has been implicated in the pathogenesis of GBM through interactions with microRNAs and long noncoding RNAs. LINC00470 is a long noncoding RNA that was shown to induce malignant characteristics of GBM and has been proposed as a prognostic marker for astrocytoma patients (Liu et al., 2018). LINC00470 was shown to rely on interaction with FUS to activate AKT and induce this GBM phenotype (Liu et al., 2018). Another long noncoding RNA implicated in GBM is ADAMTS9-AS2 (Yan et al., 2019). ADAMTS9-AS2 was shown to promote GBM invasion and migration in TMZ resistance GBM cells and was associated with poor TMZ response in GBM patients. It was then

suggested that ADAMTS9-AS2 induced TMZ resistance by stabilising FUS and preventing its degradation mediated by MDM2 (Yan et al., 2019). Alongside the transcription factor BACH2, FUS was found to be expressed at high levels in GBM tissue compared with normal tissue and is thought to act as a coactivator with BACH2 to ultimately block the Hippo signalling pathway and promote malignancy in glioma cells (Yang et al., 2020). This inhibition of the Hippo signalling pathway was dependant on FUS's regulation of the long noncoding RNA, TSLNC8, and the microRNA, miR-10b05p (Yang et al., 2020). Another signalling pathway often impacted in cancer pathogenesis, the Hedgehog pathway, has also been shown to be regulated by FUS (Wu et al., 2021). FUS was shown to positively regulate the transcription of SMO-193a.a, a circular RNA that encodes for the SMO protein that is required for the sustained hedgehog signalling to promote proliferation and self-renewal (Wu et al., 2021). An important aspect of tumour biology is the formation of blood vessels, angiogenesis. FUS has been shown to promote this process in GBM cells through upregulation of the circular RNA circ_002136, forming part of a positive feedback loop involving miR-138-5p, SOX13 and SPON2 (He et al., 2019). Due to FUS's multifunctional role and number of interactions with noncoding RNAs, it presents a novel target for GBM therapy. Its ability to promote angiogenesis and TMZ resistance offers an alternative mechanism to combat the disease when used in combination with other drugs.

FUS has previously been demonstrated to contain at least 20 arginine residues that are asymmetrically methylated (Rappsilber et al., 2003). In a study conducted by Du et al., R216, R218, R242 and R394 were shown to be consistently methylated in HeLa cells, although it was not specified if these were ADMA or SDMA marks (Du et al., 2011). The group demonstrated FUS in a complex with PRMT1 and showed increased methylation of FUS following the enhanced expression of PRMT1. They also found that this co-expression of PRMT1 and FUS in HeLa cells caused a synergistic activation of the Survivin promoter. Survivin is a member of the Inhibitor of apoptosis (IAP) family of proteins. It is involved in the inhibition of apoptosis and is increased in expression in a number of cancers (Jaioswol et al., 2015). The mass spectrometry experiments conducted in this chapter suggest that treatment with MS023 induces a switch from asymmetrical to symmetrical dimethylation of FUS at R394. It is currently unknown what the specific effect of FUS asymmetrical dimethylation at R394 may be. The loss of PRMT1 activity and induction of type II PRMT activity could inhibit FUS's interaction with the Survivin promoter region and therefore the activation gene expression. This could present a mechanism for the anti-tumour activity of MS023 seen by other groups through the induction of apoptosis. For this reason, it may be useful to quantify changes in apoptotic markers, such as cleaved-PARP, by IHC, rather than the use of proliferative markers. This could also overcome the issues evident by the reduction in Ki-67 index in samples incubated on chip compared with pre-chip samples.

As previously mentioned in chapter 3, PRMT1 has been shown to stimulate the acetylation of lysine residues in histone tails by p300 (Wang et al., 2001, Geoghegan et al., 2015). FUS normally undergoes allosteric alteration by the long non-encoding RNA, pncRNA-D, allowing for its binding to and inhibition of CBP/p300 and its histone acetyl transferase (HAT) activity (Wang et al., 2008b). Methylation of FUS by PRMT1, however, was shown to inhibit this modification by pncRNA-D, resulting in the increased HAT activity of CBP/p300 (Cui et al., 2018). This HAT activity was specific towards the *CCND1* promoter. It is unclear if a switch of ADMA to SDMA of FUS by type II PRMTs would also result in the same activity of FUS in this scenario.

PRMT1 was found to be required for the accumulation of FUS with Amyotrophic lateral sclerosis (ALS) linked mutations within the cytoplasm rather than the nucleus (Tradewell et al., 2012), and autopsies of ALS patients show FUS granular like inclusions within neurons and glial cells of the brain (Rademakers et al., 2010). Methylation of FUS within RGG motifs in FUS' C-terminal domain has also been shown to inhibit the ability of FUS to take part in phase separation, by disrupting protein-protein interactions (Qamar et al., 2018). Alongside PRMT1, PRMT8 has also been shown to interact with and methylate FUS (Pahlich et al., 2008, Simandi et al., 2018).

There are fewer studies that investigate the presence of SDMA marks within the FUS protein and the consequences of this modification. Fedoriw et al. (2019) and Fon et al. (2019) identified FUS in similar experiments to the SILAC mass spectrometry investigations in this chapter. Using the type I PRMT inhibitor, GSK3368715, in a wide range of cancer cell lines, Fedoriw et al. demonstrated that FUS was methylated, along with other proteins associated with pre-mRNA processing (Fedoriw et al., 2019). The peptide identified was also shown to be symmetrically dimethylated at residue 394 in the presence of GSK3368715, although it was not shown to be monomethylated at 394. Symmetrical dimethylation of FUS at R394 has also been identified by other groups (Chitiprolu et al., 2018). The paper did not focus on this specific modification but did find that symmetrical dimethylation by PRMT5 of arginines in neighbouring RGG motifs, facilitated the binding of FUS to p62, a protein involved in autophagy (Rusten & Harald Stenmark 2010).

6.5.6) Limitations of hmSILAC Approach

A limited proportion of peptides were found to be methylated in these samples, suggesting inefficiency in the immunoaffinity purification stages. Hartel et al. showed multiple techniques are required in order to reveal complete methylome data (Hartel et al., 2019). They found that there was minimal overlap between the peptides identified following enrichment by two different techniques: immunopurification and high pH strong cation exchange. This suggests that many modified peptides were overlooked during the enrichment stage of lysate processing. This may be due to the unspecific

nature of high pH ion exchange, compared with the RGG motif recognition found in immunoaffinity purification.

Our mass spectrometry experiments demonstrated that FUS was symmetrically dimethylated in U-87MG cells and monomethylated in patient tissue in response to treatment with MS023. Although evidence suggests FUS is most likely normally asymmetrically dimethylated in cells (Rappsilber et al., 2003, Du et al., 2011, Qamar et al., 2018), due to the immunoprecipitation step of the experiments, the methylation state of FUS prior to treatment with MS023 is unknown. To overcome this, antibodies against ArgMe, rather than MMA or SDMA specifically could be used, and LC MS/MS used to identify the presence of ADMA or SDMA marks. To investigate the methylation status of FUS, specific methyl FUS antibodies could be used, although currently, none are available for R392 methylFUS. Another possibility is the use of immunoprecipitation to isolate the FUS protein and then a simpler MALDI mass spectrometry procedure to identify any methylation marks on the peptides. Treatment of the cells with FUS siRNA could also help confirm the identity of the FUS band prior to isolation.

6.5.7) Conclusions

As PRMT inhibitors targeting type I PRMTs are currently under investigation in clinical trials, it is important to address the cross-talk activity that occurs between type I and type II PRMTs, as they could have number of consequences in terms of cancer treatment. These changes could, for instance, result in drug resistance, if the resulting SDMA marks were functionally similar to the ADMA marks or could provide the drug mechanism of action. Western blot experiments demonstrated this cross-talk activity in 6 samples, judged by the increased SDMA in treated samples. Possible consequences of this shift from ADMA to SDMA are changes in protein-protein interacts, such as with Myc and CHTOP, leading to changes in the expression of genes including *SOX2, CCND1/2, EGFR, AKT3, CDK6,* and *BRA.* To identify specific proteins monomethylated or symmetrically dimethylated as a result of MS023 treatment, SILAC mass spectrometry was utilised. Using this method, FUS was identified as being monomethylated in a patient sample and symmetrically dimethylated in U-87MG cells, as a consequence of type I PRMT inhibition. As this was only investigated in a single patient sample, it is not certain whether this methylation pattern of FUS is apparent in a wider range of GBM tumours and therefore whether it is important in GBM pathogenesis or PRMT targeted treatment. Methylation of FUS has previously been demonstrated, supporting these findings (Du et al., 2011, Rappsilber et al., 2003, Cui et al., 2018, Tradewell et al., 2012, Qamar et al., 2018, Pahlich et al., 2008, Simandi et al., 2018). These studies each suggest varying consequences of FUS methylation. The ADMA of FUS has been shown to alter its cellular localisation, the activation of the Survivin promoter region, and the inhibition of CBP/p300 and its HAT activity. SDMA of FUS, however, has been shown to facilitate its binding to p62. It remains unclear what consequence a shift from ADMA to SDMA will result in. The

vast majority of research that has been carried out on FUS has been in the setting of Amyotrophic lateral sclerosis (ALS) (Ishigaki & Sobue 2018) and there are limited studies that have investigated FUS in GBM in terms of ArgMe. It is therefore difficult to determine if these functional consequences of FUS methylation discussed here will be applicable in GBM. However, the change in methylation status following type I PRMT inhibition may alter its functionality and attenuate pathways such as the Hedgehog, Hippo and those involved in GBM stemness, proliferation and angiogenesis to contribute towards to activity of PRMT inhibitors.

Chapter 7 – Discussion

7.1) Overview

PRMTs have presented a novel target for the treatment of GBM, a cancer with no curative therapies available for patients. Currently, GBM patients are most commonly given concurrent radiotherapy and chemotherapy, following surgical removal of the tumour. Despite this aggressive intervention, prognosis is poor with patients surviving approximately 15 months from diagnosis. Small molecule inhibitors of PRMTs are currently in clinical trials to evaluate both the safety of administration, and to determine if this devastating prognosis can be improved. As PRMT inhibitors are being investigated in human trials, it is important to fully understand the role of ArgMe in GBM in clinically relevant model. Here, an *ex vivo* microfluidic model was evaluated and the consequences of PRMT loss in GBM cells and tissue were characterised. The model successfully maintained GBM patient tissue in a viable state, allowing for the pharmacological treatment with a variety of PRMT inhibiting drugs. Drawbacks of the model included a reduced proliferative capacity of the tissues, meaning more thought would be needed for the appropriate end point. With the assays and markers used in these experiments, i.e., LDH assay, MTS assay and IHC, it is difficult to define the patient response to PRMT inhibition. However, cross-talk activity between PRMT enzymes was demonstrated and a protein identified that may play an important role in the cellular response to PRMT inhibition, something that had previously not been shown in GBM tissue.

Out of all the PRMT inhibitors tested in the monolayer and spheroid cell line model, Furamidine was the only drug to induce a reduction is cell viability as judged by MTS assay. Differences in the response to Furamidine and MS023 are likely due to their differing specificities for PRMT enzymes and other targets, including TDP1. Treatment with Furamidine caused the loss of acetyl lysine marks, suggesting cross-talk mechanisms between PRMT1 and lysine acetyltransferases. Other cross-talk events were also observed between type I and type II PRMTs, as there was an increase in SDMA following treatment with MS023. These cross-talk mechanisms are also being investigated by other groups (Dhar et al., 2013, Fedoriw et al., 2019, Hartel et al., 2019, Gao et al., 2019b), but have not yet been demonstrated in tissue. For this reason, MS023 was the focus of further investigations into PRMT activity in GBM using patient biopsies.

The microfluidic model was initially evaluated by measuring the release of LDH into effluent samples, where the presence of LDH would indicate cell death of the GBM biopsy. This methodology was used to determine how long the patient samples could be incubated on chip and remain viable. Minimal release of LDH into the effluent was observed up to 192 hr. Although previous microfluidic studies

were limited to incubation times of up to 72 hr (Riley et al., 2019, Olubajo et al., 2020) longer periods were investigated as this would allow for greater drug penetration and clinical relevance.

As TMZ is given to GBM patient as standard care (Stupp et al., 2009), this drug was used to further evaluate the model's efficacy. However, treatment with TMZ did not result in a tumour response when judged by LDH assay, MTS assay or Ki-67 quantification. This was surprising as patient sample SD0026 was found to have a methylated MGMT promoter, meaning they were theoretically sensitive to TMZ treatment due to a reduction in DNA repair capacity. However, this was the only biopsy to show methylation of the MGMT promoter and definite conclusions cannot be made. Ki-67 was found to be statistically reduced in the on-chip samples, regardless of treatment. This suggests that although there is no increase in cell death on-chip, the biopsies have a reduced proliferative capacity after incubation on-chip for 8 days. This may help explain the lack of response seen in treated samples, due to the need for active cell division and protein turnover for both TMZ and MS023 to be effective. It may also be difficult to identify differences in ki-67 staining as all on-chip samples had ki-56 index values of less than 10%, meaning any differences may not be obvious or statistically significant.

Treatment with TMZ was also used to determine the presence of intra-tumour heterogeneity in the GBM patient biopsies used. This was important as variance amongst slices taken from the same biopsy could introduce misleading observations when comparing to differently treated groups. Slices taken from the same biopsy that were ran in parallel with the same treatment showed small variances in LDH release throughout the microfluidic incubation and showed greater variance in Ki-67 index following immunohistochemical processing.

Due to the demonstrable cross-talk events and clear inhibition of type I PRMT activity, MS023 was the focus of ArgMe experiments in later chapters. The efficacy of MS023 as a PRMT inhibiting drug to treat GBM patients was first evaluated using LDH assay and Ki-67 index. MS023 was initially given as a singular treatment, however, following a lack of response in 5 patient samples, it was given in combination with TMZ, due to the role of PRMT's in the repair of DNA damage (Auclair & Richard 2013). No change in LDH release or Ki-67 index was observed in the two patients tested. Drug concentrations were then increased ten-fold in an attempt to induce a cellular response, however no response was observed. It is hypothesised that the lack of response is due to the reduced proliferative activity of the patient biopsies during the microfluidic incubation leading to a loss of sensitivity of the GBM cells towards PRMT inhibition.

Following inhibition of type I PRMTs by MS023 in both U-87MG cells and patient biopsies, an induction in the symmetrical dimethylation of certain proteins was observed, including one weighing approximately 70 kDa, as judged by the increased intensity of the SDMA band at the 70 kDa marker.

In order to shed some light on the identity of this protein, or other proteins with an increase in ArgMe, hmSILAC mass spectrometry was utilised. Using this method, FUS, a protein with a molecular of approx. 70 kDa, was the only protein to be identified as being monomethylated only in the presence of MS023.

7.2) Patient Samples Had Reduced Proliferative Activity Following Microfluidic Incubation

Many previous studies and some of the experiments in this thesis have been carried out on GBM cell lines, including U-87MG. Although this cell line allows for a comparable view of GBM cell characteristics when investigating PRMT activity, it is limited by the lack of genetic heterogeneity that is present both amongst patients and within a tumour itself. For this reason, future work could involve repeating these experiments on other GBM cell lines in order to increase the data reproducibility and confidence on the GBM tumour responses observed. An interesting cell line that could be investigated is T98G, as it is PTEN wildtype, whereas U-87MG cells are PTEN mutant, as previously described (Dong et al., 2018). In later chapters, experiments were predominantly carried out on GBM patient samples in an *ex vivo* model, a more representative and accurate model of both GBM tumours and their microenvironment.

The minimal release of LDH into the effluent suggested the patient samples remained viable during incubation using this microfluidic model, and that the samples did not experience an increase in cell death. However, following quantification of Ki-67, it became apparent that the cells had a reduced proliferative activity. This is important as treatments such as TMZ act upon cells by inducing replication fork collapse and DNA breaks, resulting in ATR dependant cell cycle arrest and apoptosis (Mojas et al., 2007). For this to occur, the cells need to go through rounds of replication, which may not be occurring at a sufficient rate in these patient samples whilst on chip. Due to PRMTs role in DNA repair (Auclair & Richard 2013), proliferative signalling (Wang et al., 2019) and RNA processing (Braun et al., 2017), inhibition of PRMT enzymes is also most effective in proliferating cells. Any tumour response to PRMT inhibition may therefore be muted in this microfluidic model. To further elucidate the trend in Ki-67 expression and proliferative activity of the tumour cells, Ki-67 expression could be assessed at increasing time points up to 192 hr. The length of incubation prior to Ki-67 downregulation would then be used. Work carried out on tumour samples using similar microfluidic concepts found no decrease in Ki-67 following 72 hr (GBM, Olubajo et al., 2020) or 96 hr incubation (Thyroid, Riley et al., 2019). This suggests the loss of proliferation is most likely to occur between 72/96 and 192 hr.

Markers of other cellular processes, including apoptosis and senescence, are available to quantify by IHC or by western blotting. Cleavage of poly (ADP-ribose) polymerase (PARP), for example, is a marker

of apoptosis (Kaufmann et al., 1993) and has been shown to increase in GBM cells following treatment with TMZ (Ciechomska et al., 2018) and has also been shown to increase upon inhibition of PRMT1 in neuroblastoma cells (Hua et al., 2020). Unpublished work carried out by colleagues also demonstrated a lack of response when judged by Ki-67 index when using a similar microfluidic model but have shown changes in cleaved PARP by IHC on Thyroid malignancies (Riley, et al., unpublished). This evidence suggests that cleavage of PARP would be a suitable marker of cellular response for future microfluidic incubation with classical chemotherapeutic and PRMT inhibiting drugs.

Further investigation should be carried out to identify changes in flow rate or growing medium composition that could improve the maintenance of patient tissue on-chip. A flow rate of 3 µL/min was used here based on previous work carried out by colleagues at the University of Hull. However, it may be beneficial to use either a higher flow rate to aid in the removal of waste and provision of nutrients, or a lower rate to reduce stress upon the patient tissue. The growing medium used in this microfluidic model was the same as used in the earlier experiments with U-87MG cells. The use of a growing medium with greater resemblance to the CSF may be advantageous (Jacob et al., 2020). The use of growing medium without serum may also support the proliferation of a stem-like population of cells with greater robustness during microfluidic incubation.

7.4) Further Investigation of ArgMe in GBM

The changes in ADMA, SDMA and MMA levels observed by western blotting and mass spectrometry were used in these experiments to determine changes in PRMT activity. However, further methodologies exist that could provide a more in-depth elucidation of methylation within GBM cells. Such methodologies include the synthesis of enzymatically inactive PRMTs (Radzisheuskaya et al., 2019), site-directed mutagenesis to produce unmethylated proteins (Jeong et al., 2019, Liu et al., 2020), the use of ArgMe site specific antibodies (khumar et al., 2020), including a methyl-FUS specific antibody (Dormann et al., 2012), and finally, the measurement of PRMT activity through kinetic assays (Hevel and Price 2020).

Our mass spectrometry investigations have identified FUS as being both monomethylated (in biopsies) and symmetrically methylated (in cells) following treatment with MS023. It is therefore a possible candidate for the 70 kDa protein identified in the U-87MG and tissue studies carried out here. In order to confirm this, immunoprecipitation experiments could be carried out on these lysates. This could be done in several ways. Cells or tissue samples treated with and without MS023 could be lysed and separated through SDS-polyacrylamide gel electrophoresis (SDS-PAGE). Following staining of the gel and visualisation of the protein bands, the 70 kDa band could be excised and processed for mass spectrometry using SDMA specific antibodies to isolate methylated peptides. Using a Maxquant search

(Musiani et al., 2019), the presence of methyl-FUS could then be searched for in a very comprehensive and targeted manner. Alternatively, following cell lysis, immunoprecipitation could be carried out to isolate FUS, and the resulting lysate separated by SDS-PAGE. The proteins could be transferred onto a nitrocellulose membrane and an SDMA specific antibody used to visualise methyl-FUS if present on the membrane.

To determine the functional consequences of asymmetrical and symmetrical dimethylation of FUS, a FUS peptide could be synthesised bearing either modification and conjugated to biotin. Following incubation of these peptides with GBM cells or tissue, the peptides could be isolated using a streptavidin system. If these two modifications were functionally distinct on the FUS peptide, then different binding partners or substrates would be isolated alongside the modified FUS peptide.

There are currently possible biomarkers being investigated for patient stratification and response to PRMT inhibition. One such biomarker is MTAP deletion. Loss of MTAP results in an increase of its metabolite MTA, which can act as a selective inhibitor of PRMT5 (Fedoriw et al. 2019). This would offer an intrinsic method to produce the combinational loss of both PRMT1 and PRMT5, acting specifically on MTAP deleted cancer cells. This may be particularly useful in GBM treatment by allowing the stratification of patients, as loss of MTAP is relatively common in GBM tumours, making these patients suitable for treatment via PRMT inhibition (Bidinotto et al., 2016, Menezes et al., 2020). This is currently being investigated as a patient selection biomarker (NCT03666988) for clinical trials involving PRMT inhibitors.

A possible biomarker for PRMT inhibition has been identified in peripheral blood mononuclear cells and in cancer cell lines (Noto et al., 2020). As PRMT inhibitors are administered either intravenously or orally (systemically), total PRMT activity is likely to decrease, meaning there should be a measurable decrease in the proteolytic products of methylated proteins (mMA, aDMA and sDMA). Levels of these products could therefore be used to determine patient response to small molecular inhibitors of PRMTs currently being investigated in clinical trials.

7.5) Further Improvements and Applications of the Microfluidic Workflow

7.5.1) Overview

Microfluidics has provided a useful tool in the preclinical modelling of cancers, something that is greatly needed in the study of brain tumours (Aldape et al., 2019). Compared with conventional cell culture, microfluidics has a greater resemblance to the tumour environment and therefore allows for more accurate testing of pharmacological drugs. The use of patient tissue on-chip also provides the opportunity for improved precision medicine, either through the investigation of new therapeutic avenues or patient screening (Xiao et al., 2019, Yi et al., 2019, Linkous et al., 2019). In order to

characterise GBM biology, microfluidic devices have been integrated with various techniques to further understand different aspects of GBM tumour cells including proliferation, migration, and genomic and proteomic contents (Logun et al., 2018, Cai et al., 2020). To achieve this, microfluidic chips have been fabricated in series with a number of analytical tools, such as qPCR (Shao et al., 2015) and immunocytochemistry array chip (Sun et al., 2010).

7.5.2) Liquid Biopsies

Individuals with GBM have the worst prognosis of all glioma patients, with a median survival of 1.5 years following initial diagnosis (Ostrom et al, 2019). This is because GBM tumours are advanced and aggressive, being classed as grade IV astrocytomas. By the time of disease presentation and diagnosis, there are limited treatment options due to the diffuse nature of the tumour (Sahm et al., 2012). Therefore, there is a need for new methods that allow for the early detection and diagnosis of GBM. One such method being investigated is the use of liquid biopsies (Saenz-Antoñanzas et al., 2019).

Surgery may not be an always be an option for GBM patients due to location of the tumour (Simpson et al., 1993). Due to the nature of the tissue that tumour is situated in, there is always a risk of affecting normal neurological function during the procedure (Shankar et al., 2017). When surgery is not an option, a liquid biopsy could be used to confirm the presence of GBM. GBM liquid biopsies can provide a wide range of information. For example, proteins, DNA and RNA can be isolated from circulating tumour cell, extracellular vesicles (EVs) and from a cell free fraction (Shankar et al., 2017). These can be collected through a number of methods, including blood, CSF, urine and saliva samples, as EVs have been shown to cross the BBB (García-Romero et al., 2017). EVs are membrane enclosed bodies that are released by cells, including cancer cells, that contain a variety of cellular components (Haraszti et al., 2016). When released by GBM cells, these vesicles mirror the phenotypical signature of their parent cell, meaning they can be used to not only diagnose GBM, but identify the molecular subtype prior to surgical intervention (Lane et al., 2019).

Liquid biopsies allow for longitudinal tracking of tumour growth following treatment. Currently, imaging is used to track the progression of tumours following surgery and/or chemotherapy and radiotherapy. However, it is difficult to distinguish between progression of the tumour, and pseudo progression, the presence contrast-enhancing lesions caused by swelling as a result of treatment (Brandsma et al., 2008, Delgado-López et al., 2018). Liquid biopsies may therefore present a more reliable form of tracking patient recovery and possible progression. As well as being useful in a clinical setting, longitudinal sampling of GBM patient tumour cells has massive potential in investigating resistance mechanisms following chemotherapy to help progress the development of more effective treatments. Studies with this objective have been carried out in GBM but were limited to the use of primary and recurrent samples for their longitudinal experiments (Barthel et al., 2019).

The microfluidic model utilised in this thesis could be used to identity useful biomarkers for GBM diagnosis, patient stratification and response to treatment, and disease progression, by using the effluent samples collected at multiple time points through the incubation. Several methods could be utilised to identify these markers including ELISA; to identify cellular proteins in shed tumour cells, EVs, or soluble proteins released directly into the effluent, and qPCR to identify DNA or RNA. There are a limited number of known biomarkers of TMZ response. Studies evaluating the expression of CD36, EGFR and the GBM specific variant EGFRvIII, found that expression of these biomarkers was reduced in EVs released by GBM cells following TMZ treatment (Shao et al., 2012). However, more recent studies did not identify markers of TMZ response in cell lines when evaluating the expression of expression of EGFR, EGFRvIII, IDH1, PDPN, Hsp25, Hsp70, and Hsp90 through western blotting (Elisa et al., 2020). To increase sensitivity and to cast a wider net, differential expression studies following RNA-seq could be used on isolated EVs in our microfluidic model to identify biomarkers of TMZ response.

7.5.3) Other Cell Models

Many previous uses of microfluidics in GBM research involve the use of classic cell lines such as U-87MG and U-251s (Jie et al., 2017). This does not account for patient specific variability or intra-tumour heterogeneity. To overcome this, another cell model utilised in GBM microfluidics is patient derived stem cell lines, where patient tumours are macerated following surgical removal and cultured in growing medium (Cui et al., 2020). These cells more closely resemble the genetic phenotypes of GBM tumours as well as incorporating the inter-tumour heterogeneity amongst patients (Ishiguro et al., 2017). These stem cells are also able to differentiate into various cell types with a similar proportion to the original tumour (Tchoghandjian et al., 2010). However, as these cells would be resected into a single cell suspension, some tumour architecture is lost, and histology would be uninformative. To overcome this, a group have developed a protocol for producing GBM organoids from patient tumours without the need for mechanical or enzymatic dissociation (Jacob et al., 2020). Following resection of the tumour, it is sliced into smaller sections and incubated on an orbital shaker in serum free growing medium, where it forms spherical bodies within 1-2 weeks. This method of organoid culture of primary samples could be carried out prior to microfluidic incubation carried out here, and perhaps improve issues with the loss of proliferative capacity, as the group were able to demonstrate a reduction in ki-67 following a weeklong treatment 10 Gy radiation and 50 µM TMZ. This may also provide greater replicates as a single tumour piece can develop many more propagated slices.

7.6) Conclusion

The cross-talk between ADMA and SDMA marks identified here, along with evidence collated from other groups (Dhar et al., 2013, Fedoriw et al., 2019, Hartel et al., 2019, Gao et al., 2019b), opens the possibility that this is a mechanism by which GBM cells may be able to develop resistance to PRMT inhibitors. This is important because several type I and type II PRMT inhibitors are currently in preclinical and patient trials. The cross-talk may be due to the overlap in PRMT substrates, enhanced by the increased availability of substrate upon loss of type I PRMT activity. Although it was not evident here, most likely due to the limitations of this microfluidic model, the loss of both type and type II enzymes, namely PRMT1 and PRMT5, results in a synergistic effect upon cells (Fedoriw et al., 2019). Therefore, to effectively kills cancer cells with a reduced likelihood of drug resistance, a dual treatment should be explored. This could, however, produce unwanted side effects as PRMT1 and PRMT5 are responsible for the majority of ArgMe activity in human cells. In order to target only tumour cells specifically during treatment, a lack of either PRMT1 or PRMT5 activity should be endogenous, for instance, in tumours with an MTAP loss.

To further investigate this, improvements to this microfluidic model should be made. The length of incubation that allows for sufficient drug penetration and activity, without the loss of proliferative activity should be assessed. To do this, markers of cellular responses such as Ki-67 for proliferation, and cleaved PARP for apoptosis, could be quantified at increasing time points throughout the incubation, by IHC.

Chapter 8 - Bibliography

Abdelzaher, E. (2017) WHO grading of astrocytomas (2016). Available online: https://www.pathologyoutlines.com/topic/cnstumorwhograding.html [Accessed 11/04/ 2020].

Akhil, A. V., Raj, D. D. D., Raj, M. K., Bhat, S. R., Akshay, V., Bhowmik, S., Ramanathan, S. & Ahmed, S. (2016) Vaporized solvent bonding of polymethyl methacrylate. Null, 30 (8), 826-841.

Alcantara Llaguno, S. R., Wang, Z., Sun, D., Chen, J., Xu, J., Kim, E., Hatanpaa, K. J., Raisanen, J. M., Burns, D. K., Johnson, J. E., & Parada, L. F. (2015). Adult Lineage-Restricted CNS Progenitors Specify Distinct Glioblastoma Subtypes. Cancer cell, 28(4), 429–440.

Aldape, K., Brindle, K. M., Chesler, L., Chopra, R., Gajjar, A., Gilbert, M. R., Gottardo, N., Gutmann, D. H., Hargrave, D., Holland, E. C., Jones, D. T. W., Joyce, J. A., Kearns, P., Kieran, M. W., Mellinghoff, I. K., Merchant, M., Pfister, S. M., Pollard, S. M., Ramaswamy, V., Rich, J. N., Robinson, G. W., Rowitch, D. H., Sampson, J. H., Taylor, M. D., Workman, P. & Gilbertson, R. J. (2019) Challenges to curing primary brain tumours. Nature Reviews Clinical Oncology, 16 (8), 509-520.

Al-Kharboosh, R., ReFaey, K., Lara-Velazquez, M., Grewal, S. S., Imitola, J. & Quiñones-Hinojosa, A. (2020) Inflammatory mediators in glioma microenvironment play a dual role in gliomagenesis and mesenchymal stem cell homing: Implication for cellular therapy. Mayo Clinic Proceedings.Innovations, Quality & Outcomes, 4 (4), 443-459.

Alnahhas, I., Alsawas, M., Rayi, A., Palmer, J. D., Raval, R., Ong, S., Giglio, P., Murad, H. M. & Puduvalli, V. (2020) Characterizing benefit from temozolomide in MGMT promoter unmethylated and methylated glioblastoma: A systematic review and meta-analysis. Neuro-Oncology Advances, 2 (1), vdaa082.

Andreas, v. D., Louis, D. N., Klaus, v. A., Petersen, I., Hoell, T., Chung, R. Y., Martuza, R. L., Schoenfeld, D. A., Gazi Yaşargil, M., Wiestler, O. D. & Seizinger, B. R. (1992) Association of epidermal growth factor receptor gene amplification with loss of chromosome 10 in human glioblastoma multiforme. Journal of Neurosurgery, 77 (2), 295-301.

Anselmi, E., Vallisa, D., Bertè, R., Vanzo, C. & Cavanna, L. (2006) Post-traumatic glioma: Report of two cases. Tumori, 92 (2), 175-177.

Antony, S., Marchand, C., Stephen, A. G., Thibaut, L., Agama, K. K., Fisher, R. J. & Pommier, Y. (2007) Novel high-throughput electrochemiluminescent assay for identification of human tyrosyl-DNA phosphodiesterase (Tdp1) inhibitors and characterization of furamidine (NSC 305831) as an inhibitor of Tdp1. Nucleic Acids Research, 35 (13), 4474-4484.

Antonysamy, S., Bonday, Z., Campbell, R. M., Doyle, B., Druzina, Z., Gheyi, T., Han, B., Jungheim, L. N., Qian, Y., Rauch, C., Russell, M., Sauder, J. M., Wasserman, S. R., Weichert, K., Willard, F. S., Zhang, A. & Emtage, S. (2012) Crystal structure of the human PRMT5:MEP50 complex. Proceedings of the National Academy of Sciences of the United States of America, 109 (44), 17960-17965.

Aubert, J., Stavridis, M. P., Tweedie, S., O'Reilly, M., Vierlinger, K., Li, M., Ghazal, P., Pratt, T., Mason, J. O., Roy, D. & Smith, A. (2003) Screening for mammalian neural genes via fluorescence-activated cell sorter purification of neural precursors from Sox1-gfp knock-in mice. Proc Natl Acad Sci USA, 100 11836.

Auclair, Y. & Richard, S. (2013) The role of arginine methylation in the DNA damage response. DNA Repair, 12 (7), 459-465.

Auffinger, B., Ahmed, A. U. & Lesniak, M. S. (2013) Oncolytic virotherapy for malignant glioma: Translating laboratory insights into clinical practice. Frontiers in Oncology, 3 32.

Bady, P., Delorenzi, M. & Hegi, M. E. (2016) Sensitivity analysis of the MGMT-STP27 model and impact of genetic and epigenetic context to predict the MGMT methylation status in gliomas and other tumors. The Journal of Molecular Diagnostics, 18 (3), 350-361.

Banasavadi-Siddegowda, Y., Russell, L., Frair, E., Karkhanis, V. A., Relation, T., Yoo, J. Y., Zhang, J., Sif, S., Imitola, J., Baiocchi, R. & Kaur, B. (2017) PRMT5–PTEN molecular pathway regulates senescence and self-renewal of primary glioblastoma neurosphere cells. Oncogene, 36 (2), 263-274.

Bao, X., Siprashvili, Z., Zarnegar, B. J., Shenoy, R. M., Rios, E. J., Nady, N., Qu, K., Mah, A., Webster, D. E., Rubin, A. J., Wozniak, G. G., Tao, S., Wysocka, J. & Khavari, P. A. (2017) CSNK1a1 regulates PRMT1 to maintain the progenitor state in self-renewing somatic tissue. Developmental Cell, 43 (2), 227-239.e5.

Barbero, S., Bonavia, R., Bajetto, A., Porcile, C., Pirani, P., Ravetti, J. L., Zona, G. L., Spaziante, R., Florio, T., & Schettini, G. (2003). Stromal cell-derived factor 1alpha stimulates human glioblastoma cell growth through the activation of both extracellular signal-regulated kinases 1/2 and Akt. Cancer Research, 63(8), 1969-1974.

Barthel, F. P., Johnson, K. C., Varn, F. S., Moskalik, A. D., Tanner, G., Kocakavuk, E., Anderson, K. J., Abiola, O., Aldape, K., Alfaro, K. D., Alpar, D., Amin, S. B., Ashley, D. M., Bandopadhayay, P., Barnholtz-Sloan, J., Beroukhim, R., Bock, C., Brastianos, P. K., Brat, D. J., Brodbelt, A. R., Bruns, A. F., Bulsara, K. R., Chakrabarty, A., Chakravarti, A., Chuang, J. H., Claus, E. B., Cochran, E. J., Connelly, J., Costello, J. F., Finocchiaro, G., Fletcher, M. N., French, P. J., Gan, H. K., Gilbert, M. R., Gould, P. V.,

Grimmer, M. R., Iavarone, A., Ismail, A., Jenkinson, M. D., Khasraw, M., Kim, H., Kouwenhoven, M. C. M., LaViolette, P. S., Li, M., Lichter, P., Ligon, K. L., Lowman, A. K., Malta, T. M., Mazor, T., McDonald, K. L., Molinaro, A. M., Nam, D., Nayyar, N., Ng, H. K., Ngan, C. Y., Niclou, S. P., Niers, J. M., Noushmehr, H., Noorbakhsh, J., Ormond, D. R., Park, C., Poisson, L. M., Rabadan, R., Radlwimmer, B., Rao, G., Reifenberger, G., Sa, J. K., Schuster, M., Shaw, B. L., Short, S. C., Smitt, P. A. S., Sloan, A. E., Smits, M., Suzuki, H., Tabatabai, G., Van Meir, E.,G., Watts, C., Weller, M., Wesseling, P., Westerman, B. A., Widhalm, G., Woehrer, A., Yung, W. K. A., Zadeh, G., Huse, J. T., De Groot, J.,F., Stead, L. F., Verhaak, R. G. W. & Consortium, G. (2019) Longitudinal molecular trajectories of diffuse glioma in adults. Nature, 576 (7785), 112-120.

Bayin, N. S., Ma, L., Thomas, C., Baitalmal, R., Sure, A., Fansiwala, K., Bustoros, M., Golfinos, J. G., Pacione, D., Snuderl, M., Zagzag, D., Barcellos-Hoff, M. H., & Placantonakis, D. (2016). Patient-Specific Screening Using High-Grade Glioma Explants to Determine Potential Radiosensitization by a TGF-β Small Molecule Inhibitor. Neoplasia, 18(12), 795–805.

Beaver, J. E. & Waters, M. L. (2016) Molecular recognition of lys and arg methylation. ACS Chemical Biology, 11 (3), 643-653.

Bedford, M. T. & Clarke, S. G. (2009) Protein arginine methylation in mammals: Who, what, and why. Molecular Cell, 33 (1), 1-13.

Bedford, M. T. & Richard, S. (2005) Arginine methylation: An emerging regulatorof protein function. Molecular Cell, 18 (3), 263-272.

Beltran-Alvarez, P., Espejo, A., Schmauder, R., Beltran, C., Mrowka, R., Linke, T., Batlle, M., Pérez-Villa, F., Pérez, G. J., Scornik, F. S., Benndorf, K., Pagans, S., Zimmer, T. & Brugada, R. (2013) Protein arginine methyl transferases-3 and -5 increase cell surface expression of cardiac sodium channel. FEBS Letters, 587 (19), 3159-3165.

Ben-David, U., Beroukhim, R. & Golub, T. R. (2019) Genomic evolution of cancer models: Perils and opportunities. Nature Reviews.Cancer, 19 (2), 97-109.

Bezzi, M., Teo, S. X., Muller, J., Mok, W. C., Sahu, S. K., Vardy, L. A., Bonday, Z. Q. & Guccione, E. (2013) Regulation of constitutive and alternative splicing by PRMT5 reveals a role for Mdm4 pre-mRNA in sensing defects in the spliceosomal machinery. Genes & Development, 27 (17), 1903-1916.

Bhuripanyo, K., Wang, Y., Liu, X., Zhou, L., Liu, R., Duong, D., Zhao, B., Bi, Y., Zhou, H., Chen, G., Seyfried, N. T., Chazin, W. J., Kiyokawa, H. & Yin, J. (2018) Identifying the substrate proteins of U-box E3s E4B and CHIP by orthogonal ubiquitin transfer. Science Advances, 4 (1), e1701393.

Bidinotto, L. T., Torrieri, R., Mackay, A., Almeida, G. C., Viana-Pereira, M., Cruvinel-Carloni, A., Spina, M. L., Campanella, N. C., Pereira de Menezes, W., Clara, C. A., Becker, A. P., Jones, C. & Reis, R. M. (2016) Copy number profiling of brazilian astrocytomas. G3 (Bethesda, Md.), 6 (7), 1867-1878.

Bielamowicz, K., Fousek, K., Byrd, T. T., Samaha, H., Mukherjee, M., Aware, N., Wu, M., Orange, J. S., Sumazin, P., Man, T., Joseph, S. K., Hegde, M. & Ahmed, N. (2018) Trivalent CAR T cells overcome interpatient antigenic variability in glioblastoma. Neuro-Oncology, 20 (4), 506-518.

Bissinger, E., Heinke, R., Spannhoff, A., Eberlin, A., Metzger, E., Cura, V., Hassenboehler, P., Cavarelli, J., Schüle, R., Bedford, M. T., Sippl, W. & Jung, M. (2011) Acyl derivatives of p-aminosulfonamides and dapsone as new inhibitors of the arginine methyltransferase hPRMT1. Bioorganic & Medicinal Chemistry; Epigenetic Drug Discovery, 19 (12), 3717-3731.

Blanc, R. S. & Richard, S. (2017) Arginine methylation: The coming of age. Molecular Cell, 65 (1), 8-24.

Bloch, O., Han, S. J., Cha, S., Sun, M. Z., Aghi, M. K., McDermott, M. W., Berger, M. S. & Parsa, A. T. (2012) Impact of extent of resection for recurrent glioblastoma on overall survival. Journal of Neurosurgery JNS, 117 (6), 1032-1038.

Blythe, S. A., Cha, S., Tadjuidje, E., Heasman, J. & Klein, P. S. (2010) Beta-catenin primes organizer gene expression by recruiting a histone H3 arginine 8 methyltransferase, Prmt2. Developmental Cell, 19 (2), 220-231.

Bobola, M. S., Kolstoe, D. D., Blank, A., Chamberlain, M. C. & Silber, J. R. (2012) Repair of 3-methyladenine and abasic sites by base excision repair mediates glioblastoma resistance to temozolomide. Frontiers in Oncology, 2 176.

Bohn, A., Braley, A., Rodriguez de la Vega, Pura, Zevallos, J. C. & Barengo, N. C. (2018) The association between race and survival in glioblastoma patients in the US: A retrospective cohort study. PloS One, 13 (6), e0198581.

Boisvert, F., Déry, U., Masson, J. & Richard, S. (2005) Arginine methylation of MRE11 by PRMT1 is required for DNA damage checkpoint control. Genes & Development, 19 (6), 671-676.

Boisvert, F., Rhie, A., Richard, S. & Doherty, A. J. (2005) The GAR motif of 53BP1 is arginine methylated by PRMT1 and is necessary for 53BP1 DNA binding activity. Cell Cycle, 4 (12), 1834-1841.

Bonday, Z. Q., Cortez, G. S., Grogan, M. J., Antonysamy, S., Weichert, K., Bocchinfuso, W. P., Li, F., Kennedy, S., Li, B., Mader, M. M., Arrowsmith, C. H., Brown, P. J., Eram, M. S., Szewczyk, M. M., Barsyte-Lovejoy, D., Vedadi, M., Guccione, E. & Campbell, R. M. (2018) LLY-283, a potent and

selective inhibitor of arginine methyltransferase 5, PRMT5, with antitumor activity. ACS Medicinal Chemistry Letters, 9 (7), 612-617.

Bondy, M. L., Scheurer, M. E., Malmer, B., Barnholtz-Sloan, J., Davis, F. G., Il'yasova, D., Kruchko, C., McCarthy, B. J., Rajaraman, P., Schwartzbaum, J. A., Sadetzki, S., Schlehofer, B., Tihan, T., Wiemels, J. L., Wrensch, M., Buffler, P. A. & Brain Tumor, E. C. (2008) Brain tumor epidemiology: Consensus from the brain tumor epidemiology consortium. Cancer, 113 (7), 1953-1968.

Bonnici, J., Tumber, A., Kawamura, A., & Schofield, C. J. (2018). Inhibitors of both the N-methyl lysyl- and arginyl-demethylase activities of the JmjC oxygenases. Philosophical transactions of the Royal Society of London. Series B, Biological sciences, 373(1748), 20170071.

Borghaei, H., Paz-Ares, L., Horn, L., Spigel, D. R., Steins, M., Ready, N. E., Chow, L. Q., Vokes, E. E., Felip, E., Holgado, E., Barlesi, F., Kohlhäufl, M., Arrieta, O., Burgio, M. A., Fayette, J., Lena, H., Poddubskaya, E., Gerber, D. E., Gettinger, S. N., Rudin, C. M., Rizvi, N., Crinò, L., Blumenschein,George R.,,Jr, Antonia, S. J., Dorange, C., Harbison, C. T., Graf Finckenstein, F. & Brahmer, J. R. (2015) Nivolumab versus docetaxel in advanced nonsquamous non-small-cell lung cancer. The New England Journal of Medicine, 373 (17), 1627-1639.

Böttger, A., Islam, M., Chowdhury, R., Schofield, C. & Wolf, A. (2015) The oxygenase Jmjd6–a case study in conflicting assignments. Biochemical Journal, 468 (2), 191-202.

Bouffet, E., Larouche, V., Campbell, B. B., Merico, D., de Borja, R., Aronson, M., Durno, C., Krueger, J., Cabric, V., Ramaswamy, V., Zhukova, N., Mason, G., Farah, R., Afzal, S., Yalon, M., Rechavi, G., Magimairajan, V., Walsh, M. F., Constantini, S., Dvir, R., Elhasid, R., Reddy, A., Osborn, M., Sullivan, M., Hansford, J., Dodgshun, A., Klauber-Demore, N., Peterson, L., Patel, S., Lindhorst, S., Atkinson, J., Cohen, Z., Laframboise, R., Dirks, P., Taylor, M., Malkin, D., Albrecht, S., Dudley, R. W. R., Jabado, N., Hawkins, C. E., Shlien, A. & Tabori, U. (2016) Immune checkpoint inhibition for hypermutant glioblastoma multiforme resulting from germline biallelic mismatch repair deficiency. American Society of Clinical Oncology.

Boulanger, M., Liang, C., Russell, R. S., Lin, R., Bedford, M. T., Wainberg, M. A. & Richard, S. (2005) Methylation of tat by PRMT6 regulates human immunodeficiency virus type 1 gene expression. Journal of Virology, 79 (1), 124-131.

Bowman, R. L., Klemm, F., Akkari, L., Pyonteck, S. M., Sevenich, L., Quail, D. F., Dhara, S., Simpson, K., Gardner, E. E., Iacobuzio-Donahue, C. A., Brennan, C. W., Tabar, V., Gutin, P. H. & Joyce, J. A. (2016) Macrophage ontogeny underlies differences in tumor-specific education in brain malignancies. Cell Reports, 17 (9), 2445-2459.

Brandsma, D., Stalpers, L., Taal, W., Sminia, P. & van den Bent, M., J. (2008) Clinical features, mechanisms, and management of pseudoprogression in malignant gliomas. The Lancet Oncology, 9 (5), 453-461.

Braun, C. J., Stanciu, M., Boutz, P. L., Patterson, J. C., Calligaris, D., Higuchi, F., Neupane, R., Fenoglio, S., Cahill, D. P., Wakimoto, H., Agar, N. Y. R., Yaffe, M. B., Sharp, P. A., Hemann, M. T. & Lees, J. A. (2017) Coordinated splicing of regulatory detained introns within oncogenic transcripts creates an exploitable vulnerability in malignant glioma. Cancer Cell, 32 (4), 411-426.e11.

Brat, D. J. & Van Meir, E. G. (2001) Glomeruloid microvascular proliferation orchestrated by VPF/VEGF: A new world of angiogenesis research. The American Journal of Pathology, 158 (3), 789-796.

Brennan, C. W., Verhaak, R. G. W., McKenna, A., Campos, B., Noushmehr, H., Salama, S. R., Zheng, S., Chakravarty, D., Sanborn, J. Z., Berman, S. H., Beroukhim, R., Bernard, B., Wu, C., Genovese, G., Shmulevich, I., Barnholtz-Sloan, J., Zou, L., Vegesna, R., Shukla, S. A., Ciriello, G., Yung, W. K., Zhang, W., Sougnez, C., Mikkelsen, T., Aldape, K., Bigner, D. D., Van Meir, E.,G., Prados, M., Sloan, A., Black, K. L., Eschbacher, J., Finocchiaro, G., Friedman, W., Andrews, D. W., Guha, A., Iacocca, M., O'Neill, B.,P., Foltz, G., Myers, J., Weisenberger, D. J., Penny, R., Kucherlapati, R., Perou, C. M., Hayes, D. N., Gibbs, R., Marra, M., Mills, G. B., Lander, E., Spellman, P., Wilson, R., Sander, C., Weinstein, J., Meyerson, M., Gabriel, S., Laird, P. W., Haussler, D., Getz, G., Chin, L. & TCGA, R. N. (2013) The somatic genomic landscape of glioblastoma. Cell, 155 (2), 462-477.

Brodbelt, A., Williams, M., Thorpe, A., Mills, S., Price, S., Lekka, E., Watts, C., Davis, C. & Jenkinson, M. (2018) A pilot study of the acceptance and tolerability of tumour treating fields in adult glioblastoma patients. Neuro-Oncology, 20 v349.

Brown, C. E., Alizadeh, D., Starr, R., Weng, L., Wagner, J. R., Naranjo, A., Ostberg, J. R., Blanchard, M. S., Kilpatrick, J., Simpson, J., Kurien, A., Priceman, S. J., Wang, X., Harshbarger, T. L., D'Apuzzo, M., Ressler, J. A., Jensen, M. C., Barish, M. E., Chen, M., Portnow, J., Forman, S. J. & Badie, B. (2016) Regression of glioblastoma after chimeric antigen receptor T-cell therapy. N Engl J Med, 375 (26), 2561-2569.

Bryan, T. M., Englezou, A., Dalla-Pozza, L., Dunham, M. A. & Reddel, R. R. (1997) Evidence for an alternative mechanism for maintaining telomere length in human tumors and tumor-derived cell lines. Nature Medicine, 3 (11), 1271-1274.

Bryant, J., Heiss, J. & Banasavadi-Siddegowda, Y. K. (2021) Arginine methylation in brain tumors: Tumor biology and therapeutic strategies. 10 (1), 124.

Butler, J. S., Zurita-Lopez, C., Clarke, S. G., Bedford, M. T. & Dent, S. Y. R. (2011) Protein-arginine methyltransferase 1 (PRMT1) methylates Ash2L, a shared component of mammalian histone H3K4 methyltransferase complexes. The Journal of Biological Chemistry, 286 (14), 12234-12244.

Cai, J., Chen, J., Zhang, W., Yang, P., Zhang, C., Li, M., Yao, K., Wang, H., Li, Q., Jiang, C., & Jiang, T. (2015). Loss of ATRX, associated with DNA methylation pattern of chromosome end, impacted biological behaviors of astrocytic tumors. Oncotarget, 6(20), 18105–18115.

Cai, X., Briggs, R. G., Homburg, H. B., Young, I. M., Davis, E. J., Lin, Y., Battiste, J. D. & Sughrue, M. E. (2020) Application of microfluidic devices for glioblastoma study: Current status and future directions. Biomedical Microdevices, 22 (3), 60.

Calabretta, S., Vogel, G., Yu, Z., Choquet, K., Darbelli, L., Nicholson, T. B., Kleinman, C. L. & Richard, S. (2018) Loss of PRMT5 promotes PDGFRα degradation during oligodendrocyte differentiation and myelination. Developmental Cell, 46 (4), 426-440.e5.

Calinescu, A. A., Yadav, V. N., Carballo, E., Kadiyala, P., Tran, D., Zamler, D. B., Doherty, R., Srikanth, M., Lowenstein, P. R., & Castro, M. G. (2017). Survival and Proliferation of Neural Progenitor-Derived Glioblastomas Under Hypoxic Stress is Controlled by a CXCL12/CXCR4 Autocrine-Positive Feedback Mechanism. Clinical cancer research : an official journal of the American Association for Cancer Research, 23(5), 1250–1262.

Cancer Genome Atlas Research Network (2008) Comprehensive genomic characterization defines human glioblastoma genes and core pathways. Nature, 455 (7216), 1061-1068.

Cantanhede, I. G. & de Oliveira, J., Ricardo Mendes (2017) PDGF family expression in glioblastoma multiforme: Data compilation from ivy glioblastoma atlas project database. Scientific Reports, 7 (1), 15271.

Cao, X., Zee, B. M. & Garcia, B. A. (2013) Heavy methyl-SILAC labeling coupled with liquid chromatography and high-resolution mass spectrometry to study the dynamics of site-specific histone methylation. Methods in Molecular Biology (Clifton, N.J.), 977 299-313.

Carmeliet, P. (2005) Angiogenesis in life, disease and medicine. Nature, 438 (7070), 932-936.

Carr, S. D., Green, V. L., Stafford, N. D. & Greenman, J. (2014) Analysis of radiation-induced cell death in head and neck squamous cell carcinoma and rat liver maintained in microfluidic devices. Otolaryngol Head Neck Surg, 150 (1), 73-80.

Casadio, F., Lu, X., Pollock, S. B., LeRoy, G., Garcia, B. A., Muir, T. W., Roeder, R. G. & Allis, C. D. (2013a) H3R42me2a is a histone modification with positive transcriptional effects. Proceedings of the National Academy of Sciences of the United States of America, 110 (37), 14894-14899.

Casadio, F., Lu, X., Pollock, S. B., LeRoy, G., Garcia, B. A., Muir, T. W., Roeder, R. G. & Allis, C. D. (2013b) H3R42me2a is a histone modification with positive transcriptional effects. Proc Natl Acad Sci USA, 110 (37), 14894.

Ceschin, D. G., Walia, M., Wenk, S. S., Duboé, C., Gaudon, C., Xiao, Y., Fauquier, L., Sankar, M., Vandel, L. & Gronemeyer, H. (2011) Methylation specifies distinct estrogen-induced binding site repertoires of CBP to chromatin. Genes & Development, 25 (11), 1132-1146.

Chakrapani, B., Khan, M. I. K., Kadumuri, R. V., Gupta, S., Verma, M., Awasthi, S., Govindaraju, G., Mahesh, A., Rajavelu, A., Chavali, S. & Dhayalan, A. (2020) The uncharacterized protein FAM47E interacts with PRMT5 and regulates its functions. Life Science Alliance, 4 (3), e202000699.

Chakravarti, A., Zhai, G., Suzuki, Y., Sarkesh, S., Black, P. M., Muzikansky, A. & Loeffler, J. S. (2004) The prognostic significance of phosphatidylinositol 3-kinase pathway activation in human gliomas. Jco, 22 (10), 1926-1933.

Chan-Penebre, E., Kuplast, K. G., Majer, C. R., Boriack-Sjodin, P., Wigle, T. J., Johnston, L. D., Rioux, N., Munchhof, M. J., Jin, L., Jacques, S. L., West, K. A., Lingaraj, T., Stickland, K., Ribich, S. A., Raimondi, A., Scott, M. P., Waters, N. J., Pollock, R. M., Smith, J. J., Barbash, O., Pappalardi, M., Ho, T. F., Nurse, K., Oza, K. P., Gallagher, K. T., Kruger, R., Moyer, M. P., Copeland, R. A., Chesworth, R. & Duncan, K. W. (2015) A selective inhibitor of PRMT5 with in vivo and in vitro potency in MCL models. Nature Chemical Biology, 11 (6), 432-437.

Chang, B., Chen, Y., Zhao, Y. & Bruick, R. K. (2007) JMJD6 is a histone arginine demethylase. Science, 318 (5849), 444.

Chang, N. C., Sincennes, M., Chevalier, F. P., Brun, C. E., Lacaria, M., Segalés, J., Muñoz-Cánoves, P., Ming, H. & Rudnicki, M. A. (2018) The dystrophin glycoprotein complex regulates the epigenetic activation of muscle stem cell commitment. Cell Stem Cell, 22 (5), 755-768.e6.

Chaturvedi, N. K., Mahapatra, S., Kesherwani, V., Kling, M. J., Shukla, M., Ray, S., Kanchan, R., Perumal, N., McGuire, T. R., Sharp, J. G., Joshi, S. S. & Coulter, D. W. (2019) Role of protein arginine methyltransferase 5 in group 3 (MYC-driven) medulloblastoma. BMC Cancer, 19 (1), 1056.

Chen, C., Hutzen, B., Wedekind, M. F. & Cripe, T. P. (2018) Oncolytic virus and PD-1/PD-L1 blockade combination therapy. Oncolytic Virotherapy, 7 65-77.

Chen, C., Jin, J., James, D. A., Adams-Cioaba, M. A., Park, J. G., Guo, Y., Tenaglia, E., Xu, C., Gish, G., Min, J., & Pawson, T. (2009). Mouse Piwi interactome identifies binding mechanism of Tdrkh Tudor domain to arginine methylated Miwi. Proceedings of the National Academy of Sciences of the United States of America, 106(48), 20336–20341.

Chen, C., Nott, T. J., Jin, J. & Pawson, T. (2011) Deciphering arginine methylation: Tudor tells the tale. Nature Reviews Molecular Cell Biology, 12 (10), 629-642.

Chen, D., Ma, H., Hong, H., Koh, S. S., Huang, S., Schurter, B. T., Aswad, D. W. & Stallcup, M. R. (1999) Regulation of transcription by a protein methyltransferase. Science, 284 (5423), 2174.

Chen, M., Qu, X., Zhang, Z., Wu, H., Qin, X., Li, F., Liu, Z., Tian, L., Miao, J. & Shu, W. (2016) Cross-talk between arg methylation and ser phosphorylation modulates apoptosis signal-regulating kinase 1 activation in endothelial cells. Molecular Biology of the Cell, 27 (8), 1358-1366.

Chen, M., Yi, B., & Sun, J. (2014). Inhibition of cardiomyocyte hypertrophy by protein arginine methyltransferase 5. The Journal of biological chemistry, 289(35), 24325–24335.

Chen, W., Gao, D., Xie, L., Wang, A., Zhao, H., Guo, C., Sun, Y., Nie, Y., Hong, A. & Xiong, S. (2020) SCF-FBXO24 regulates cell proliferation by mediating ubiquitination and degradation of PRMT6. Biochemical and Biophysical Research Communications, 530 (1), 75-81.

Cheng, D., Gao, G., Di Lorenzo, A., Jayne, S., Hottiger, M. O., Richard, S. & Bedford, M. T. (2020) Genetic evidence for partial redundancy between the arginine methyltransferases CARM1 and PRMT6. The Journal of Biological Chemistry, 295 (50), 17060-17070.

Cheng, D., Côté, J., Shaaban, S. & Bedford, M. T. (2007) The arginine methyltransferase CARM1 regulates the coupling of transcription and mRNA processing. Molecular Cell, 25 (1), 71-83.

Cheng, D., Yadav, N., King, R. W., Swanson, M. S., Weinstein, E. J. & Bedford, M. T. (2004) Small molecule regulators of protein arginine methyltransferases.

Cheng, X., Collins, R. E. & Zhang, X. (2005) Structural and sequence motifs of protein (histone) methylation enzymes. Annual Review of Biophysics and Biomolecular Structure, 34 267-294.

Chiang, K., Zielinska, A. E., Shaaban, A. M., Sanchez-Bailon, M., Jarrold, J., Clarke, T. L., Zhang, J., Francis, A., Jones, L. J., Smith, S., Barbash, O., Guccione, E., Farnie, G., Smalley, M. J. & Davies, C. C. (2017) PRMT5 is a critical regulator of breast cancer stem cell function via histone methylation and FOXP1 expression. Cell Reports, 21 (12), 3498-3513.

Chitiprolu, M., Jagow, C., Tremblay, V., Bondy-Chorney, E., Paris, G., Savard, A., Palidwor, G., Barry, F. A., Zinman, L., Keith, J., Rogaeva, E., Robertson, J., Lavallée-Adam, M., Woulfe, J., Couture, J., Côté, J. & Gibbings, D. (2018) A complex of C9ORF72 and p62 uses arginine methylation to eliminate stress granules by autophagy. Nature Communications, 9 (1), 2794.

Chittka, A. (2010) Dynamic distribution of histone H4 arginine 3 methylation marks in the developing murine cortex. PloS One, 5 (11), e13807.

Chittka, A., Nitarska, J., Grazini, U. & Richardson, W. D. (2012) Transcription factor positive regulatory domain 4 (PRDM4) recruits protein arginine methyltransferase 5 (PRMT5) to mediate histone arginine methylation and control neural stem cell proliferation and differentiation. The Journal of Biological Chemistry, 287 (51), 42995-43006.

Chonan, Y., Taki, S., Sampetrean, O., Saya, H. & Sudo, R. (2017) Endothelium-induced three-dimensional invasion of heterogeneous glioma initiating cells in a microfluidic coculture platform. Integrative Biology, 9 (9), 762-773.

Chongsathidkiet, P., Jackson, C., Koyama, S., Loebel, F., Cui, X., Farber, S. H., Woroniecka, K., Elsamadicy, A. A., Dechant, C. A., Kemeny, H. R., Sanchez-Perez, L., Cheema, T. A., Souders, N. C., Herndon, J. E., Coumans, J., Everitt, J. I., Nahed, B. V., Sampson, J. H., Gunn, M. D., Martuza, R. L., Dranoff, G., Curry, W. T. & Fecci, P. E. (2018) Sequestration of T cells in bone marrow in the setting of glioblastoma and other intracranial tumors. Nature Medicine, 24 (9), 1459-1468.

Choucair, A., Pham, T. H., Omarjee, S., Jacquemetton, J., Kassem, L., Trédan, O., Rambaud, J., Marangoni, E., Corbo, L., Treilleux, I. & Le Romancer, M. (2019) The arginine methyltransferase PRMT1 regulates IGF-1 signaling in breast cancer. Oncogene, 38 (21), 4015-4027.

Chowdhary, S. A., Ryken, T. & Newton, H. B. (2015) Survival outcomes and safety of carmustine wafers in the treatment of high-grade gliomas: A meta-analysis. Journal of Neuro-Oncology, 122 (2), 367-382.

Ciechomska, I. A., Marciniak, M. P., Jackl, J. & Kaminska, B. (2018) Pre-treatment or post-treatment of human glioma cells with BIX01294, the inhibitor of histone methyltransferase G9a, sensitizes cells to temozolomide. Frontiers in Pharmacology, 9 1271.

Cipolla, M. J. (2009) The cerebral circulation. San Rafael (CA). Morgan & Claypool Life Sciences.

Clark, K. H., Villano, J. L., Nikiforova, M. N., Hamilton, R. L. & Horbinski, C. (2013) 1p/19q testing has no significance in the workup of glioblastomas. Neuropathology and Applied Neurobiology, 39 (6), 706-717.

Clarke, T. L., Sanchez-Bailon, M., Chiang, K., Reynolds, J. J., Herrero-Ruiz, J., Bandeiras, T. M., Matias, P. M., Maslen, S. L., Skehel, J. M., Stewart, G. S. & Davies, C. C. (2017) PRMT5-dependent methylation of the TIP60 coactivator RUVBL1 is a key regulator of homologous recombination. Molecular Cell, 65 (5), 900-916.e7.

Cloughesy, T. F., Mochizuki, A. Y., Orpilla, J. R., Hugo, W., Lee, A. H., Davidson, T. B., Wang, A. C., Ellingson, B. M., Rytlewski, J. A., Sanders, C. M., Kawaguchi, E. S., Du, L., Li, G., Yong, W. H., Gaffey, S. C., Cohen, A. L., Mellinghoff, I. K., Lee, E. Q., Reardon, D. A., O'Brien, B.,J., Butowski, N. A., Nghiemphu, P. L., Clarke, J. L., Arrillaga-Romany, I., Colman, H., Kaley, T. J., de Groot, J.,F., Liau, L. M., Wen, P. Y. & Prins, R. M. (2019) Neoadjuvant anti-PD-1 immunotherapy promotes a survival benefit with intratumoral and systemic immune responses in recurrent glioblastoma.

Cohen, A. L., Holmen, S. L. & Colman, H. (2013) IDH1 and IDH2 mutations in gliomas. Current Neurology and Neuroscience Reports, 13 (5), 345.

Cohen, M. H., Shen, Y. L., Keegan, P. & Pazdur, R. (2009) FDA drug approval summary: Bevacizumab (avastin®) as treatment of recurrent glioblastoma multiforme. The Oncologist, 14 (11), 1131-1138.

Côté, J. & Richard, S. (2005) Tudor domains bind symmetrical dimethylated arginines. Journal of Biological Chemistry, 280 (31), 28476-28483.

Cui, W., Yoneda, R., Ueda, N. & Kurokawa, R. (2018) Arginine methylation of translocated in liposarcoma (TLS) inhibits its binding to long noncoding RNA, abrogating TLS-mediated repression of CBP/p300 activity. The Journal of Biological Chemistry, 293 (28), 10937-10948.

Cui, X., Ma, C., Vasudevaraja, V., Serrano, J., Tong, J., Peng, Y., Delorenzo, M., Shen, G., Frenster, J., Morales, R. T., Qian, W., Tsirigos, A., Chi, A. S., Jain, R., Kurz, S. C., Sulman, E. P., Placantonakis, D. G., Snuderl, M. & Chen, W. (2020) Dissecting the immunosuppressive tumor microenvironments in glioblastoma-on-a-chip for optimized PD-1 immunotherapy. eLife, 9 e52253.

Cura, V., Marechal, N., Troffer-Charlier, N., Strub, J., van Haren, M. J., Martin, N. I., Cianférani, S., Bonnefond, L. & Cavarelli, J. (2017) Structural studies of protein arginine methyltransferase 2 reveal its interactions with potential substrates and inhibitors. The FEBS Journal, 284 (1), 77-96.

Cura, V., Troffer-Charlier, N., Wurtz, J., Bonnefond, L. & Cavarelli, J. (2014) Structural insight into arginine methylation by the mouse protein arginine methyltransferase 7: A zinc finger freezes the mimic of the dimeric state into a single active site. Acta Crystallographica Section D, 70.

Cuthbert, G. L., Daujat, S., Snowden, A. W., Erdjument-Bromage, H., Hagiwara, T., Yamada, M., Schneider, R., Gregory, P. D., Tempst, P., Bannister, A. J., & Kouzarides, T. (2004). Histone deimination antagonizes arginine methylation. Cell, 118(5), 545–553.

Dang, L., White, D. W., Gross, S., Bennett, B. D., Bittinger, M. A., Driggers, E. M., Fantin, V. R., Jang, H. G., Jin, S., Keenan, M. C., Marks, K. M., Prins, R. M., Ward, P. S., Yen, K. E., Liau, L. M., Rabinowitz, J. D., Cantley, L. C., Thompson, C. B., Vander Heiden, M.,G. & Su, S. M. (2009) Cancer-associated IDH1 mutations produce 2-hydroxyglutarate. Nature, 462 (7274), 739-744.

D'Angelo, F., Ceccarelli, M., Tala, Garofano, L., Zhang, J., Frattini, V., Caruso, F. P., Lewis, G., Alfaro, K. D., Bauchet, L., Berzero, G., Cachia, D., Cangiano, M., Capelle, L., de Groot, J., DiMeco, F., Ducray, F., Farah, W., Finocchiaro, G., Goutagny, S., Kamiya-Matsuoka, C., Lavarino, C., Loiseau, H., Lorgis, V., Marras, C. E., McCutcheon, I., Nam, D., Ronchi, S., Saletti, V., Seizeur, R., Slopis, J., Suñol, M., Vandenbos, F., Varlet, P., Vidaud, D., Watts, C., Tabar, V., Reuss, D. E., Kim, S., Meyronet, D., Mokhtari, K., Salvador, H., Bhat, K. P., Eoli, M., Sanson, M., Lasorella, A. & Iavarone, A. (2019) The molecular landscape of glioma in patients with neurofibromatosis 1. Nature Medicine, 25 (1), 176-187.

Davis, M. E. (2016) Glioblastoma: Overview of disease and treatment. Clinical Journal of Oncology Nursing, 20 (5), S2-S8.

Debler, E. W., Jain, K., Warmack, R. A., Feng, Y., Clarke, S. G., Blobel, G. & Stavropoulos, P. (2016) A glutamate/aspartate switch controls product specificity in a protein arginine methyltransferase. Proceedings of the National Academy of Sciences of the United States of America, 113 (8), 2068-2073.

Deeken, J. F. & Löscher, W. (2007) The blood-brain barrier and cancer: Transporters, treatment, and trojan horses. Clinical Cancer Research : An Official Journal of the American Association for Cancer Research, 13 (6), 1663-1674.

Delgado-López, P. D., Riñones-Mena, E. & Corrales-García, E. M. (2018) Treatment-related changes in glioblastoma: A review on the controversies in response assessment criteria and the concepts of true progression, pseudoprogression, pseudoresponse and radionecrosis. Clinical and Translational Oncology, 20 (8), 939-953.

Deng, Q., Holler, C. J., Taylor, G., Hudson, K. F., Watkins, W., Gearing, M., Ito, D., Murray, M. E., Dickson, D. W., Seyfried, N. T. & Kukar, T. (2014) FUS is phosphorylated by DNA-PK and accumulates in the cytoplasm after DNA damage. The Journal of Neuroscience : The Official Journal of the Society for Neuroscience, 34 (23), 7802-7813.

Desjardins, A., Gromeier, M., Herndon,James E., Beaubier, N., Bolognesi, D. P., Friedman, A. H., Friedman, H. S., McSherry, F., Muscat, A. M., Nair, S., Peters, K. B., Randazzo, D., Sampson, J. H., Vlahovic, G., Harrison, W. T., McLendon, R. E., Ashley, D. & Bigner, D. D. (2018) Recurrent glioblastoma treated with recombinant poliovirus. The New England Journal of Medicine, 379 (2), 150-161.

Dhar, S., Vemulapalli, V., Patananan, A. N., Huang, G. L., Di Lorenzo, A., Richard, S., Comb, M. J., Guo, A., Clarke, S. G. & Bedford, M. T. (2013a) Loss of the major type I arginine methyltransferase PRMT1 causes substrate scavenging by other PRMTs. Scientific Reports, 3 1311.

Dhar, S., Vemulapalli, V., Patananan, A. N., Huang, G. L., Di Lorenzo, A., Richard, S., Comb, M. J., Guo, A., Clarke, S. G. & Bedford, M. T. (2013b) Loss of the major type I arginine methyltransferase PRMT1 causes substrate scavenging by other PRMTs. Scientific Reports, 3 1311.

Di Trapani, G., Carnevale, A., Scerrati, M., Colosimo, C., Vaccario, M. L. & Mei, D. (1996) Post-traumatic malignant glioma. report of a case. Italian Journal of Neurological Sciences, 17 (4), 283-286.

Diaz, R. J., Ali, S., Qadir, M. G., De La Fuente, Macarena I., Ivan, M. E. & Komotar, R. J. (2017) The role of bevacizumab in the treatment of glioblastoma. Journal of Neuro-Oncology, 133 (3), 455-467.

Diez, B. D., Statkevich, P., Zhu, Y., Abutarif, M. A., Xuan, F., Kantesaria, B., Cutler, D., Cantillon, M., Schwarz, M., Pallotta, M. G. & Ottaviano, F. H. (2010a) Evaluation of the exposure equivalence of oral versus intravenous temozolomide. Cancer Chemotherapy and Pharmacology, 65 (4), 727-734.

Diez, B. D., Statkevich, P., Zhu, Y., Abutarif, M. A., Xuan, F., Kantesaria, B., Cutler, D., Cantillon, M., Schwarz, M., Pallotta, M. G. & Ottaviano, F. H. (2010b) Evaluation of the exposure equivalence of oral versus intravenous temozolomide. Cancer Chemotherapy and Pharmacology, 65 (4), 727-734.

Dillon, M. B. C., Rust, H. L., Thompson, P. R. & Mowen, K. A. (2013) Automethylation of protein arginine methyltransferase 8 (PRMT8) regulates activity by impeding S-adenosylmethionine sensitivity. The Journal of Biological Chemistry, 288 (39), 27872-27880.

Djamgoz, M. B. A., Fraser, S. P. & Brackenbury, W. J. (2019) In vivo evidence for voltage-gated sodium channel expression in carcinomas and potentiation of metastasis. Cancers, 11 (11), 1675. doi: 10.3390/cancers11111675.

Dodd, P. R., Hardy, J. A., Baig, E. B., Kidd, A. M., Bird, E. D., Watson, W. E. J. & Johnston, G. A. R. (1986) Optimization of freezing, storage, and thawing conditions for the preparation of metabolically active synaptosomes from frozen rat and human brain. Neurochemical Pathology, 4 (3), 177-198.

Dolezal, E., Infantino, S., Drepper, F., Börsig, T., Singh, A., Wossning, T., Fiala, G. J., Minguet, S., Warscheid, B., Tarlinton, D. M., Jumaa, H., Medgyesi, D. & Reth, M. (2017) The BTG2-PRMT1 module limits pre-B cell expansion by regulating the CDK4-cyclin-D3 complex. Nature Immunology, 18 (8), 911-920.

Dong, F., Li, Q., Yang, C., Huo, D., Wang, X., Ai, C., Kong, Y., Sun, X., Wang, W., Zhou, Y., Liu, X., Li, W., Gao, W., Liu, W., Kang, C. & Wu, X. (2018) PRMT2 links histone H3R8 asymmetric dimethylation to oncogenic activation and tumorigenesis of glioblastoma. Nature Communications, 9 (1), 4552.

Dormann, D., Madl, T., Valori, C. F., Bentmann, E., Tahirovic, S., Abou-Ajram, C., Kremmer, E., Ansorge, O., Mackenzie, I. R. A., Neumann, M. & Haass, C. (2012) Arginine methylation next to the PY-NLS modulates transportin binding and nuclear import of FUS. The EMBO Journal, 31 (22), 4258-4275.

Drabløs, F., Feyzi, E., Aas, P. A., Vaagbø, C. B., Kavli, B., Bratlie, M. S., Peña-Diaz, J., Otterlei, M., Slupphaug, G. & Krokan, H. E. (2004) Alkylation damage in DNA and RNA—repair mechanisms and medical significance. DNA Repair, 3 (11), 1389-1407.

Du, K., Arai, S., Kawamura, T., Matsushita, A. & Kurokawa, R. (2011) TLS and PRMT1 synergistically coactivate transcription at the survivin promoter through TLS arginine methylation. Biochemical and Biophysical Research Communications, 404 (4), 991-996.

Duan, S., Cermak, L., Pagan, J. K., Rossi, M., Martinengo, C., di Celle, P. F., Chapuy, B., Shipp, M., Chiarle, R. & Pagano, M. (2012) FBXO11 targets BCL6 for degradation and is inactivated in diffuse large B-cell lymphomas. Nature, 481 (7379), 90-93.

Duncan, K. W., Rioux, N., Boriack-Sjodin, P., Munchhof, M. J., Reiter, L. A., Majer, C. R., Jin, L., Johnston, L. D., Chan-Penebre, E., Kuplast, K. G., Porter Scott, M., Pollock, R. M., Waters, N. J., Smith, J. J., Moyer, M. P., Copeland, R. A. & Chesworth, R. (2015) Structure and property guided design in the identification of PRMT5 tool compound EPZ015666. ACS Medicinal Chemistry Letters, 7 (2), 162-166.

Dutoit, V., Migliorini, D., Dietrich, P. & Walker, P. R. (2016) Immunotherapy of malignant tumors in the brain: How different from other sites? Frontiers Media S.A.

Dutoit, V., Migliorini, D., Ranzanici, G., Marinari, E., Widmer, V., Lobrinus, J. A., Momjian, S., Costello, J., Walker, P. R., Okada, H., Weinschenk, T., Herold-Mende, C. & Dietrich, P. (2017) Antigenic expression and spontaneous immune responses support the use of a selected peptide set from the

IMA950 glioblastoma vaccine for immunotherapy of grade II and III glioma. Oncoimmunology, 7 (2), e1391972.

Dyer, M. A., Qadeer, Z. A., Valle-Garcia, D. & Bernstein, E. (2017) ATRX and DAXX: Mechanisms and mutations. Cold Spring Harbor Perspectives in Medicine, 7 (3), a026567.

Eberhardt, A., Hansen, J. N., Koster, J., Lotta, Louis T., Wang, S., Livingstone, E., Qian, K., Valentijn, L. J., Zheng, Y. G., Schor, N. F. & Li, X. (2016) Protein arginine methyltransferase 1 is a novel regulator of MYCN in neuroblastoma. Oncotarget, 7 (39), 63629-63639.

Eckel-Passow, J., Lachance, D. H., Molinaro, A. M., Walsh, K. M., Decker, P. A., Sicotte, H., Pekmezci, M., Rice, T., Kosel, M. L., Smirnov, I. V., Sarkar, G., Caron, A. A., Kollmeyer, T. M., Praska, C. E., Chada, A. R., Halder, C., Hansen, H. M., McCoy, L. S., Bracci, P. M., Marshall, R., Zheng, S., Reis, G. F., Pico, A. R., O'Neill, B.,P., Buckner, J. C., Giannini, C., Huse, J. T., Perry, A., Tihan, T., Berger, M. S., Chang, S. M., Prados, M. D., Wiemels, J., Wiencke, J. K., Wrensch, M. R. & Jenkins, R. B. (2015) Glioma groups based on 1p/19q, IDH, and TERT promoter mutations in tumors. The New England Journal of Medicine, 372 (26), 2499-2508.

Ehtesham, M., Winston, J. A., Kabos, P., & Thompson, R. C. (2006). CXCR4 expression mediates glioma cell invasiveness. Oncogene, 25(19), 2801–2806.

Ehrlich, P. (1885) Das sauerstoff-bedürfnis des organismus. eine farbenanalytische studie. Berlin: Herschwald.

Ellor, S. V., Pagano-Young, T. & Avgeropoulos, N. G. (2014) Glioblastoma: Background, standard treatment paradigms, and supportive care considerations. J Law Med Ethics, 42 (2), 171-182.

EMBL-EBI (2019) CHEBI:16467 - L-arginine. Available online: https://www.ebi.ac.uk/chebi/searchId.do?chebiId=CHEBI:16467 [Accessed 18/05/20.

Eram, M. S., Shen, Y., Szewczyk, M., Wu, H., Senisterra, G., Li, F., Butler, K. V., Kaniskan, H. Ü, Speed, B. A., Dela Seña, C., Dong, A., Zeng, H., Schapira, M., Brown, P. J., Arrowsmith, C. H., Barsyte-Lovejoy, D., Liu, J., Vedadi, M. & Jin, J. (2016) A potent, selective, and cell-active inhibitor of human type I protein arginine methyltransferases. ACS Chemical Biology, 11 (3), 772-781.

Esse, R. (2012) Deciphering protein arginine methylation in mammals. In Paula Leandro (ed) Methylation. Rijeka: IntechOpen, Ch. 4.

Fan, B., Mellinghoff, I. K., Wen, P. Y., Lowery, M. A., Goyal, L., Tap, W. D., Pandya, S. S., Manyak, E., Jiang, L., Liu, G., Nimkar, T., Gliser, C., Prahl Judge, M., Agresta, S., Yang, H. & Dai, D. (2020) Clinical

pharmacokinetics and pharmacodynamics of ivosidenib, an oral, targeted inhibitor of mutant IDH1, in patients with advanced solid tumors. Investigational New Drugs, 38 (2), 433-444.

Favia, A., Salvatori, L., Nanni, S., Iwamoto-Stohl, L., Valente, S., Mai, A., Scagnoli, F., Fontanella, R. A., Totta, P., Nasi, S. & Illi, B. (2019) The protein arginine methyltransferases 1 and 5 affect myc properties in glioblastoma stem cells. Scientific Reports, 9 (1), 15925.

Fawcett, J.W., Oohashi, T. & Pizzorusso, T. The roles of perineuronal nets and the perinodal extracellular matrix in neuronal function. Nat Rev Neurosci 20, 451–465 (2019).

Fedoriw, A., Rajapurkar, S. R., O'Brien, S., Gerhart, S. V., Mitchell, L. H., Adams, N. D., Rioux, N., Lingaraj, T., Ribich, S. A., Pappalardi, M. B., Shah, N., Laraio, J., Liu, Y., Butticello, M., Carpenter, C. L., Creasy, C., Korenchuk, S., McCabe, M. T., McHugh, C. F., Nagarajan, R., Wagner, C., Zappacosta, F., Annan, R., Concha, N. O., Thomas, R. A., Hart, T. K., Smith, J. J., Copeland, R. A., Moyer, M. P., Campbell, J., Stickland, K., Mills, J., Jacques-O'Hagan, S., Allain, C., Johnston, D., Raimondi, A., Porter Scott, M., Waters, N., Swinger, K., Boriack-Sjodin, A., Riera, T., Shapiro, G., Chesworth, R., Prinjha, R. K., Kruger, R. G., Barbash, O. & Mohammad, H. P. (2019) Anti-tumor activity of the type I PRMT inhibitor, GSK3368715, synergizes with PRMT5 inhibition through MTAP loss. Cancer Cell, 36 (1), 100-114.e25.

Feng, J., Dang, Y., Zhang, W., Zhao, X., Zhang, C., Hou, Z., Jin, Y., McNutt, M. A., Marks, A. R. & Yin, Y. (2019) PTEN arginine methylation by PRMT6 suppresses PI3K–AKT signaling and modulates pre-mRNA splicing. Proc Natl Acad Sci USA, 116 (14), 6868.

Feng, Q., He, B., Jung, S., Song, Y., Qin, J., Tsai, S. Y., Tsai, M. & O'Malley, B., W. (2009) Biochemical control of CARM1 enzymatic activity by phosphorylation. The Journal of Biological Chemistry, 284 (52), 36167-36174.

Feng, Y., Hadjikyriacou, A. & Clarke, S. G. (2014) Substrate specificity of human protein arginine methyltransferase 7 (PRMT7): The importance of acidic residues in the double E loop. The Journal of Biological Chemistry, 289 (47), 32604-32616.

Feng, Y., Maity, R., Whitelegge, J. P., Hadjikyriacou, A., Li, Z., Zurita-Lopez, C., Al-Hadid, Q., Clark, A. T., Bedford, M. T., Masson, J. & Clarke, S. G. (2013) Mammalian protein arginine methyltransferase 7 (PRMT7) specifically targets RXR sites in lysine- and arginine-rich regions. The Journal of Biological Chemistry, 288 (52), 37010-37025.

Fitch, C. A., Platzer, G., Okon, M., Garcia-Moreno, B. & McIntosh, L. P. (2015) Arginine: Its pKa value revisited. Protein Science : A Publication of the Protein Society, 24 (5), 752-761.

Fong, J. Y., Pignata, L., Goy, P., Kawabata, K. C., Lee, S. C., Koh, C. M., Musiani, D., Massignani, E., Kotini, A. G., Penson, A., Wun, C. M., Shen, Y., Schwarz, M., Low, D. H., Rialdi, A., Ki, M., Wollmann, H., Mzoughi, S., Gay, F., Thompson, C., Hart, T., Barbash, O., Luciani, G. M., Szewczyk, M. M., Wouters, B. J., Delwel, R., Papapetrou, E. P., Barsyte-Lovejoy, D., Arrowsmith, C. H., Minden, M. D., Jin, J., Melnick, A., Bonaldi, T., Abdel-Wahab, O. & Guccione, E. (2019) Therapeutic targeting of RNA splicing catalysis through inhibition of protein arginine methylation. Cancer Cell, 36 (2), 194-209.e9.

Fox, A. H., Nakagawa, S., Hirose, T. & Bond, C. S. (2018) Paraspeckles: Where long noncoding RNA meets phase separation. Trends in Biochemical Sciences, 43 (2), 124-135.

Franco, R. S. (2012) Measurement of red cell lifespan and aging. Transfusion Medicine and Hemotherapy : Offizielles Organ Der Deutschen Gesellschaft Fur Transfusionsmedizin Und Immunhamatologie, 39 (5), 302-307.

Frankel, A., Yadav, N., Lee, J., Branscombe, T. L., Clarke, S. & Bedford, M. T. (2002) The novel human protein arginine N-methyltransferase PRMT6 is a nuclear enzyme displaying unique substrate specificity.

Friesen, W. J., Massenet, S., Paushkin, S., Wyce, A., & Dreyfuss, G. (2001). SMN, the product of the spinal muscular atrophy gene, binds preferentially to dimethylarginine-containing protein targets. Molecular cell, 7(5), 1111–1117.

Friesen, W. J., Wyce, A., Paushkin, S., Abel, L., Rappsilber, J., Mann, M. & Dreyfuss, G. (2002) A novel WD repeat protein component of the methylosome binds sm proteins. Journal of Biological Chemistry, 277 (10), 8243-8247.

Frohne, C. C., Llano, E. M., Perkovic, A., Cohen, R. D. & Luke, J. J. (2019) Complete response of metastatic melanoma in a patient with crohn's disease simultaneously receiving anti-α4β7 and anti-PD1 antibodies. J Immunother Cancer, 7 (1), 1.

Fults, D., Pedone, C., Thompson, G., Uchiyama, C., Gumpper, K., Iliev, D., Vinson, V., Tavtigian, S., Perry, W. (1998) Microsatellite deletion mapping on chromosome 10q and mutation analysis of MMAC1, FAS, and MXI1 in human glioblastoma multiforme. International Journal of Oncology, 12 (4), 905-915.

Fung, L. K., Shin, M., Tyler, B., Brem, H. & Saltzman, W. M. (1996) Chemotherapeutic drugs released from polymers: Distribution of 1,3-bis(2-chloroethyl)-l-nitrosourea in the rat brain. Pharmaceutical Research, 13 (5), 671-682.

Gallivan, J. P. & Dougherty, D. A. (1999) Cation-π interactions in structural biology. Proc Natl Acad Sci USA, 96 (17), 9459.

Gamm, D. M., Melvan, J. N., Shearer, R. L., Pinilla, I., Sabat, G., Svendsen, C. N., & Wright, L. S. (2008) A Novel Serum-Free Method for Culturing Human Prenatal Retinal Pigment Epithelial Cells. Invest. Ophthalmol. Vis. Sci., 49(2), 788-799.

Ganesh, L., Yoshimoto, T., Moorthy, N. C., Akahata, W., Boehm, M., Nabel, E. G. & Nabel, G. J. (2006) Protein methyltransferase 2 inhibits NF-kappaB function and promotes apoptosis. Molecular and Cellular Biology, 26 (10), 3864-3874.

Gao, G., Dhar, S. & Bedford, M. T. (2017) PRMT5 regulates IRES-dependent translation via methylation of hnRNP A1. Nucleic Acids Research, 45 (8), 4359-4369.

Gao, G., Zhang, L., Villarreal, O. D., He, W., Su, D., Bedford, E., Moh, P., Shen, J., Shi, X., Bedford, M. T. & Xu, H. (2019) PRMT1 loss sensitizes cells to PRMT5 inhibition. Nucleic Acids Research, 47 (10), 5038-5048.

Gao, L., Huang, S., Zhang, H., Hua, W., Xin, S., Cheng, L., Guan, W., Yu, Y., Mao, Y. & Pei, G. (2019) Suppression of glioblastoma by a drug cocktail reprogramming tumor cells into neuronal like cells. Scientific Reports, 9 (1), 3462.

Gao, X., Zhao, X., Zhu, Y., He, J., Shao, J., Su, C., Zhang, Y., Zhang, W., Saarikettu, J., Silvennoinen, O., Yao, Z., & Yang, J. (2012). Tudor staphylococcal nuclease (Tudor-SN) participates in small ribonucleoprotein (snRNP) assembly via interacting with symmetrically dimethylated Sm proteins. The Journal of biological chemistry, 287(22), 18130–18141.

Garay, P. G., Martin, O. A., Scheraga, H. A. & Vila, J. A. (2016) Detection of methylation, acetylation and glycosylation of protein residues by monitoring (13)C chemical-shift changes: A quantum-chemical study. PeerJ, 4 e2253.

García-Romero, N., Carrión-Navarro, J., Esteban-Rubio, S., Lázaro-Ibáñez, E., Peris-Celda, M., Alonso, M. M., Guzmán-De-Villoria, J., Fernández-Carballal, C., de Mendivil, A. O., García-Duque, S., Escobedo-Lucea, C., Prat-Acín, R., Belda-Iniesta, C. & Ayuso-Sacido, A. (2017) DNA sequences within glioma-derived extracellular vesicles can cross the intact blood-brain barrier and be detected in peripheral blood of patients. Oncotarget, 8 (1), 1416-1428.

Geoghegan, V., Guo, A., Trudgian, D., Thomas, B. & Acuto, O. (2015) Comprehensive identification of arginine methylation in primary T cells reveals regulatory roles in cell signalling. Nature Communications, 6 (1), 6758.

Gerdes, J., Lemke, H., Baisch, H., Wacker, H. H., Schwab, U. & Stein, H. (1984) Cell cycle analysis of a cell proliferation-associated human nuclear antigen defined by the monoclonal antibody ki-67. The Journal of Immunology, 133 (4), 1710.

Gerhart, S. V., Kellner, W. A., Thompson, C., Pappalardi, M. B., Zhang, X., Montes de Oca, R., Penebre, E., Duncan, K., Boriack-Sjodin, A., Le, B., Majer, C., McCabe, M. T., Carpenter, C., Johnson, N., Kruger, R. G. & Barbash, O. (2018) Activation of the p53-MDM4 regulatory axis defines the anti-tumour response to PRMT5 inhibition through its role in regulating cellular splicing. Scientific Reports, 8 (1), 9711.

Ghanbarpanah, E., Kohanpour, M. A., Hosseini-Beheshti, F., Yari, L. & Keshvari, M. (2018) Structure and function of FUS gene in prostate cancer. Bratislavske Lekarske Listy, 119 (10), 660-663.

Goldmann, E. E. (1913) Vitalfärbung am zentralnervensystem Abh Preuss Akad Wiss Phys-Math, 1-60.

Golebiewska, A., Hau, A., Oudin, A., Stieber, D., Yabo, Y. A., Baus, V., Barthelemy, V., Klein, E., Bougnaud, S., Keunen, O., Wantz, M., Michelucci, A., Neirinckx, V., Muller, A., Kaoma, T., Nazarov, P. V., Azuaje, F., De Falco, A., Flies, B., Richart, L., Poovathingal, S., Arns, T., Grzyb, K., Mock, A., Herold-Mende, C., Steino, A., Brown, D., May, P., Miletic, H., Malta, T. M., Noushmehr, H., Kwon, Y., Jahn, W., Klink, B., Tanner, G., Stead, L. F., Mittelbronn, M., Skupin, A., Hertel, F., Bjerkvig, R. & Niclou, S. P. (2020) Patient-derived organoids and orthotopic xenografts of primary and recurrent gliomas represent relevant patient avatars for precision oncology. Acta Neuropathologica, 140 (6), 919-949.

Gonsalvez, G. B., Tian, L., Ospina, J. K., Boisvert, F., Lamond, A. I. & Matera, A. G. (2007) Two distinct arginine methyltransferases are required for biogenesis of sm-class ribonucleoproteins. Journal of Cell Biology, 178 (5), 733-740.

Gorlia, T., Stupp, R., Brandes, A. A., Rampling, R. R., Fumoleau, P., Dittrich, C., Campone, M. M., Twelves, C. C., Raymond, E., Hegi, M. E., Lacombe, D. & van den Bent, Martin J. (2012) New prognostic factors and calculators for outcome prediction in patients with recurrent glioblastoma: A pooled analysis of EORTC brain tumour group phase I and II clinical trials. European Journal of Cancer, 48 (8), 1176-1184.

Goulet, I., Gauvin, G., Boisvenue, S. & Côté, J. (2007) Alternative splicing yields protein arginine methyltransferase 1 isoforms with distinct activity, substrate specificity, and subcellular localization. Journal of Biological Chemistry, 282 (45), 33009-33021.

Grasbon-Frodl, E., Kreth, F. W., Ruiter, M., Schnell, O., Bise, K., Felsberg, J. ö, Reifenberger, G., Tonn, J. & Kretzschmar, H. A. (2007) Intratumoral homogeneity of MGMT promoter hypermethylation as demonstrated in serial stereotactic specimens from anaplastic astrocytomas and glioblastomas. International Journal of Cancer, 121 (11), 2458-2464.

Gros, L., Delaporte, C., Frey, S., Decesse, J., de Saint-Vincent, B. R., Cavarec, L., Dubart, A., Gudkov, A. V. & Jacquemin-Sablon, A. (2003) Identification of new drug sensitivity genes using genetic suppressor elements. Cancer Res, 63 (1), 164.

Guccione, E. & Richard, S. (2019) The regulation, functions and clinical relevance of arginine methylation. Nature Reviews.Molecular Cell Biology, 20 (10), 642-657.

Guderian, G., Peter, C., Wiesner, J., Sickmann, A., Schulze-Osthoff, K., Fischer, U. & Grimmler, M. (2011) RioK1, a new interactor of protein arginine methyltransferase 5 (PRMT5), competes with pICln for binding and modulates PRMT5 complex composition and substrate specificity. The Journal of Biological Chemistry, 286 (3), 1976-1986.

Guendel, I., Carpio, L., Pedati, C., Schwartz, A., Teal, C., Kashanchi, F. & Kehn-Hall, K. (2010) Methylation of the tumor suppressor protein, BRCA1, influences its transcriptional cofactor function. PloS One, 5 (6), e11379.

Gui, S., Gathiaka, S., Li, J., Qu, J., Acevedo, O., & Hevel, J. M. (2014). A remodeled protein arginine methyltransferase 1 (PRMT1) generates symmetric dimethylarginine. The Journal of biological chemistry, 289(13), 9320–9327.

Guo, A., Gu, H., Zhou, J., Mulhern, D., Wang, Y., Lee, K. A., Yang, V., Aguiar, M., Kornhauser, J., Jia, X., Ren, J., Beausoleil, S. A., Silva, J. C., Vemulapalli, V., Bedford, M. T. & Comb, M. J. (2014) Immunoaffinity enrichment and mass spectrometry analysis of protein methylation. Molecular & Cellular Proteomics : MCP, 13 (1), 372-387.

Guo, Z., Zheng, L., Xu, H., Dai, H., Zhou, M., Pascua, M. R., Chen, Q. M. & Shen, B. (2010) Methylation of FEN1 suppresses nearby phosphorylation and facilitates PCNA binding. Nature Chemical Biology, 6 (10), 766-773.

Gutenberg, A., Lumenta, C. B., Braunsdorf, W. E. K., Sabel, M., Mehdorn, H. M., Westphal, M. & Giese, A. (2013) The combination of carmustine wafers and temozolomide for the treatment of malignant gliomas. A comprehensive review of the rationale and clinical experience. Journal of Neuro-Oncology, 113 (2), 163-174.

Hadjikyriacou, A., Yang, Y., Espejo, A., Bedford, M. T. & Clarke, S. G. (2015) Unique features of human protein arginine methyltransferase 9 (PRMT9) and its substrate RNA splicing factor SF3B2. The Journal of Biological Chemistry, 290 (27), 16723-16743.

Hainsworth, J. D., Ervin, T., Friedman, E., Priego, V., Murphy, P. B., Clark, B. L. & Lamar, R. E. (2010) Concurrent radiotherapy and temozolomide followed by temozolomide and sorafenib in the first-line treatment of patients with glioblastoma multiforme. John Wiley & Sons, Ltd.

Halabelian, L., & Barsyte-Lovejoy, D. (2021). Structure and Function of Protein Arginine Methyltransferase PRMT7. Life, 11(8), 768.

Halatsch, M., Schmidt, U., Behnke-Mursch, J., Unterberg, A. & Wirtz, C. R. (2006) Epidermal growth factor receptor inhibition for the treatment of glioblastoma multiforme and other malignant brain tumours. Cancer Treatment Reviews, 32 (2), 74-89.

Han, X., Li, R., Zhang, W., Yang, X., Wheeler, C. G., Friedman, G. K., Province, P., Ding, Q., You, Z., Fathallah-Shaykh, H., Gillespie, G. Y., Zhao, X., King, P. H. & Nabors, L. B. (2014) Expression of PRMT5 correlates with malignant grade in gliomas and plays a pivotal role in tumor growth in vitro. Journal of Neuro-Oncology, 118 (1), 61-72.

Haraszti, R. A., Didiot, M. C., Sapp, E., Leszyk, J., Shaffer, S. A., Rockwell, H. E., Gao, F., Narain, N. R., DiFiglia, M., Kiebish, M. A., Aronin, N. & Khvorova, A. (2016) High-resolution proteomic and lipidomic analysis of exosomes and microvesicles from different cell sources. Journal of Extracellular Vesicles, 5 32570.

Hartel, N. G., Chew, B., Qin, J., Xu, J., & Graham, N. A. (2019). Deep Protein Methylation Profiling by Combined Chemical and Immunoaffinity Approaches Reveals Novel PRMT1 Targets. Molecular & cellular proteomics, 18(11), 2149–2164.

Hartley, A. & Lu, T. (2020) Modulating the modulators: Regulation of protein arginine methyltransferases by post-translational modifications. Drug Discovery Today, 25 (9), 1735-1743.

Hartley, A., Wang, B., Jiang, G., Wei, H., Sun, M., Prabhu, L., Martin, M., Safa, A., Sun, S., Liu, Y. & Lu, T. (2020) Regulation of a PRMT5/NF-κB axis by phosphorylation of PRMT5 at serine 15 in colorectal cancer. International Journal of Molecular Sciences, 21 (10), 3684.

Hartmann, C., Meyer, J., Balss, J., Capper, D., Mueller, W., Christians, A., Felsberg, J., Wolter, M., Mawrin, C., Wick, W., Weller, M., Herold-Mende, C., Unterberg, A., Jeuken, J. W. M., Wesseling, P., Reifenberger, G. & von Deimling, A. (2009) Type and frequency of IDH1 and IDH2 mutations are

related to astrocytic and oligodendroglial differentiation and age: A study of 1,010 diffuse gliomas. Acta Neuropathologica, 118 (4), 469-474.

Hasegawa, M., Toma-Fukai, S., Kim, J., Fukamizu, A. & Shimizu, T. (2014) Protein arginine methyltransferase 7 has a novel homodimer-like structure formed by tandem repeats. FEBS Letters, 588 (10), 1942-1948.

Hashimoto, M., Kumabe, A., Kim, J., Murata, K., Sekizar, S., Williams, A., Lu, W., Ishida, J., Nakagawa, T., Endo, M., Minami, Y. & Fukamizu, A. (2020) Loss of PRMT1 in the central nervous system (CNS) induces reactive astrocytes and microglia during postnatal brain development. Journal of Neurochemistry, 156(6), 834-847.

Hashimoto, M., Murata, K., Ishida, J., Kanou, A., Kasuya, Y. & Fukamizu, A. (2016) Severe hypomyelination and developmental defects are caused in mice lacking protein arginine methyltransferase 1 (PRMT1) in the central nervous system. The Journal of Biological Chemistry, 291 (5), 2237-2245.

Hatanpaa, K. J., Burma, S., Zhao, D. & Habib, A. A. (2010) Epidermal growth factor receptor in glioma: Signal transduction, neuropathology, imaging, and radioresistance. Neoplasia (New York, N.Y.), 12 (9), 675-684.

He, W., Ma, X., Yang, X., Zhao, Y., Qiu, J. & Hang, H. (2011) A role for the arginine methylation of Rad9 in checkpoint control and cellular sensitivity to DNA damage. Nucleic Acids Research, 39 (11), 4719-4727.

He, Z., Ruan, X., Liu, X., Zheng, J., Liu, Y., Liu, L., Ma, J., Shao, L., Wang, D., Shen, S., Yang, C., & Xue, Y. (2019). FUS/circ_002136/miR-138-5p/SOX13 feedback loop regulates angiogenesis in Glioma. Journal of experimental & clinical cancer research : CR, 38(1), 65.

Heaphy, C. M., Subhawong, A. P., Hong, S., Goggins, M. G., Montgomery, E. A., Gabrielson, E., Netto, G. J., Epstein, J. I., Lotan, T. L., Westra, W. H., Shih, I., Iacobuzio-Donahue, C., Maitra, A., Li, Q. K., Eberhart, C. G., Taube, J. M., Rakheja, D., Kurman, R. J., Wu, T. C., Roden, R. B., Argani, P., De Marzo, A.,M., Terracciano, L., Torbenson, M. & Meeker, A. K. (2011) Prevalence of the alternative lengthening of telomeres telomere maintenance mechanism in human cancer subtypes. The American Journal of Pathology, 179 (4), 1608-1615.

Hegi, M. E., Diserens, A., Bady, P., Kamoshima, Y., Kouwenhoven, M. C. M., Delorenzi, M., Lambiv, W. L., Hamou, M., Matter, M. S., Koch, A., Heppner, F. L., Yonekawa, Y., Merlo, A., Frei, K., Mariani, L. &

Hofer, S. (2011) Pathway analysis of glioblastoma tissue after preoperative treatment with the EGFR tyrosine kinase inhibitor Gefitinib—A phase II trial. Mol Cancer Ther, 10 (6), 1102.

Hegi, M. E., Diserens, A., Gorlia, T., Hamou, M., de Tribolet, N., Weller, M., Kros, J. M., Hainfellner, J. A., Mason, W., Mariani, L., Bromberg, J. E. C., Hau, P., Mirimanoff, R. O., Cairncross, J. G., Janzer, R. C. & Stupp, R. (2005) MGMT gene silencing and benefit from temozolomide in glioblastoma. N Engl J Med, 352 (10), 997-1003.

Heiland, D. H., Haaker, G., Watzlawick, R., Delev, D., Masalha, W., Franco, P., Machein, M., Staszewski, O., Oelhke, O., Nicolay, N. H. & Schnell, O. (2018) One decade of glioblastoma multiforme surgery in 342 elderly patients: What have we learned? Journal of Neuro-Oncology, 140 (2), 385-391.

Hernandez, S. J., Dolivo, D. M. & Dominko, T. (2017) PRMT8 demonstrates variant-specific expression in cancer cells and correlates with patient survival in breast, ovarian and gastric cancer. Oncology Letters, 13 (3), 1983-1989.

Hernandez, S. & Dominko, T. (2016) Novel protein arginine methyltransferase 8 isoform is essential for cell proliferation. Journal of Cellular Biochemistry, 117 (9), 2056-2066.

Herrmann, F., Bossert, M., Schwander, A., Akgün, E. & Fackelmayer, F. O. (2004) Arginine methylation of scaffold attachment factor A by heterogeneous nuclear ribonucleoprotein particle-associated PRMT1. Journal of Biological Chemistry, 279 (47), 48774-48779.

Herrmann, F., Lee, J., Bedford, M. T. & Fackelmayer, F. O. (2005) Dynamics of human protein arginine methyltransferase 1(PRMT1) in vivo. Journal of Biological Chemistry, 280 (45), 38005-38010.

Hevel, J. M. & Price, O. M. (2020) Rapid and direct measurement of methyltransferase activity in about 30 min. Methods (San Diego, Calif.), 175 3-9.

Higashimoto, K., Kuhn, P., Desai, D., Cheng, X. & Xu, W. (2007) Phosphorylation-mediated inactivation of coactivator-associated arginine methyltransferase 1. Proceedings of the National Academy of Sciences of the United States of America, 104 (30), 12318-12323.

Hodges, T. R., Ott, M., Xiu, J., Gatalica, Z., Swensen, J., Zhou, S., Huse, J. T., de Groot, J., Li, S., Overwijk, W. W., Spetzler, D. & Heimberger, A. B. (2017) Mutational burden, immune checkpoint expression, and mismatch repair in glioma: Implications for immune checkpoint immunotherapy. Oxford University Press.

Holdhoff, M., Ye, X., Supko, J. G., Nabors, L. B., Desai, A. S., Walbert, T., Lesser, G. J., Read, W. L., Lieberman, F. S., Lodge, M. A., Leal, J., Fisher, J. D., Desideri, S., Grossman, S. A., Wahl, R. L. & Schiff,

D. (2017) Timed sequential therapy of the selective T-type calcium channel blocker mibefradil and temozolomide in patients with recurrent high-grade gliomas. Neuro-Oncology, 19 (6), 845-852.

Holmes, B., Benavides-Serrato, A., Saunders, J. T., Landon, K. A., Schreck, A. J., Nishimura, R. N. & Gera, J. (2019) The protein arginine methyltransferase PRMT5 confers therapeutic resistance to mTOR inhibition in glioblastoma. Journal of Neuro-Oncology, 145 (1), 11-22.

Honda, M., Nakashima, K. & Katada, S. (2017) PRMT1 regulates astrocytic differentiation of embryonic neural stem/precursor cells. Journal of Neurochemistry, 142 (6), 901-907.

Hong, X., Zang, J., White, J., Wang, C., Pan, C., Zhao, R., Murphy, R. C., Dai, S., Henson, P., Kappler, J. W., Hagman, J. & Zhang, G. (2010) Interaction of JMJD6 with single-stranded RNA. Proceedings of the National Academy of Sciences of the United States of America, 107 (33), 14568-14572.

Hornbeck, P. V., Zhang, B., Murray, B., Kornhauser, J. M., Latham, V. & Skrzypek, E. (2015) PhosphoSitePlus, 2014: Mutations, PTMs and recalibrations. Nucleic Acids Research, 43 (Database issue), 512.

Houillier, C., Lejeune, J., Benouaich-Amiel, A., Laigle-Donadey, F., Criniere, E., Mokhtari, K., Thillet, J., Delattre, J., Hoang-Xuan, K. & Sanson, M. (2006) Prognostic impact of molecular markers in a series of 220 primary glioblastomas. Cancer, 106 (10), 2218-2223.

Howlader, N., Noone, A. M., Krapcho, M., Garshell, J., Neyman, N., Altekruse, S. F., Kosary, C. L., Yu, M., Ruhl, J., Tatalovich, Z., Cho, H., Mariotto, A., Lewis, D. R., Chen, H. S., Feuer, E. J. & Cronin, K. A. (2013) SEER cancer statistics review, 1975-2010. Available online: https://seer.cancer.gov/archive/csr/1975_2010/ [Accessed 09/11/ 2020].

Hsu, J., Chen, C., Chou, C., Kuo, H., Li, L., Lin, C., Lee, H., Wang, Y., Liu, M., Liao, H., Shi, B., Lai, C., Bedford, M. T., Tsai, C. & Hung, M. (2011) Crosstalk between arg 1175 methylation and tyr 1173 phosphorylation negatively modulates EGFR-mediated ERK activation. Nature Cell Biology, 13 (2), 174-181.

Hu, G., Yan, C., Xie, P., Cao, Y., Shao, J. & Ge, J. (2020) PRMT2 accelerates tumorigenesis of hepatocellular carcinoma by activating Bcl2 via histone H3R8 methylation. Experimental Cell Research, 394 (2), 112152.

Hu, Y., Shi, G., Zhang, L., Li, F., Jiang, Y., Jiang, S., Ma, W., Zhao, Y., Songyang, Z. & Huang, J. (2016) Switch telomerase to ALT mechanism by inducing telomeric DNA damages and dysfunction of ATRX and DAXX. Scientific Reports, 6 32280.

Hu, Y., Gao, H., Vo, C., Ke, C., Pan, F., Yu, L., Siegel, E., Hess, K. R., Linskey, M. E., & Zhou, Y. H. (2014). Anti-EGFR function of EFEMP1 in glioma cells and patient prognosis. Oncoscience, 1(3), 205–215.

Hua, Z., Hansen, J. N., He, M., Dai, S., Choi, Y., Fulton, M. D., Lloyd, S. M., Szemes, M., Sen, J., Ding, H., Angelastro, J. M., Fei, X., Li, H., Wu, C., Yang, S., Malik, K., Bao, X., George Zheng, Y., Liu, C., Schor, N. F., Li, Z. & Li, X. (2020) PRMT1 promotes neuroblastoma cell survival through ATF5. Oncogenesis, 9 (5), 50.

Huang, J., Yu, J., Tu, L., Huang, N., Li, H. & Luo, Y. (2019) Isocitrate dehydrogenase mutations in glioma: From basic discovery to therapeutics development. Frontiers in Oncology, 9 506.

Huang, J., Vogel, G., Yu, Z., Almazan, G. & Richard, S. (2011) Type II arginine methyltransferase PRMT5 regulates gene expression of inhibitors of differentiation/DNA binding Id2 and Id4 during glial cell differentiation.

Huang, P. H., Cavenee, W. K., Furnari, F. B. & White, F. M. (2007) Uncovering therapeutic targets FOR glioblastoma: A systems biology approach. Cell Cycle, 6 (22), 2750-2754.

Huang, S., Litt, M. & Felsenfeld, G. (2005) Methylation of histone H4 by arginine methyltransferase PRMT1 is essential in vivo for many subsequent histone modifications. Genes & Development, 19 (16), 1885-1893.

Hubert, C. G., Rivera, M., Spangler, L. C., Wu, Q., Mack, S. C., Prager, B. C., Couce, M., McLendon, R. E., Sloan, A. E. & Rich, J. N. (2016) A three-dimensional organoid culture system derived from human glioblastomas recapitulates the hypoxic gradients and cancer stem cell heterogeneity of tumors found in vivo. Cancer Research, 76 (8), 2465-2477.

Humpel, C. (2015) Organotypic brain slice cultures: A review. Neuroscience, 305 86-98.

Humphrey, P. A., Wong, A. J., Vogelstein, B., Zalutsky, M. R., Fuller, G. N., Archer, G. E., Friedman, H. S., Kwatra, M. M., Bigner, S. H. & Bigner, D. D. (1990) Anti-synthetic peptide antibody reacting at the fusion junction of deletion-mutant epidermal growth factor receptors in human glioblastoma. Proceedings of the National Academy of Sciences of the United States of America, 87 (11), 4207-4211.

Hupalowska, A., Jedrusik, A., Zhu, M., Bedford, M. T., Glover, D. M. & Zernicka-Goetz, M. (2018) CARM1 and paraspeckles regulate pre-implantation mouse embryo development. Cell, 175 (7), 1902-1916.e13.

Iberg, A. N., Espejo, A., Cheng, D., Kim, D., Michaud-Levesque, J., Richard, S. & Bedford, M. T. (2008) Arginine methylation of the histone H3 tail impedes effector binding. Journal of Biological Chemistry, 283 (6), 3006-3010.

Idbaih, A., Carvalho Silva, R., Crinière, E., Marie, Y., Carpentier, C., Boisselier, B., Taillibert, S., Rousseau, A., Mokhtari, K., Ducray, F., Thillet, J., Sanson, M., Hoang-Xuan, K. & Delattre, J. (2008) Genomic changes in progression of low-grade gliomas. Journal of Neuro-Oncology, 90 (2), 133-140.

Ikenaka, K., Miyata, S., Mori, Y., Koyama, Y., Taneda, T., Okuda, H., Kousaka, A. & Tohyama, M. (2006) Immunohistochemical and western analyses of protein arginine N-methyltransferase 3 in the mouse brain. Neuroscience, 141 (4), 1971-1982.

Ishigaki, S. & Sobue, G. (2018) Importance of functional loss of FUS in FTLD/ALS. Frontiers in Molecular Biosciences, 5 44.

Ishiguro, T., Ohata, H., Sato, A., Yamawaki, K., Enomoto, T. & Okamoto, K. (2017) Tumor-derived spheroids: Relevance to cancer stem cells and clinical applications. Cancer Science, 108 (3), 283-289.

Izumikawa, K., Ishikawa, H., Yoshikawa, H., Terukina, G., Miyazawa, N., Nakayama, H., Nobe, Y., Taoka, M., Yamauchi, Y., Philipsen, S., Isobe, T. & Takahashi, N. (2014) Friend of Prmt1, FOP is a novel component of the nuclear SMN complex isolated using biotin affinity purification. Journal of Proteomics & Bioinformatics, 7 1-11.

Jacob, F., Salinas, R. D., Zhang, D. Y., Nguyen, P. T. T., Schnoll, J. G., Wong, S. Z. H., Thokala, R., Sheikh, S., Saxena, D., Prokop, S., Liu, D. A., Qian, X., Petrov, D., Lucas, T., Chen, H. I., Dorsey, J. F., Christian, K. M., Binder, Z. A., Nasrallah, M., Brem, S., O'Rourke, D. M., Ming, G. L. & Song, H. (2020) A patient-derived glioblastoma organoid model and biobank recapitulates inter- and intra-tumoral heterogeneity. Cell, 180 (1), 188-204.e22.

Jacob, F., Salinas, R. D., Zhang, D. Y., Nguyen, P. T. T., Schnoll, J. G., Wong, S. Z. H., Thokala, R., Sheikh, S., Saxena, D., Prokop, S., Liu, D., Qian, X., Petrov, D., Lucas, T., Chen, H. I., Dorsey, J. F., Christian, K. M., Binder, Z. A., Nasrallah, M., Brem, S., O'Rourke, D.,M., Ming, G. & Song, H. (2020) A patient-derived glioblastoma organoid model and biobank recapitulates inter- and intra-tumoral heterogeneity. Cell, 180 (1), 188-204.e22.

Jaiswal, P. K., Goel, A. & Mittal, R. D. (2015) Survivin: A molecular biomarker in cancer. The Indian Journal of Medical Research, 141 (4), 389-397.

Jarzebska, N., Mangoni, A. A., Martens-Lobenhoffer, J., Bode-Böger, S. M. & Rodionov, R. N. (2019) The second life of methylarginines as cardiovascular targets. International Journal of Molecular Sciences, 20 (18), 4592. doi: 10.3390/ijms20184592.

Jelinic, P., Stehle, J. C. & Shaw, P. (2006) The testis-specific factor CTCFL cooperates with the protein methyltransferase PRMT7 in H19 imprinting control region methylation. PLoS Biology, 4 (11), e355.

Jeong, H. J., Lee, S. J., Lee, H. J., Kim, H. B., Anh Vuong, T., Cho, H., Bae, G. U. & Kang, J. S. (2020) Prmt7 promotes myoblast differentiation via methylation of p38MAPK on arginine residue 70. Cell Death and Differentiation, 27 (2), 573-586.

Jeong, M., Jeong, H., Ahn, B., Pyun, J., Kwon, I., Cho, H. & Kang, J. (2019) PRMT1 suppresses ATF4-mediated endoplasmic reticulum response in cardiomyocytes. Cell Death & Disease, 10 (12), 903.

Jie, M., Mao, S., Liu, H., He, Z., Li, H. & Lin, J. (2017) Evaluation of drug combination for glioblastoma based on an intestine–liver metabolic model on microchip. Analyst, 142 (19), 3629-3638.

Jihong Zhang & Malcolm F.G. Stevens and Tracey D. Bradshaw. (2012) Temozolomide: Mechanisms of action, repair and resistance. Current Molecular Pharmacology, 5 (1), 102-114.

Jill S. Barnholtz-Sloan, Sloan, A. E. & Schwartz, A. G. (2003a) Relative survival rates and patterns of diagnosis analyzed by time period for individuals with primary malignant brain tumor, 1973–1997. Journal of Neurosurgery, 99 (3), 458-466.

Jill S. Barnholtz-Sloan, Sloan, A. E. & Schwartz, A. G. (2003b) Relative survival rates and patterns of diagnosis analyzed by time period for individuals with primary malignant brain tumor, 1973–1997. Journal of Neurosurgery, 99 (3), 458-466.

Jin, J., Martin, M., Hartley, A. & Lu, T. (2019) PRMTs and miRNAs: Functional cooperation in cancer and beyond. Null, 18 (15), 1676-1686.

Johanns, T. M., Miller, C. A., Dorward, I. G., Tsien, C., Chang, E., Perry, A., Uppaluri, R., Ferguson, C., Schmidt, R. E., Dahiya, S., Ansstas, G., Mardis, E. R. & Dunn, G. P. (2016) Immunogenomics of hypermutated glioblastoma: A patient with germline POLE deficiency treated with checkpoint blockade immunotherapy. Cancer Discovery, 6 (11), 1230-1236.

Johnson, D., Fogh, S., Giannini, C., Kaufmann, T., Raghunathan, A., Theodosopoulos, P. & Clarke, J. (2015) Case-based review: Newly diagnosed glioblastoma. Neuro-Oncology Practice, 2 (3), 106-121.

Jones, D., Wilson, L., Thomas, H., Gaughan, L. & Wade, M. A. (2019) The histone demethylase enzymes KDM3A and KDM4B co-operatively regulate chromatin transactions of the estrogen receptor in breast cancer. Cancers, 11 (8), 1122. doi: 10.3390/cancers11081122.

Ju, U., Park, J., Park, H., Kim, S. J. & Chun, Y. (2015) FBXO11 represses cellular response to hypoxia by destabilizing hypoxia-inducible factor-1α mRNA. Biochemical and Biophysical Research Communications, 464 (4), 1008-1015.

Jung, G. A., Shin, B. S., Jang, Y. S., Sohn, J. B., Woo, S. R., Kim, J. E., Choi, G., Lee, K. M., Min, B. H., Lee, K. H. & Park, G. H. (2011) Methylation of eukaryotic elongation factor 2 induced by basic fibroblast growth factor via mitogen-activated protein kinase. Experimental & Molecular Medicine, 43 (10), 550-560.

Kakkar, A., Suri, V., Jha, P., Srivastava, A., Sharma, V., Pathak, P., Sharma, M., Sharma, M., Kale, S., Chosdol, K., Phalak, M. & Sarkar, C. (2011) Loss of heterozygosity on chromosome 10q in glioblastomas, and its association with other genetic alterations and survival in indian patients. Neurol India, 59 (2), 254-261.

Kaley, T. J., Panageas, K. S., Mellinghoff, I. K., Nolan, C., Gavrilovic, I. T., DeAngelis, L. M., Abrey, L. E., Holland, E. C. & Lassman, A. B. (2019) Phase II trial of an AKT inhibitor (perifosine) for recurrent glioblastoma. Journal of Neuro-oncology, 144(2), 403-407.

Kalokhe, G., Grimm, S. A., Chandler, J. P., Helenowski, I., Rademaker, A. & Raizer, J. J. (2012) Metastatic glioblastoma: Case presentations and a review of the literature. Journal of Neuro-Oncology, 107 (1), 21-27.

Kalpathy-Cramer, J., Gerstner, E. R., Emblem, K. E., Andronesi, O. & Rosen, B. (2014) Advanced magnetic resonance imaging of the physical processes in human glioblastoma. Cancer Research, 74 (17), 4622-4637.

Kamath, A. A., Friedman, D. D., Akbari, S. H., Kim, A. H., Tao, Y., Luo, J. & Leuthardt, E. C. (2019) Glioblastoma treated with magnetic resonance imaging-guided laser interstitial thermal therapy: Safety, efficacy, and outcomes. Neurosurgery, 84 (4), 836-843.

Kaneshiro, D., Kobayashi, T., Chao, S. T., Suh, J. & Prayson, R. A. (2009) Chromosome 1p and 19q deletions in glioblastoma multiforme. Applied Immunohistochemistry & Molecular Morphology, 17 (6), 512-516.

Kappadakunnel, M., Eskin, A., Dong, J., Nelson, S. F., Mischel, P. S., Liau, L. M., Ngheimphu, P., Lai, A., Cloughesy, T. F., Goldin, J. & Pope, W. B. (2010) Stem cell associated gene expression in glioblastoma

multiforme: Relationship to survival and the subventricular zone. Journal of Neuro-Oncology, 96 (3), 359-367.

Katsanis, N., Yaspo, M. -. & Fisher, E. M. C. (1997) Identification and mapping of a novel human gene, HRMT1L1, homologous to the rat protein arginine N-methyltransferase 1 (PRMT1) gene. Mammalian Genome, 8 (7), 526-529.

Katsuno, Y., Qin, J., Oses-Prieto, J., Wang, H., Jackson-Weaver, O., Zhang, T., Lamouille, S., Wu, J., Burlingame, A., Xu, J. & Derynck, R. (2018) Arginine methylation of SMAD7 by PRMT1 in TGF-β-induced epithelial-mesenchymal transition and epithelial stem-cell generation. The Journal of Biological Chemistry, 293 (34), 13059-13072.

Katz, J. E., Dlakić, M. & Clarke, S. (2003) Automated identification of putative methyltransferases from genomic open reading frames. Mol Cell Proteomics, 2 (8), 525.

Kaufmann, S. H., Desnoyers, S., Ottaviano, Y., Davidson, N. E. & Poirier, G. G. (1993) Specific proteolytic cleavage of poly(ADP-ribose) polymerase: An early marker of chemotherapy-induced apoptosis. Cancer Research, 53 (17), 3976-3985.

Kfoury, N., Sun, T., Yu, K. et al. Cooperative p16 and p21 action protects female astrocytes from transformation. Acta Neuropathologica Communications, 6(12).

Khot, M. I., Levenstein, M. A., de Boer, G. N., Armstrong, G., Maisey, T., Svavarsdottir, H. S., Andrew, H., Perry, S. L., Kapur, N. & Jayne, D. G. (2020) Characterising a PDMS based 3D cell culturing microfluidic platform for screening chemotherapeutic drug cytotoxic activity. Scientific Reports, 10 (1), 15915.

Kim, D., Park, M., Lim, S., Park, J., Yoon, K., Han, H., Gustafsson, J., Lim, J. & Park, S. (2015) PRMT3 regulates hepatic lipogenesis through direct interaction with LXRα. Diabetes, 64 (1), 60.

Kim, J., Daniel, J., Espejo, A., Lake, A., Krishna, M., Xia, L., Zhang, Y., & Bedford, M. T. (2006). Tudor, MBT and chromo domains gauge the degree of lysine methylation. EMBO reports, 7(4), 397–403.

Kim, J. H., Yoo, B. C., Yang, W. S., Kim, E., Hong, S. & Cho, J. Y. (2016) The role of protein arginine methyltransferases in inflammatory responses. Mediators of Inflammation, 2016 4028353.

Kim, J., Park, K., Ishida, J., Kako, K., Hamada, J., Kani, S., Takeuchi, M., Namiki, K., Fukui, H., Fukuhara, S., Hibi, M., Kobayashi, M., Kanaho, Y., Kasuya, Y., Mochizuki, N. & Fukamizu, A. (2015) PRMT8 as a phospholipase regulates purkinje cell dendritic arborization and motor coordination. Sci Adv, 1 (11), e1500615.

Kimelberg, H. K. & Norenberg, M. D. (1989) Astrocytes. Scientific American, 260 (4), 66-77.

Kirino, Y., Vourekas, A., Sayed, N., de Lima Alves, F., Thomson, T., Lasko, P., Rappsilber, J., Jongens, T. A., & Mourelatos, Z. (2010). Arginine methylation of Aubergine mediates Tudor binding and germ plasm localization. RNA, 16(1), 70–78.

Kirson, E. D., Gurvich, Z., Schneiderman, R., Dekel, E., Itzhaki, A., Wasserman, Y., Schatzberger, R. & Palti, Y. (2004) Disruption of cancer cell replication by alternating electric fields. Cancer Res, 64 (9), 3288.

Kleinman, H. K., Klebe, R. J. & Martin, G. R. (1981) Role of collagenous matrices in the adhesion and growth of cells. J Cell Biol, 88 (3), 473–485.

Kleihues, P. & Ohgaki, H. (2000) Phenotype vs genotype in the evolution of astrocytic brain tumors. Toxicol Pathol, 28 (1), 164-170.

Kodack, D. P., Farago, A. F., Dastur, A., Held, M. A., Dardaei, L., Friboulet, L., von Flotow, F., Damon, L. J., Lee, D., Parks, M., Dicecca, R., Greenberg, M., Kattermann, K. E., Riley, A. K., Fintelmann, F. J., Rizzo, C., Piotrowska, Z., Shaw, A. T., Gainor, J. F., Sequist, L. V., Niederst, M. J., Engelman, J. A. & Benes, C. H. (2017) Primary patient-derived cancer cells and their potential for personalized cancer patient care. Cell Reports, 21 (11), 3298-3309.

Komander, D. & Rape, M. (2012) The ubiquitin code. Annual Review of Biochemistry, 81 (1), 203-229.

Krzyzanowski, A., Gasper, R., Adihou, H., Hart, P. '., & Waldmann, H. (2021). Biochemical Investigation of the Interaction of pICln, RioK1 and COPR5 with the PRMT5-MEP50 Complex. Chembiochem : a European journal of chemical biology, 22(11), 1908–1914.

Kuhn, P., Chumanov, R., Wang, Y., Ge, Y., Burgess, R. R. & Xu, W. (2011) Automethylation of CARM1 allows coupling of transcription and mRNA splicing. Nucleic Acids Research, 39 (7), 2717-2726.

Kumar, A., Zhong, Y., Albrecht, A., Sang, P. B., Maples, A., Liu, Z., Vinayachandran, V., Reja, R., Lee, C. F., Kumar, A., Chen, J., Xiao, J., Park, B., Shen, J., Liu, B., Person, M. D., Trybus, K. M., Zhang, K. Y. J., Pugh, B. F., Kamm, K. E., Milewicz, D. M., Shen, X. & Kapoor, P. (2020) Actin R256 mono-methylation is a conserved post-translational modification involved in transcription. Cell Reports, 32 (13), 108172.

Kumari, N., Hassan, M. A., Lu, X., Roeder, R. G. & Biswas, D. (2019) AFF1 acetylation by p300 temporally inhibits transcription during genotoxic stress response. Proc Natl Acad Sci USA, 116 (44), 22140.

Kurz, S. C., Cabrera, L. P., Hastie, D., Huang, R., Unadkat, P., Rinne, M., Nayak, L., Lee, E. Q., Reardon, D. A. & Wen, P. Y. (2018) PD-1 inhibition has only limited clinical benefit in patients with recurrent high-grade glioma. Neurology, 91(14), e1355-e1359.

Kzhyshkowska, J., Schütt, H., Liss, M., Kremmer, E., Stauber, R., Wolf, H. & Dobner, T. (2001) Heterogeneous nuclear ribonucleoprotein E1B-AP5 is methylated in its arg-gly-gly (RGG) box and interacts with human arginine methyltransferase HRMT1L1. The Biochemical Journal, 358 305-314.

Labussière, M., Di Stefano, A. L., Gleize, V., Boisselier, B., Giry, M., Mangesius, S., Bruno, A., Paterra, R., Marie, Y., Rahimian, A., Finocchiaro, G., Houlston, R. S., Hoang-Xuan, K., Idbaih, A., Delattre, J., Mokhtari, K. & Sanson, M. (2014) TERT promoter mutations in gliomas, genetic associations and clinico-pathological correlations. British Journal of Cancer, 111 (10), 2024-2032.

Lacroix, M., El Messaoudi, S., Rodier, G., Le Cam, A., Sardet, C. & Fabbrizio, E. (2008) The histone-binding protein COPR5 is required for nuclear functions of the protein arginine methyltransferase PRMT5. EMBO Reports, 9 (5), 452-458.

Lai, Y., Song, M., Hakala, K., Weintraub, S. T. & Shiio, Y. (2011) Proteomic dissection of the von hippel-lindau (VHL) interactome. Journal of Proteome Research, 10 (11), 5175-5182.

Laity, J. H., Lee, B. M. & Wright, P. E. (2001) Zinc finger proteins: New insights into structural and functional diversity. Current Opinion in Structural Biology, 11 (1), 39-46.

Lakowski, T. & Frankel, A. (2009) Kinetic analysis of human protein arginine N-methyltransferase 2: Formation of monomethyl- and asymmetric dimethyl-arginine residues on histone H4. Biochemical Journal, 421 (2), 253-261.

Lander, E. S., Linton, L. M., Birren, B., Nusbaum, C., Zody, M. C., Baldwin, J., Devon, K., Dewar, K., Doyle, M., FitzHugh, W., Funke, R., Gage, D., Harris, K., Heaford, A., Howland, J., Kann, L., Lehoczky, J., LeVine, R., McEwan, P., McKernan, K., Meldrim, J., Mesirov, J. P., Miranda, C., Morris, W., Naylor, J., Raymond, C., Rosetti, M., Santos, R., Sheridan, A., Sougnez, C., Stange-Thomann, N., Stojanovic, N., Subramanian, A., Wyman, D., Rogers, J., Sulston, J., Ainscough, R., Beck, S., Bentley, D., Burton, J., Clee, C., Carter, N., Coulson, A., Deadman, R., Deloukas, P., Dunham, A., Dunham, I., Durbin, R., French, L., Grafham, D., Gregory, S., Hubbard, T., Humphray, S., Hunt, A., Jones, M., Lloyd, C., McMurray, A., Matthews, L., Mercer, S., Milne, S., Mullikin, J. C., Mungall, A., Plumb, R., Ross, M., Shownkeen, R., Sims, S., Waterston, R. H., Wilson, R. K., Hillier, L. W., McPherson, J. D., Marra, M. A., Mardis, E. R., Fulton, L. A., Chinwalla, A. T., Pepin, K. H., Gish, W. R., Chissoe, S. L., Wendl, M. C., Delehaunty, K. D., Miner, T. L., Delehaunty, A., Kramer, J. B., Cook, L. L., Fulton, R. S., Johnson, D. L., Minx, P. J., Clifton, S. W., Hawkins, T., Branscomb, E., Predki, P., Richardson, P., Wenning, S., Slezak,

T., Doggett, N., Cheng, J., Olsen, A., Lucas, S., Elkin, C., Uberbacher, E., Frazier, M., Gibbs, R. A., Muzny, D. M., Scherer, S. E., Bouck, J. B., Sodergren, E. J., Worley, K. C., Rives, C. M., Gorrell, J. H., Metzker, M. L., Naylor, S. L., Kucherlapati, R. S., Nelson, D. L., Weinstock, G. M., Sakaki, Y., Fujiyama, A., Hattori, M., Yada, T., Toyoda, A., Itoh, T., Kawagoe, C., Watanabe, H., Totoki, Y., Taylor, T., Weissenbach, J., Heilig, R., Saurin, W., Artiguenave, F., Brottier, P., Bruls, T., Pelletier, E., Robert, C., Wincker, P., Rosenthal, A., Platzer, M., Nyakatura, G., Taudien, S., Rump, A., Smith, D. R., Doucette-Stamm, L., Rubenfield, M., Weinstock, K., Lee, H. M., Dubois, J., Yang, H., Yu, J., Wang, J., Huang, G., Gu, J., Hood, L., Rowen, L., Madan, A., Qin, S., Davis, R. W., Federspiel, N. A., Abola, A. P., Proctor, M. J., Roe, B. A., Chen, F., Pan, H., Ramser, J., Lehrach, H., Reinhardt, R., McCombie, W. R., de la Bastide, M., Dedhia, N., Blöcker, H., Hornischer, K., Nordsiek, G., Agarwala, R., Aravind, L., Bailey, J. A., Bateman, A., Batzoglou, S., Birney, E., Bork, P., Brown, D. G., Burge, C. B., Cerutti, L., Chen, H., Church, D., Clamp, M., Copley, R. R., Doerks, T., Eddy, S. R., Eichler, E. E., Furey, T. S., Galagan, J., Gilbert, J. G. R., Harmon, C., Hayashizaki, Y., Haussler, D., Hermjakob, H., Hokamp, K., Jang, W., Johnson, L. S., Jones, T. A., Kasif, S., Kaspryzk, A., Kennedy, S., Kent, W. J., Kitts, P., Koonin, E. V., Korf, I., Kulp, D., Lancet, D., Lowe, T. M., McLysaght, A., Mikkelsen, T., Moran, J. V., Mulder, N., Pollara, V. J., Ponting, C. P., Schuler, G., Schultz, J. ö, Slater, G., Smit, A. F. A., Stupka, E., Szustakowki, J., Thierry-Mieg, D., Thierry-Mieg, J., Wagner, L., Wallis, J., Wheeler, R., Williams, A., Wolf, Y. I., Wolfe, K. H., Yang, S., Yeh, R., Collins, F., Guyer, M. S., Peterson, J., Felsenfeld, A., Wetterstrand, K. A., Myers, R. M., Schmutz, J., Dickson, M., Grimwood, J., Cox, D. R., Olson, M. V., Kaul, R., Raymond, C., Shimizu, N., Kawasaki, K., Minoshima, S., Evans, G. A., Athanasiou, M., Schultz, R., Patrinos, A. & Morgan, M. J. (2001) Initial sequencing and analysis of the human genome. Nature, 409 (6822), 860-921.

Lane, R., Simon, T., Vintu, M., Solkin, B., Koch, B., Stewart, N., Benstead-Hume, G., Pearl, F. M. G., Critchley, G., Stebbing, J. & Giamas, G. (2019) Cell-derived extracellular vesicles can be used as a biomarker reservoir for glioblastoma tumor subtyping. Communications Biology, 2 (1), 315.

Lang, F. F., Conrad, C., Gomez-Manzano, C., Yung, W. K. A., Sawaya, R., Weinberg, J. S., Prabhu, S. S., Rao, G., Fuller, G. N., Aldape, K. D., Gumin, J., Vence, L. M., Wistuba, I., Rodriguez-Canales, J., Villalobos, P. A., Dirven, C. M. F., Tejada, S., Valle, R. D., Alonso, M. M., Ewald, B., Peterkin, J. J., Tufaro, F. & Fueyo, J. (2018) Phase I study of DNX-2401 (delta-24-RGD) oncolytic adenovirus: Replication and immunotherapeutic effects in recurrent malignant glioma. Journal of Clinical Oncology : Official Journal of the American Society of Clinical Oncology, 36 (14), 1419-1427.

Larsen, S. C., Sylvestersen, K. B., Mund, A., Lyon, D., Mullari, M., Madsen, M. V., Daniel, J. A., Jensen, L. J. & Nielsen, M. L. (2016) Proteome-wide analysis of arginine monomethylation reveals widespread occurrence in human cells. Science Signaling, 9 (443), rs9.

Lawrence, T. (2009) The nuclear factor NF-kappaB pathway in inflammation. Cold Spring Harbor Perspectives in Biology, 1 (6), a001651.

Lawton, C. D., Nagasawa, D. T., Yang, I., Fessler, R. G. & Smith, Z. A. (2012) Leptomeningeal spinal metastases from glioblastoma multiforme: Treatment and management of an uncommon manifestation of disease. Journal of Neurosurgery: Spine SPI, 17 (5), 438-448.

Le Romancer, M., Treilleux, I., Leconte, N., Robin-Lespinasse, Y., Sentis, S., Bouchekioua-Bouzaghou, K., Goddard, S., Gobert-Gosse, S. & Corbo, L. (2008) Regulation of estrogen rapid signaling through arginine methylation by PRMT1. Molecular Cell, 31 (2), 212-221.

Lee, J., Cook, J. R., Yang, Z., Mirochnitchenko, O., Gunderson, S. I., Felix, A. M., Herth, N., Hoffmann, R. & Pestka, S. (2005) PRMT7, a new protein arginine methyltransferase that synthesizes symmetric dimethylarginine.

Lee, J., Kotliarova, S., Kotliarov, Y., Li, A., Su, Q., Donin, N. M., Pastorino, S., Purow, B. W., Christopher, N., Zhang, W., Park, J. K. & Fine, H. A. (2006) Tumor stem cells derived from glioblastomas cultured in bFGF and EGF more closely mirror the phenotype and genotype of primary tumors than do serum-cultured cell lines. Cancer Cell, 9 (5), 391-403.

Lee, J., Sayegh, J., Daniel, J., Clarke, S. & Bedford, M. T. (2005) PRMT8, a new membrane-bound tissue-specific member of the protein arginine methyltransferase family.

Lee, P. K. M., Goh, W. W. B. & Sng, J. C. G. (2017) Network-based characterization of the synaptic proteome reveals that removal of epigenetic regulator Prmt8 restricts proteins associated with synaptic maturation. Journal of Neurochemistry, 140 (4), 613-628.

Leroy, B., Fournier, J. L., Ishioka, C., Monti, P., Inga, A., Fronza, G. & Soussi, T. (2013) The TP53 website: An integrative resource centre for the TP53 mutation database and TP53 mutant analysis. Nucleic Acids Research, 41 D962-D969.

Lester-Coll, N., Supko, J. G., Kluytenaar, J., Pavlik, K. F., Yu, J. B., Moliterno, J., Piepmeier, J., Becker, K., Baehring, J. M., Huttner, A., Vortmeyer, A., Contessa, J. N., Ramani, R., Lampert, R., Yao, X. & Bindra, R. (2018) Mibefradil dihydrochoride with hypofractionated radiation for recurrent glioblastoma: A phase I dose expansion trial. Jco, 36 (15), e14046.

Leuthardt, E. C., Duan, C., Kim, M. J., Campian, J. L., Kim, A. H., Miller-Thomas, M., Shimony, J. S. & Tran, D. D. (2016) Hyperthermic laser ablation of recurrent glioblastoma leads to temporary disruption of the peritumoral blood brain barrier. PloS One, 11 (2), e0148613.

Levy, D., Darnell, J. (2002). STATs: transcriptional control and biological impact. Nature Reviews Molecular Cell Biology, 3, 651–662.

Li, B., Liu, L., Li, X. & Wu, L. (2015) miR-503 suppresses metastasis of hepatocellular carcinoma cell by targeting PRMT1. Biochemical and Biophysical Research Communications, 464 (4), 982-987.

Li, J., Zhao, Z., Carter, C., Ehrlich, L. I. R., Bedford, M. T. & Richie, E. R. (2013) Coactivator-associated arginine methyltransferase 1 regulates fetal hematopoiesis and thymocyte development. The Journal of Immunology, 190 (2), 597.

Li, J., Liang, R., Song, C., Xiang, Y. & Liu, Y. (2018) Prognostic significance of epidermal growth factor receptor expression in glioma patients. OncoTargets and Therapy, 11, 731-742.

Li, S., Ali, S., Duan, X., Liu, S., Du, J., Liu, C., Dai, H., Zhou, M., Zhou, L., Yang, L., Chu, P., Li, L., Bhatia, R., Schones, D. E., Wu, X., Xu, H., Hua, Y., Guo, Z., Yang, Y., Zheng, L. & Shen, B. (2018) JMJD1B demethylates H4R3me2s and H3K9me2 to facilitate gene expression for development of hematopoietic stem and progenitor cells. Cell Reports, 23 (2), 389-403.

Liau, L. M., Ashkan, K., Tran, D. D., Campian, J. L., Trusheim, J. E., Cobbs, C. S., Heth, J. A., Salacz, M., Taylor, S., D'Andre, S.,D., Iwamoto, F. M., Dropcho, E. J., Moshel, Y. A., Walter, K. A., Pillainayagam, C. P., Aiken, R., Chaudhary, R., Goldlust, S. A., Bota, D. A., Duic, P., Grewal, J., Elinzano, H., Toms, S. A., Lillehei, K. O., Mikkelsen, T., Walbert, T., Abram, S. R., Brenner, A. J., Brem, S., Ewend, M. G., Khagi, S., Portnow, J., Kim, L. J., Loudon, W. G., Thompson, R. C., Avigan, D. E., Fink, K. L., Geoffroy, F. J., Lindhorst, S., Lutzky, J., Sloan, A. E., Schackert, G., Krex, D., Meisel, H., Wu, J., Davis, R. P., Duma, C., Etame, A. B., Mathieu, D., Kesari, S., Piccioni, D., Westphal, M., Baskin, D. S., New, P. Z., Lacroix, M., May, S., Pluard, T. J., Tse, V., Green, R. M., Villano, J. L., Pearlman, M., Petrecca, K., Schulder, M., Taylor, L. P., Maida, A. E., Prins, R. M., Cloughesy, T. F., Mulholland, P. & Bosch, M. L. (2018) First results on survival from a large phase 3 clinical trial of an autologous dendritic cell vaccine in newly diagnosed glioblastoma. Journal of Translational Medicine, 16 (1), 142.

Lim, Y., Lee, J. Y., Ha, S. J., Yu, S., Shin, J. K. & Kim, H. C. (2020) Proteome-wide identification of arginine methylation in colorectal cancer tissues from patients. Proteome Science, 18 (1), 6.

Lin, W., Gary, J. D., Yang, M. C., Clarke, S. & Herschman, H. R. (1996) The mammalian immediate-early TIS21 protein and the leukemia-associated BTG1 protein interact with a protein-arginine N-methyltransferase.

Linkous, A., Balamatsias, D., Snuderl, M., Edwards, L., Miyaguchi, K., Milner, T., Reich, B., Cohen-Gould, L., Storaska, A., Nakayama, Y., Schenkein, E., Singhania, R., Cirigliano, S., Magdeldin, T., Lin, Y.,

Nanjangud, G., Chadalavada, K., Pisapia, D., Liston, C. & Fine, H. A. (2019) Modeling patient-derived glioblastoma with cerebral organoids. Cell Reports, 26 (12), 3203-3211.e5.

Liu, C., Zhang, Y., She, X., Fan, L., Li, P., Feng, J., Fu, H., Liu, Q., Liu, Q., Zhao, C., Sun, Y., & Wu, M. (2018). A cytoplasmic long noncoding RNA LINC00470 as a new AKT activator to mediate glioblastoma cell autophagy. Journal of hematology & oncology, 11(1), 77.

Liu, F., Zhao, X., Perna, F., Wang, L., Koppikar, P., Abdel-Wahab, O., Harr, M. W., Levine, R. L., Xu, H., Tefferi, A., Deblasio, A., Hatlen, M., Menendez, S. & Nimer, S. D. (2011) JAK2V617F-mediated phosphorylation of PRMT5 downregulates its methyltransferase activity and promotes myeloproliferation. Cancer Cell, 19 (2), 283-294.

Liu, K., Chen, C., Guo, Y., Lam, R., Bian, C., Xu, C., Zhao, D. Y., Jin, J., MacKenzie, F., Pawson, T., & Min, J. (2010). Structural basis for recognition of arginine methylated Piwi proteins by the extended Tudor domain. Proceedings of the National Academy of Sciences of the United States of America, 107(43), 18398–18403.

Liu, N., Yang, R., Shi, Y., Chen, L., Liu, Y., Wang, Z., Liu, S., Ouyang, L., Wang, H., Lai, W., Mao, C., Wang, M., Cheng, Y., Liu, S., Wang, X., Zhou, H., Cao, Y., Xiao, D. & Tao, Y. (2020) The cross-talk between methylation and phosphorylation in lymphoid-specific helicase drives cancer stem-like properties. Signal Transduction and Targeted Therapy, 5 (1), 197.

Liu, S., & Chen, Z. J. (2011). Expanding role of ubiquitination in NF-κB signaling. Cell research, 21(1), 6–21.

Liu, T., Li, A., Xu, Y. & Xin, Y. (2019) Momelotinib sensitizes glioblastoma cells to temozolomide by enhancement of autophagy via JAK2/STAT3 inhibition. Oncol Rep; Oncology Reports, 41 (3), 1883-1892.

Liu, X., Wu, G., Shan, Y., Hartmann, C., von Deimling, A. & Xing, M. (2013) Highly prevalent TERT promoter mutations in bladder cancer and glioblastoma. Cell Cycle (Georgetown, Tex.), 12 (10), 1637-1638.

Liu, Y., Li, L., Liu, X., Wang, Y., Liu, L., Peng, L., Liu, J., Zhang, L., Wang, G., Li, H., Liu, D., Huang, B., Lu, J. & Zhang, Y. (2020) Arginine methylation of SHANK2 by PRMT7 promotes human breast cancer metastasis through activating endosomal FAK signalling. eLife, 9 e57617.

Lo Sardo, A., Altamura, S., Pegoraro, S., Maurizio, E., Sgarra, R. & Manfioletti, G. (2013) Identification and characterization of new molecular partners for the protein arginine methyltransferase 6 (PRMT6). PloS One, 8 (1), e53750.

Logun, M., Zhao, W., Mao, L. & Karumbaiah, L. (2018) Microfluidics in malignant glioma research and precision medicine. Advanced Biosystems, 2 (5), 1700221.

Lombard, A., Goffart, N. & Rogister, B. (2015) Glioblastoma circulating cells: Reality, trap or illusion? Stem Cells International, 182985.

Louis, D. N., Ohgaki, H., Wiestler, O. D., Cavenee, W. K., Burger, P. C., Jouvet, A., Scheithauer, B. W. & Kleihues, P. (2007) The 2007 WHO classification of tumours of the central nervous system. Acta Neuropathologica, 114 (2), 97-109.

Louis, D. N., Perry, A., Reifenberger, G., von Deimling, A., Figarella-Branger, D., Cavenee, W. K., Ohgaki, H., Wiestler, O. D., Kleihues, P. & Ellison, D. W. (2016) The 2016 world health organization classification of tumors of the central nervous system: A summary. Acta Neuropathologica, 131 (6), 803-820.

Lu, J., Xu, Z., Duan, H., Ji, H., Zhen, Z., Li, B., Wang, H., Tang, H., Zhou, J., Guo, T., Wu, B., Wang, D., Liu, Y., Niu, Y. & Zhang, R. (2020) Tumor-associated macrophage interleukin-β promotes glycerol-3-phosphate dehydrogenase activation, glycolysis and tumorigenesis in glioma cells. Cancer Science, 111 (6), 1979-1990.

Lu, Y. -., Cai, X. -., Li, Z. -., Lv, J., Xiang, Y., Chen, J. -., Chen, W. -., Sun, W. -., Liu, X. -. & Chen, J. -. (2018) LncRNA SNHG16 functions as an oncogene by sponging MiR-4518 and up-regulating PRMT5 expression in glioma. Cellular Physiology and Biochemistry, 45 (5), 1975-1985.

Lun, M., Lok, E., Gautam, S., Wu, E. & Wong, E. T. (2011) The natural history of extracranial metastasis from glioblastoma multiforme. Journal of Neuro-Oncology, 105 (2), 261-273.

Luo, Q., Wu, T., Wu, W., Chen, G., Luo, X., Jiang, L., Tao, H., Rong, M., Kang, S. & Deng, M. (2020) The functional role of voltage-gated sodium channel Nav1.5 in metastatic breast cancer. Frontiers in Pharmacology, 11 1111.

Mahmoudi, K., Bouras, A., Bozec, D., Ivkov, R. & Hadjipanayis, C. (2018) Magnetic hyperthermia therapy for the treatment of glioblastoma: A review of the therapy's history, efficacy and application in humans. International Journal of Hyperthermia : The Official Journal of European Society for Hyperthermic Oncology, North American Hyperthermia Group, 34 (8), 1316-1328.

Malchow, S., Loosse, C., Sickmann, A. & Lorenz, C. (2017) Quantification of cardiovascular disease biomarkers in human platelets by targeted mass spectrometry. Proteomes, 5 (4), 31.

Marques-Torrejon, M., Gangoso, E. & Pollard, S. M. (2018) Modelling glioblastoma tumour-host cell interactions using adult brain organotypic slice co-culture. Dis Models Mech, 11 (2), dmm031435.

Meister, G., Eggert, C., Bühler, D., Brahms, H., Kambach, C. & Fischer, U. (2001) Methylation of sm proteins by a complex containing PRMT5 and the putative U snRNP assembly factor pICln. Current Biology, 11 (24), 1990-1994.

Mellinghoff, I. K., Cloughesy, T. F., Wen, P. Y., Taylor, J. W., Maher, E. A., Arrillaga, I., Peters, K. B., Choi, C., Ellingson, B. M., Lin, A. P., Thakur, S. B., Nicolay, B., Lu, M., Le, K., Yin, F., Tai, F., Schoenfeld, S., Steelman, L., Pandya, S. S. & Clarke, J. L. (2019) A phase I, open label, perioperative study of AG-120 and AG-881 in recurrent IDH1 mutant, low-grade glioma: Results from cohort 1. Jco, 37 (15), 2003.

Menezes, W. P. d., Silva, V. A. O., Gomes, I. N. F., Rosa, M. N., Spina, M. L. C., Carloni, A. C., Alves, A. L. V., Melendez, M., Almeida, G. C., Silva, L. S. d., Clara, C., da Cunha, I. W., Hajj, G. N. M., Jones, C., Bidinotto, L. T. & Reis, R. M. (2020) Loss of 5'-methylthioadenosine phosphorylase (MTAP) is frequent in high-grade gliomas; nevertheless, it is not associated with higher tumor aggressiveness. Cells, 9 (2), 492.

Merz, F., Gaunitz, F., Dehghani, F., Renner, C., Meixensberger, J., Gutenberg, A., Giese, A., Schopow, K., Hellwig, C., Schäfer, M., Bauer, M., Stöcker, H., Taucher-Scholz, G., Durante, M., & Bechmann, I. (2013). Organotypic slice cultures of human glioblastoma reveal different susceptibilities to treatments. Neuro-oncology, 15(6), 670–681.

Meyer, R., Wolf, S. S. & Obendorf, M. (2007) PRMT2, a member of the protein arginine methyltransferase family, is a coactivator of the androgen receptor. The Journal of Steroid Biochemistry and Molecular Biology, 107 (1), 1-14.

Migliori, V., Müller, J., Phalke, S., Low, D., Bezzi, M., Mok, W. C., Sahu, S. K., Gunaratne, J., Capasso, P., Bassi, C., Cecatiello, V., De Marco, A., Blackstock, W., Kuznetsov, V., Amati, B., Mapelli, M., & Guccione, E. (2012). Symmetric dimethylation of H3R2 is a newly identified histone mark that supports euchromatin maintenance. Nature structural & molecular biology, 19(2), 136–144.

Miles Cunningham Freezing biological samples. Available online: https://www.leicabiosystems.com/knowledge-pathway/freezing-biological-samples/ [Accessed 17/12/ 2020].

Miranda, T. B., Khusial, P., Cook, J. R., Lee, J., Gunderson, S. I., Pestka, S., Zieve, G. W. & Clarke, S. (2004) Spliceosome sm proteins D1, D3, and B/B′ are asymmetrically dimethylated at arginine residues in the nucleus. Biochemical and Biophysical Research Communications, 323 (2), 382-387.

Mischel, P. S., Shai, R., Shi, T., Horvath, S., Lu, K. V., Choe, G., Seligson, D., Kremen, T. J., Palotie, A., Liau, L. M., Cloughesy, T. F. & Nelson, S. F. (2003) Identification of molecular subtypes of glioblastoma by gene expression profiling. Oncogene, 22 (15), 2361-2373.

Mishra, M., Tiwari, S. & Gomes, A. V. (2017) Protein purification and analysis: Next generation western blotting techniques. Expert Review of Proteomics, 14 (11), 1037-1053.

Mohammadi, A. M., Hawasli, A. H., Rodriguez, A., Schroeder, J. L., Laxton, A. W., Elson, P., Tatter, S. B., Barnett, G. H. & Leuthardt, E. C. (2014) The role of laser interstitial thermal therapy in enhancing progression-free survival of difficult-to-access high-grade gliomas: A multicenter study. Cancer Medicine, 3 (4), 971-979.

Mojas, N., Lopes, M. & Jiricny, J. (2007) Mismatch repair-dependent processing of methylation damage gives rise to persistent single-stranded gaps in newly replicated DNA. Genes & Development, 21 (24), 3342-3355.

Momota, H., Nerio, E., & Holland, E. C. (2005). Perifosine inhibits multiple signaling pathways in glial progenitors and cooperates with temozolomide to arrest cell proliferation in gliomas in vivo. Cancer research, 65(16), 7429–7435.

Mondesir, J., Willekens, C., Touat, M. & de Botton, S. (2016) IDH1 and IDH2 mutations as novel therapeutic targets: Current perspectives. Journal of Blood Medicine, 7 171-180.

Mongiardi, M. P., Savino, M., Bartoli, L., Beji, S., Nanni, S., Scagnoli, F., Falchetti, M. L., Favia, A., Farsetti, A., Levi, A., Nasi, S. & Illi, B. (2015) Myc and omomyc functionally associate with the protein arginine methyltransferase 5 (PRMT5) in glioblastoma cells. Scientific Reports, 5 15494.

Monteith, G. R., Prevarskaya, N. & Roberts-Thomson, S. (2017) The calcium–cancer signalling nexus.

Montenegro, M. F., González-Guerrero, R., Sánchez-del-Campo, L., Piñero-Madrona, A., Cabezas-Herrera, J. & Rodríguez-López, J. N. (2020) PRMT1-dependent methylation of BRCA1 contributes to the epigenetic defense of breast cancer cells against ionizing radiation. Scientific Reports, 10 (1), 13275.

Morales, Y., Cáceres, T., May, K. & Hevel, J. M. (2016) Biochemistry and regulation of the protein arginine methyltransferases (PRMTs). Archives of Biochemistry and Biophysics, 590 138-152.

Morales, Y., Nitzel, D. V., Price, O. M., Gui, S., Li, J., Qu, J. & Hevel, J. M. (2015) Redox control of protein arginine methyltransferase 1 (PRMT1) activity. The Journal of Biological Chemistry, 290 (24), 14915-14926.

Müller, C., Holtschmidt, J., Auer, M., Heitzer, E., Lamszus, K., Schulte, A., Matschke, J., Langer-Freitag, S., Gasch, C., Stoupiec, M., Mauermann, O., Peine, S., Glatzel, M., Speicher, M. R., Geigl, J. B., Westphal, M., Pantel, K. & Riethdorf, S. (2014) Hematogenous dissemination of glioblastoma multiforme. Science Translational Medicine, 6 (247), 247ra101.

Musiani, D., Bok, J., Massignani, E., Wu, L., Tabaglio, T., Ippolito, M. R., Cuomo, A., Ozbek, U., Zorgati, H., Ghoshdastider, U., Robinson, R. C., Guccione, E. & Bonaldi, T. (2019) Proteomics profiling of arginine methylation defines PRMT5 substrate specificity. Science Signaling, 12 (575), eaat8388.

Musiani, D., Giambruno, R., Massignani, E., Ippolito, M. R., Maniaci, M., Jammula, S., Manganaro, D., Cuomo, A., Nicosia, L., Pasini, D. & Bonaldi, T. (2020) PRMT1 is recruited via DNA-PK to chromatin where it sustains the senescence-associated secretory phenotype in response to cisplatin. Cell Reports, 30 (4), 1208-1222.e9.

Nagai, Y., Ji, M. Q., Zhu, F., Xiao, Y., Tanaka, Y., Kambayashi, T., Fujimoto, S., Goldberg, M. M., Zhang, H., Li, B., Ohtani, T. & Greene, M. I. (2019) PRMT5 associates with the FOXP3 homomer and when disabled enhances targeted p185erbB2/neu tumor immunotherapy. Frontiers in Immunology, 10 174.

Nakakido, M., Deng, Z., Suzuki, T., Dohmae, N., Nakamura, Y. & Hamamoto, R. (2015) PRMT6 increases cytoplasmic localization of p21CDKN1A in cancer cells through arginine methylation and makes more resistant to cytotoxic agents. Oncotarget, 6 (31), 30957-30967.

National Institute for Health and Care Excellence (2018) Brain tumours (primary) and brain metastases in adults

NICE guideline [NG99]. Available online: https://www.nice.org.uk/guidance/ng99 [Accessed 09/11/ 2020].

Neault, M., Mallette, F. A., Vogel, G., Michaud-Levesque, J. & Richard, S. (2012) Ablation of PRMT6 reveals a role as a negative transcriptional regulator of the p53 tumor suppressor. Nucleic Acids Research, 40 (19), 9513-9521.

Newcomb, E. W., Cohen, H., Lee, S. R., Bhalla, S. K., Bloom, J., Hayes, R. L. & Miller, D. C. (1998) Survival of patients with glioblastoma multiforme is not influenced by altered expression of P16, P53, EGFR, MDM2 or bcl-2 genes. Brain Pathology, 8 (4), 655-667.

Neyns, B., Sadones, J., Joosens, E., Bouttens, F., Verbeke, L., Baurain, J. -., D'Hondt, L., Strauven, T., Chaskis, C., In't Veld, P., Michotte, A. & De Greve, J. (2009) Stratified phase II trial of cetuximab in patients with recurrent high-grade glioma. Annals of Oncology, 20 (9), 1596-1603.

Ni, H., Wang, K., Xie, P., Zuo, J., Liu, W. & Liu, C. (2020) LncRNA SAMMSON knockdown inhibits the malignancy of glioblastoma cells by inactivation of the PI3K/akt pathway. Cellular and Molecular Neurobiology, .

Nie, M., Wang, Y., Guo, C., Li, X., Wang, Y., Deng, Y., Yao, B., Gui, T., Ma, C., Liu, M., Wang, P., Wang, R., Tan, R., Fang, M., Chen, B., He, Y., Huang, D. C. S., Ju, J. & Zhao, Q. (2018) CARM1-mediated methylation of protein arginine methyltransferase 5 represses human γ-globin gene expression in erythroleukemia cells. The Journal of Biological Chemistry, 293 (45), 17454-17463.

Niyazi, M., Harter, P. N., Hattingen, E., Rottler, M., von Baumgarten, L., Proescholdt, M., Belka, C., Lauber, K. & Mittelbronn, M. (2016) Bevacizumab and radiotherapy for the treatment of glioblastoma: Brothers in arms or unholy alliance? Oncotarget, 7 (3), 2313-2328.

Nonoguchi, N., Ohta, T., Oh, J., Kim, Y., Kleihues, P. & Ohgaki, H. (2013) TERT promoter mutations in primary and secondary glioblastomas. Acta Neuropathologica, 126 (6), 931-937.

Noto, P. B., Sikorski, T. W., Zappacosta, F., Wagner, C. D., Montes de Oca, R., Szapacs, M. E., Annan, R. S., Liu, Y., McHugh, C. F., Mohammad, H. P., Piccoli, S. P. & Creasy, C. L. (2020) Identification of hnRNP-A1 as a pharmacodynamic biomarker of type I PRMT inhibition in blood and tumor tissues. Scientific Reports, 10 (1), 22155.

Obianyo, O., Osborne, T. C. & Thompson, P. R. (2008) Kinetic mechanism of protein arginine methyltransferase 1. Biochemistry, 47 (39), 10420-10427.

Ohgaki, H. & Kleihues, P. (2007) Genetic pathways to primary and secondary glioblastoma. The American Journal of Pathology, 170 5 1445-1453.

Ohgaki, H., Dessen, P., Jourde, B., Horstmann, S., Nishikawa, T., Di Patre, P., Burkhard, C., Schüler, D., Probst-Hensch, N., Maiorka, P. C., Baeza, N., Pisani, P., Yonekawa, Y., Yasargil, M. G., Lütolf, U. M. & Kleihues, P. (2004) Genetic pathways to glioblastoma. Cancer Res, 64 (19), 6892.

Ohgaki, H. & Kleihues, P. (2009) Genetic alterations and signaling pathways in the evolution of gliomas. Cancer Science, 100 (12), 2235-2241.

Ohgaki, H. & Kleihues, P. (2013a) The definition of primary and secondary glioblastoma. Clin Cancer Res, 19 (4), 764.

Ohgaki, H. & Kleihues, P. (2013b) The definition of primary and secondary glioblastoma. Clin Cancer Res, 19 (4), 764.

Olubajo, F., Achawal, S. & Greenman, J. (2020) Development of a microfluidic culture paradigm for ex vivo maintenance of human glioblastoma tissue: A new glioblastoma model? Translational Oncology, 13 (1), 1-10.

Ong, S. & Mann, M. (2006) Identifying and quantifying sites of protein methylation by heavy methyl SILAC. Current Protocols in Protein Science, 46 (1), 14.9.1-14.9.12.

Ono, A., Kanno, H., Hayashi, A., Nishimura, S., Kyuma, Y., Sato, H., Ito, S., Shimizu, N., Chang, C. C., Gondo, G., Yamamoto, I., Sasaki, T., & Tanaka, M. (2007). Collagen gel matrix assay as an in vitro chemosensitivity test for malignant astrocytic tumors. International journal of clinical oncology, 12(2), 125–130.

Onwuli, D., Rigau-Roca, L., Cawthorne, C. & Beltran-Alvarez, P. (2017) Mapping arginine methylation in the human body and cardiac disease. Proteomics.Clinical Applications, 11 (1-2), 10.1002/prca.201600106. Epub 2016 Nov 25.

Oprita, A., Baloi, S., Staicu, G., Alexandru, O., Tache, D. E., Danoiu, S., Micu, E. S. & Sevastre, A. (2021) Updated insights on EGFR signaling pathways in glioma. International Journal of Molecular Sciences, 22 (2), 587.

O'Rourke, D.,M., Nasrallah, M. P., Desai, A., Melenhorst, J. J., Mansfield, K., Morrissette, J. J. D., Martinez-Lage, M., Brem, S., Maloney, E., Shen, A., Isaacs, R., Mohan, S., Plesa, G., Lacey, S. F., Navenot, J., Zheng, Z., Levine, B. L., Okada, H., June, C. H., Brogdon, J. L. & Maus, M. V. (2017) A single dose of peripherally infused EGFRvIII-directed CAR T cells mediates antigen loss and induces adaptive resistance in patients with recurrent glioblastoma. Science Translational Medicine, 9 (399), eaaa0984.

Orrego, E., Castaneda, C. A., Castillo, M., Bernabe, L. A., Casavilca, S., Chakravarti, A., Meng, W., Garcia-Corrochano, P., Villa-Robles, M., Zevallos, R., Mejia, O., Deza, P., Belmar-Lopez, C. & Ojeda, L. (2018) Distribution of tumor-infiltrating immune cells in glioblastoma. CNS Oncology, 7 (4), CNS21.

Ortensi, B., Setti, M., Osti, D. & Pelicci, G. (2013) Cancer stem cell contribution to glioblastoma invasiveness. Stem Cell Research & Therapy, 4 (1), 18.

Ostermann, S., Csajka, C., Buclin, T., Leyvraz, S., Lejeune, F., Decosterd, L. A. & Stupp, R. (2004) Plasma and cerebrospinal fluid population pharmacokinetics of temozolomide in malignant glioma patients. Clin Cancer Res, 10 (11), 3728.

Ostrom, Q. T., Cioffi, G., Gittleman, H., Patil, N., Waite, K., Kruchko, C. & Barnholtz-Sloan, J. (2019) CBTRUS statistical report: Primary brain and other central nervous system tumors diagnosed in the United States in 2012–2016. Neuro-Oncology, 21 v1-v100.

Ostrom, Q. T., Gittleman, H., Fulop, J., Liu, M., Blanda, R., Kromer, C., Wolinsky, Y., Kruchko, C. & Barnholtz-Sloan, J. (2015) CBTRUS statistical report: Primary brain and central nervous system tumors diagnosed in the United States in 2008-2012. Neuro-Oncology, 17 iv1-iv62.

Ostrom, Q. T., Gittleman, H., Truitt, G., Boscia, A., Kruchko, C. & Barnholtz-Sloan, J. (2018) CBTRUS statistical report: Primary brain and other central nervous system tumors diagnosed in the United States in 2011-2015. Neuro-Oncology, 20 iv1-iv86.

Pahlich, S., Zakaryan, R. P. & Gehring, H. (2008) Identification of proteins interacting with protein arginine methyltransferase 8: The ewing sarcoma (EWS) protein binds independent of its methylation state. Proteins: Structure, Function, and Bioinformatics, 72 (4), 1125-1137.

Paik, W. K. & Kim, S. (1967). Enzymatic methylation of protein fractions from calf thymus nuclei. Biochemical and Biophysical Research Communications, 29 (1), 14-20.

Pak, M. L., Lakowski, T. M., Thomas, D., Vhuiyan, M. I., Hüsecken, K. & Frankel, A. (2011) A protein arginine N-methyltransferase 1 (PRMT1) and 2 heteromeric interaction increases PRMT1 enzymatic activity. Biochemistry, 50 (38), 8226-8240.

Pal, S., Baiocchi, R. A., Byrd, J. C., Grever, M. R., Jacob, S. T. & Sif, S. (2007) Low levels of miR-92b/96 induce PRMT5 translation and H3R8/H4R3 methylation in mantle cell lymphoma. The EMBO Journal, 26 (15), 3558-3569.

Pal, S., Vishwanath, S. N., Erdjument-Bromage, H., Tempst, P. & Sif, S. (2004) Human SWI/SNF-associated PRMT5 methylates histone H3 arginine 8 and negatively regulates expression of ST7 and NM23 tumor suppressor genes. Molecular and Cellular Biology, 24 (21), 9630-9645.

Palte, R. L., Schneider, S. E., Altman, M. D., Hayes, R. P., Kawamura, S., Lacey, B. M., Mansueto, M. S., Reutershan, M., Siliphaivanh, P., Sondey, C., Xu, H., Xu, Z., Ye, Y. & Machacek, M. R. (2020) Allosteric modulation of protein arginine methyltransferase 5 (PRMT5). ACS Medicinal Chemistry Letters, 11 (9), 1688-1693.

Panicker, S. P., Raychaudhuri, B., Sharma, P., Tipps, R., Mazumdar, T., Mal, A. K., Palomo, J. M., Vogelbaum, M. A. & Haque, S. J. (2010) p300- and myc-mediated regulation of glioblastoma multiforme cell differentiation. Oncotarget, 1 (4), 289-303.

Panzarini, E., Tacconi, S., Carata, E., Mariano, S., Tata, A. M. & Dini, L. (2020) Molecular characterization of temozolomide-treated and non-temozolomide-treated glioblastoma cells released extracellular vesicles and their role in the macrophage response. International Journal of Molecular Sciences, 21 (21), 8353.

Park, J. H., Szemes, M., Vieira, G. C., Melegh, Z., Malik, S., Heesom, K. J., Von Wallwitz-Freitas, L., Greenhough, A., Brown, K. W., Zheng, Y. G., Catchpoole, D., Deery, M. J. & Malik, K. (2015) Protein arginine methyltransferase 5 is a key regulator of the MYCN oncoprotein in neuroblastoma cells. Molecular Oncology, 9 (3), 617-627.

Park, J., Kwon, M., Kim, K. H., Kim, T., Hong, S., Kim, C. G., Kang, S., Moon, J. H., Kim, E. H., Park, S., Chang, J. H. & Shin, E. (2019) Immune checkpoint inhibitor-induced reinvigoration of tumor-infiltrating CD8+ T cells is determined by their differentiation status in glioblastoma.

Parsons, D. W., Jones, S., Zhang, X., Lin, J. C., Leary, R. J., Angenendt, P., Mankoo, P., Carter, H., Siu, I., Gallia, G. L., Olivi, A., McLendon, R., Rasheed, B. A., Keir, S., Nikolskaya, T., Nikolsky, Y., Busam, D. A., Tekleab, H., Diaz,Luis A.,,Jr, Hartigan, J., Smith, D. R., Strausberg, R. L., Marie, S. K. N., Shinjo, S. M. O., Yan, H., Riggins, G. J., Bigner, D. D., Karchin, R., Papadopoulos, N., Parmigiani, G., Vogelstein, B., Velculescu, V. E. & Kinzler, K. W. (2008) An integrated genomic analysis of human glioblastoma multiforme. Science (New York, N.Y.), 321 (5897), 1807-1812.

Patel, A. P., Tirosh, I., Trombetta, J. J., Shalek, A. K., Gillespie, S. M., Wakimoto, H., Cahill, D. P., Nahed, B. V., Curry, W. T., Martuza, R. L., Louis, D. N., Rozenblatt-Rosen, O., Suvà, M., L., Regev, A. & Bernstein, B. E. (2014) Single-cell RNA-seq highlights intratumoral heterogeneity in primary glioblastoma. Science (New York, N.Y.), 344 (6190), 1396-1401.

Patel, M., McCully, C., Godwin, K. & Balis, F. M. (2003) Plasma and cerebrospinal fluid pharmacokinetics of intravenous temozolomide in non-human primates. Journal of Neuro-Oncology, 61 (3), 203-207.

Patel, N. P., Lyon, K. A. & Huang, J. H. (2019) The effect of race on the prognosis of the glioblastoma patient: A brief review. Neurological Research, 41 (11), 967-971.

Patrizii, M., Bartucci, M., Pine, S. R. & Sabaawy, H. E. (2018) Utility of glioblastoma patient-derived orthotopic xenografts in drug discovery and personalized therapy. Frontiers in Oncology, 8 23.

Pawlak, M. R., Scherer, C. A., Chen, J., Roshon, M. J. & Ruley, H. E. (2000) Arginine N-methyltransferase 1 is required for early postimplantation mouse development, but cells deficient in the enzyme are viable. Molecular and Cellular Biology, 20 (13), 4859-4869.

Pawson, T. (2004) Specificity in signal transduction: From phosphotyrosine-SH2 domain interactions to complex cellular systems. Cell, 116 (2), 191-203.

Pawson, T. & Gish, G. D. (1992) SH2 and SH3 domains: From structure to function. Cell, 71 (3), 359-362.

Pegg, A. E., Dolan, M. E. & Moschel, R. C. (1995) Structure, function, and inhibition of O6-alkylguanine-DNA alkyltransferase. In Waldo E. Cohn and Kivie Moldave (eds) Progress in nucleic acid research and molecular biology. Academic Press, 167-223.

Pekmezci, M., Rice, T., Molinaro, A. M., Walsh, K. M., Decker, P. A., Hansen, H., Sicotte, H., Kollmeyer, T. M., McCoy, L. S., Sarkar, G., Perry, A., Giannini, C., Tihan, T., Berger, M. S., Wiemels, J. L., Bracci, P. M., Eckel-Passow, J., Lachance, D. H., Clarke, J., Taylor, J. W., Luks, T., Wiencke, J. K., Jenkins, R. B. & Wrensch, M. R. (2017) Adult infiltrating gliomas with WHO 2016 integrated diagnosis: Additional prognostic roles of ATRX and TERT. Acta Neuropathologica, 133 (6), 1001-1016.

Penney, J., Seo, J., Kritskiy, O., Elmsaouri, S., Gao, F., Pao, P., Su, S. C. & Tsai, L. (2017) Loss of protein arginine methyltransferase 8 alters synapse composition and function, resulting in behavioral defects. The Journal of Neuroscience, 37 (36), 8655.

Perrot, V. & Rechler, M. M. (2005) The coactivator p300 directly acetylates the forkhead transcription factor Foxo1 and stimulates Foxo1-induced transcription. Molecular Endocrinology (Baltimore, Md.), 19 (9), 2283-2298.

Peruzzi, P. & Chiocca, E. A. (2018) Viruses in cancer therapy - from benchwarmers to quarterbacks. Nature Reviews.Clinical Oncology, 15 (11), 657-658.

Phillips, H. S., Kharbanda, S., Chen, R., Forrest, W. F., Soriano, R. H., Wu, T. D., Misra, A., Nigro, J. M., Colman, H., Soroceanu, L., Williams, P. M., Modrusan, Z., Feuerstein, B. G. & Aldape, K. (2006) Molecular subclasses of high-grade glioma predict prognosis, delineate a pattern of disease progression, and resemble stages in neurogenesis. Cancer Cell, 9 (3), 157-173.

Plotnikov, A., Kozer, N., Cohen, G., Carvalho, S., Duberstein, S., Almog, O., Solmesky, L. J., Shurrush, K. A., Babaev, I., Benjamin, S., Gilad, S., Kupervaser, M., Levin, Y., Gershovits, M., Ben-Avraham, D. & Barr, H. M. (2020) PRMT1 inhibition induces differentiation of colon cancer cells. Scientific Reports, 10 (1), 20030.

Pollack, B. P., Kotenko, S. V., He, W., Izotova, L. S., Barnoski, B. L. & Pestka, S. (1999) The human homologue of the yeast proteins Skb1 and Hsl7p interacts with jak kinases and contains protein methyltransferase activity. Journal of Biological Chemistry, 274 (44), 31531-31542.

Popovici-Muller, J., Lemieux, R. M., Artin, E., Saunders, J. O., Salituro, F. G., Travins, J., Cianchetta, G., Cai, Z., Zhou, D., Cui, D., Chen, P., Straley, K., Tobin, E., Wang, F., David, M. D., Penard-Lacronique, V., Quivoron, C., Saada, V., de Botton, S., Gross, S., Dang, L., Yang, H., Utley, L., Chen, Y., Kim, H., Jin, S., Gu, Z., Yao, G., Luo, Z., Lv, X., Fang, C., Yan, L., Olaharski, A., Silverman, L., Biller, S., Su, S. M. & Yen, K. (2018) Discovery of AG-120 (ivosidenib): A first-in-class mutant IDH1 inhibitor for the treatment of IDH1 mutant cancers. ACS Medicinal Chemistry Letters, 9 (4), 300-305.

Prabhu, S., Goda, J. S., Mutalik, S., Mohanty, B. S., Chaudhari, P., Rai, S., Udupa, N. & Rao, B. S. S. (2017) A polymeric temozolomide nanocomposite against orthotopic glioblastoma xenograft: Tumor-specific homing directed by nestin. Nanoscale, 9 (30), 10919-10932.

Prados, M. D., Chang, S. M., Butowski, N., DeBoer, R., Parvataneni, R., Carliner, H., Kabuubi, P., Ayers-Ringler, J., Rabbitt, J., Page, M., Fedoroff, A., Sneed, P. K., Berger, M. S., McDermott, M. W., Parsa, A. T., Vandenberg, S., James, C. D., Lamborn, K. R., Stokoe, D. & Haas-Kogan, D. (2009) Phase II study of erlotinib plus temozolomide during and after radiation therapy in patients with newly diagnosed glioblastoma multiforme or gliosarcoma. Journal of Clinical Oncology : Official Journal of the American Society of Clinical Oncology, 27 (4), 579-584.

Primon, M., Huszthy, P. C., Motaln, H., Talasila, K. M., Torkar, A., Bjerkvig, R. & Lah Turnšek, T. (2013) Cathepsin L silencing enhances arsenic trioxide mediated in vitro cytotoxicity and apoptosis in glioblastoma U87MG spheroids. Experimental Cell Research, 319 (17), 2637-2648.

Qamar, S., Wang, G., Randle, S. J., Ruggeri, F. S., Varela, J. A., Lin, J. Q., Phillips, E. C., Miyashita, A., Williams, D., Ströhl, F., Meadows, W., Ferry, R., Dardov, V. J., Tartaglia, G. G., Farrer, L. A., Kaminski Schierle, G.,S., Kaminski, C. F., Holt, C. E., Fraser, P. E., Schmitt-Ulms, G., Klenerman, D., Knowles, T., Vendruscolo, M. & St George-Hyslop, P. (2018) FUS phase separation is modulated by a molecular chaperone and methylation of arginine cation-π interactions. Cell, 173 (3), 720-734.e15.

Qi, C., Chang, J., Zhu, Y., Yeldandi, A. V., Rao, S. M. & Zhu, Y. (2002) Identification of protein arginine methyltransferase 2 as a coactivator for estrogen receptor α. Journal of Biological Chemistry, 277 (32), 28624-28630.

Rademakers, R., Stewart, H., Dejesus-Hernandez, M., Krieger, C., Graff-Radford, N., Fabros, M., Briemberg, H., Cashman, N., Eisen, A. & Mackenzie, I. R. A. (2010) Fus gene mutations in familial and sporadic amyotrophic lateral sclerosis. Muscle & Nerve, 42 (2), 170-176.

Radzisheuskaya, A., Shliaha, P. V., Grinev, V., Lorenzini, E., Kovalchuk, S., Shlyueva, D., Gorshkov, V., Hendrickson, R. C., Jensen, O. N. & Helin, K. (2019) PRMT5 methylome profiling uncovers a direct link

to splicing regulation in acute myeloid leukemia. Nature Structural & Molecular Biology, 26 (11), 999-1012.

Raizer, J. J., Abrey, L. E., Lassman, A. B., Chang, S. M., Lamborn, K. R., Kuhn, J. G., Yung, W. K. A., Gilbert, M. R., Aldape, K. A., Wen, P. Y., Fine, H. A., Mehta, M., Deangelis, L. M., Lieberman, F., Cloughesy, T. F., Robins, H. I., Dancey, J., Prados, M. D. & North American Brain, Tumor Consortium (2010) A phase II trial of erlotinib in patients with recurrent malignant gliomas and nonprogressive glioblastoma multiforme postradiation therapy. Neuro-Oncology, 12 (1), 95-103.

Rajpurohit, R., Lee, S. O., Park, J. O., Paik, W. K. & Kim, S. (1994) Enzymatic methylation of recombinant heterogeneous nuclear RNP protein A1. dual substrate specificity for S-adenosylmethionine:Histone-arginine N-methyltransferase. The Journal of Biological Chemistry, 269 (2), 1075-1082.

Rampling, R., Peoples, S., Mulholland, P. J., James, A., Al-Salihi, O., Twelves, C. J., McBain, C., Jefferies, S., Jackson, A., Stewart, W., Lindner, J., Kutscher, S., Hilf, N., McGuigan, L., Peters, J., Hill, K., Schoor, O., Singh-Jasuja, H., Halford, S. E. & Ritchie, J. W. A. (2016) A cancer research UK first time in human phase I trial of IMA950 (novel multipeptide therapeutic vaccine) in patients with newly diagnosed glioblastoma. Clinical Cancer Research : An Official Journal of the American Association for Cancer Research, 22 (19), 4776-4785.

Rao, S. K., Edwards, J., Joshi, A. D., Siu, I. & Riggins, G. J. (2010) A survey of glioblastoma genomic amplifications and deletions. Journal of Neuro-Oncology, 96 (2), 169-179.

Rappsilber, J., Ajuh, P., Lamond, A. I., & Mann, M. (2001). SPF30 is an essential human splicing factor required for assembly of the U4/U5/U6 tri-small nuclear ribonucleoprotein into the spliceosome. The Journal of biological chemistry, 276(33), 31142–31150.

Rappsilber, J., Friesen, W. J., Paushkin, S., Dreyfuss, G. & Mann, M. (2003) Detection of arginine dimethylated peptides by parallel precursor ion scanning mass spectrometry in positive ion mode. Analytical Chemistry, 75 (13), 3107-3114.

Raymond, E., Brandes, A. A., Dittrich, C., Fumoleau, P., Coudert, B., Clement, P. M. J., Frenay, M., Rampling, R., Stupp, R., Kros, J. M., Heinrich, M. C., Gorlia, T., Lacombe, D., van den Bent, M.,J. & European Organisation for Research and Treatment of Cancer Brain Tumor, Group Study. (2008) Phase II study of imatinib in patients with recurrent gliomas of various histologies: A european organisation for research and treatment of cancer brain tumor group study. American Society of Clinical Oncology.

Rehman, I., Basu, S. M., Das, S. K., Bhattacharjee, S., Ghosh, A., Pommier, Y. & Das, B. B. (2018) PRMT5-mediated arginine methylation of TDP1 for the repair of topoisomerase I covalent complexes. Nucleic Acids Research, 46 (11), 5601-5617.

Reilly, K. M., Loisel, D. A., Bronson, R. T., McLaughlin, M. E., & Jacks, T. (2000). Nf1;Trp53 mutant mice develop glioblastoma with evidence of strain-specific effects. Nature genetics, 26(1), 109–113.

Reintjes, A., Fuchs, J. E., Kremser, L., Lindner, H. H., Liedl, K. R., Huber, L. A. & Valovka, T. (2016) Asymmetric arginine dimethylation of RelA provides a repressive mark to modulate TNFα/NF-κB response. Proceedings of the National Academy of Sciences of the United States of America, 113 (16), 4326-4331.

Reiss, S. N., Yerram, P., Modelevsky, L. & Grommes, C. (2017) Retrospective review of safety and efficacy of programmed cell death-1 inhibitors in refractory high grade gliomas. BioMed Central.

Reithmeier, T., Graf, E., Piroth, T., Trippel, M., Pinsker, M. O. & Nikkhah, G. (2010) BCNU for recurrent glioblastoma multiforme: Efficacy, toxicity and prognostic factors. BMC Cancer, 10 (1), 30.

Reuter, M., Chuma, S., Tanaka, T., Franz, T., Stark, A., & Pillai, R. S. (2009). Loss of the Mili-interacting Tudor domain-containing protein-1 activates transposons and alters the Mili-associated small RNA profile. Nature structural & molecular biology, 16(6), 639–646.

Riehle, R. D., Cornea, S. & Degterev, A. (2013) Role of phosphatidylinositol 3,4,5-trisphosphate in cell signaling. In Daniel G. S. Capelluto (ed) Lipid-mediated protein signaling. Dordrecht: Springer Netherlands, 105-139.

Riley, A., Green, V., Cheah, R., McKenzie, G., Karsai, L., England, J. & Greenman, J. (2019) A novel microfluidic device capable of maintaining functional thyroid carcinoma specimens ex vivo provides a new drug screening platform. BMC Cancer, 19 (1), 259.

Rivlin, N., Brosh, R., Oren, M. & Rotter, V. (2011) Mutations in the p53 tumor suppressor gene: Important milestones at the various steps of tumorigenesis. Genes & Cancer, 2 (4), 466-474.

Robin-Lespinasse, Y., Sentis, S., Kolytcheff, C., Rostan, M., Corbo, L. & Le Romancer, M. (2007) hCAF1, a new regulator of PRMT1-dependent arginine methylation. Journal of Cell Science, 120 (4), 638.

Rottenberg, D. A., Ginos, J. Z., Kearfott, K. J., Junck, L. & Bigner, D. D. (1984) In vivo measurement of regional brain tissue pH using positron emission tomography. Annals of Neurology, 15 98-102.

Rust, H. L., Subramanian, V., West, G. M., Young, D. D., Schultz, P. G. & Thompson, P. R. (2014) Using unnatural amino acid mutagenesis to probe the regulation of PRMT1. ACS Chemical Biology, 9 (3), 649-655.

Rusten, T. E. & Stenmark, H. (2010) P62, an autophagy hero or culprit? Nature Cell Biology, 12 (3), 207-209.

Rusthoven, C. G., Carlson, J. A., Waxweiler, T. V., Dally, M. J., Barón, A. E., Yeh, N., Gaspar, L. E., Liu, A. K., Ney, D. E., Damek, D. M., Lillehei, K. O. & Kavanagh, B. D. (2014) The impact of adjuvant radiation therapy for high-grade gliomas by histology in the United States population. International Journal of Radiation Oncology • Biology • Physics, 90 (4), 894-902.

Saenz-Antoñanzas, A., Auzmendi-Iriarte, J., Carrasco-Garcia, E., Moreno-Cugnon, L., Ruiz, I., Villanua, J., Egaña, L., Otaegui, D., Samprón, N. & Matheu, A. (2019) Liquid biopsy in glioblastoma: Opportunities, applications and challenges. Cancers, 11 (7), 950.

Sachamitr, P., Ho, J. C., Ciamponi, F. E., Ba-Alawi, W., Coutinho, F. J., Guilhamon, P., Kushida, M. M., Cavalli, F., Lee, L., Rastegar, N., Vu, V., Sánchez-Osuna, M., Coulombe-Huntington, J., Kanshin, E., Whetstone, H., Durand, M., Thibault, P., Hart, K., Mangos, M., Veyhl, J., … Dirks, P. B. (2021). PRMT5 inhibition disrupts splicing and stemness in glioblastoma. Nature communications, 12(1), 979.

Sahm, F., Capper, D., Jeibmann, A., Habel, A., Paulus, W., Troost, D. & von Deimling, A. (2012) Addressing diffuse glioma as a systemic brain disease with single-cell analysis. Archives of Neurology, 69 (4), 523-526.

Said, M. Y., Bollenbach, A., Minović, I., van Londen, M., Frenay, A. R., de Borst, M. H., van den Berg, E., Kayacelebi, A. A., Tsikas, D., van Goor, H., Navis, G. & Bakker, S. J. L. (2019) Plasma ADMA, urinary ADMA excretion, and late mortality in renal transplant recipients. Amino Acids, 51 (6), 913-927.

Samson, A., Scott, K. J., Taggart, D., West, E. J., Wilson, E., Nuovo, G. J., Thomson, S., Corns, R., Mathew, R. K., Fuller, M. J., Kottke, T. J., Thompson, J. M., Ilett, E. J., Cockle, J. V., van Hille, P., Sivakumar, G., Polson, E. S., Turnbull, S. J., Appleton, E. S., Migneco, G., Rose, A. S., Coffey, M. C., Beirne, D. A., Collinson, F. J., Ralph, C., Alan Anthoney, D., Twelves, C. J., Furness, A. J., Quezada, S. A., Wurdak, H., Errington-Mais, F., Pandha, H., Harrington, K. J., Selby, P. J., Vile, R. G., Griffin, S. D., Stead, L. F., Short, S. C. & Melcher, A. A. (2018) Intravenous delivery of oncolytic reovirus to brain tumor patients immunologically primes for subsequent checkpoint blockade. Science Translational Medicine, 10 (422), eaam7577.

Sarbassov, D. D., Guertin, D. A., Ali, S. M. & Sabatini, D. M. (2005) Phosphorylation and regulation of akt/PKB by the rictor-mTOR complex. Science, 307 (5712), 1098.

Sayegh, J., Webb, K., Cheng, D., Bedford, M. T. & Clarke, S. G. (2007) Regulation of protein arginine methyltransferase 8 (PRMT8) activity by its N-terminal domain. Journal of Biological Chemistry, 282 (50), 36444-36453.

Scaglione, A., Patzig, J., Liang, J., Frawley, R., Bok, J., Mela, A., Yattah, C., Zhang, J., Teo, S. X., Zhou, T., Chen, S., Bernstein, E., Canoll, P., Guccione, E. & Casaccia, P. (2018) PRMT5-mediated regulation of developmental myelination. Nature Communications, 9 (1), 2840.

Schäfer, N., Gielen, G. H., Rauschenbach, L., Kebir, S., Till, A., Reinartz, R., Simon, M., Niehusmann, P., Kleinschnitz, C., Herrlinger, U., Pietsch, T., Scheffler, B. & Glas, M. (2019) Longitudinal heterogeneity in glioblastoma: Moving targets in recurrent versus primary tumors. Journal of Translational Medicine, 17 (1), 96.

Schapira, M. & Ferreira de Freitas, R. (2014) Structural biology and chemistry of protein arginine methyltransferases. MedChemComm, 5 (12), 1779-1788.

Schiff, D., Lee, E. Q., Nayak, L., Norden, A. D., Reardon, D. A. & Wen, P. Y. (2015) Medical management of brain tumors and the sequelae of treatment. Neuro-Oncology, 17 (4), 488-504.

Schurter, B. T., Koh, S. S., Chen, D., Bunick, G. J., Harp, J. M., Hanson, B. L., Henschen-Edman, A., Mackay, D. R., Stallcup, M. R. & Aswad, D. W. (2001) Methylation of histone H3 by coactivator-associated arginine methyltransferase 1. Biochemistry, 40 (19), 5747-5756.

Schuster, J., Lai, R. K., Recht, L. D., Reardon, D. A., Paleologos, N. A., Groves, M. D., Mrugala, M. M., Jensen, R., Baehring, J. M., Sloan, A., Archer, G. E., Bigner, D. D., Cruickshank, S., Green, J. A., Keler, T., Davis, T. A., Heimberger, A. B. & Sampson, J. H. (2015) A phase II, multicenter trial of rindopepimut (CDX-110) in newly diagnosed glioblastoma: The ACT III study. Neuro-Oncology, 17 (6), 854-861.

Scott, H. S., Antonarakis, S. E., Lalioti, M. D., Rossier, C., Silver, P. A. & Henry, M. F. (1998) Identification and characterization of two putative human arginine methyltransferases (HRMT1L1 and HRMT1L2). Genomics, 48 (3), 330-340.

Segelman, J., Granath, F., Holm, T., Machado, M., Mahteme, H. & Martling, A. (2012) Incidence, prevalence and risk factors for peritoneal carcinomatosis from colorectal cancer. The British Journal of Surgery, 99 (5), 699-705.

Selvi, B. R., Swaminathan, A., Maheshwari, U., Nagabhushana, A., Mishra, R. K. & Kundu, T. K. (2015) CARM1 regulates astroglial lineage through transcriptional regulation of nanog and posttranscriptional regulation by miR92a. Molecular Biology of the Cell, 26 (2), 316-326.

Shackleton, M., Quintana, E., Fearon, E. R. & Morrison, S. J. (2009) Heterogeneity in cancer: Cancer stem cells versus clonal evolution. Cell, 138 (5), 822-829.

Shankar, G. M., Balaj, L., Stott, S. L., Nahed, B. & Carter, B. S. (2017) Liquid biopsy for brain tumors. Expert Review of Molecular Diagnostics, 17 (10), 943-947.

Shao, H., Chung, J., Balaj, L., Charest, A., Bigner, D. D., Carter, B. S., Hochberg, F. H., Breakefield, X. O., Weissleder, R. & Lee, H. (2012) Protein typing of circulating microvesicles allows real-time monitoring of glioblastoma therapy. Nature Medicine, 18 (12), 1835-1840.

Shao, H., Chung, J., Lee, K., Balaj, L., Min, C., Carter, B. S., Hochberg, F. H., Breakefield, X. O., Lee, H. & Weissleder, R. (2015) Chip-based analysis of exosomal mRNA mediating drug resistance in glioblastoma. Nature Communications, 6 6999.

Shao, L., Zhang, X. & Yao, Q. (2020) The F-box protein FBXO11 restrains hepatocellular carcinoma stemness via promotion of ubiquitin-mediated degradation of snail. FEBS Open Bio, n/a .

Shih, A. H., Dai, C., Hu, X., Rosenblum, M. K., Koutcher, J. A., & Holland, E. C. (2004). Dose-dependent effects of platelet-derived growth factor-B on glial tumorigenesis. Cancer research, 64(14), 4783–4789.

Shin, H. R., Kim, H., Oh, S., Lee, J., Kee, M., Ko, H., Kweon, M., Won, K. & Baek, S. H. (2016) AMPK–SKP2–CARM1 signalling cascade in transcriptional regulation of autophagy. Nature, 534 (7608), 553-557.

Simandi, Z., Czipa, E., Horvath, A., Koszeghy, A., Bordas, C., Póliska, S., Juhász, I., Imre, L., Szabó, G., Dezso, B., Barta, E., Sauer, S., Karolyi, K., Kovacs, I., Hutóczki, G., Bognár, L., Klekner, Á, Szucs, P., Bálint, B. L. & Nagy, L. (2015) PRMT1 and PRMT8 regulate retinoic acid-dependent neuronal differentiation with implications to neuropathology. Stem Cells, 33 (3), 726-741.

Simandi, Z., Pajer, K., Karolyi, K., Sieler, T., Jiang, L., Kolostyak, Z., Sari, Z., Fekecs, Z., Pap, A., Patsalos, A., Contreras, G. A., Reho, B., Papp, Z., Guo, X., Horvath, A., Kiss, G., Keresztessy, Z., Vámosi, G., Hickman, J., Xu, H., Dormann, D., Hortobagyi, T., Antal, M., Nógrádi, A. & Nagy, L. (2018) Arginine methyltransferase PRMT8 provides cellular stress tolerance in aging motoneurons. The Journal of Neuroscience : The Official Journal of the Society for Neuroscience, 38 (35), 7683-7700.

Simpson, J. R., Horton, J., Scott, C., Curran, W. J., Rubin, P., Fischbach, J., Isaacson, S., Rotman, M., Asbell, S. O. & Nelson, J. S. (1993) Influence of location and extent of surgical resection on survival of patients with glioblastoma multiforme: Results of three consecutive radiation therapy oncology group (RTOG) clinical trials. International Journal of Radiation Oncology, Biology, Physics, 26 (2), 239-244.

Sims, R. J., 3rd, Rojas, L. A., Beck, D. B., Bonasio, R., Schüller, R., Drury, W. J., 3rd, Eick, D., & Reinberg, D. (2011). The C-terminal domain of RNA polymerase II is modified by site-specific methylation. Science (New York, N.Y.), 332(6025), 99–103.

Singh, V., Miranda, T. B., Jiang, W., Frankel, A., Roemer, M. E., Robb, V. A., Gutmann, D. H., Herschman, H. R., Clarke, S. & Newsham, I. F. (2004) DAL-1/4.1B tumor suppressor interacts with protein arginine N-methyltransferase 3 (PRMT3) and inhibits its ability to methylate substrates in vitro and in vivo. Oncogene, 23 (47), 7761-7771.

Singhroy, D. N., Mesplède, T., Sabbah, A., Quashie, P. K., Falgueyret, J. & Wainberg, M. A. (2013) Automethylation of protein arginine methyltransferase 6 (PRMT6) regulates its stability and its anti-HIV-1 activity. Retrovirology, 10 73.

Smil, D., Eram, M. S., Li, F., Kennedy, S., Szewczyk, M. M., Brown, P. J., Barsyte-Lovejoy, D., Arrowsmith, C. H., Vedadi, M. & Schapira, M. (2015) Discovery of a dual PRMT5-PRMT7 inhibitor. ACS Medicinal Chemistry Letters, 6 (4), 408-412.

Smith, J. S., Perry, A., Borell, T. J., Lee, H. K., O'Fallon, J., Hosek, S. M., Kimmel, D., Yates, A., Burger, P. C., Scheithauer, B. W. & Jenkins, R. B. (2000) Alterations of chromosome arms 1p and 19q as predictors of survival in oligodendrogliomas, astrocytomas, and mixed oligoastrocytomas. Jco, 18 (3), 636.

Smith, J. S., Tachibana, I., Passe, S. M., Huntley, B. K., Borell, T. J., Iturria, N., O'Fallon, J. R., Schaefer, P. L., Scheithauer, B. W., James, C. D., Buckner, J. C. & Jenkins, R. B. (2001) PTEN mutation, EGFR amplification, and outcome in patients with anaplastic astrocytoma and glioblastoma multiforme. JNCI: Journal of the National Cancer Institute, 93 (16), 1246-1256.

Snyder, H., Robinson, K., Shah, D., Brennan, R. & Handrigan, M. (1993) Signs and symptoms of patients with brain tumors presenting to the emergency department. Journal of Emergency Medicine, 11 (3), 253-258.

Solomón, M. T., Selva, J. C., Figueredo, J., Vaquer, J., Toledo, C., Quintanal, N., Salva, S., Domíngez, R., Alert, J., Marinello, J. J., Catalá, M., Griego, M. G., Martell, J. A., Luaces, P. L., Ballesteros, J., de-

Castro, N., Bach, F. & Crombet, T. (2013) Radiotherapy plus nimotuzumab or placebo in the treatment of high grade glioma patients: Results from a randomized, double blind trial. BMC Cancer, 13 (1), 299.

Sottoriva, A., Spiteri, I., Piccirillo, S. G. M., Touloumis, A., Collins, V. P., Marioni, J. C., Curtis, C., Watts, C. & Tavaré, S. (2013) Intratumor heterogeneity in human glioblastoma reflects cancer evolutionary dynamics. Proceedings of the National Academy of Sciences of the United States of America, 110 (10), 4009-4014.

Spadotto, V., Giambruno, R., Massignani, E., Mihailovich, M., Maniaci, M., Patuzzo, F., Ghini, F., Nicassio, F. & Bonaldi, T. (2020) PRMT1-mediated methylation of the microprocessor-associated proteins regulates microRNA biogenesis. Nucleic Acids Research, 48 (1), 96-115.

Spannhoff, A., Heinke, R., Bauer, I., Trojer, P., Metzger, E., Gust, R., Schüle, R., Brosch, G., Sippl, W. & Jung, M. (2007) Target-based approach to inhibitors of histone arginine methyltransferases. Journal of Medicinal Chemistry, 50 (10), 2319-2325.

Spannhoff, A., Machmur, R., Heinke, R., Trojer, P., Bauer, I., Brosch, G., Schüle, R., Hanefeld, W., Sippl, W. & Jung, M. (2007) A novel arginine methyltransferase inhibitor with cellular activity. Bioorganic & Medicinal Chemistry Letters, 17 (15), 4150-4153.

Steeg, P. S. (2016) Targeting metastasis. Nature Reviews Cancer, 16 (4), 201-218.

Stommel, J. M., Kimmelman, A. C., Ying, H., Nabioullin, R., Ponugoti, A. H., Wiedemeyer, R., Stegh, A. H., Bradner, J. E., Ligon, K. L., Brennan, C., Chin, L. & DePinho, R. A. (2007) Coactivation of receptor tyrosine kinases affects the response of tumor cells to targeted therapies.

Stringer, B. W., Day, B. W., D'Souza, R. C. J., Jamieson, P. R., Ensbey, K. S., Bruce, Z. C., Lim, Y. C., Goasdoué, K., Offenhäuser, C., Akgül, S., Allan, S., Robertson, T., Lucas, P., Tollesson, G., Campbell, S., Winter, C., Do, H., Dobrovic, A., Inglis, P., Jeffree, R. L., Johns, T. G. & Boyd, A. W. (2019) A reference collection of patient-derived cell line and xenograft models of proneural, classical and mesenchymal glioblastoma. Scientific Reports, 9 (1), 4902.

Stupp, R., Hegi, M. E., Mason, W. P., van den Bent, M.,J., Taphoorn, M. J. B., Janzer, R. C., Ludwin, S. K., Allgeier, A., Fisher, B., Belanger, K., Hau, P., Brandes, A. A., Gijtenbeek, J., Marosi, C., Vecht, C. J., Mokhtari, K., Wesseling, P., Villa, S., Eisenhauer, E., Gorlia, T., Weller, M., Lacombe, D., Cairncross, J. G. & Mirimanoff, R. (2009) Effects of radiotherapy with concomitant and adjuvant temozolomide versus radiotherapy alone on survival in glioblastoma in a randomised phase III study: 5-year analysis of the EORTC-NCIC trial. The Lancet Oncology, 10 (5), 459-466.

Stupp, R., Mason, W. P., van den Bent, Martin J., Weller, M., Fisher, B., Taphoorn, M. J. B., Belanger, K., Brandes, A. A., Marosi, C., Bogdahn, U., Curschmann, J., Janzer, R. C., Ludwin, S. K., Gorlia, T., Allgeier, A., Lacombe, D., Cairncross, J. G., Eisenhauer, E. & Mirimanoff, R. O. (2005) Radiotherapy plus concomitant and adjuvant temozolomide for glioblastoma. N Engl J Med, 352 (10), 987-996.

Stupp, R., Taillibert, S., Kanner, A., Read, W., Steinberg, D., Lhermitte, B., Toms, S., Idbaih, A., Ahluwalia, M. S., Fink, K., Di Meco, F., Lieberman, F., Zhu, J., Stragliotto, G., Tran, D., Brem, S., Hottinger, A., Kirson, E. D., Lavy-Shahaf, G., Weinberg, U., Kim, C., Paek, S., Nicholas, G., Bruna, J., Hirte, H., Weller, M., Palti, Y., Hegi, M. E. & Ram, Z. (2017) Effect of tumor-treating fields plus maintenance temozolomide vs maintenance temozolomide alone on survival in patients with glioblastoma: A randomized clinical trial. Jama, 318 (23), 2306-2316.

Stupp, R., Wong, E. T., Kanner, A. A., Steinberg, D., Engelhard, H., Heidecke, V., Kirson, E. D., Taillibert, S., Liebermann, F., Dbalý, V., Ram, Z., Villano, J. L., Rainov, N., Weinberg, U., Schiff, D., Kunschner, L., Raizer, J., Honnorat, J., Sloan, A., Malkin, M., Landolfi, J. C., Payer, F., Mehdorn, M., Weil, R. J., Pannullo, S. C., Westphal, M., Smrcka, M., Chin, L., Kostron, H., Hofer, S., Bruce, J., Cosgrove, R., Paleologous, N., Palti, Y. & Gutin, P. H. (2012) NovoTTF-100A versus physician's choice chemotherapy in recurrent glioblastoma: A randomised phase III trial of a novel treatment modality. European Journal of Cancer, 48 (14), 2192-2202.

Su, X., Zhu, G., Ding, X., Lee, S. Y., Dou, Y., Zhu, B., Wu, W. & Li, H. (2014) Molecular basis underlying histone H3 lysine-arginine methylation pattern readout by spin/ssty repeats of Spindlin1. Genes & Development, 28 (6), 622-636.

Suchorska, B., Weller, M., Tabatabai, G., Senft, C., Hau, P., Sabel, M. C., Herrlinger, U., Ketter, R., Schlegel, U., Marosi, C., Reifenberger, G., Wick, W., Tonn, J. & Wirsching, H. (2016) Complete resection of contrast-enhancing tumor volume is associated with improved survival in recurrent glioblastoma-results from the DIRECTOR trial. Neuro-Oncology, 18 (4), 549-556.

Suire, S., Hawkins, P. & Stephens, L. (2002) Activation of phosphoinositide 3-kinase γ by ras. Current Biology, 12 (13), 1068-1075.

Sun, T., Plutynski, A., Ward, S. & Rubin, J. B. (2015) An integrative view on sex differences in brain tumors. Cellular and Molecular Life Sciences : CMLS, 72 (17), 3323-3342.

Sun, T., Warrington, N. M., Luo, J., Brooks, M. D., Dahiya, S., Snyder, S. C., Sengupta, R., & Rubin, J. B. (2014). Sexually dimorphic RB inactivation underlies mesenchymal glioblastoma prevalence in males. The Journal of clinical investigation, 124(9), 4123–4133.

Suzuki, H., Aoki, K., Chiba, K. et al. (2015) Mutational landscape and clonal architecture in grade II and III gliomas. Nature Genetics, 47, 458–468.

Swiercz, R., Cheng, D., Kim, D. & Bedford, M. T. (2007) Ribosomal protein rpS2 is hypomethylated in PRMT3-deficient mice. Journal of Biological Chemistry, 282 (23), 16917-16923.

Szewczyk, M. M., Ishikawa, Y., Organ, S., Sakai, N., Li, F., Halabelian, L., Ackloo, S., Couzens, A. L., Eram, M., Dilworth, D., Fukushi, H., Harding, R., dela Seña, C. C., Sugo, T., Hayashi, K., McLeod, D., Zepeda, C., Aman, A., Sánchez-Osuna, M., Bonneil, E., Takagi, S., Al-Awar, R., Tyers, M., Richard, S., Takizawa, M., Gingras, A., Arrowsmith, C. H., Vedadi, M., Brown, P. J., Nara, H. & Barsyte-Lovejoy, D. (2020) Pharmacological inhibition of PRMT7 links arginine monomethylation to the cellular stress response. Nature Communications, 11 (1), 2396.

Szewczyk, M. M., Ishikawa, Y., Organ, S., Sakai, N., Li, F., Halabelian, L., Ackloo, S., Couzens, A. L., Eram, M., Dilworth, D., Fukushi, H., Harding, R., Dela Seña, C.,C., Sugo, T., Hayashi, K., McLeod, D., Zepeda, C., Aman, A., Sánchez-Osuna, M., Bonneil, E., Takagi, S., Al-Awar, R., Tyers, M., Richard, S., Takizawa, M., Gingras, A., Arrowsmith, C. H., Vedadi, M., Brown, P. J., Nara, H. & Barsyte-Lovejoy, D. (2020) Pharmacological inhibition of PRMT7 links arginine monomethylation to the cellular stress response. Nature Communications, 11 (1), 2396.

Taal, W., Oosterkamp, H. M., Walenkamp, A. M. E., Dubbink, H. J., Beerepoot, L. V., Hanse, M. C. J., Buter, J., Honkoop, A. H., Boerman, D., de Vos, F.,Y.F., Dinjens, W. N. M., Enting, R. H., Taphoorn, M. J. B., van den Berkmortel, F.,W.P.J., Jansen, R. L. H., Brandsma, D., Bromberg, J. E. C., van Heuvel, I., Vernhout, R. M., van der Holt, B. & van den Bent, M.,J. (2014) Single-agent bevacizumab or lomustine versus a combination of bevacizumab plus lomustine in patients with recurrent glioblastoma (BELOB trial): A randomised controlled phase 2 trial. The Lancet Oncology, 15 (9), 943-953.

Takai, H., Masuda, K., Sato, T., Sakaguchi, Y., Suzuki, T., Suzuki, T., Koyama-Nasu, R., Nasu-Nishimura, Y., Katou, Y., Ogawa, H., Morishita, Y., Kozuka-Hata, H., Oyama, M., Todo, T., Ino, Y., Mukasa, A., Saito, N., Toyoshima, C., Shirahige, K. & Akiyama, T. (2014) 5-hydroxymethylcytosine plays a critical role in glioblastomagenesis by recruiting the CHTOP-methylosome complex. Cell Reports, 9 (1), 48-60.

Takano, S., Yoshii, Y., Kondo, S., Suzuki, H., Maruno, T., Shirai, S. & Nose, T. (1996) Concentration of vascular endothelial growth factor in the serum and tumor tissue of brain tumor patients. Cancer Res, 56 (9), 2185.

Tang, J., Frankel, A., Cook, R. J., Kim, S., Paik, W. K., Williams, K. R., Clarke, S. & Herschman, H. R. (2000) PRMT1 is the predominant type I protein arginine methyltransferase in mammalian cells.

Tang, J., Gary, J. D., Clarke, S. & Herschman, H. R. (1998) PRMT 3, a type I protein arginine N-methyltransferase that differs from PRMT1 in its oligomerization, subcellular localization, substrate specificity, and regulation.

Tao, B. B., Liu, X. Q., Zhang, W., Li, S., Dong, D., Xiao, M., & Zhong, J. (2017). Evidence for the association of chromatin and microRNA regulation in the human genome. Oncotarget, 8(41), 70958–70966.

Taphoorn, M. J. B., Dirven, L., Kanner, A. A., Lavy-Shahaf, G., Weinberg, U., Taillibert, S., Toms, S. A., Honnorat, J., Chen, T. C., Sroubek, J., David, C., Idbaih, A., Easaw, J. C., Kim, C., Bruna, J., Hottinger, A. F., Kew, Y., Roth, P., Desai, R., Villano, J. L., Kirson, E. D., Ram, Z. & Stupp, R. (2018) Influence of treatment with tumor-treating fields on health-related quality of life of patients with newly diagnosed glioblastoma: A secondary analysis of a randomized clinical trial. JAMA Oncology, 4 (4), 495-504.

Tarighat, S. S., Santhanam, R., Frankhouser, D., Radomska, H. S., Lai, H., Anghelina, M., Wang, H., Huang, X., Alinari, L., Walker, A., Caligiuri, M. A., Croce, C. M., Li, L., Garzon, R., Li, C., Baiocchi, R. A., & Marcucci, G. (2016). The dual epigenetic role of PRMT5 in acute myeloid leukemia: gene activation and repression via histone arginine methylation. Leukemia, 30(4), 789–799.

Tchoghandjian, A., Baeza, N., Colin, C., Cayre, M., Metellus, P., Beclin, C., Ouafik, L. & Figarella-Branger, D. (2010) A2B5 cells from human glioblastoma have cancer stem cell properties. Brain Pathology, 20 (1), 211-221.

The GLASS Consortium (2018) Glioma through the looking GLASS: Molecular evolution of diffuse gliomas and the glioma longitudinal analysis consortium. Neuro-Oncology, 20 (7), 873-884.

The Human Protein Atlas CARM1 HPA RNA-seq data. Available online: http://www.proteinatlas.org [Accessed 11/11/ 2020].

Thomas, A., Tanaka, M., Trepel, J., Reinhold, W. C., Rajapakse, V. N. & Pommier, Y. (2017) Temozolomide in the era of precision medicine. Cancer Research, 77 (4), 823-826.

Thomas, J. G., Rao, G., Kew, Y. & Prabhu, S. S. (2016) Laser interstitial thermal therapy for newly diagnosed and recurrent glioblastoma. Neurosurgical Focus FOC, 41 (4), E12.

Tian, M., Ma, W., Chen, Y., Yu, Y., Zhu, D., Shi, J. & Zhang, Y. (2018) Impact of gender on the survival of patients with glioblastoma. Bioscience Reports, 38 (6), BSR20180752.

Topalian, S. L., Drake, C. G. & Pardoll, D. M. (2015) Immune checkpoint blockade: A common denominator approach to cancer therapy.

Touat, M., Idbaih, A., Sanson, M. & Ligon, K. L. (2017) Glioblastoma targeted therapy: Updated approaches from recent biological insights. Annals of Oncology : Official Journal of the European Society for Medical Oncology, 28 (7), 1457-1472.

Touat, M., Li, Y. Y., Boynton, A. N., Spurr, L. F., Iorgulescu, J. B., Bohrson, C. L., Cortes-Ciriano, I., Birzu, C., Geduldig, J. E., Pelton, K., Lim-Fat, M., Pal, S., Ferrer-Luna, R., Ramkissoon, S. H., Dubois, F., Bellamy, C., Currimjee, N., Bonardi, J., Qian, K., Ho, P., Malinowski, S., Taquet, L., Jones, R. E., Shetty, A., Chow, K., Sharaf, R., Pavlick, D., Albacker, L. A., Younan, N., Baldini, C., Verreault, M., Giry, M., Guillerm, E., Ammari, S., Beuvon, F., Mokhtari, K., Alentorn, A., Dehais, C., Houillier, C., Laigle-Donadey, F., Psimaras, D., Lee, E. Q., Nayak, L., McFaline-Figueroa, J., Carpentier, A., Cornu, P., Capelle, L., Mathon, B., Barnholtz-Sloan, J., Chakravarti, A., Bi, W. L., Chiocca, E. A., Fehnel, K. P., Alexandrescu, S., Chi, S. N., Haas-Kogan, D., Batchelor, T. T., Frampton, G. M., Alexander, B. M., Huang, R. Y., Ligon, A. H., Coulet, F., Delattre, J., Hoang-Xuan, K., Meredith, D. M., Santagata, S., Duval, A., Sanson, M., Cherniack, A. D., Wen, P. Y., Reardon, D. A., Marabelle, A., Park, P. J., Idbaih, A., Beroukhim, R., Bandopadhayay, P., Bielle, F. & Ligon, K. L. (2020) Mechanisms and therapeutic implications of hypermutation in gliomas. Nature, 580 (7804), 517-523.

Tradewell, M. L., Yu, Z., Tibshirani, M., Boulanger, M., Durham, H. D. & Richard, S. (2012) Arginine methylation by PRMT1 regulates nuclear-cytoplasmic localization and toxicity of FUS/TLS harbouring ALS-linked mutations. Human Molecular Genetics, 21 (1), 136-149.

Tripsianes, K., Madl, T., Machyna, M., Fessas, D., Englbrecht, C., Fischer, U., Neugebauer, K. M. & Sattler, M. (2011) Structural basis for dimethylarginine recognition by the tudor domains of human SMN and SPF30 proteins. Nature Structural & Molecular Biology, 18 (12), 1414-1420.

Troffer-Charlier, N., Cura, V., Hassenboehler, P., Moras, D. & Cavarelli, J. (2007) Functional insights from structures of coactivator-associated arginine methyltransferase 1 domains. The EMBO Journal, 26 (20), 4391-4401.

Tsai, W., Reineke, L. C., Jain, A., Jung, S. Y. & Lloyd, R. E. (2017) Histone arginine demethylase JMJD6 is linked to stress granule assembly through demethylation of the stress granule-nucleating protein G3BP1. The Journal of Biological Chemistry, 292 (46), 18886-18896.

Tsikas, D., Bollenbach, A., Hanff, E. & Kayacelebi, A. A. (2018) Asymmetric dimethylarginine (ADMA), symmetric dimethylarginine (SDMA) and homoarginine (hArg): The ADMA, SDMA and hArg paradoxes. Cardiovascular Diabetology, 17 (1), 1-x.

Tumeh, P. C., Harview, C. L., Yearley, J. H., Shintaku, I. P., Taylor, E. J. M., Robert, L., Chmielowski, B., Spasic, M., Henry, G., Ciobanu, V., West, A. N., Carmona, M., Kivork, C., Seja, E., Cherry, G., Gutierrez, A. J., Grogan, T. R., Mateus, C., Tomasic, G., Glaspy, J. A., Emerson, R. O., Robins, H., Pierce, R. H., Elashoff, D. A., Robert, C. & Ribas, A. (2014) PD-1 blockade induces responses by inhibiting adaptive immune resistance. Nature, 515 (7528), 568-571.

Turcan, S., Rohle, D., Goenka, A., Walsh, L. A., Fang, F., Yilmaz, E., Campos, C., Fabius, A. W. M., Lu, C., Ward, P. S., Thompson, C. B., Kaufman, A., Guryanova, O., Levine, R., Heguy, A., Viale, A., Morris, L. G. T., Huse, J. T., Mellinghoff, I. K. & Chan, T. A. (2012) IDH1 mutation is sufficient to establish the glioma hypermethylator phenotype. Nature, 483 (7390), 479-483.

Turkalp, Z., Karamchandani, J. & Das, S. (2014) IDH mutation in glioma: New insights and promises for the future. JAMA Neurology, 71 (10), 1319-1325.

Turkez, H., Nóbrega, F. R. d., Ozdemir, O., Bezerra Filho, Carlos da,Silva Maia, Almeida, R. N. d., Tejera, E., Perez-Castillo, Y. & Sousa, D. P. d. (2019) NFBTA: A potent cytotoxic agent against glioblastoma. Molecules (Basel, Switzerland), 24 (13), 2411.

Uhlen, M., Zhang, C., Lee, S., Sjöstedt, E., Fagerberg, L., Bidkhori, G., Benfeitas, R., Arif, M., Liu, Z., Edfors, F., Sanli, K., von Feilitzen, K., Oksvold, P., Lundberg, E., Hober, S., Nilsson, P., Mattsson, J., Schwenk, J. M., Brunnström, H., Glimelius, B., Sjöblom, T., Edqvist, P., Djureinovic, D., Micke, P., Lindskog, C., Mardinoglu, A. & Ponten, F. (2017) A pathology atlas of the human cancer transcriptome. Science, 357 (6352), eaan2507.

Vagin, V. V., Wohlschlegel, J., Qu, J., Jonsson, Z., Huang, X., Chuma, S., Girard, A., Sachidanandam, R., Hannon, G. J., & Aravin, A. A. (2009). Proteomic analysis of murine Piwi proteins reveals a role for arginine methylation in specifying interaction with Tudor family members. Genes & development, 23(15), 1749–1762.

van Dijk, T. B., Gillemans, N., Stein, C., Fanis, P., Demmers, J., van de Corput, M., Essers, J., Grosveld, F., Bauer, U. & Philipsen, S. (2010) Friend of Prmt1, a novel chromatin target of protein arginine methyltransferases. Molecular and Cellular Biology, 30 (1), 260-272.

Verhaak, R. G. W., Hoadley, K. A., Purdom, E., Wang, V., Qi, Y., Wilkerson, M. D., Miller, C. R., Ding, L., Golub, T., Mesirov, J. P., Alexe, G., Lawrence, M., O'Kelly, M., Tamayo, P., Weir, B. A., Gabriel, S., Winckler, W., Gupta, S., Jakkula, L., Feiler, H. S., Hodgson, J. G., James, C. D., Sarkaria, J. N., Brennan, C., Kahn, A., Spellman, P. T., Wilson, R. K., Speed, T. P., Gray, J. W., Meyerson, M., Getz, G., Perou, C. M., Hayes, D. N. & Cancer Genome Atlas, Research Network (2010) Integrated genomic analysis

identifies clinically relevant subtypes of glioblastoma characterized by abnormalities in PDGFRA, IDH1, EGFR, and NF1. Cancer Cell, 17 (1), 98-110.

Verkhratsky, A. & Nedergaard, M. (2018) Physiology of astroglia. Physiological Reviews, 98 (1), 239-389.

Vhuiyan, M. I., Pak, M. L., Park, M. A., Thomas, D., Lakowski, T. M., Chalfant, C. E. & Frankel, A. (2017) PRMT2 interacts with splicing factors and regulates the alternative splicing of BCL-X. Journal of Biochemistry, 162 (1), 17-25.

Vieira de Castro, J., Gonçalves, C., S., Hormigo, A. & Costa, B. M. (2020) Exploiting the complexities of glioblastoma stem cells: Insights for cancer initiation and therapeutic targeting. International Journal of Molecular Sciences, 21 (15), 5278.

Vuong, T. A., Jeong, H., Lee, H., Kim, B., Leem, Y., Cho, H. & Kang, J. (2020) PRMT7 methylates and suppresses GLI2 binding to SUFU thereby promoting its activation. Cell Death & Differentiation, 27 (1), 15-28.

Waite, K. J., Wharton, S. B., Old, S. E. & Burnet, N. G. (1999) Systemic metastases of glioblastoma multiforme. Clinical Oncology, 11 (3), 205-207.

Waldmann, T., Izzo, A., Kamieniarz, K., Richter, F., Vogler, C., Sarg, B., Lindner, H., Young, N. L., Mittler, G., Garcia, B. A. & Schneider, R. (2011) Methylation of H2AR29 is a novel repressive PRMT6 target. Epigenetics & Chromatin, 4 (1), 11.

Walport, L. J., Hopkinson, R. J., Chowdhury, R., Schiller, R., Ge, W., Kawamura, A. & Schofield, C. J. (2016) Arginine demethylation is catalysed by a subset of JmjC histone lysine demethylases. Nature Communications, 7 11974.

Wang, D., Starr, R., Chang, W., Aguilar, B., Alizadeh, D., Wright, S. L., Yang, X., Brito, A., Sarkissian, A., Ostberg, J. R., Li, L., Shi, Y., Gutova, M., Aboody, K., Badie, B., Forman, S. J., Barish, M. E. & Brown, C. E. (2020) Chlorotoxin-directed CAR T cells for specific and effective targeting of glioblastoma. Science Translational Medicine, 12 (533), eaaw2672.

Wang, H., Guo, W., Mitra, J., Hegde, P. M., Vandoorne, T., Eckelmann, B. J., Mitra, S., Tomkinson, A. E., Van Den Bosch, L. & Hegde, M. L. (2018) Mutant FUS causes DNA ligation defects to inhibit oxidative damage repair in amyotrophic lateral sclerosis. Nature Communications, 9 (1), 3683.

Wang, H., Huang, Z., Xia, L., Feng, Q., Erdjument-Bromage, H., Strahl, B. D., Briggs, S. D., Allis, C. D., Wong, J., Tempst, P. & Zhang, Y. (2001) Methylation of histone H4 at arginine 3 facilitating transcriptional activation by nuclear hormone receptor. Science, 293 (5531), 853.

Wang, J., Chen, L., Sinha, S. H., Liang, Z., Chai, H., Muniyan, S., Chou, Y., Yang, C., Yan, L., Feng, Y., Kathy Li, K., Lin, M., Jiang, H., George Zheng, Y. & Luo, C. (2012) Pharmacophore-based virtual screening and biological evaluation of small molecule inhibitors for protein arginine methylation. Journal of Medicinal Chemistry, 55 (18), 7978-7987.

Wang, J., Saxe, J. P., Tanaka, T., Chuma, S., & Lin, H. (2009). Mili interacts with tudor domain-containing protein 1 in regulating spermatogenesis. Current biology, 19(8), 640–644.

Wang, L., Pal, S. & Sif, S. (2008) Protein arginine methyltransferase 5 suppresses the transcription of the RB family of tumor suppressors in leukemia and lymphoma cells. Molecular and Cellular Biology, 28 (20), 6262-6277.

Wang, L., Qin, H., Li, L., Zhang, Y., TU, Y., Feng, F., Ji, P., Zhang, J., Li, G., Zhao, Z. & Gao, G. (2012) Overexpression of CCL20 and its receptor CCR6 predicts poor clinical prognosis in human gliomas. Medical Oncology, 29 (5), 3491-3497.

Wang, L., Charoensuksai, P., Watson, N. J., Wang, X., Zhao, Z., Coriano, C. G., Kerr, L. R. & Xu, W. (2013) CARM1 automethylation is controlled at the level of alternative splicing. Nucleic Acids Research, 41 (14), 6870-6880.

Wang, S., Chen, C., Li, J., Xu, X., Chen, W., & Li, F. (2020). The CXCL12/CXCR4 axis confers temozolomide resistance to human glioblastoma cells via up-regulation of FOXM1. Journal of the neurological sciences, 414, 116837.

Wang, S., Tan, X., Yang, B., Yin, B. & Peng, X. (2012) Screening of substrates of protein arginine methyltransferase 1 in glioma. Chinese Medical Sciences Journal, 27 (1), 1-6.

Wang, S., Tan, X., Yang, B., Yin, B., Yuan, J., Qiang, B. & Peng, X. (2012) The role of protein arginine-methyltransferase 1 in gliomagenesis. BMB Reports, 45 470-5.

Wang, W., Pan, K., Chen, Y., Huang, C. & Zhang, X. (2012) The acetylation of transcription factor HBP1 by p300/CBP enhances p16INK4A expression. Nucleic Acids Research, 40 (3), 981-995.

Wang, W., Hsu, J., Wang, Y., Lee, H., Yamaguchi, H., Liao, H. & Hung, M. (2019) An essential role of PRMT1-mediated EGFR methylation in EGFR activation by ribonuclease 5. American Journal of Cancer Research, 9 (1), 180-185.

Wang, X., Arai, S., Song, X., Reichart, D., Du, K., Pascual, G., Tempst, P., Rosenfeld, M. G., Glass, C. K. & Kurokawa, R. (2008) Induced ncRNAs allosterically modify RNA-binding proteins in cis to inhibit transcription. Nature, 454 (7200), 126-130.

Wang, X., Zhen, X., Wang, J., Zhang, J., Wu, W. & Jiang, X. (2013) Doxorubicin delivery to 3D multicellular spheroids and tumors based on boronic acid-rich chitosan nanoparticles. Biomaterials, 34 (19), 4667-4679.

Wang, X., Huang, Y., Zhao, J., Zhang, Y., Lu, J. & Huang, B. (2012) Suppression of PRMT6-mediated arginine methylation of p16 protein potentiates its ability to arrest A549 cell proliferation. The International Journal of Biochemistry & Cell Biology, 44 (12), 2333-2341.

Wang, Y., Pan, L., Sheng, X., Chen, S. & Dai, J. (2016) Nimotuzumab, a humanized monoclonal antibody specific for the EGFR, in combination with temozolomide and radiation therapy for newly diagnosed glioblastoma multiforme: First results in chinese patients. Asia-Pacific Journal of Clinical Oncology, 12 (1), e23-e29.

Wang, Y., Wysocka, J., Sayegh, J., Lee, Y., Perlin, J. R., Leonelli, L., Sonbuchner, L. S., McDonald, C. H., Cook, R. G., Dou, Y., Roeder, R. G., Clarke, S., Stallcup, M. R., Allis, C. D. & Coonrod, S. A. (2004) Human PAD4 regulates histone arginine methylation levels via demethylimination. Science, 306 (5694), 279.

Watanabe, K., Tachibana, O., Sato, K., Yonekawa, Y., Kleihues, P. & Ohgaki, H. (1996) Overexpression of the EGF receptor and p53 mutations are mutually exclusive in the evolution of primary and secondary glioblastomas. Brain Pathology, 6 (3), 217-223.

Watanabe, T., Nobusawa, S., Kleihues, P. & Ohgaki, H. (2009) IDH1 mutations are early events in the development of astrocytomas and oligodendrogliomas. The American Journal of Pathology, 174 (4), 1149-1153.

Waugh, M. G. (2016) Chromosomal instability and phosphoinositide pathway gene signatures in glioblastoma multiforme. Molecular Neurobiology, 53 (1), 621-630.

Wei, H., Mundade, R., Lange, K. C. & Lu, T. (2014) Protein arginine methylation of non-histone proteins and its role in diseases. Cell Cycle (Georgetown, Tex.), 13 (1), 32-41.

Weller, M., Butowski, N., Tran, D. D., Recht, L. D., Lim, M., Hirte, H., Ashby, L., Mechtler, L., Goldlust, S. A., Iwamoto, F., Drappatz, J., O'Rourke, D.,M., Wong, M., Hamilton, M. G., Finocchiaro, G., Perry, J., Wick, W., Green, J., He, Y., Turner, C. D., Yellin, M. J., Keler, T., Davis, T. A., Stupp, R., Sampson, J. H., Butowski, N., Campian, J., Recht, L., Lim, M., Ashby, L., Drappatz, J., Hirte, H., Iwamoto, F., Mechtler, L., Goldlust, S., Becker, K., Barnett, G., Nicholas, G., Desjardins, A., Benkers, T., Wagle, N., Groves, M., Kesari, S., Horvath, Z., Merrell, R., Curry, R., O'Rourke, J., Schuster, D., Wong, M., Mrugala, M., Jensen, R., Trusheim, J., Lesser, G., Belanger, K., Sloan, A., Purow, B., Fink, K., Raizer, J.,

Schulder, M., Nair, S., Peak, S., Perry, J., Brandes, A., Weller, M., Mohile, N., Landolfi, J., Olson, J., Finocchiaro, G., Jennens, R., DeSouza, P., Robinson, B., Crittenden, M., Shih, K., Flowers, A., Ong, S., Connelly, J., Hadjipanayis, C., Giglio, P., Mott, F., Mathieu, D., Lessard, N., Sepulveda, S. J., Lövey, J., Wheeler, H., Inglis, P., Hardie, C., Bota, D., Lesniak, M., Portnow, J., Frankel, B., Junck, L., Thompson, R., Berk, L., McGhie, J., Macdonald, D., Saran, F., Soffietti, R., Blumenthal, D., André de, Sá Barreto,Costa Marcos, Nowak, A., Singhal, N., Hottinger, A., Schmid, A., Srkalovic, G., Baskin, D., Fadul, C., Nabors, L., LaRocca, R., Villano, J., Paleologos, N., Kavan, P., Pitz, M., Thiessen, B., Idbaih, A., Frenel, J. S., Domont, J., Grauer, O., Hau, P., Marosi, C., Sroubek, J., Hovey, E., Sridhar, P. S., Cher, L., Dunbar, E., Coyle, T., Raymond, J., Barton, K., Guarino, M., Raval, S., Stea, B., Dietrich, J., Hopkins, K., Erridge, S., Steinbach, J., Pineda, L. E., Balana, Q. C., Sonia del, B. B., Wenczl, M., Molnár, K., Hideghéty, K., Lossos, A., Myra van, L., Levy, A., Harrup, R., Patterson, W., Lwin, Z., Sathornsumetee, S., Lee, E., Ho, J., Emmons, S., Duic, J. P., Shao, S., Ashamalla, H., Weaver, M., Lutzky, J., Avgeropoulos, N., Hanna, W., Nadipuram, M., Cecchi, G., O'Donnell, R., Pannullo, S., Carney, J., Hamilton, M., MacNeil, M., Beaney, R., Fabbro, M., Schnell, O., Fietkau, R., Stockhammer, G., Malinova, B., Odrazka, K., Sames, M., Miguel Gil, G., Razis, E., Lavrenkov, K., Castro, G., Ramirez, F., Baldotto, C., Viola, F., Malheiros, S., Lickliter, J., Gauden, S., Dechaphunkul, A., Thaipisuttikul, I., Thotathil, Z., Ma, H., Cheng, W., Chang, C., Salas, F., Dietrich, P., Mamot, C., Nayak, L. & Nag, S. (2017) Rindopepimut with temozolomide for patients with newly diagnosed, EGFRvIII-expressing glioblastoma (ACT IV): A randomised, double-blind, international phase 3 trial. The Lancet Oncology, 18 (10), 1373-1385.

Weller, M., Roth, P., Preusser, M., Wick, W., Reardon, D. A., Platten, M. & Sampson, J. H. (2017) Vaccine-based immunotherapeutic approaches to gliomas and beyond. Nature Reviews Neurology, 13 (6), 363-374.

Wen, P. Y., Touat, M., Alexander, B. M., Mellinghoff, I. K., Ramkissoon, S., McCluskey, C. S., Pelton, K., Haidar, S., Basu, S. S., Gaffey, S. C., Brown, L. E., Martinez-Ledesma, J., Wu, S., Kim, J., Wei, W., Park, M., Huse, J. T., Kuhn, J. G., Rinne, M. L., Colman, H., Agar, N. Y. R., Omuro, A. M., DeAngelis, L. M., Gilbert, M. R., de Groot, J.,F., Cloughesy, T. F., Chi, A. S., Roberts, T. M., Zhao, J. J., Lee, E. Q., Nayak, L., Heath, J. R., Horky, L. L., Batchelor, T. T., Beroukhim, R., Chang, S. M., Ligon, A. H., Dunn, I. F., Koul, D., Young, G. S., Prados, M. D., Reardon, D. A., Yung, W. K. A. & Ligon, K. L. (2019) Buparlisib in patients with recurrent glioblastoma harboring phosphatidylinositol 3-kinase pathway activation: An open-label, multicenter, multi-arm, phase II trial. American Society of Clinical Oncology.

Westphal, M., Heese, O., Steinbach, J. P., Schnell, O., Schackert, G., Mehdorn, M., Schulz, D., Simon, M., Schlegel, U., Senft, C., Geletneky, K., Braun, C., Hartung, J. G., Reuter, D., Metz, M. W., Bach, F. &

Pietsch, T. (2015) A randomised, open label phase III trial with nimotuzumab, an anti-epidermal growth factor receptor monoclonal antibody in the treatment of newly diagnosed adult glioblastoma. European Journal of Cancer, 51 (4), 522-532.

Wick, W., Weller, M., van den Bent, M., Sanson, M., Weiler, M., von Deimling, A., Plass, C., Hegi, M., Platten, M. & Reifenberger, G. (2014) MGMT testing—the challenges for biomarker-based glioma treatment. Nature Reviews Neurology, 10 (7), 372-385.

Wu, X., Xiao, S., Zhang, M., Yang, L., Zhong, J., Li, B., Li, F., Xia, X., Li, X., Zhou, H., Liu, D., Huang, N., Yang, X., Xiao, F., & Zhang, N. (2021). A novel protein encoded by circular SMO RNA is essential for Hedgehog signaling activation and glioblastoma tumorigenicity. Genome biology, 22(1), 33.

Xiao, Y., Kim, D., Dura, B., Zhang, K., Yan, R., Li, H., Han, E., Ip, J., Zou, P., Liu, J., Chen, A. T., Vortmeyer, A. O., Zhou, J. & Fan, R. (2019) Ex vivo dynamics of human glioblastoma cells in a microvasculature-on-a-chip system correlates with tumor heterogeneity and subtypes. Advanced Science, 6 (8), 1801531.

Xie, Y., Zhou, R., Lian, F., Liu, Y., Chen, L., Shi, Z., Zhang, N., Zheng, M., Shen, B., Jiang, H., Liang, Z. & Luo, C. (2014) Virtual screening and biological evaluation of novel small molecular inhibitors against protein arginine methyltransferase 1 (PRMT1). Organic & Biomolecular Chemistry, 12 (47), 9665-9673.

Xiong, D., Wu, Y. B., Jin, C., Li, J. J., Gu, J., Liao, Y. F., Long, X., Zhu, S. Q., Wu, H. B., Xu, J. J., & Ding, J. Y. (2018). Elevated FUS/TLS expression is negatively associated with E-cadherin expression and prognosis of patients with non-small cell lung cancer. Oncology letters, 16(2), 1791–1800.

Xu, J., Wang, A. H., Oses-Prieto, J., Makhijani, K., Katsuno, Y., Pei, M., Yan, L., Zheng, Y. G., Burlingame, A., Brückner, K. & Derynck, R. (2013) Arginine methylation initiates BMP-induced smad signaling. Molecular Cell, 51 (1), 5-19.

Xu, W., Cho, H., Kadam, S., Banayo, E. M., Anderson, S., Yates, J. R.,3rd, Emerson, B. M. & Evans, R. M. (2004) A methylation-mediator complex in hormone signaling. Genes & Development, 18 (2), 144-156.

Xu, W., Chen, H., Du, K., Asahara, H., Tini, M., Emerson, B. M., Montminy, M. & Evans, R. M. (2001) A transcriptional switch mediated by cofactor methylation. Science, 294 (5551), 2507.

Xu, W., Yang, H., Liu, Y., Yang, Y., Wang, P., Kim, S., Ito, S., Yang, C., Wang, P., Xiao, M., Liu, L., Jiang, W., Liu, J., Zhang, J., Wang, B., Frye, S., Zhang, Y., Xu, Y., Lei, Q., Guan, K., Zhao, S. & Xiong, Y. (2011)

Oncometabolite 2-hydroxyglutarate is a competitive inhibitor of α-ketoglutarate-dependent dioxygenases. Cancer Cell, 19 (1), 17-30.

Yadav, N., Lee, J., Kim, J., Shen, J., Mickey C. -T. Hu, Aldaz, C. M. & Bedford, M. T. (2003) Specific protein methylation defects and gene expression perturbations in coactivator-associated arginine methyltransferase 1-deficient mice. Proceedings of the National Academy of Sciences of the United States of America, 100 (11), 6464-6468.

Yan, F., Alinari, L., Lustberg, M. E., Martin, L. K., Cordero-Nieves, H., Banasavadi-Siddegowda, Y., Virk, S., Barnholtz-Sloan, J., Bell, E. H., Wojton, J., Jacob, N. K., Chakravarti, A., Nowicki, M. O., Wu, X., Lapalombella, R., Datta, J., Yu, B., Gordon, K., Haseley, A., Patton, J. T., Smith, P. L., Ryu, J., Zhang, X., Mo, X., Marcucci, G., Nuovo, G., Kwon, C., Byrd, J. C., Chiocca, E. A., Li, C., Sif, S., Jacob, S., Lawler, S., Kaur, B. & Baiocchi, R. A. (2014) Genetic validation of the protein arginine methyltransferase PRMT5 as a candidate therapeutic target in glioblastoma. Cancer Research, 74 (6), 1752-1765.

Yan, H., Parsons, D. W., Jin, G., McLendon, R., Rasheed, B. A., Yuan, W., Kos, I., Batinic-Haberle, I., Jones, S., Riggins, G. J., Friedman, H., Friedman, A., Reardon, D., Herndon, J., Kinzler, K. W., Velculescu, V. E., Vogelstein, B. & Bigner, D. D. (2009) IDH1 and IDH2 mutations in gliomas. The New England Journal of Medicine, 360 (8), 765-773.

Yan, L., Yan, C., Qian, K., Su, H., Kofsky-Wofford, S., Lee, W., Zhao, X., Ho, M., Ivanov, I. & Zheng, Y. G. (2014) Diamidine compounds for selective inhibition of protein arginine methyltransferase 1. Journal of Medicinal Chemistry, 57 (6), 2611-2622.

Yan, Y., Xu, Z., Chen, X., Wang, X., Zeng, S., Zhao, Z., Qian, L., Li, Z., Wei, J., Huo, L., Li, X., Gong, Z., & Sun, L. (2019). Novel Function of lncRNA ADAMTS9-AS2 in Promoting Temozolomide Resistance in Glioblastoma via Upregulating the FUS/MDM2 Ubiquitination Axis. Frontiers in cell and developmental biology, 7, 217.

Yang, Y. & Bedford, M. T. (2013) Protein arginine methyltransferases and cancer. Nature Reviews Cancer, 13 (1), 37-50.

Yang, Y., Hadjikyriacou, A., Xia, Z., Gayatri, S., Kim, D., Zurita-Lopez, C., Kelly, R., Guo, A., Li, W., Clarke, S. G. & Bedford, M. T. (2015) PRMT9 is a type II methyltransferase that methylates the splicing factor SAP145. Nature Communications, 6 (1), 6428.

Yang, Y., Lu, Y., Espejo, A., Wu, J., Xu, W., Liang, S., & Bedford, M. T. (2010). TDRD3 is an effector molecule for arginine-methylated histone marks. Molecular cell, 40(6), 1016–1023.

Yang, Y., McBride, K. M., Hensley, S., Lu, Y., Chedin, F., & Bedford, M. T. (2014). Arginine methylation facilitates the recruitment of TOP3B to chromatin to prevent R loop accumulation. Molecular cell, 53(3), 484–497.

Yi, H., Jeong, Y. H., Kim, Y., Choi, Y., Moon, H. E., Park, S. H., Kang, K. S., Bae, M., Jang, J., Youn, H., Paek, S. H. & Cho, D. (2019) A bioprinted human-glioblastoma-on-a-chip for the identification of patient-specific responses to chemoradiotherapy. Nature Biomedical Engineering, 3 (7), 509-519.

Yi, M., Ma, Y., Chen, Y., Liu, C., Wang, Q. & Deng, H. (2020) Glutathionylation decreases methyltransferase activity of PRMT5 and inhibits cell proliferation. Mol Cell Proteomics, 19 (11), 1910.

Yoshimoto, T., Boehm, M., Olive, M., Crook, M. F., San, H., Langenickel, T. & Nabel, E. G. (2006) The arginine methyltransferase PRMT2 binds RB and regulates E2F function. Experimental Cell Research, 312 (11), 2040-2053.

Young, R. M., Jamshidi, A., Davis, G. & Sherman, J. H. (2015) Current trends in the surgical management and treatment of adult glioblastoma. Annals of Translational Medicine, 3 (9), 121.

Yung, W. K. A., Vredenburgh, J. J., Cloughesy, T. F., Nghiemphu, P., Klencke, B., Gilbert, M. R., Reardon, D. A. & Prados, M. D. (2010) Safety and efficacy of erlotinib in first-relapse glioblastoma: A phase II open-label study. Neuro-Oncology, 12 (10), 1061-1070.

Zakharenko, A., Dyrkheeva, N. & Lavrik, O. (2019) Dual DNA topoisomerase 1 and tyrosyl-DNA phosphodiesterase 1 inhibition for improved anticancer activity. Medicinal Research Reviews, 39 (4), 1427-1441.

Zeng, A., Hu, Q., Liu, Y., Wang, Z., Cui, X., Li, R., Yan, W. & You, Y. (2015) IDH1/2 mutation status combined with ki-67 labeling index defines distinct prognostic groups in glioma. Oncotarget, 6 (30), 30232-30238.

Zhang, H., Guo, X., Feng, X., Wang, T., Hu, Z., Que, X., Tian, Q., Zhu, T., Guo, G., Huang, W. & Li, X. (2017) MiRNA-543 promotes osteosarcoma cell proliferation and glycolysis by partially suppressing PRMT9 and stabilizing HIF-1α protein. Oncotarget, 8 (2), 2342-2355.

Zhang, H., Liu, K., Izumi, N., Huang, H., Ding, D., Ni, Z., Sidhu, S. S., Chen, C., Tomari, Y., & Min, J. (2017). Structural basis for arginine methylation-independent recognition of PIWIL1 by TDRD2. Proceedings of the National Academy of Sciences of the United States of America, 114(47), 12483–12488.

Zhang, H., Zeng, L., He, Q., Tao, W. A., Zha, Z. & Hu, C. (2016) The E3 ubiquitin ligase CHIP mediates ubiquitination and proteasomal degradation of PRMT5. Biochimica Et Biophysica Acta, 1863 (2), 335-346.

Zhang, X., Zhou, L. & Cheng, X. (2000) Crystal structure of the conserved core of protein arginine methyltransferase PRMT3. The EMBO Journal, 19 (14), 3509-3519.

Zhao, Y., Wang, Z., Cao, C., Weng, H., Xu, C., Li, K., Li, J., Lan, J., Zeng, X. & Li, Z. (2018) The clinical significance of O(6)-methylguanine-DNA methyltransferase promoter methylation status in adult patients with glioblastoma: A meta-analysis. Frontiers in Neurology, 9 127.

Zheng, L., Chen, J., Zhou, Z. & He, Z. (2017) miR-195 enhances the radiosensitivity of colorectal cancer cells by suppressing CARM1. OncoTargets and Therapy, 10 1027-1038.

Zheng, S., Moehlenbrink, J., Lu, Y. C., Zalmas, L. P., Sagum, C. A., Carr, S., McGouran, J. F., Alexander, L., Fedorov, O., Munro, S., Kessler, B., Bedford, M. T., Yu, Q., & La Thangue, N. B. (2013). Arginine methylation-dependent reader-writer interplay governs growth control by E2F-1. Molecular cell, 52(1), 37–51.

Zheng, Y., Zhang, X., & Li, H. (2020). Molecular basis for histidine N3-specific methylation of actin H73 by SETD3. Cell discovery, 6, 3.

Zhong, J., Cao, R., Zu, X., Hong, T., Yang, J., Liu, L., Xiao, X., Ding, W., Zhao, Q., Liu, J. & Wen, G. (2012) Identification and characterization of novel spliced variants of PRMT2 in breast carcinoma. The FEBS Journal, 279 (2), 316-335.

Zhou, B. & Liu, W. (2010) Post-traumatic glioma: Report of one case and review of the literature. International Journal of Medical Sciences, 7 (5), 248-250.

Zhou, Z., Sun, X., Zou, Z., Sun, L., Zhang, T., Guo, S., Wen, Y., Liu, L., Wang, Y., Qin, J., Li, L., Gong, W. & Bao, S. (2010) PRMT5 regulates golgi apparatus structure through methylation of the golgin GM130. Cell Research, 20 (9), 1023-1033.

Zhu, H., Acquaviva, J., Ramachandran, P., Boskovitz, A., Woolfenden, S., Pfannl, R., Bronson, R. T., Chen, J. W., Weissleder, R., Housman, D. E. & Charest, A. (2009) Oncogenic EGFR signaling cooperates with loss of tumor suppressor gene functions in gliomagenesis. Proceedings of the National Academy of Sciences of the United States of America, 106 (8), 2712-2716.

Zhu, H., Zheng, T., Yu, J., Zhou, L., & Wang, L. (2018). LncRNA XIST accelerates cervical cancer progression via upregulating Fus through competitively binding with miR-200a. Biomedicine & pharmacotherapy = Biomedecine & pharmacotherapie, 105, 789–797.

Zurita Rendón, O., Silva Neiva, L., Sasarman, F. & Shoubridge, E. A. (2014) The arginine methyltransferase NDUFAF7 is essential for complex I assembly and early vertebrate embryogenesis. Human Molecular Genetics, 23 (19), 5159-5170.

Zurita-Lopez, C., Sandberg, T., Kelly, R. & Clarke, S. G. (2012) Human protein arginine methyltransferase 7 (PRMT7) is a type III enzyme forming ω-NG-monomethylated arginine residues. The Journal of Biological Chemistry, 287 (11), 7859-7870.

Chapter 9 - Appendices

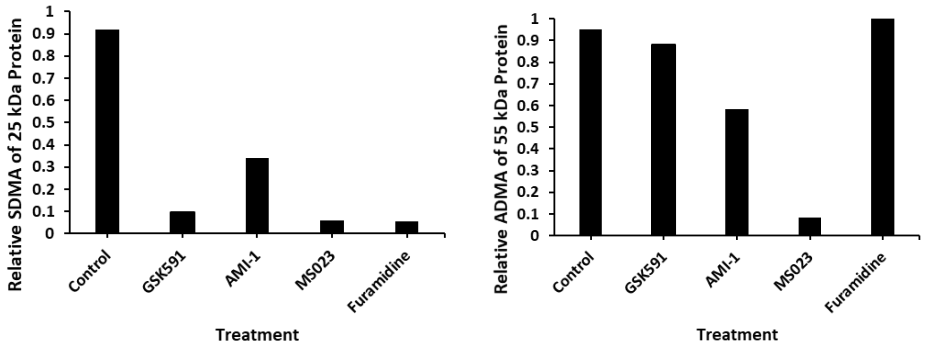

Appendix 1: *Figure 3.4 Quantification carried on Image J software by band densitometry. Each band density was measured and normalised against the corresponding loading control for that lane.*

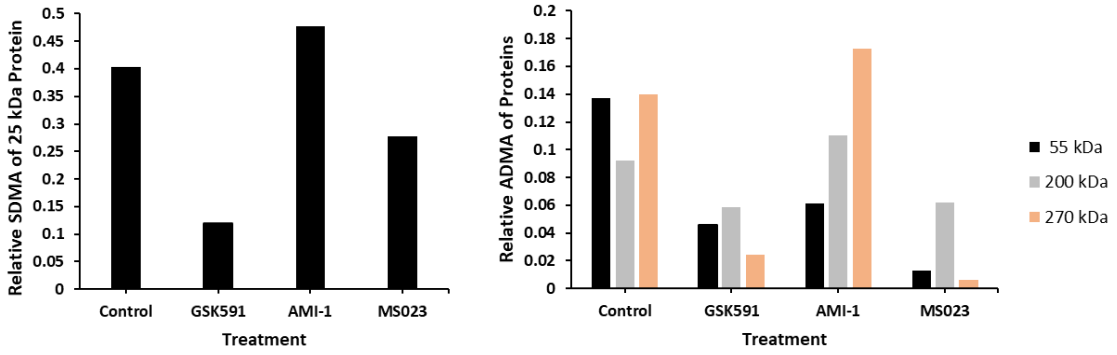

Appendix 2: *Figure 3.5 Quantification carried on Image J software by band densitometry. Each band density was measured and normalised against the corresponding loading control for that lane.*

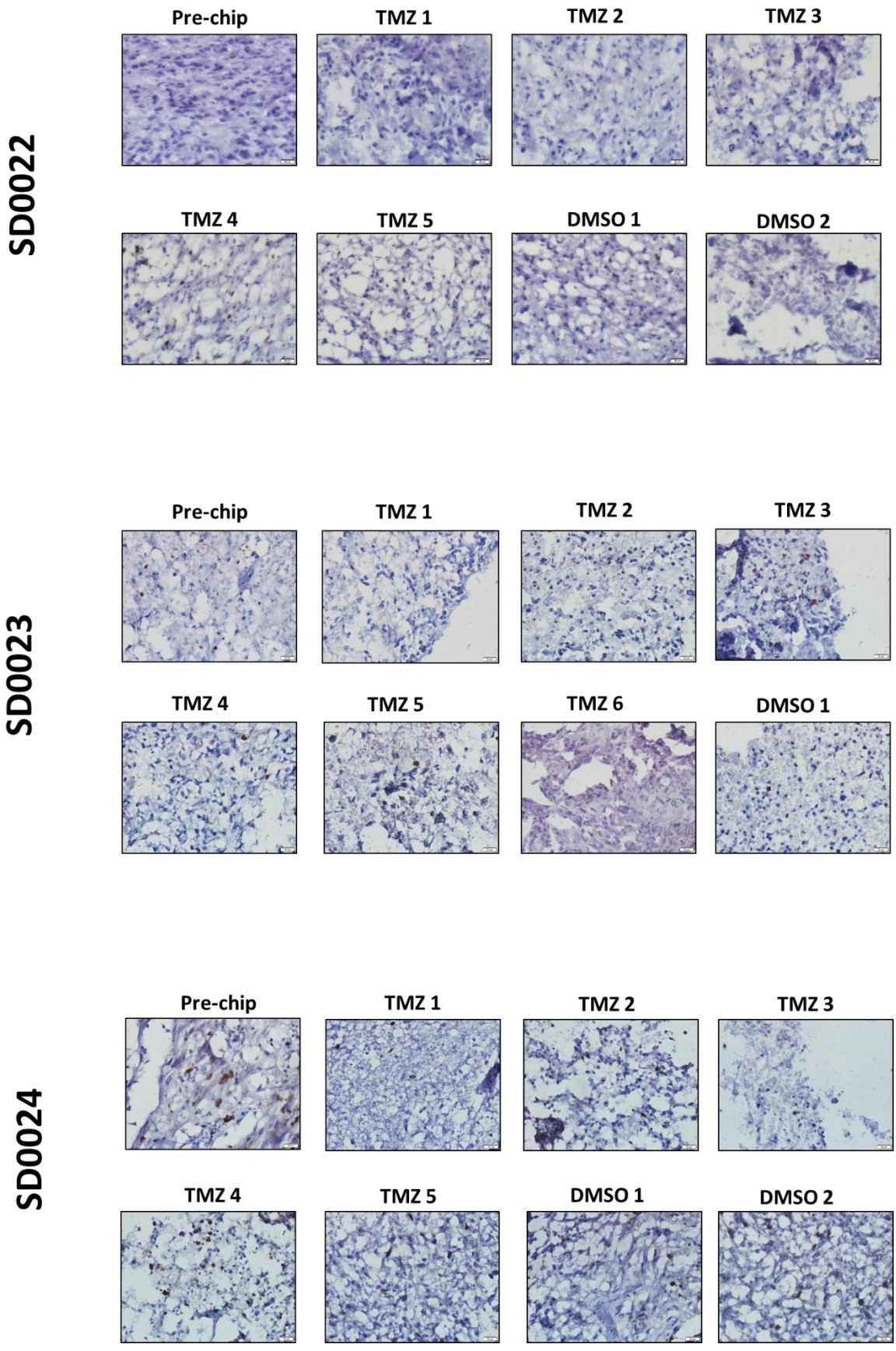

Appendix 3: *Representative images of patient biopsy slices treated with and without TMZ on the microfluidic device (x40). A pre-chip slice is also included. Quantifications can be found in Figure 4.2.*

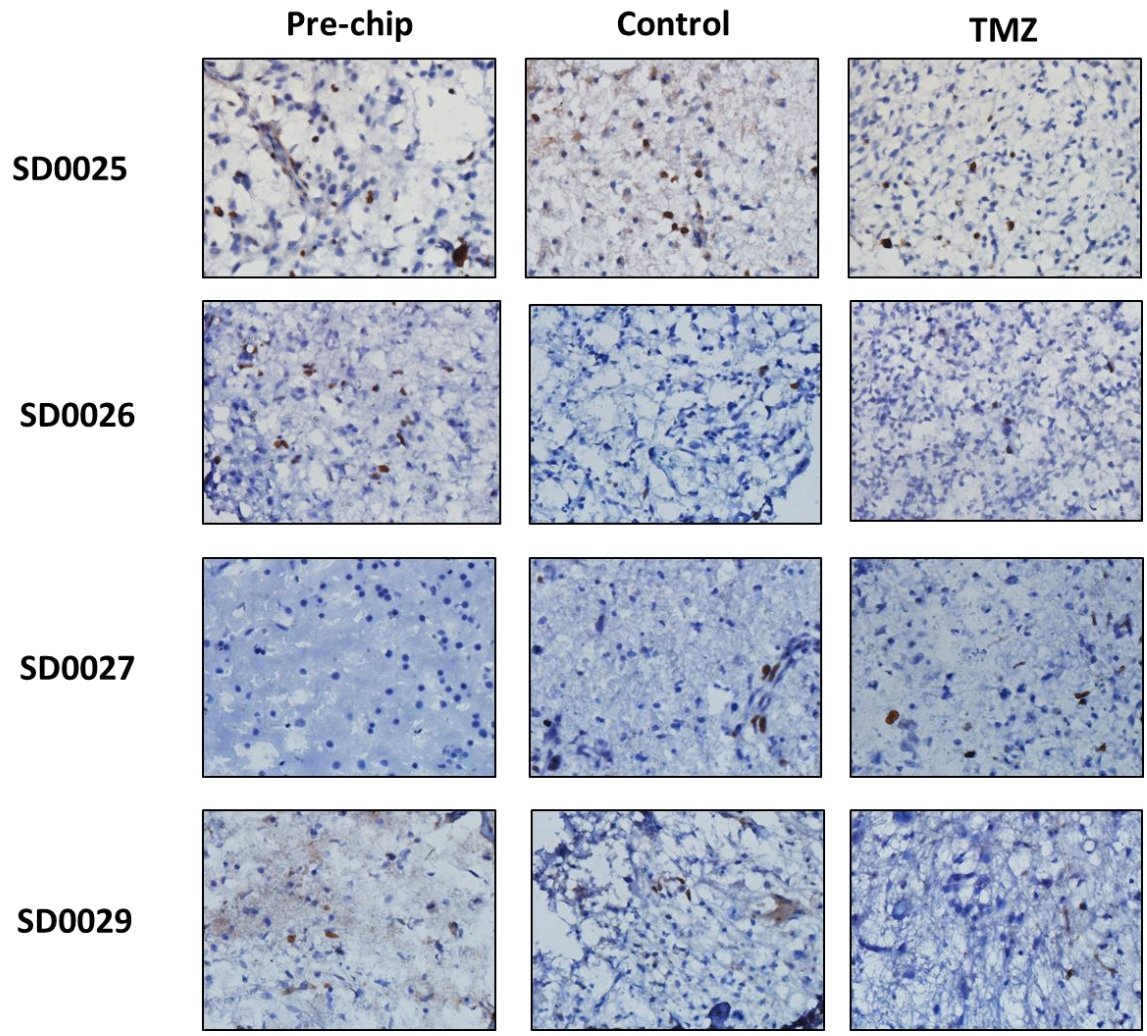

***Appendix 4**: Representative images of patient biopsy slices treated with and without TMZ on the microfluidic device (x40). A pre-chip slice is also included. Quantifications can be found in Figure 4.3.*

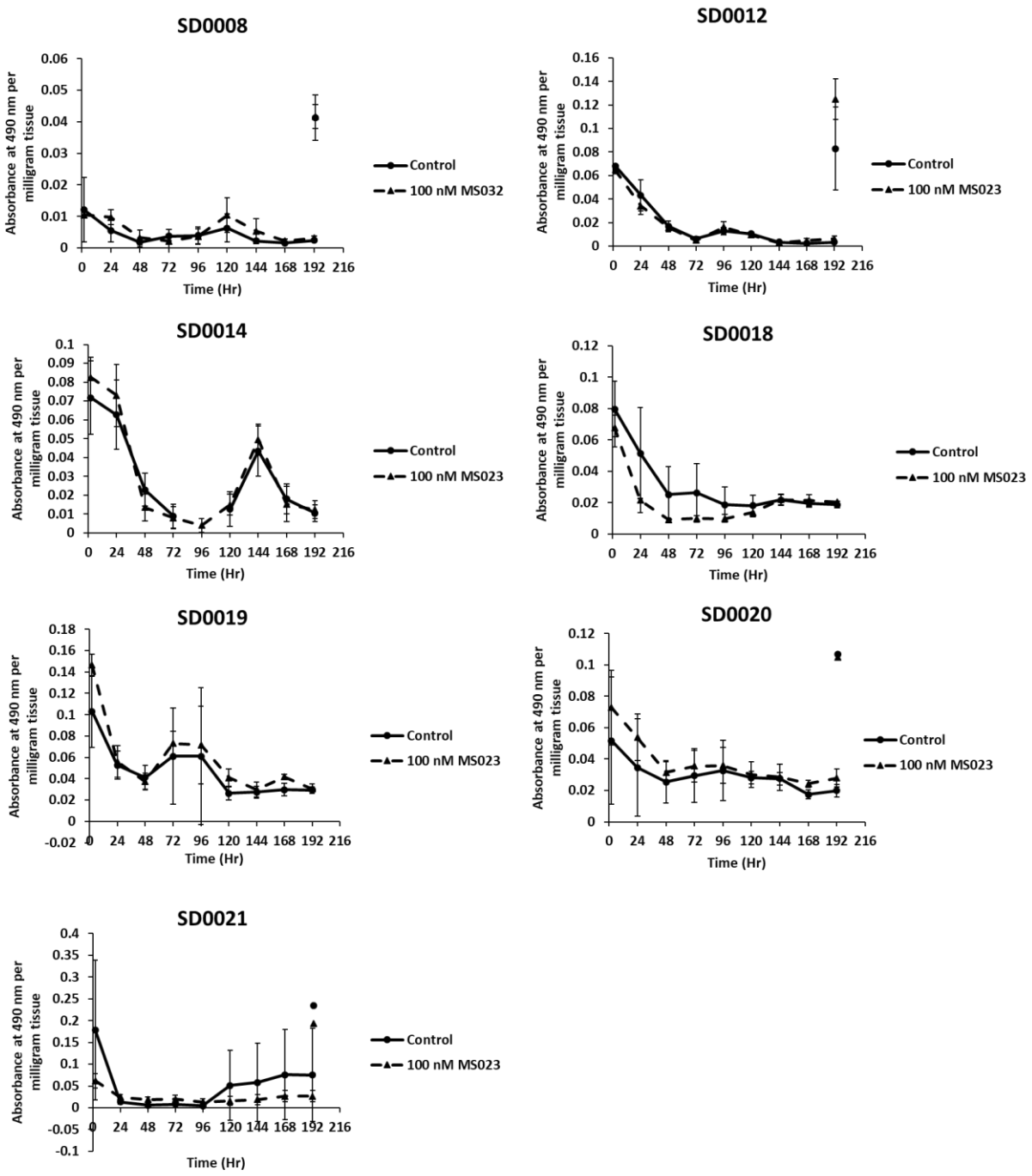

Appendix 5: *The LDH release for each individual patient sample used in Figure 5.5. Treated with 100 nM MS023 and control samples incubated with growing medium alone for 192 hr. Effluent samples were taken at regular intervals and samples were lysed at the end of the incubation. Error bars represent standard deviation amongst biological replicates (N=4).*

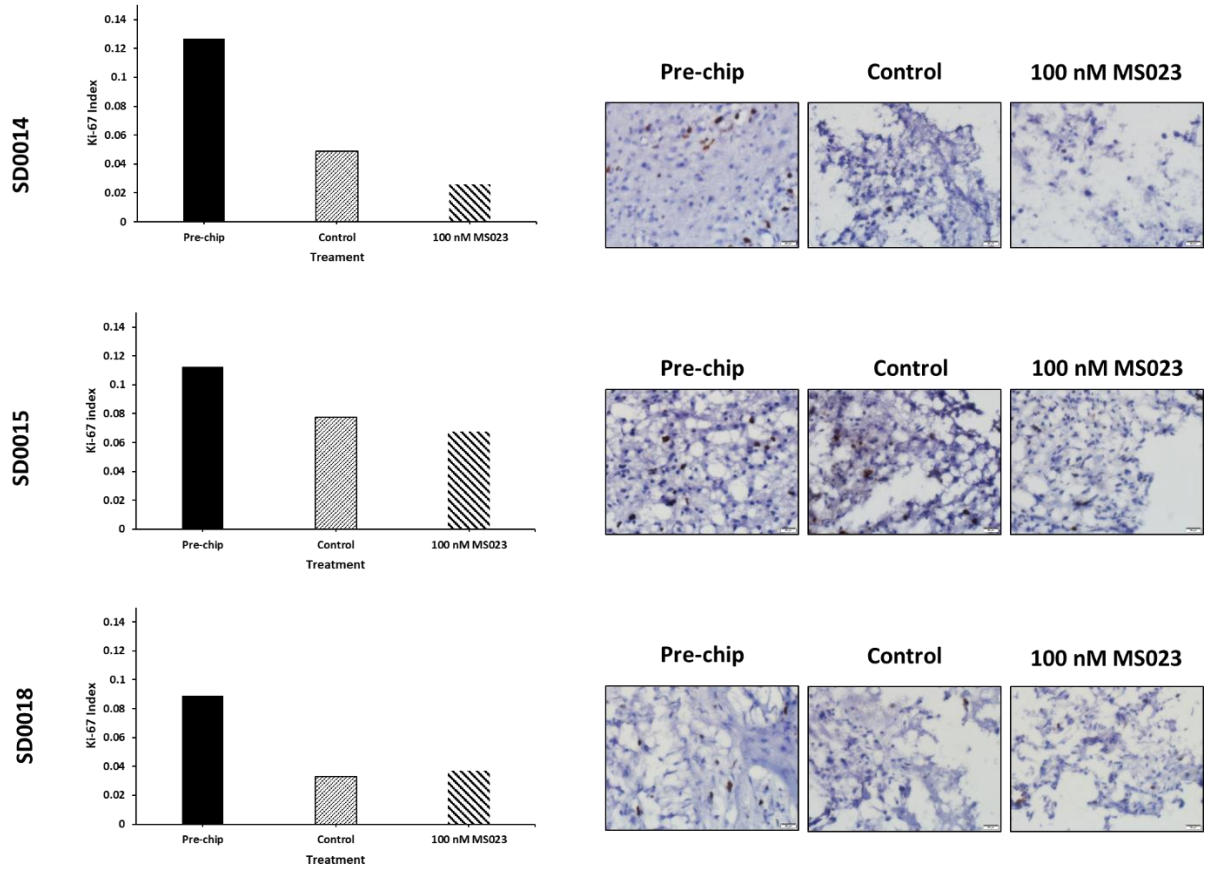

Appendix 6: *(A) The individual ki-67 index values for individual patient samples used in Figure 5.6. (B) Representative images of patient biopsy slices treated with and without MS023 on the microfluidic device (x40). A pre-chip slice is also included for each patient. Quantifications can be found in Figure 5.6.*

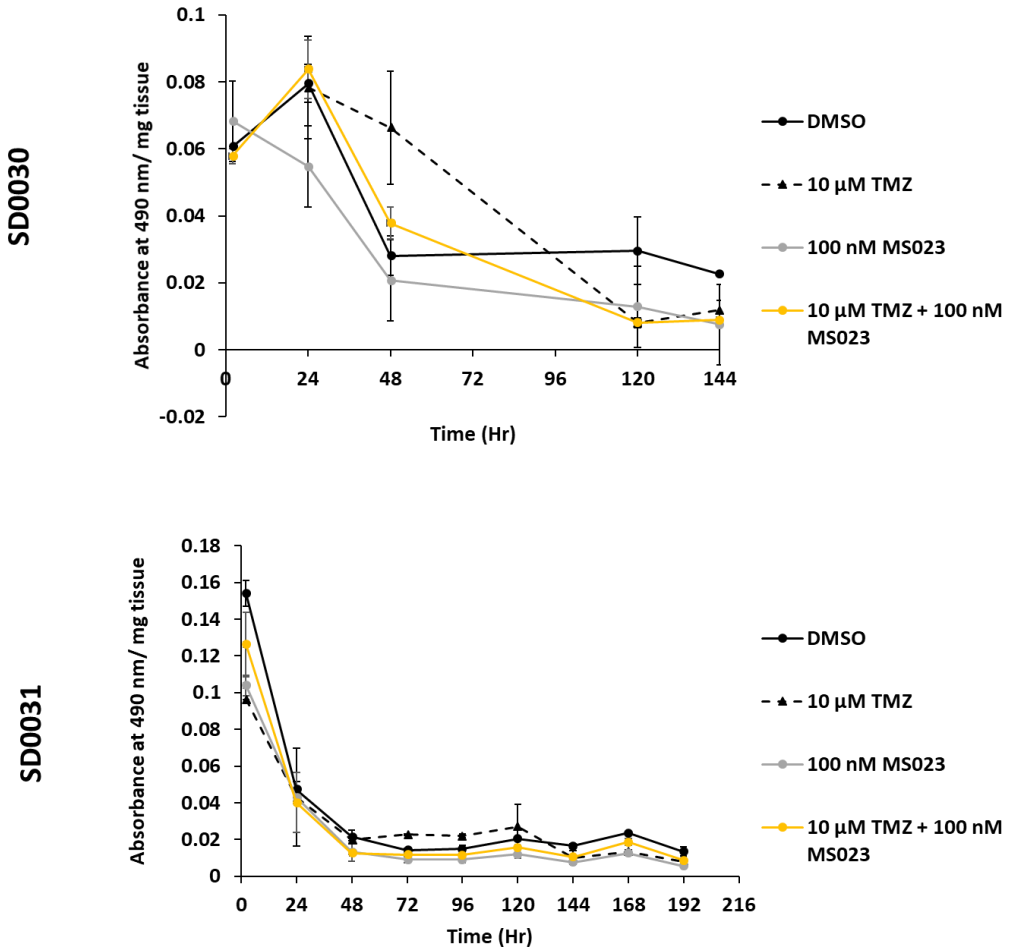

Appendix 7: *The release of LDH into the effluent for each individual patient biopsies given as absorbance at 490 nm per milligram of tissue. Error bars represent standard deviation of biological replicates (N=2) The collective LDH release can be found in Figure 5.7A.*

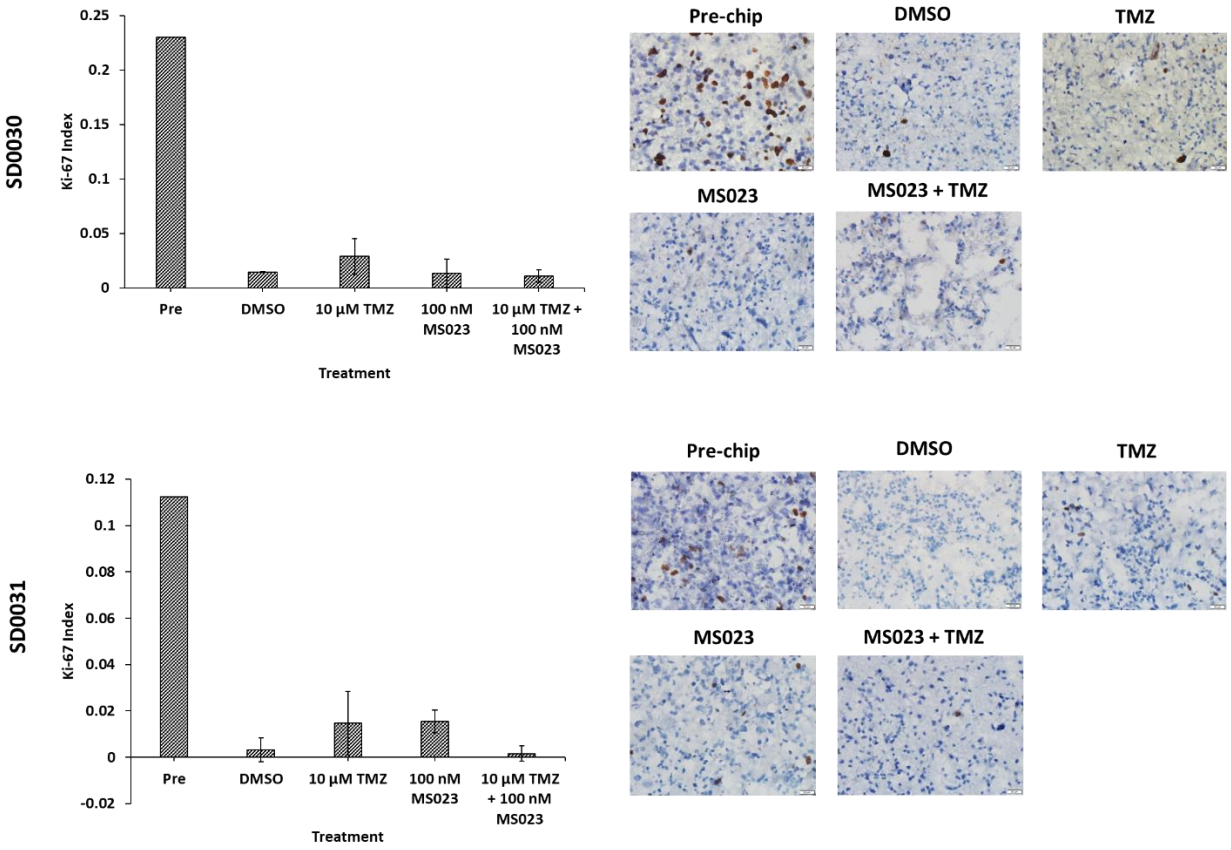

Appendix 8: *Ki-67 index of individual patient biopsies. Error bars represent standard deviation of biological replicates (N=2) Collective Ki-67 index can be found in Figure 5.7B.*

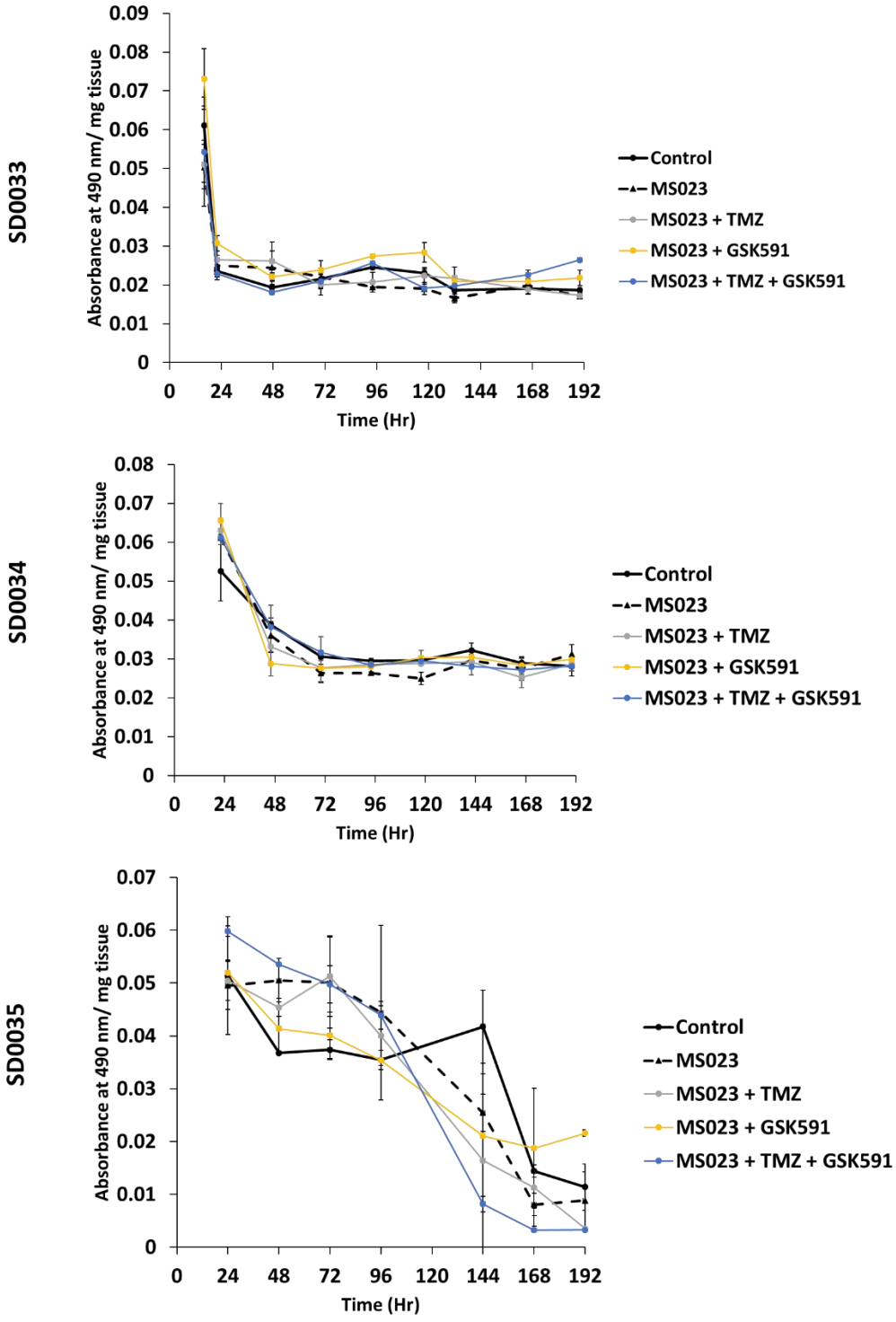

Appendix 9: *The release of LDH into the effluent for each individual patient biopsies, depicted in Figure 5.9, given as absorbance at 490 nm per milligram of tissue. Error bars represent standard deviation of biological replicates (N=2) Collective LDH release can be ound in Figure 5.9.*

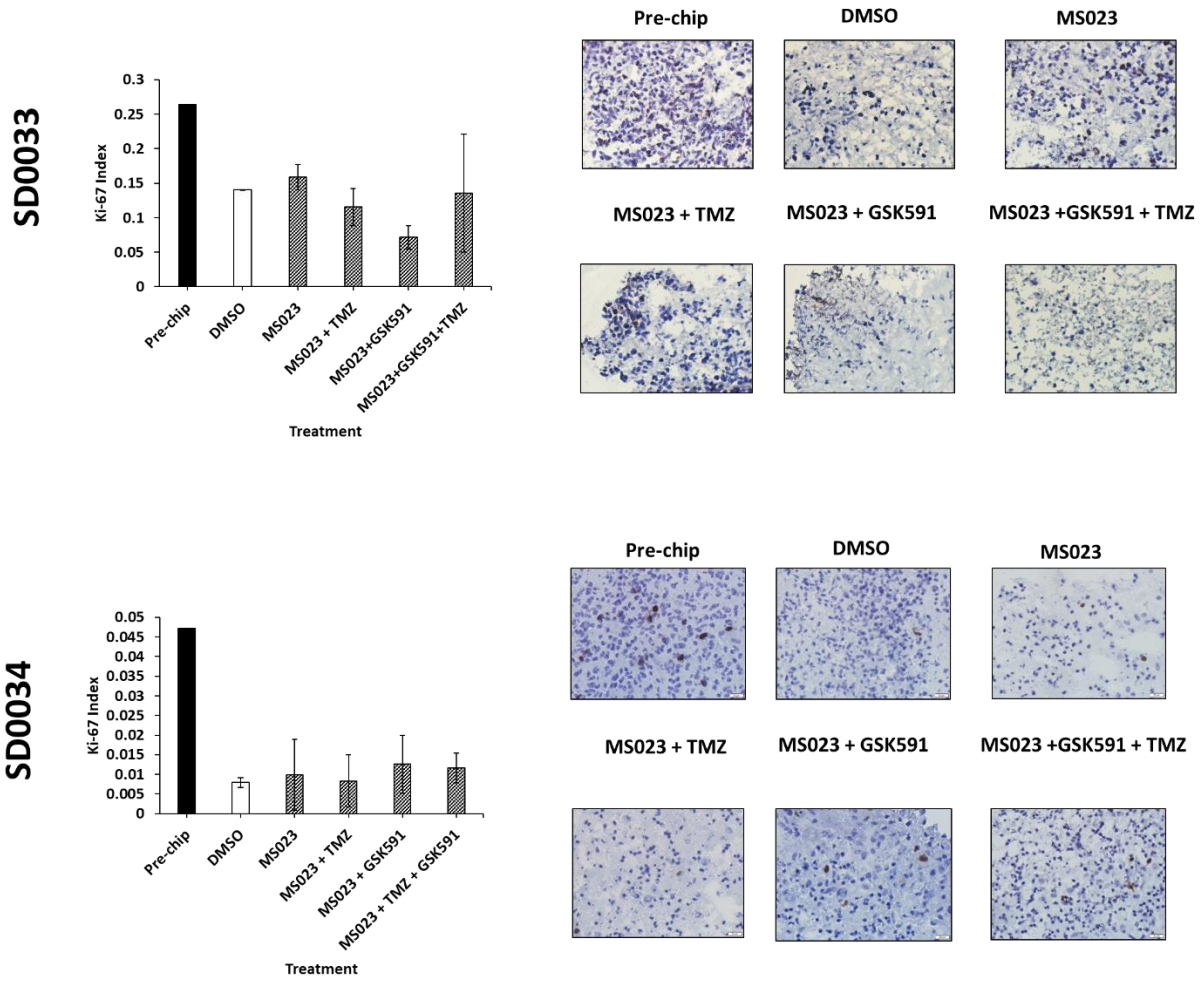

Appendix 10: *Ki-67 index for individual patient biopsies treated with combinations of TMZ and PRMT inhibitors, visualised in Figure 5.10, including representative images (x40). Error bars represent standard deviation of biological replicates (N=2) Collective Ki-67 index can be found in Figure 5.10.*

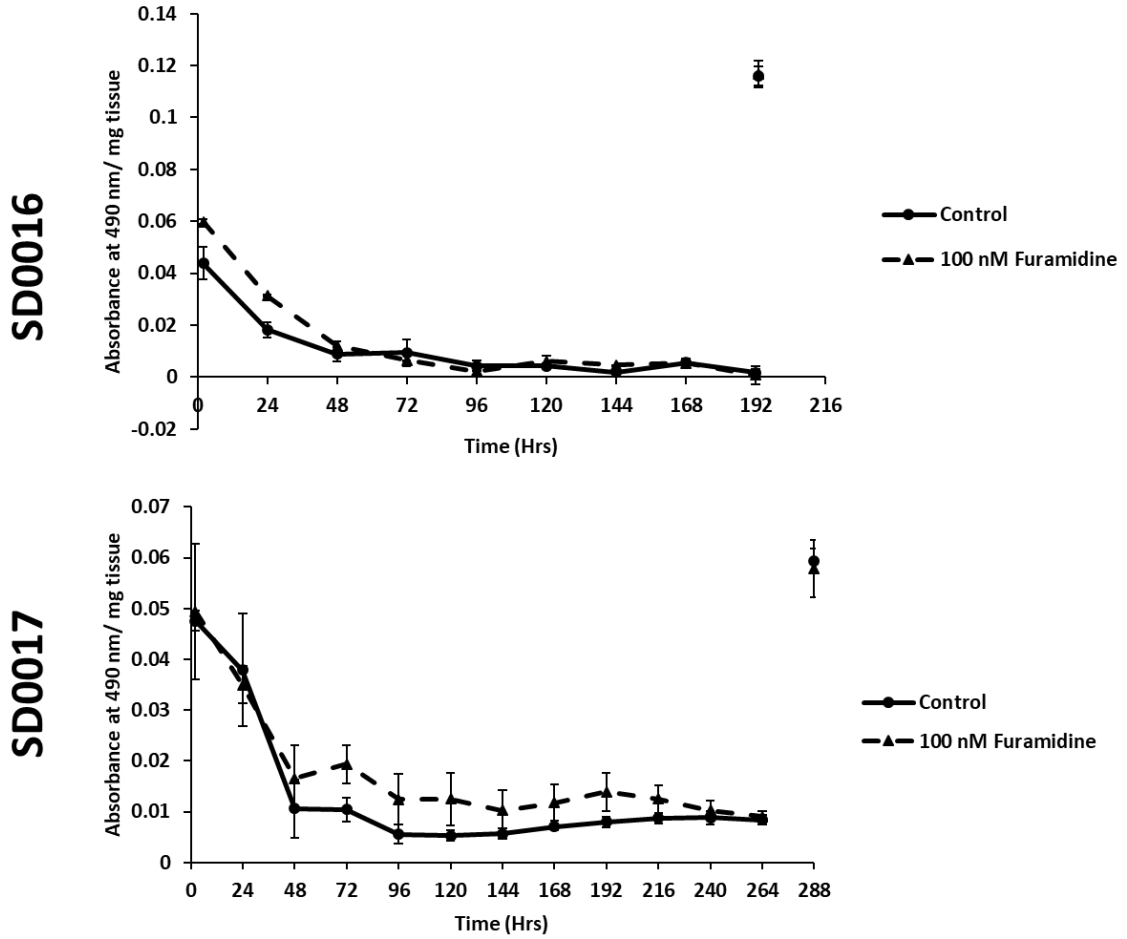

Appendix 11: *The release of LDH into the effluent for each individual patient biopsies, depicted in Figure 5.11, given as absorbance at 490 nm per milligram of tissue. Error bars represent standard deviation of biological replicates (N=3). Collective LDH release can be found in Figure 5.11.*

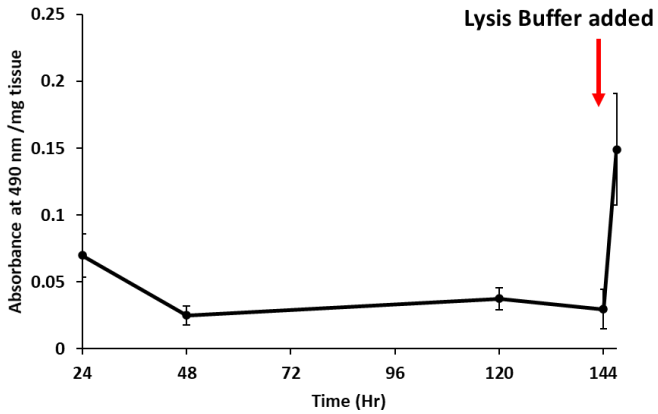

Appendix 12: *Two biopsy slices from SD0031 were incubated with lysis buffer (1 % (v/v) triton X-100 in PBS) for 2 hr at the end of the microfluidic incubation.*

Appendix 13: *Table of top GO terms for Control vs MS023 Treated and Pre-chip vs Control for SD0021 RNA analysis.*

Control vs Treated		Pre-chip vs Control					
immune system process	extra cellular region	immune system process	cell adhesion	transmembrane transporter activity	extracellular region	peptidase activity	transport
CXCL2	ESM1	CXCL10	CCDC18	KCNJ10	SEC11C	PSEN1	ARHGAP35
IL32	CCL28	PPBP	CDH19	ATP6V0E2	APOL6	KCNJ10	IL16
C1QL2	LUCAT1	BGLAP	DSG2	SCAMP5	SCAMP5	PRTN3	BCAS3
CXCL8	PDE10A	HLA-DPB1	PCDHGB7	KCNB1	ADAMTS15	CTSF	IDH1
CCL28	CXCL3	IKBIP	PCDHGB4	KCNJ14	ZC3H12B	DPEP1	PPFIA2
CCL20	CXCL5	SBSPON	PCDH18	AL390879.1	CLEC10A	PLA2G7	LTF
IL1A	MMP9	CXCL3	PCDHA10	ABCB1	CCDC18	ADAMTS4	CEP112
TNFSF14	PLAT	CXCL5	NECTIN4	KCNS1	CSF3	ADAMTS16	SLC13A3
CXCL5	MMP10	HLA-DQA2	TSGA10	GABRB3	SLC4A11	ASIC3	RGS9BP
CXCL9	IL32	ULBP1	STAB2	GPR137C	ADAMTS4	TLL2	KCNN3
IL1B	CXCL8	CXCL1	CDH3	BATF3	ADAMTS16	GZMA	PDZK1
CXCL3	PI3	AC022167.2	PCDHA4	SCN2B	MXRA7P1	MMP14	HERC2P3
IL6	SLPI	HLA-F	PCDHA5	SLC29A4	CXCL3	ADAM20	NECTIN4
C1QL4	IL6	CD70	PCDHA7	KCNN4	HHIPL1	JMJD7-PLA2G4B	ABCD2
ENPP1	SBSN	DYRK2	PCDHA2	SLC31A1	TLL2	AEBP1	SPARCL1
CD70	CXCL2	IL12A	PCDHA3	AC005682.1	TRAF3IP3	KLRA1P	KCNJ16
	AC044797.1	IL32	PCDHGA3	ARHGAP35	WNT2B	NECTIN4	SLCO3A1
	CCL20	CXCL11	SPECC1	CACNB2	METTL17	TPSG1	ATP7A
	IL1A	C1QB	FLT1	ASIC3	CALCB	ADAM1A	DNAH9
	MMP1	HLA-DPA1	BX664727.3	AC007000.1	CXCL11	SPARCL1	IDH2
	VEGFC	C1QC	CNTNAP2	KRT8P50	EFNA5	CES3	SGTB
	MMP3	HLA-DOB	AL121748.2	AC027279.1	MMP11	ARL6IP4	SYT2
	C3	CCL24	CDH10	COX7A1	MMP14	HHIPL1	ITPKB
	GAL	HLA-DQB2	PCDH12	SORT1	CXCL10	ECEL1	SLC6A13
	LTF	CXCL13	CD24P4	KCNN3	ADAM20	ERMP1	FRS2
	TINCR	SARM1	PCDH17	COX5BP2	SPTBN1	ADAMTS15	SLC26A9
	IGFBP6	IL6	PCDH8	ATAD5	TTC16	NAALADL2	SLC6A6
	AL672207.1	C1QL4	PCDHB1	SLC4A1	PJA1	CRB1	ITM2C
	ACAN	LST1	THBS2	HERC2P3	MME	CMBL	ASIC4
	KCNIP2	CD1D	ASGR1	MT-ATP6	CCL24	DHX34	FLVCR1
	ADM2	CXCL2	SCARB2	NECTIN4	CXCL13	TFDP2	PCDH12
	CXCL9	CCL8	LZIC	RABL3	GAST	CREG1	HBD
	ADAMTS8	CCL26	PCDHAC2	P2RX7	IL1RN	CPD	ASXL2
		IL23A	AC040162.3	KCNE1	SCRT2	ADAM21	PRF1
		HFE	SHISA9	SPARCL1	ADAM1A	ACE	STXBP6
		CCL20	CDH2	KCNJ16	SAA4	ADAMTS18	MEGF10
		IL1A	FAM120AOS	SCNN1D	KCTD8	SMARCA2	BAAT
		SHISA9	F8	ATP5PB	CXCL2	CTSK	RND2
		CD8A	PCDHGA2	ATP1A1	ADAMTSL2	KCNK13	B4GALT5
		HLA-H	F5	SV2A	STAB2	ADAMTSL4	APOLD1
		MR1	BCAN	SLC2A13	DGKB	TPP1	AP5M1
		TNFSF14	PCDHB18P	KCNQ5	OCLN	DNAH10OS	CACNG4
		SUSD1	CELSR1	SLC6A16	MGP	LPAL2	PRKAR1A
		HLA-DQB1	RASSF8-AS1	ARGLU1	KCNQ5	KLK14	ABCC2
		BCORP1	CDH22	AL031708.1	PRAP1	ASXL2	SLC10A5
		CSF3	CNTN2	SLC1A3	VEGFC	HTRA1	CACNB2
		TTC16	NPIPA8	SLC39A1	PYY2	C1orf74	MYH16
		PRG4	CDH15	SLC47A2	COBL	PCSK2	TRIM46
		HLA-DRB6	TRAF3IP3	SLC6A6	C3	CARMIL1	MFSD6
		OSM	PCDH19	KIF3C	B3GNT9	ELANE	ABCD3
		HLA-DMA	HAPLN1	SCN7A	NCAN	ACR	TRAK1
		CD74	PCDHGC3	SLC17A5	NPC1L1	CTSL	ERAS
		PROCR	PCDHGB6	ITPR3	C5orf46	MTDH	SLC8A3
		CCL7	SCARA3	ATP6V1D	UBAP1L	ACY1	KCNC1
		PF4V1	MATN2	KCNMB1	SVEP1	PRSS36	OLR1
		AL162231.4	DSC2	LAIR1	TBC1D10C	PIGK	UBALD1
		SIGLEC12	CTNNA1	KCNQ1	BTBD11	HFE	RANBP6
		SIGLEC16	ACAN	TCERG1	IGFBP6	SLC2A12	EMP2
		SLAMF1	PCDHB14	CACNA1G	LRP1	MMP1	SCN2A
		CXCL6	FGL2	AP003119.3	SPECC1	PLCXD3	IL1R2
		C1QA	AC068768.2	AL512353.2	ADM2	ADAM17	SCN3A
		HLA-DRB5	SUSD5	UNC119B	UCN	PRSS35	STXBP2
		RAB11FIP1	DMPK	KCNE5	ADAMTS18	AKAP14	DES
		HLA-K	PCDHB12	ATP6V1H	MFAP5	MBTPS2	CHMP4BP1
		ENPP2	KRT8P33	SLC16A8	ESM1	ADAMTS17	KIAA0825
			CDH6	TMCO3	ADHFE1	SLC9A5	CXCR3
			AC098614.1	ZNF253	ADAMTSL4	MMP11	C1QB
			CDH4	MIR1-1HG-AS1	RCN1P2	ADAM10	XPOTP1

			OMG	AP001486.2	MT1H	PBXIP1	ATP1B1
			MYO15B	GRIK3	GRM6	PCSK6	SLC30A2
			OCLN	FCGR1B	STRCP1	SCPEP1	NAA16
			CPXM2	CACNA1H	PPP1R9A	ADAMTS10	SLC5A3
			CDH5	GRIK2	HTRA1	PHEX	SDK1
			LINC00304	AC010329.2	DYRK2	ADAM28	FXYD5
			KCNQ1OT1	AKAP17A	BEGAIN	ZNF705E	COG6
			NINJ2	HSP90AA2P	MXRA7	CRAMP1	BDKRB2
			KTN1	VLDLR	GPC3	KLKB1	RAB9A
			FCGR3B	ASIC4	THBS2	RHBDL1	NXF1
			PCDHB17P	MT-ATP8	IL12A	DHH	GJA1
			PCDHB6	SFXN1	STXBP6	ADAM11	MT-ATP6
			PCDHB7	GPR34	ASGR1	SPG7	TMCC3
			SESN3	PPP1R12C	ZDHHC24	MMP17	PTPRG
			CNTNAP3B	KCNA1	PML	ADAMTS2	SLC16A6P1
			CNTN5	PDZK1	GPR45	CCDC85C	GAS7
			BEGAIN	FOSB	LDLRAD4	CDKL5	TPTEP2
			KRT1	SMG1P3	HEXB	INTU	CACNA2D1
			STAB1	GABRR2	LZIC	SIX6	HCN3
			EPDR1	FBXO32	APOLD1	MMP25	ARMCX1
			PCDH1	CCER2	PAWR	PCSK4	FXYD6
			DDR2	P2RY1	PRSS36	ADAMTSL2	MCC
			PCDHGA11	CACNG4	IL23A	COL12A1	MEOX2
			PCDHGA7	P2RY13	MYL9	NAA16	CLEC10A
			PCDHGA12	AC022893.1	ABCC2	NAPSA	ABCC3
			CDH8	AC119751.3	SLC6A17	LAMP1	TLR2
			FAT4	GOLGA8VP	PPP1R3D	GZMM	RAB30
			SDK2	AC009948.3	SHISA9	GOLGA2P5	CHMP6
			CTNNA1P1	SLC6A9	CFAP43	MAML2	CPNE3
			PCDH7	SFXN2	NPPA	AFG3L1P	AP3B2
			PCDHB2	UACA	XIAP	CFB	MDFI
			LAMA1	SLC35F1	ETV5	NLN	AQP3
			MRC2	AC138028.4	IL17RD	TTC9	SLITRK6
			DCHS2	MANEA-AS1	MMP1	ADAMTS6	CHRNA10
			COL18A1	EHD3	BCORP1	HPN	CLCN4
			MADCAM1	SLC30A1	EDN1	GZMB	MPZ
			ARHGAP42	SLC22A14	GHRL	GZMH	COG7
			PCDHAC1	RND2	SLC26A10	BDKRB2	KCNN1
			FAT2	SLCO2A1	RETN	HMGCS1	SLC16A5
			CDH11	SCNN1G	DAPK2	LGMN	CCDC144CP
			PCDHGB1	LZIC	WNT6	NPEPL1	OLFML3
				SLC22A3	DYNC1H1	TWIST1	KCNK5
				ATP2B2	CCN2	BICRA	SLC7A11
				LRMP	YES1P1	ADAMTS13	MCCC1
				PAWR	IFNE	UNC5A	SLC16A12
				ITM2C	BCAN	CPXM2	KCNJ9
				KRT5	LAS1L	LNPEP	ABCC5
				SH2D4A	CCN6	PRSS27	MYO1F
				PRKAR1A	CD109	TMEM154	GRIN2C
				ABCC2	HAMP	ADAMTS8	SLC7A9
				SLC6A17	WFDC3	NPIPA8	ATP6V0E2
				GIMAP4	LOXL4	CASP4LP	SCAMP5
				Z98749.2	FSD2	ACAT1	SCNN1D
				RAB6B	CNTN2	ADAMTS9	GPR137C
				CFAP43	PBXIP1	NRXN3	SLC47A2
				SLC22A7	HNF1A	CTSW	TRAF3IP3
				SLC6A13	KRT1	LONP2	SORT1
				ASXL2	LINC01480	MUC20P1	SLC26A6
				TRAK1	ADAM28	PRCP	NBAT1
				KCNH2	IGF1	AFG3L2	RABL3
				AC008147.2	CHD5	PCSK7	P2RX7
				CHRNE	DTWD2	CARD11	MFSD1
				NACC2	SPOCK2	SCRN1	SLC35F3
				GPRC5B	RASEF	PDPN	KCNQ5
				DYNC1H1	ADAM21	CAVIN2	SLC6A16
				SLC47A1	MMP17	MST1P2	ARGLU1
				YES1P1	ADAMTS2	SPPL2A	SLC1A3
				MTATP6P1	TNNC2	CAPN5	SLCO2A1
				AL049844.2	LNCOC1	ART3	MSMO1
				SLC7A3	DES	ADAM32	SCN7A
				COX4I2	SIX6	CAPN14	KCNQ1
				SLC22A20P	MMP25	TENM3	SBSN
				ALDH1A3	IL32	PSMA6	TCERG1
				B4GALT5	APOL2	PRSS56	RRAD
				ABCD3	GCG	STING1	DHX34
				GRM6	SCARA3	LOXL4	DAND5
				SLC9A5	MATN2	ADAMTS12	CCDC150

				ERAS	OXT	MMP15	HSP90AA2P
				CARMN	ADAMTS8	MMP2	TMED9
				DIRAS1	NBPF20	TINAGL1	SRPRB
				SLC33A1	KRT8P50	COL20A1	ADCY5
				SLC8A3	PI3	ATP9A	SLC26A5
				KCNC1	TINCR	ABHD12B	GABRR2
				RNF13	COL12A1	TRIM63	SLC25A37
				ITPR1	TSGA10	MMP8	SLC47A1
				OLR1	SLC5A3	THSD4	P2RY13
				SLC26A6	KRT5	SLC7A11	CLEC4GP1
				SLC2A1	LAMP1	JAM2	SLC35F1
				SLC26A9	PROS1	TMEM47	ATP6V1H
				SLC6A11	IL6	VTCN1	SSTR1
				BX322650.1	MFAP2	COL27A1	PRKCA
				SLC13A4	MAML2	CPVL	SLC19A3
				KYNU	CCL8	MST1	TMEM255A
				CHST10	IGF2	LRP1B	MFSD4A
				SLC7A8	FGL2	PLIN4	SH2D4A
				SLC35A5	F8	SNX33	CORO6
				SCN2A	ADAMTS6	EVC	DMBX1
				SLC7A2	CCL20	RHBDL3	RAB6B
				RAB26	IL1A	CTSA	AQP11
				SLC39A5	PCYT1B		GRM6
				SCN3A	DAPL1		INTS4P1
				RALBP1	OXCT2P1		LOXL4
				CACNA1A	INSL5		SLCO2B1
				SLC10A5	MROH6		UEVLD
				CXCR3	C5orf66		CD74
				RAD51-AS1	SBSPON		VMP1
				C1QB	KRT8P33		SLC7A3
				IL1R2	CDH6		ARHGAP26
				ABCC9	OSM		ALDH1A3
				SPNS1	LTF		ROS1
				KTN1	SCGN		SLC9A5
				SLC30A2	MYO15B		RNF13
				SRPRB	ADAMTS13		SLC2A12
				KIAA1549	TRIM11		SLC2A1
				MPEG1	HPCA		KYNU
				RHCG	PRSS27		HSD17B12
				SDK1	ATP2B4		SLC7A2
				GRIK4	TBC1D2		CCDC91
				SCN1A	SAA2		ITPR2
				FXYD5	KCNQ1OT1		AP1G2
				CENPF	DKK3		CACNA1A
				TMEM38A	OXCT2		CARD14
				TCIRG1	MRPS17P1		APOL2
				SLC1A2	PDCD10		XRCC4
				AC099489.1	IGFBP5		TNFAIP2
				AFAP1	LRRIQ3		DNAH17
				TTC9	ANKRD63		PALMD
				ADAMTS6	TEPSIN		ATP1B2
				LST1	KTN1		KRT8P50
				DMPK	MCC		COL6A3
				AC105052.2	STC2		GRIK4
				FLVCR1	CKAP4		SLC1A2
				ITPR2	EXTL3-AS1		TMEM38A
				AC113191.1	CCN3		PRKAA2
				KRT8P33	ALB		SLC24A2
				TTN	PLEKHF2		SERHL
				KNOP1	PPBP		LST1
				GJA1	PAM		ZNF572
				GABRA4	IL36B		FEZF2
				ATP6V1C2	ADAMTS9		SLC6A4
				SLC6A4	SOX7		GPSM2
				TMCC3	RAB30		AP2B1
				LRRFIP1P1	CXCL5		SLC7A14
				P2RX5	HSD17B13		TM7SF3
				KCNA6	CXCL1		BICD1P1
				SLC7A14	CNTN5		G3BP2
				RAB3D	PLAT		SLC23A1
				OSBPL10	PF4V1		CPLX1
				ATP2B4	FCN1		SLC4A5
				ATP6V0C	CORT		MFSD2A
				KCNQ1OT1	GUCA1B		CD93
				HCN3	KLRD1		SRL
				MTURN	CALU		KRT1
				FXYD6	RHOT2		STAB1

				MCC	HMCN2		CENPJ
				MEOX2	EPDR1		MAGEE1
				SLC22A10	CRYBG1		BATF3
				GIMAP5	NPY		LAPTM4B
				GIMAP8	ALDH5A1		ZFYVE1
				HCG27	CXCL6		SCN1A-AS1
				ABCC3	SBSN		MX1
				SLC4A5	STMN2		KCNG2
				KCNJ5	LINC00649		NCALD
				ATP8B1	QTRT1		MAML3
				TLR2	CCL26		GOLGA8VP
				RAB30	CST7		REM2
				CPNE3	DMPK		SLC13A4
				KCNE3	COL18A1		SLC4A4
				CD93	SHISA3		CACNA1I
				SRL	MIR600HG		ABHD4
				SLC2A12	KRT75		KHDC1
				BEGAIN	ADAMTS12		GABRE
				PIGCP1	MMP15		CFAP70
				KRT1	MMP2		APOL6
				SLC16A1	SUSD1		STXBP5L
				CENPJ	SAA1		KCNJ14
				SBSN	HPCAL4		ABCB1
				SLC39A11	SLC8A2		SNAP25
				RRAD	KRT14		GABRB3
				SLC39A6	TWIST1		GOLGA8N
				SMIM24	MMP8		SLC29A4
				CHRNA10	LAMA1		KCNN4
				GABRB2	THSD4		ASIC3
				CYP2U1	P2RX2		ITPR1
				CLCN4	RAB11FIP1		CPLX2
				SESN3	SLC7A11		ATP1A1
				SLC39A14	CCL7		SDAD1P1
				RPL22P24	ACAN		SLC4A1
				CHRNA7	MXRA5		ZNF496
				AC010127.1	MEGF8		SLC8A2
				ASPM	ARHGAP42		ALG10B
				SLC14A1	KHDC1		ARL6IP4
				SLC26A5	GNRH1		CCDC39
				ATP6V1C1	IGFBP4		CACNA1G
				GABRE	S100A9		SLC15A2
				GRIN3A	GRIN2C		SLC39A1
				KCNG2			KIF3C
				KIAA1549L			CRB1
				KCNN1			SLC11A1
				MAML3			ARHGAP27P1-BPTFP1-KPNA2P3
				SLC2A5			SPIRE1
				PRF1			MT-ATP8
				REM2			SPECC1
				SLC30A6			SLC16A8
				CLCN3			KCNE1
				KCNK5			AQP4
				SLC4A4			SEPTIN7
				RAB23			DIAPH3
				AC139769.1			SRSF5
				TRIM63			NDE1
				ASCL1			KCNS1
				CACNA1I			IKBIP
				ZNF572			RAD51-AS1
				P2RX2			SLC16A10
				GRIN2C			FOSB
				SLC7A11			TMTC3
				MCCC1			SEC23B
				SLC34A2			DHX40
				PCDH12			NXF3
				SLC44A1			AP3M2
				ABCC5			SFXN2
				BDKRB2			UACA
				KCNJ9			VAMP2
				MX1			SLC43A3
				GIMAP7			AQP7P1
				SLC7A9			LZIC
				TMCO1			SLC22A3
				RAB9A			PAWR
							MTX1P1

							SLC22A7
							KCNH2
							UQCRHL
							NACC2
							SLC49A4
							SLC22A20P
							NPHP3
							DIRAS1
							TOM1L1
							SLC6A11
							VAMP1
							VPS41
							STON1
							MREG
							PEX26
							ADRA2A
							ABCC9
							MYRIP
							KRT5
							CENPF
							MAML2
							TCIRG1
							CHRNA7
							ATP6V1C1
							FAM135B
							TNPO1P3
							MTATP6P1
							NPEPL1
							CCDC18
							APOB
							P2RX5
							SLC5A4
							KCNA6
							NUTF2P6
							PDCD10
							VPS35
							GIMAP8
							CLEC7A
							KCNJ5
							SESN3
							ZNF20
							KCNE5
							MOB1A
							KCNE3
							YWHAQ
							RFFL
							HMCN2
							EXOC5
							TMED10
							RPL22P24
							ITPR3
							CCER2
							CLTC
							ZNF770
							SLC2A5
							SLC30A6
							SRGAP3
							ASCL1
							SLC35B2
							SDC1
							P2RX2
							LONP2
							CHMP4A
							SLC2A13
							KCNJ10
							KCNB1
							TNPO1
							SLC6A9
							SLC4A11
							SLC31A1
							MYH3
							PIGCP1
							SMG1P3
							SLC22A14
							SMIM24
							TERF1P7
							SLC39A11

							ATP5PB
							AQP6
							SV2A
							SLC22A10
							GPRC5B
							SLC17A5
							KCNMB1
							SPN
							KCNA1
							UNC119B
							TMCO3
							MIR1-1HG-AS1
							GRIK3
							SYTL5
							GGA1
							CACNA1H
							CHST10
							VLDLR
							GPR34
							PPP1R12C
							RGPD2
							VWCE
							FBXO32
							AP4B1
							KIF1B
							RASAL3
							ASPN
							TMEM144
							EHD3
							SLC30A1
							SLC14A1
							IRAG2
							SLC6A17
							GIMAP4
							MTX3
							DYNC1H1
							SLC5A6
							AQP5
							CHRNE
							MFSD6L
							UBE2E4P
							PSTPIP1
							CARMN
							SCNN1G
							TFCP2L1
							NXT2
							SYNE3
							BGLAP
							SLC7A8
							SLC35A5
							SFXN1
							SLC39A5
							GIMAP7
							SPNS1
							PRR5
							COL12A1
							KIAA1549
							RHCG
							MPEG1
							SCN1A
							RAMP3
							AFAP1
							RAB23
							KRT8P33
							ADCYAP1R1
							GABRA4
							ATP6V1C2
							AQP8
							MORF4L1P1
							RAB3D
							OSBPL10
							SLC24A5
							ATP6V0C
							KCNQ1OT1
							FSD2
							KTN1
							NXF5

							GIMAP5
							NPIPA8
							GBP2
							PLEKHF2
							HCG27
							SLC17A7
							IGF2R
							ATP8B1
							SLC5A11
							PRDM15
							BEGAIN
							SLC16A1
							SLC39A6
							GABRB2
							PSPH
							SLC39A14
							DNAJC28
							ASPM
							DMPK
							FER1L6
							GRIN3A
							IL21-AS1
							KRT75
							PCDH7
							SLC24A3
							CLCN3
							RAB26
							AR
							KRT14
							TRIM63
							MTURN
							SLC34A2
							ELMOD2
							CLPB
							TTN